THE SPALLING OF CONCRETE IN FIRES

RAYMOND JOHN CONNOLLY

Doctor of Philosophy

THE UNIVERSITY OF ASTON IN BIRMINGHAM

April 1995

THE UNIVERSITY OF ASTON IN BIRMINGHAM

THE SPALLING OF CONCRETE IN FIRES

Raymond John Connolly PhD

1995

SUMMARY

The occurrence of spalling is a major factor in determining the fire resistance of concrete constructions. The apparently random occurrence of spalling has limited the development and application of fire resistance modelling for concrete structures. This Thesis describes an experimental investigation into the spalling of concrete on exposure to elevated temperatures. It has been shown that spalling may be categorised into four distinct types; aggregate spalling, corner spalling, surface spalling and explosive spalling.

Aggregate spalling has been found to be a form of shear failure of aggregates local to the heated surface. The susceptibility of any particular concrete to aggregate spalling can be quantified from parameters which include the coefficients of thermal expansion of both the aggregate and the surrounding mortar, the size and thermal diffusivity of the aggregate and the rate of heating. Corner spalling, which is particularly significant for the fire resistance of concrete columns, is a result of concrete losing its tensile strength at elevated temperatures.

Surface spalling is the result of excessive pore pressures within heated concretes. An empirical model has been developed to allow quantification of the pore pressures and a material failure model proposed. The dominant parameters are rate of heating, pore saturation and concrete permeability. Surface spalling may be alleviated by limiting pore pressure development and a number of methods to this end have been evaluated.

Explosive spalling involves the catastrophic failure of a concrete element and may be caused by either of two distinct mechanisms. In the first instance, excessive pore pressures can cause explosive spalling, although the effect is limited principally to unloaded or relatively small specimens. A second cause of explosive spalling is where the superimposition of thermally induced stresses on applied load stresses exceed the concrete's strength.

The influence of a range of variables on the occurrence of explosive spalling has been studied experimentally and correlation established with behavioural models derived from theoretical considerations. It was found that individual parameters can have differing effects on each of the spalling mechanisms, making it impossible to give unique criteria for spalling. The high degree of interaction between parameters needs to be considered in the assessment of any particular situation for spalling.

Keywords: Concrete, fire, spalling, explosive, failure.

To my Dad

ACKNOWLEDGEMENTS

I would like to thank my fiancée Maria not only for her love and support over the last number of years, but also for her help in producing this Thesis. I thank also my Mum and Dad, family and friends for their encouragement and understanding of my absence from the golf course. I thank also my supervisors (and I hope friends) Dr. John Purkiss and Mr. Tony Morris for their continuous help and patience.

I have many colleagues at the Building Research Establishment to whom I am particularly grateful for their help in undertaking this research. Special thanks to Alan Andrews, James Kirby, Yin Xiaolin and Dave Smit. I am also grateful for the invaluable assistance I received from Pat Walsh of BRE's Design Studio, Clive Tipple and David Richardson of BRE's Concrete Laboratory, Miles Roper in the BRE Library and Colin Thompson of Aston University.

I also thank Dr. Woolley and Dr. Warren for their constant encouragement and support of this research at The Fire Research Station. Last but not least, I am grateful to the Director of BRE for his financial support through his Programme of Strategic Research.

Thank you all.

CONTENTS

LIST OF FIGURES

LIST OF TABLES

LIST OF PLATES

CHAPTER 1. INTRODUCTION

Spalling of concrete is a natural phenomenon, whereby on exposure to a heating regime, forces are generated within a concrete's body that cause disintegration of its surface. Spalling of concrete involves the breaking up and dislodging, often violently, from the surface of particles or lumps of various sizes.

Spalling is not unique to concrete and has been well studied in the field of ceramics (Norton, 1968). Although, behaviour termed spalling has been observed in ceramics, brickwork and rocks, it is quite likely that the mechanisms leading to spalling of these materials are different to those which cause spalling in heated concrete. Although useful information may be obtained by referencing studies of spalling undertaken for other materials, researchers studying the spalling of heated concrete have realised that the underlying causative mechanisms are unique to concrete.

One of the earliest observations of the spalling of concrete were made by Gary (1916) in his study on the effects of fire on concrete houses. He observed that on setting fires in a number of purpose-built concrete houses, concrete exhibited a range of different failure modes. He reported deterioration at the corners of stair treads and the arrises of beams, pitting of floor slabs and explosive failure of large sections of beam, columns and slabs. Gary recognised that spalling had several different forms, which he set out into four categories. His early categorisation has been adopted, to a greater or lesser degree, by nearly all researchers who have since studied the phenomenon of spalling of concrete.

1.1 CATEGORISATION OF SPALLING

Gary (1916) suggested that spalling could be grouped into the categories;

(i) Aggregate Spalling
(ii) Corner Spalling
(iii) Surface Spalling
(iv) Explosive Spalling

1.1.1 AGGREGATE SPALLING (Plate 1.1)

Aggregate spalling is the bursting or splitting of concrete's component aggregates at the heated surface. It is also known as aggregate splitting or flaking. Aggregate spalling is generally restricted to areas on or near the heated surface and occurs within the first 20 minutes of exposure to the standard BS 476:Part 20:1987 heating regime. Aggregate spalling is often associated with blistering of the concrete's surface, where split aggregate particles and some surrounding cement matrix are moved but not dislodged from the concrete surface.

Gary attributed splitting to the mineralogical characteristics of the aggregate. However, other researchers (Dougill, 1971; Austin *et al.*, 1992) have suggested that aggregate spalling is a form of thermal shock.

Aggregate spalling generally leaves coin-sized craters on the surface of the concrete, with a maximum depth of 5 to 10 mm. Accordingly, aggregate spalling neither removes large amounts of the concrete's cross-section nor exposes any underlying reinforcement and aggregate spalling thus has little or no effect on the fire resistance of concrete elements of construction.

In the vast majority of applications, the effects of aggregate spalling are simply aesthetic.

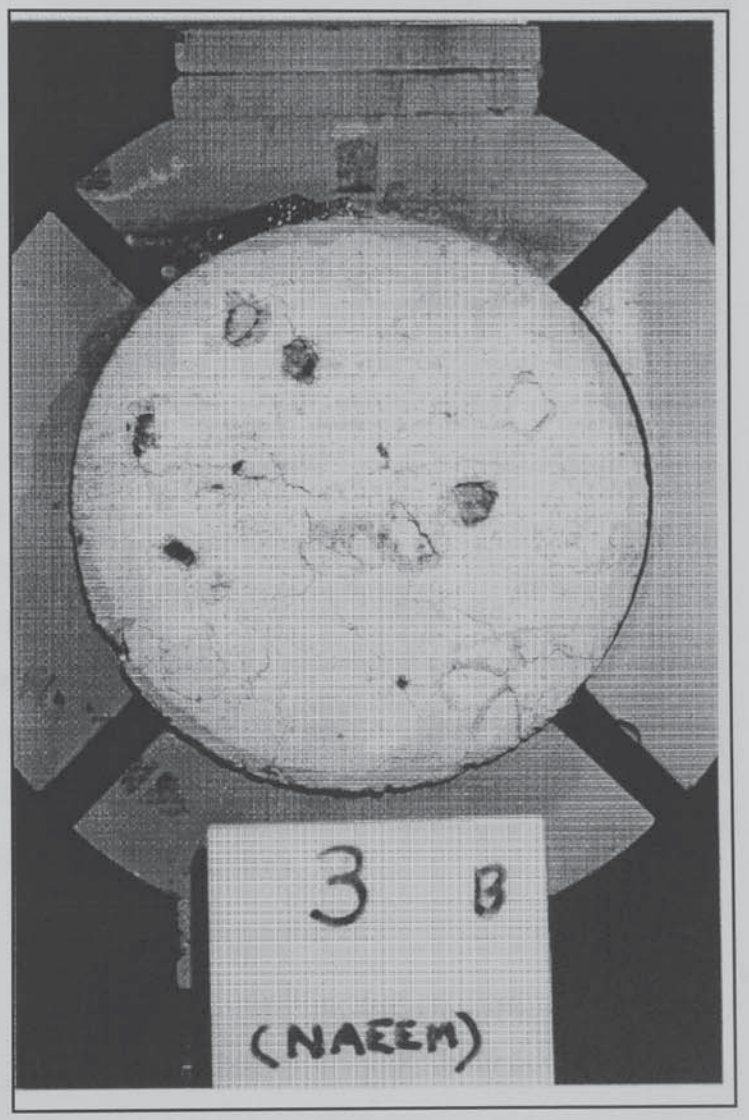

Plate 1.1 An example of aggregate spalling

1.1.2 CORNER SPALLING (Plate 1.2)

Corner spalling involves the gradual disintegration of heated concrete and occurs at the corners or arrises of concrete elements of construction such as beams or columns. It is also referred to as corner separation or sloughing-off, because of its progressive nature. Corner spalling occurs in the later stages of exposure (after 30 minutes) to the standard BS 476:Pt 20:1987 heating regime.

Corner spalling has been attributed to the loss of tensile strength in concrete at elevated temperatures (Dougill, 1971, Malhotra, 1984). The concrete at the arrises becomes cracked and weakened by heating, until bond failure occurs and the concrete outside the steel reinforcement can no longer support its self weight. Corner spalling, thus, tends to remove in sizeable lumps of concrete.

It has been suggested by some researchers (Dougill, 1971, Sertmehemetoglu, 1977) that the coincidence of strains at corners and the bursting effects of heated reinforcement are contributory factors. The presence of curvature of the concrete element, such as a loaded beam for example, may also increase the likelihood of corner. spalling.

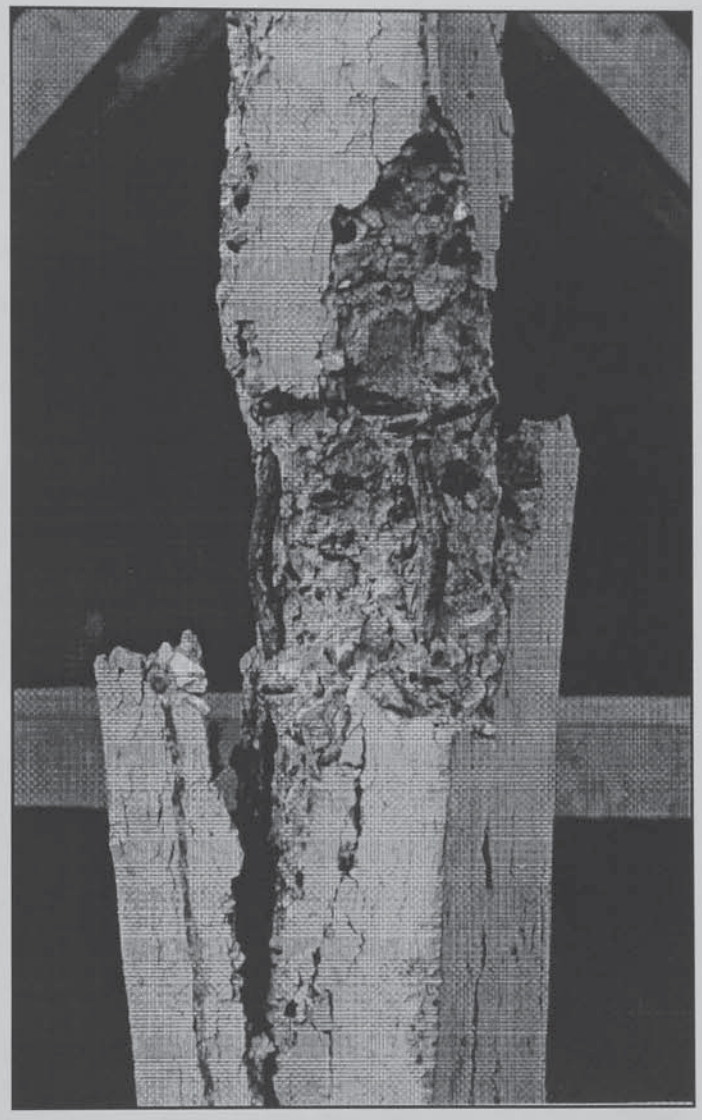

Plate 1.2 Concrete column subject to corner spalling

Corner spalling is particularly serious, as it generally involves the removal of the concrete cover to the steel reinforcement and thus can initiate global failure. It has been shown by Malhotra (1972) that provision of supplementary reinforcing mesh within the depth of the concrete cover

effectively reduces the amount of concrete that may be lost by corner spalling.

1.1.3 SURFACE SPALLING (Plates 1.3 and 1.4)

Surface spalling is a violent form of spalling at the concrete's heated surface, where lumps of concrete, of sizes up to 100 x 100 mm, are dislodged. The lumps or projectiles generally have a depth in the order of 25 to 50 mm. As such, surface spalling may result in the exposure of the steel reinforcement and has implications for the fire resistance of elements.

The implications of surface spalling are made more severe by the fact that it may occur progressively. Thus the areas damaged may extend to several square metres. The image of surface spalling presented in Plate 1.4 is very typical of the damage observed in concrete slabs exposed to real fires.

Dougill (1971) has referred to surface spalling as local destructive spalling. He suggested it resulted from bursting stresses created by super-heated steam trapped beneath the concrete surface. The violent nature of surface spalling, together with its characteristic cracking sound, has meant that many researchers (Shorter & Harmathy, 1965; Copier, 1979) have not considered it as a category of spalling in its own right and have simply viewed it as minor explosive spalling.

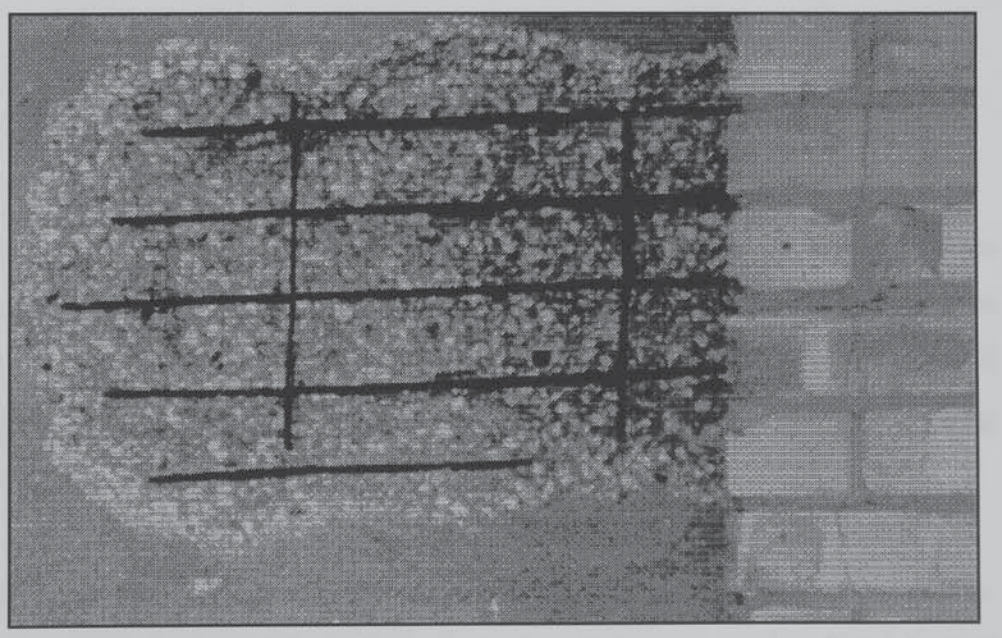

Plate 1.3 Surface spalling of concrete slab exposing steel reinforcement

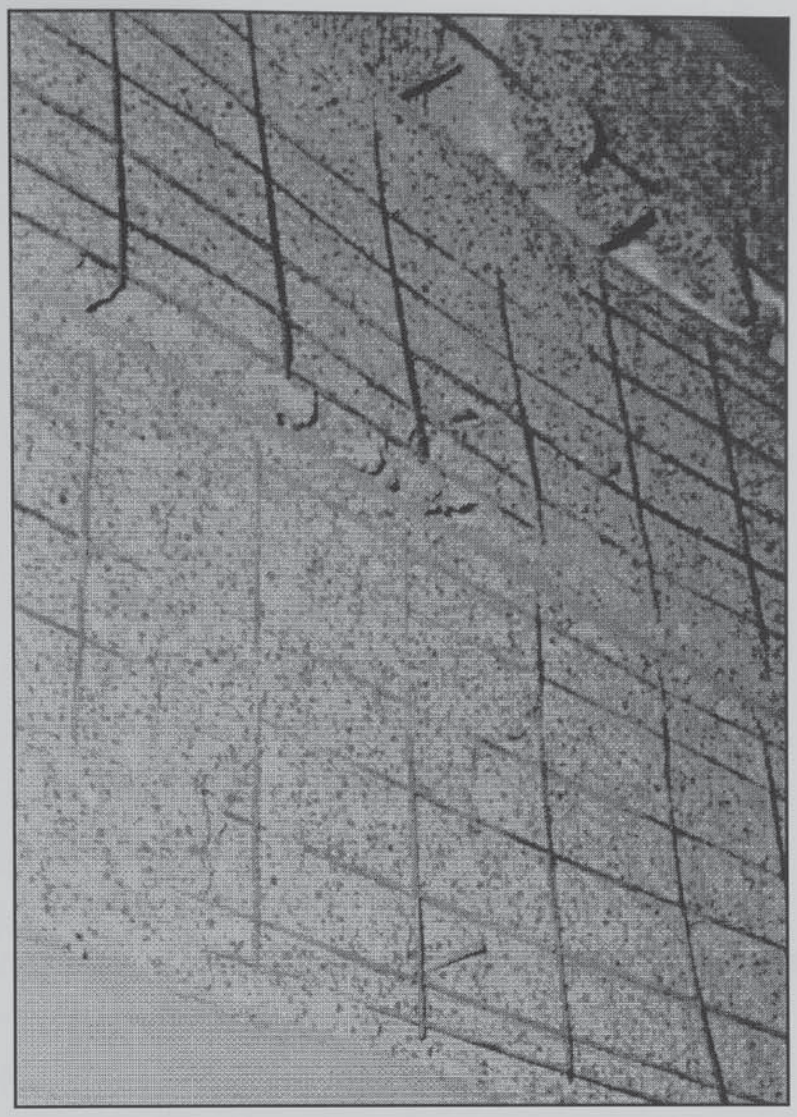

Plate 1.4 Surface spalling of Lytag concrete slab under real fire conditions

1.1.4 EXPLOSIVE SPALLING (Plates 1.5 and 1.6)

Explosive spalling, as the name suggests, is a very violent form of spalling, which involves explosive failure of heated concrete. Gary (1916) differentiated explosive spalling from surface spalling principally by its magnitude and he referred to it as the bursting of entire surfaces of wall slabs up to 1 m^2. He observed parts of slabs being ejected some 12 metres from the test building and quite reasonably classified explosive spalling as extremely dangerous.

Explosive spalling is immediately recognisable as it is accompanied by a large release of energy. It may result in a sudden and complete failure of the concrete member to sustain its load-bearing function and produces a typical explosive noise.

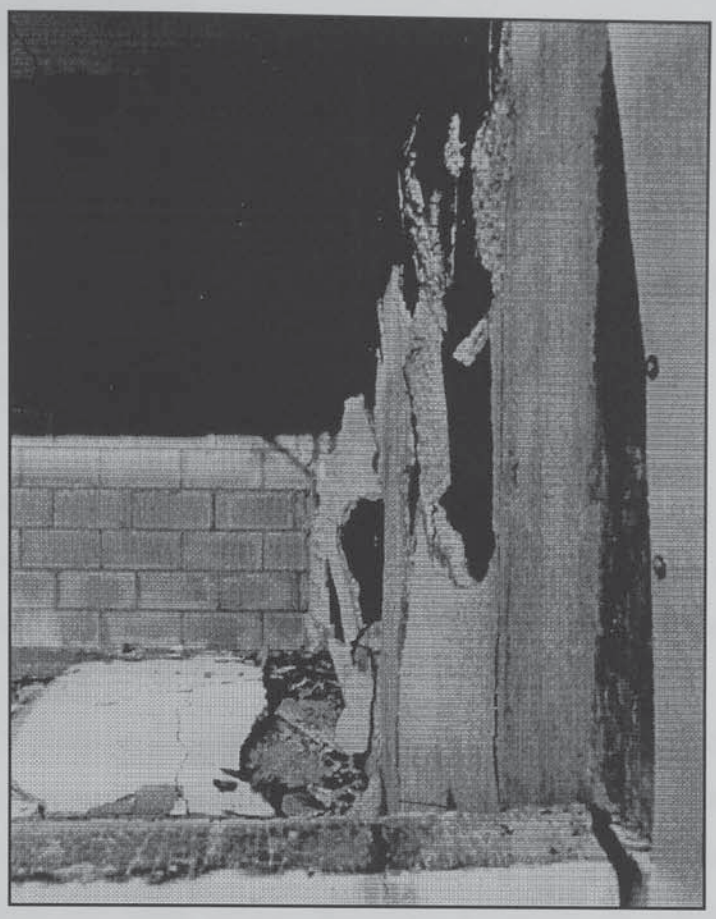

Plate 1.5 Explosive spalling of concrete slabs under real fire conditions

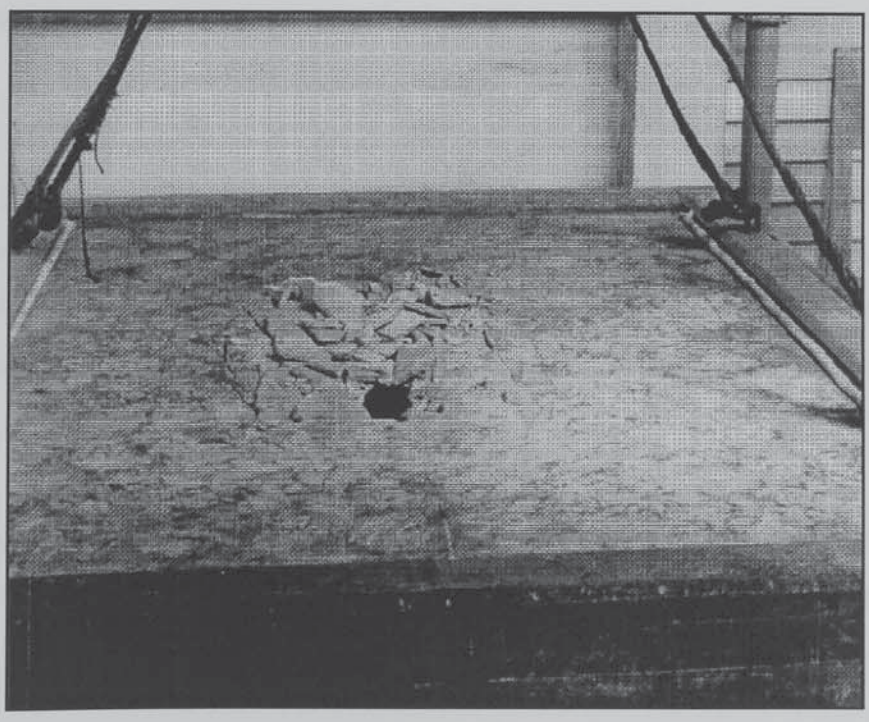

Plate 1.6 Explosive spalling leading to fire resistance integrity failure

1.2 CONSEQUENCES OF SPALLING

The extent, severity and nature of occurrence of spalling is varied. The consequences of spalling are very much effected by the application for which concrete is being used. For example, although in the majority of applications aggregate spalling may be a quite insignificant form of surface damage, it poses major problems in concrete pavements used for military aircraft (Austin *et al.*, 1992).

All forms of spalling may reduce the period of fire resistance that a concrete structural element might achieve when tested to BS 476:Part 20:1987. Spalling of concrete may cause fire resistance failure through loss of load-bearing capacity and/or loss of integrity.

Spalling may result in the loss of load-bearing capacity of a concrete member in one of two ways. In some cases, the occurrence of spalling may reduce the cross-sectional area of the concrete to such an extent that it is no longer able to sustain the compressive stresses imposed upon it. The scope for such failure has been increased by current trends towards rationalisation in design and the increasing likelihood for larger design stresses.

A second mechanism for load-bearing failure is that spalling of the concrete providing protective cover to the steel reinforcement may result in the reinforcement reaching excessive temperatures. As the yield strength of steel is considerably reduced at elevated temperatures, spalling may hasten the steel towards yield, thus precipitating flexural failure of the concrete member. With tension in the extreme fibres governing the design of most concrete elements of structure, this form of spalling failure is quite commonly found in practice. The likelihood of flexural failure is increased by the fact that spalling and crumbling of concrete from around the reinforcement may cause loss of bond and load-bearing failure could result from the loss of composite action.

Explosive spalling may be sufficiently violent to blow holes through the element's section, as shown in Plate 1.6. Thin slabs are particularly susceptible to such integrity failure.

1.3 NEED FOR CURRENT WORK

Much research on the nature of spalling and its consequences has been conducted indirectly through standard fire resistance tests. Such work has led to many anecdotal and intuitive theories regarding the importance of various parameters in governing the occurrence of spalling. In many cases, such theories are incompatible with each other and contradict reported spalling behaviour. An international survey of laboratories involved in the fire resistance testing of structural concrete members (Malhotra, 1972) confirmed that there was no real understanding of the fundamental mechanisms of spalling nor the effect of individual parameters in determining the susceptibility of concrete to spalling.

Morris (1972,personal communication) undertook a structured programme of fire tests on concrete columns to investigate the factors that effected fire resistance. Although, he was hindered in his structured study of fire resistance by the widespread occurrence of spalling, Morris provided interesting data on the effect that spalling had on fire resistance failure times. Figure 1.1 shows the effect spalling has on the fire resistance of concrete columns. The Figure suggests that regardless of the size of the column, the occurrence of spalling is critical in determining fire resistance.

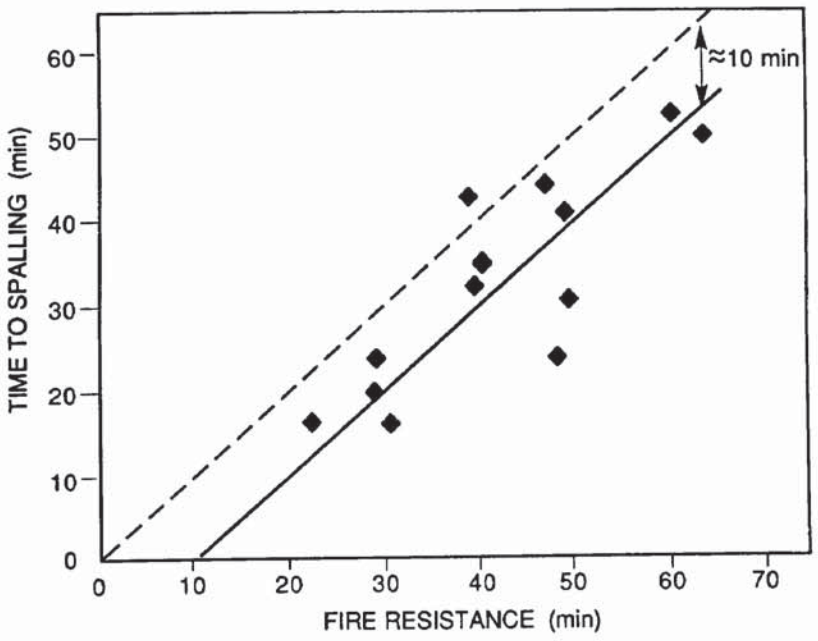

Figure 1.1 Effect of spalling on fire resistance of concrete columns

Confirmation of the crucial effect spalling has on fire resistance of concrete columns was provided using analytical methods by Mustapha (1994). He found that the amount of spalling that a column suffered was more critical in deciding its fire resistance than the patterns that heating and loading imposed. He calculated the structural response of the column using constitutive models M1, M2 and M3 based on the work of Anderberg (1976), Schneider (1986) and Lie (1984) respectively. The relationship between the amount of spalling from a 200 mm square column after 15 minutes and fire resistance time is shown in Figure 1.2 as an example of his findings.

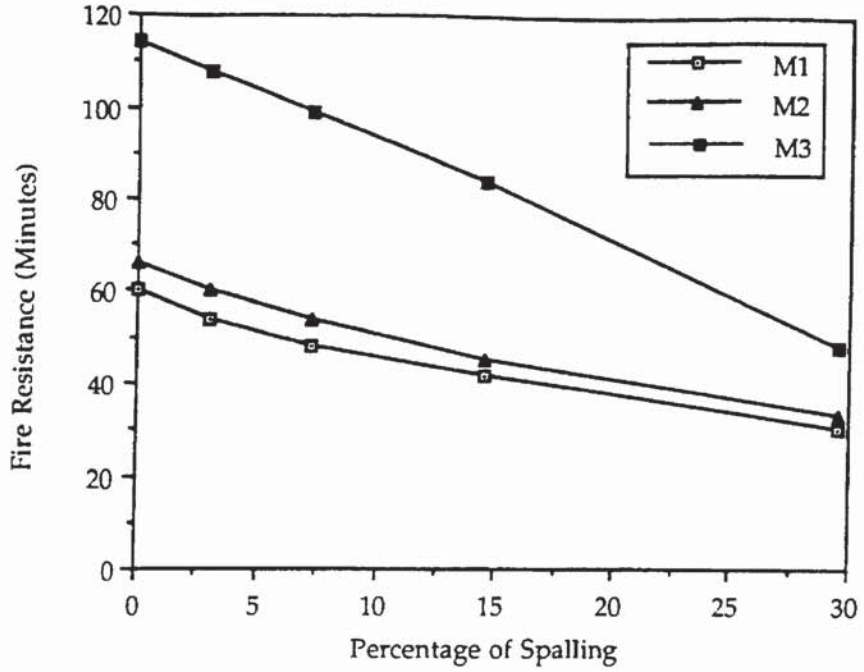

Figure 1.2 Calculated effect of spalling on fire resistance of columns

While spalling remains unpredictable, fire engineering calculations and computerised simulations of fire resistance tests will not be reliable. This has been recently demonstrated by Connolly *et al.* (1994) who showed that ignoring spalling can render numerical models for the thermal analysis of concrete members useless.

By ignoring the effects of spalling, it is possible that current engineering models used to predict the fire resistance of concrete structural elements may produce unsafe results. This possibility has been recognised by designers who, being unable to prevent spalling, have had to adopt measures to protect against its consequences.

For example, protection against the effects of spalling may be achieved by specifying the placement of supplementary reinforcement close to the surface of the concrete, thus retaining in place any concrete that may be fractured by spalling. Indeed, the Concrete Society and the Institution of Structural Engineers (1978) have suggested such an approach. However, provision of such reinforcement may cause some practical and durability difficulties (Lawson, 1985).

Spalling has been shown by Meyer-Ottens (1972) to be related to the rate at which concrete is heated. Accordingly, the susceptibility of any particular concrete to spalling will be related to the nature and severity of the fire to which it is exposed. This poses a major difficulty for the design of concrete structures to safely withstand fire. Concrete structural elements which have been tested for fire resistance are heated using a single standard heating regime. Despite apparently good fire resistance characteristics, exposure of such elements to more severe heating conditions may result in spalling and radically inferior performance in fire than that expected from the test.

Reports of a recent fire during construction of the Storebaelt Tunnel in Denmark (Bolton,1994) corroborate this very point. The 400 mm thick tunnel lining had been specified to achieve the appropriate fire resistance rating, but a fire in a boring machine exposed the concrete to very severe heating. The resultant spalling reduced the concrete thickness to a mere 100 mm in places.

It is clearly vital for the continued progress of fire safety design of concrete structures that the fundamental mechanisms that cause spalling are determined. A framework for predicting the occurrence and severity of spalling should then be established and methods to prevent spalling developed. The objective of the work reported in this Thesis was to address in part this need.

CHAPTER 2. REVIEW OF PREVIOUS WORK

2.1 EARLY EXPERIMENTAL INVESTIGATIONS

Much of the early research into the spalling of concrete was carried out in Germany in the first half of this century. As a result of their observations from fire tests, Bottke (1931) and Hasenjager (1935) developed basic explanations for spalling, which will be discussed later in Chapter 3.

It was not until after the Second World War that the fire performance of concrete was investigated in the United Kingdom and many observations regarding spalling ensued. A report from the Joint Committee on the Fire Grading of Buildings (1946) recognised that the spalling of concrete could greatly reduce the strength of columns exposed to fire. Ashton and Davey (1953) noted, after a comprehensive series of fire resistance tests, that the "*process of disintegration*" made it difficult to regulate the sizes of concrete slabs necessary to achieve periods of fire resistance. They observed further that thin concrete sections were more susceptible to the process of disintegration than thicker sections.

In an extensive study of the fire resistance of concrete columns, Thomas and Webster (1953) found that the use of a light mesh cover could limit the extent of spalling and significantly improve the performance of the columns with regards to fire resistance. At the same time, Ashton and Bate (1960), who were studying the behaviour of prestressed beams in fires, observed that extensive spalling from the arrises of the beams had a significant adverse effect on their fire resistance.

In Japan, prestressed concrete slabs were observed to spall in fire tests by Kawagoe (1958) and Nisugi *et al.*(1959). It was upon their work that Saito (1965) subsequently based his explanation of spalling which will be discussed in Chapter 3.

Hanneman and Thoms (1959) mentioned the spalling of concrete and bricks in their study of the fire damage sustained by 12 war-damaged houses in Berlin. In addition to the forms of appearance of spalling already mentioned, they found that floors and beams exhibited increased levels of spalling, particularly if the elements had a thin cross-section and were exposed to fire

on all sides.

Gustaferro and Carlson (1962) working in the United States and later Malhotra (1969) in the United Kingdom, confirmed from the results of an extensive series of tests on prestressed and reinforced concrete beams that destructive spalling may occur. Malhotra concluded from his practical experience that *"old dense concretes could well generate enough steam pressure to blow off the concrete cover, whereas young concrete still being quite permeable, could release steam pressures without much damage. Thus, poor concrete was superior to good concrete in spalling*".

Unlike the dominant view held in the United Kingdom at that time, Gustaferro and Carlson (1962) considered the nature of the aggregate to be of minor importance in determining the susceptibility of concrete to spalling. However, their opinions must be set in the context of the reduced incidence of spalling in the United States.

2.2 INVESTIGATIONS INTO THE FIRE RESISTANCE OF CONCRETE COLUMNS AT THE FIRE RESEARCH STATION (1964-1972)

A major experimental investigation into the fire resistance of concrete columns was undertaken by the Joint Fire Research Organisation (later to become part of the Building Research Establishment) at the Fire Research Station, Borehamwood between 1964 and 1972. Although some of the work was reported in brief by Malhotra (1970), the majority of the experimental results went unreported. This was due to the fact that the experimental programme was geared towards the study of the fire resistance of concrete columns and the widespread occurrence of spalling severly limited the application of the results.

The experimental records and some initial analysis of the findings recorded at the time by Morris*(1972, personal communication) have been retrospectively examined to give the basis for the following overview of the work.

(*) The help of Mr. W.A.Morris with this work is gratefully acknowledged

2.2.1 INITIAL FIRE RESISTANCE TESTS (1964-1969)

Morris's investigation commenced in 1964 and was aimed at producing guidelines on the dimensions of concrete columns necessary to achieve fire resistance ratings, in accordance with BS 476: Part 1: 1953. His tests were undertaken using a gas-fired furnace, of the type shown in Figure 2.1.

Initially, fire resistance tests were undertaken on columns made with two different aggregates, i.e. Ham River Gravel (max. size 10mm) and Aglite expanded clay (max. size 12mm). The concrete had water/cement ratios of 0.5 and 0.6 respectively and were tested at ages ranging from 5 to 30 weeks. The columns were tested under a variety of different levels of load.

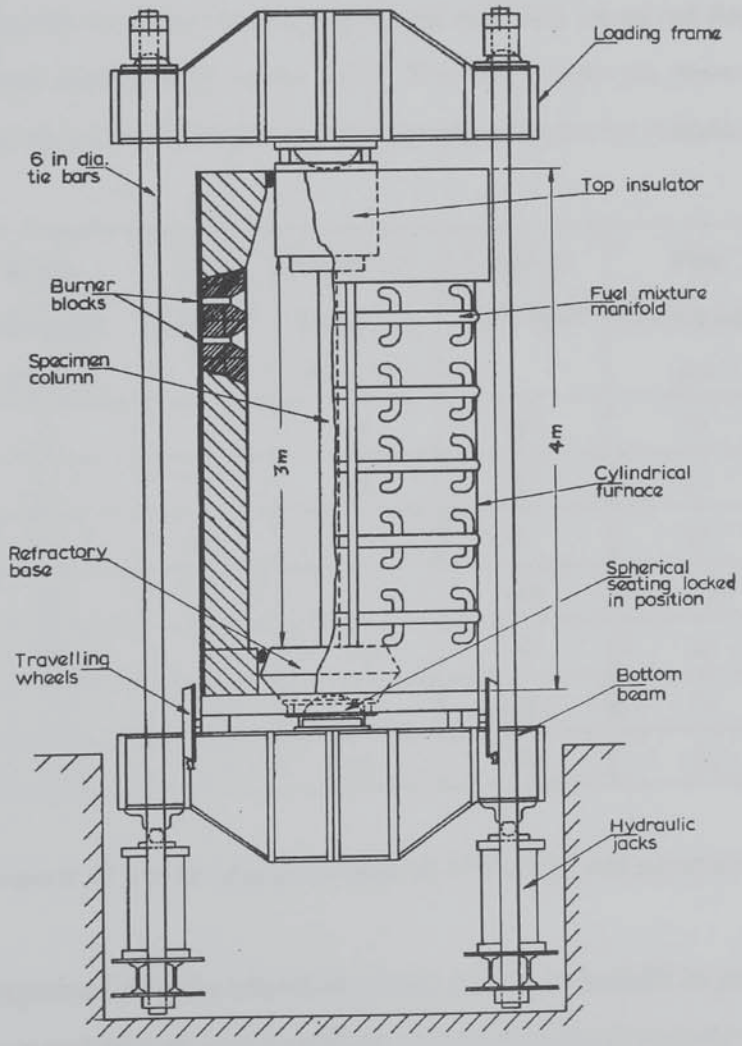

Figure 2.1. Furnace for fire resistance testing of columns

The results of these early tests showed that columns of relatively small cross-sectional area could achieve fire resistance ratings of over 1 hour by reducing the applied load to some 80% of its ultimate load capacity. One of the principal reasons for the surprisingly good performances observed was the absence of spalling with both the Gravel and Aglite concrete columns. It had been planned to develop the test programme further to establish a definite relationship between fire resistance and applied load, but staffing difficulties forced the work to be postponed for a period of five years.

2.2.2 FURTHER FIRE RESISTANCE TESTS (1969-1972)

When the experimental programme was reactivated in 1969, a number of the 5 year old 150mm square columns were tested in the furnace. The performance of the concrete columns had deteriorated significantly over the intervening period and their observed fire resistance ratings were reduced in some instances by up to 50%. The test results are shown in Table 2.1 and include two tests carried out on 31 N/mm^2 gravel concrete columns by Ashton and Davey (1953).

Aggregate Type	**Cube Strength** (N/mm^2)	**Age** (months)	**Moisture Content** (% by wt.)	**Load** (% of capacity)	**Fire Resistance** (min)	**Spalling**
Gravel	31	9	4.8	100	55	none
Gravel	31	9	4.8	80	77	none
Gravel	29	12	4.6	85	69	none
Gravel	28	24	4.3	100	62	none
Gravel	37	60	2.0	50	46	yes (26 min)
Gravel	32	60	2.0	100	21	yes (15 min)
Aglite	37	60	2.0	100	28	yes (12 min)

Table 2.1. Variation of fire resistance ratings of 150 x 150 mm concrete columns with age

Malhotra (1970) explained that the principal reason for the reduction in performance since the 1964 tests was the occurrence of severe spalling. Large pieces of concrete were detached from the arrises and in some cases the process was accompanied by explosive sounds. Of particular concern was the fact that the concrete made with Aglite was observed to spall explosively after

just 12 minutes heating. The data in Table 2.1 suggest that concrete with lower moisture contents were more susceptible to spalling. However, the concrete columns that were observed to spall were relatively old and it is unclear whether their propensity to spalling was related to moisture content or some other age effect, such as reduced ductility. The influence of spalling on fire resistance failure may also have been exacerbated by secondary effects such as change in slenderness ratios or the introduction of eccentricity to the column by spalling on one side.

The only variable to change between 1964 and 1969 was the age of the concrete specimens. The implications of such findings could have had a serious impact on fire resistance testing and some immediate experiments were put in hand to quantify the scope of the problem. The first of these involved testing of a 300 x 300 mm columns to confirm the significance of age on larger columns. Further experiments involved artificially raising the moisture content at the column's surface by soaking some 150 x 150 mm columns under water for 8 hours. These tests also demonstrated similarly poor performance as had been found in the rest of the series.

As has been previously discussed in Chapter 1, Morris (1972, personal communication) found that the time to spalling was important in determing the eventual fire resistance of 150 x 150 mm concrete columns. He observed a linear relationship between time to spalling and fire resistance with fire resistance failure following the onset of spalling by some 5 to 8 minutes.

Morris found a relationship, shown in Figure 2.2, between the level of load applied to a column and its susceptibility to spalling at its arrises. Spalling occured earlier in tests where the columns had high levels of load applied. He suggested that the relationship was due to the restraining effects that load has on the thermal expansion of the column. This explanation is corroborated by the data shown in Figure 2.3, which shows the relationship between expansion of a column after 30 minutes exposure to BS 476:Part 8:1972 heating and its time to spalling. These data clearly show that columns are less susceptible to spalling when free of restraint.

Fire resistance tests were also undertaken on concrete columns made of different aggregates, namely Limestone, Lytag and Aglite. With the exception of the 5 year old Aglite concrete (which had a relatively high imposed load), none of the columns spalled. Limestone concrete became significantly weak at the arrises and was easily removed by hand on cooling. The reduction in susceptibility to spalling may be explained by the reduced thermal expansions

recorded and reference to the relationship given in Figure 2.3. Gravel aggregate concrete has a coefficient of expansion in the order of 4 times that of its Light-weight or Limestone counterparts.

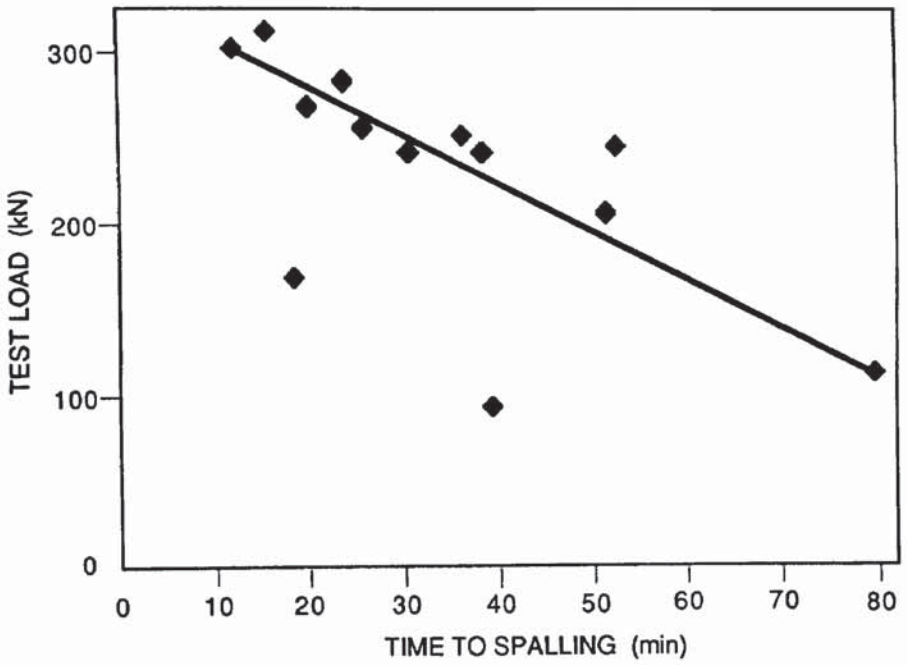

Figure 2.2. Effect of load on time to spalling

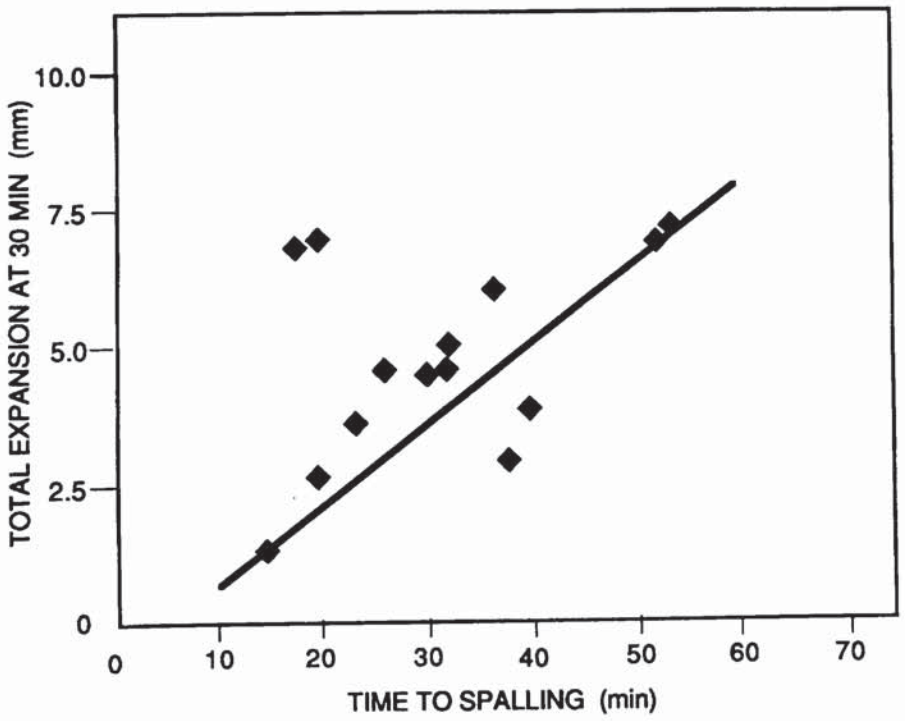

Figure 2.3. Effect of total thermal expansion on time to spalling

Morris examined the effectiveness of a range of measures designed to alleviate spalling. These measures included air-entrainment, chamferred arrises, supplementary reinforcement and protection with 6 mm glass reinforced cement (GRC) sheaths. The performance of columns including such measures was compared to that of a reference Gravel aggregate concrete. All concretes had a uniform cube strength of approximately 27 N/mm^2 and were tested 12 months after casting.

The results are given in Table 2.2 below. It is interesting to note that the control Gravel concrete column spalled later than a similar concrete column with chamferred edges. The only difference between these specimens apart from geometry was the fact that the chamferred specimen was made of 38 N/mm^2 concrete. This suggests that spalling is more likely amongst higher strength concretes and that a chamferred profile is not sufficient in itself as a measure to prevent spalling. Morris found that only glass reinforced cement sheaths offer genuine protection from spalling. Air-entrainment offered some slight reduction in susceptibility to spalling, but offered little increase in absolute fire resistance terms. Supplementary reinforcement protected concrete columns from the effects of spalling, but not from the phenomenon itself.

Concrete Details	**Fire Resistance** (min)	**Time to spalling** (min)
Control Gravel	47	41
Air-entrained	48	45
Chamferred arrises	24	18
Supplementary reinforcement	54	38
Glass reinforced cement	80	none

Table 2.2. Effectiveness of measures to alleviate spalling (after Morris, 1972 personal communication)

2.3 C.I.B. INTERNATIONAL SURVEY

In 1970, the Conseil International du Bâtiment (C.I.B.) Working Group W14 undertook a survey of 13 national fire resistance testing centres to ascertain their experiences regarding the spalling of concrete in fires and the results documented by Malhotra (1972).

Most of the laboratories questioned had encountered spalling to some extent, generally within the first 30 minutes of the standard fire resistance test. In other respects, however, their experiences were more diverse. A range of factors were suggested that might have an important influence on the occurrence of spalling;

(i)	nature of the aggregate	(v)	free moisture
(ii)	size of the aggregate	(vi)	restraint to thermal expansion
(iii)	density of the concrete	(vii)	compressive stress
(iv)	age of the concrete		

Different countries attached different levels of importance to each of the above parameters. The majority of laboratories considered the nature of the aggregate, the amount of free moisture and restraint to thermal expansion as the factors of primary importance. Concrete members constructed using siliceous aggregates were generally regarded as being more susceptible to spalling than those concretes containing calcareous or lightweight aggregates. In the United States, spalling was considered to be a relatively rare phenomenon. This could well be due to the existence of pre-test conditioning requirements in American fire test standards, which impose limits on the free moisture content permitted in concrete prior to the commencement of fire resistance tests.

2.4 ACADEMIC STUDIES (1971 - 1979)

2.4.1 DOUGILL, IMPERIAL COLLEGE, LONDON, 1971

In a study for his PhD Thesis at Imperial college, Dougill (1971) subjected concrete slabs, of a range of different compositions, to the BS 476:Part 1: 1953 heating regime in the gas-fired furnaces of the Fire Research Station, Borehamwood. The objective of his tests was to observe the temperature development and occurrence of spalling amongst different concretes. The test specimens were 3000 x 300 x 100 mm thick concrete planks, made with Thames Valley Gravel aggregate, of maximum size 12 mm. The concrete specimens were tested at ages ranging from 3 to 6 months and at cube strengths ranging from 23 to 66 N/mm^2.

Dougill found that regardless of the concrete mix details, the temperature profiles recorded in the concrete were remarkably consistent. Dougill did not encounter any explosive spalling or indeed any other form of surface deterioration, such as aggregate splitting.

2.4.2 MEYER-OTTENS, UNIVERSITY OF BRAUNSCHWEIG, GERMANY, 1972

Meyer-Ottens (1972) undertook the largest single experimental investigation into the causes of spalling for his PhD thesis at the Technical University of Braunschweig. His wide ranging test programme examined the performance of various concrete elements when subjected to heat in a gas-fired furnace. Meyer-Ottens investigated the effect of many parameters on the susceptibility of concrete to spalling including; aggregate type, concrete quality, thermal stresses, amount and arrangement of reinforcement, moisture content, section shape and applied compressive stress.

Meyer-Ottens examined both conventionally reinforced and prestressed concrete members. The behaviour of 3 different concrete mixes (with cube strengths of 22.5, 45 and 60 N/mm^2) was studied. An array of concrete elements, including beams and slabs, were subjected to 3 different heating regimes. Compressive stresses were induced in the concrete specimens by application of dead weight, external loading or prestressing.

The programme of tests undertaken by Meyer-Ottens was of immense significance to the design of concrete members against fire and the design rules which he developed are used to this day in many codes of practice (Comité Euro-International du Beton 1988, Schneider 1985, ENV 1992-1-2:1994). It is, thus, worthwhile reviewing his results in some detail.

Meyer-Ottens investigated the influence of cross-section dimensions and reinforcement detailing and concluded that thin sections with closely spaced reinforcement were more likely to spall than thick sections, with little or no reinforcement. The tendency seemed to be more pronounced for prestressed concrete specimens.

Meyer-Ottens found the rate of heating to be important. He used a gas-fired furnace to provide 3 different heating regimes as shown in Figure 2.4. He observed that in some cases spalling occurred on exposure to heating regimes II and III, but not regime I, which is similar to the BS 476:Part 20:1987.

Figure 2.4 Heating regimes used by Meyer-Ottens (1972)

Meyer-Ottens compared the susceptibility to spalling of concretes made of siliceous and calcareous aggregates. He found little difference in their behaviour and concluded that aggregate type was not important in determining susceptibility to spalling. However, neither concrete spalled in the particular situation which he tested, i.e. simply supported slabs, moisture contents 2.7 to 5.3% exposed to heating regimes I and II. It is unclear whether he would have reached the same conclusions had spalling occurred.

Although, in general, Meyer-Ottens tested concrete under heating from both sides (3 sides in the case of beams), he conducted some tests under single sided exposure. He concluded that spalling was less likely under such conditions and occurred only at higher rates of heating and with the provision of reinforcement in the central region of the slab. He explained the influence of the reinforcement in terms of its prevention of tensile cracking which allowed higher compression stresses to develop at the heated surface.

One of the most important conclusions of the work was that an increase in compressive stress, either by reduction in section size or an increase in loading, encourages explosive spalling. Meyer-Ottens produced a nomogram for the prediction of spalling, which considers the member thickness and the applied compressive stress. The nomogram, shown in Figure 2.5, is widely used in codes of practice for the fire design of concrete structures, e.g. ENV 1992-1-2: 1994.

Figure 2.5 Meyer-Ottens' (1972) design nomogram for the prediction of explosive spalling

Figure 2.5 was derived from tests carried out on concrete specimens with a cube strength of 45 N/mm^2. Sertmehemetoglu (1977) increased its applicability by plotting the spalling envelope of member thickness against the ratio of the applied compressive stresses to compressive strength, as presented in Figure 2.6. It is important to bear in mind that the compressive stresses considered in this nomogram were generated by pre-stressing as opposed to some form of end restraint.

Meyer-Ottens' nomogram clearly suggests that there are limiting combinations of compressive stress and specimen thickness, beyond which spalling is a certainty. However, Meyer-Ottens himself, actually discredited this very premise in his investigation on the influence of moisture content. Studying the performance of concretes with a wide range of moisture contents (from 0.5 to 7 % moisture by weight), he found that regardless of the stresses imposed or heating rates applied that concrete members with moisture contents less than 3.3% did not spall.

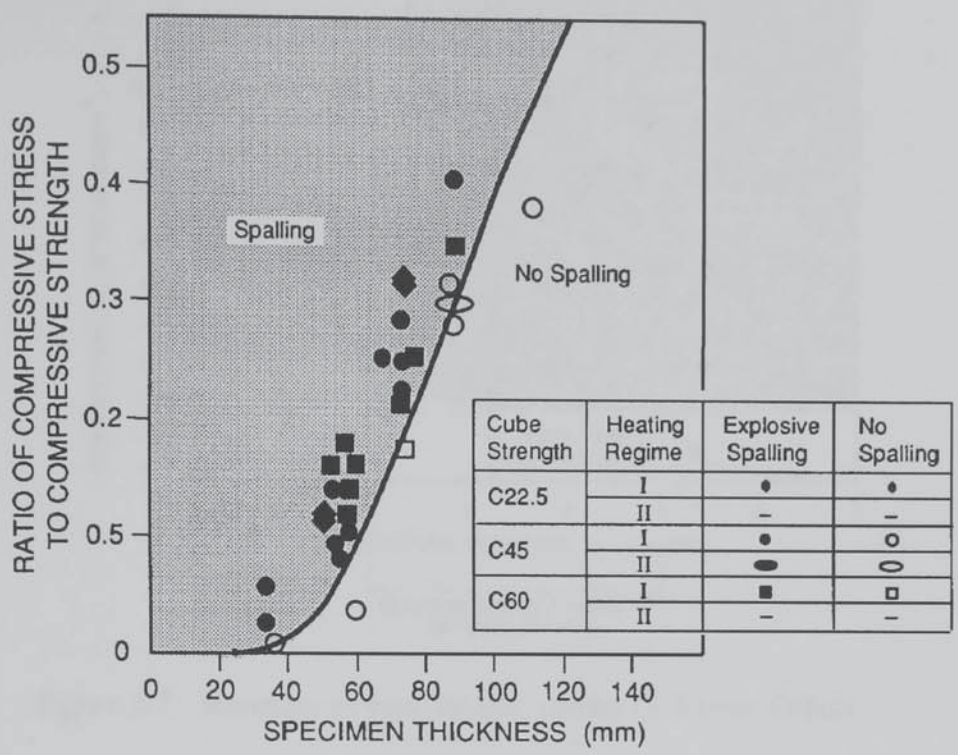

Figure 2.6 Improved design chart for predicting spalling (after Sertmehemetoglu, 1977)

This finding was largely responsible for the perception widely held since that there is a minimum moisture threshold beneath which spalling cannot occur. However, if such a perception is true, the experience of Morris (1972, personal communication) reported in Table2.1 suggests that the threshold will depend on the concrete mix, the load imposed and the heating conditions. The role of moisture content in determining the susceptibility of concrete to spalling will be examined fully later in this Thesis.

Without the application of external stresses, concretes with moisture contents between 3.3 and 7% only spalled if they were heavily reinforced or if they were of relatively thin cross-sectional width (less than 80 mm). On the introduction of relatively slight compressive stresses (say 2 N/mm^2) spalling occurred with increased regularity depending on other material parameters. Meyer-Ottens' results were elegantly summarised by Sertmehemetoglu (1977) in a design chart which is reproduced here as Figure 2.7.

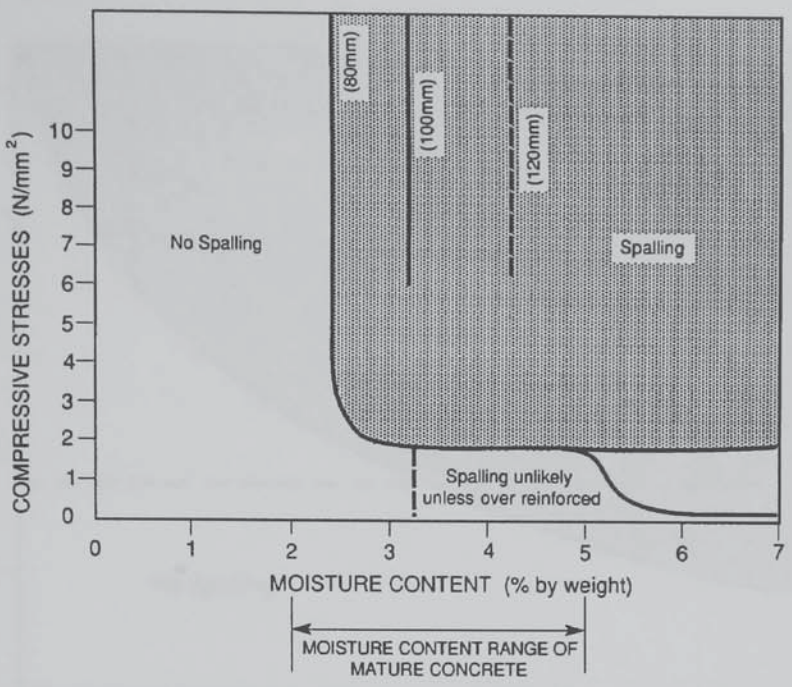

Figure 2.7 Summary of experimental results of Meyer-Ottens

The principal conclusion offered from Meyer-Ottens' monumental investigation, is that combinations of compressive stresses (above 2 N/mm^2) and moisture contents (above 3.3% by weight) make the occurrence of spalling likely. However, under the heating regimes considered, neither high compressive stresses nor high moisture contents were sufficient in isolation to cause spalling.

2.4.3 CHRISTIAANSE *et al.*, HOLLAND, 1972

A Dutch research group, led by Christiaanse *et al.* (1972), studied the behaviour of 3 week old prestressed lightweight concrete double T-beams. Like Meyer-Ottens (1972), they concluded that the occurrence of spalling in heated concrete was related to a combination of compressive stresses and moisture content. They produced a chart (given as Figure 2.8) for the design of prestressed concrete against spalling which gives the relationship between levels of prestress and moisture content and their combinations that are likely to cause spalling. Christiaanse *et al.* encountered spalling at similar moisture contents and stresses to Meyer-Ottens and concluded that spalling was not possible for concretes with moisture contents less than 4%.

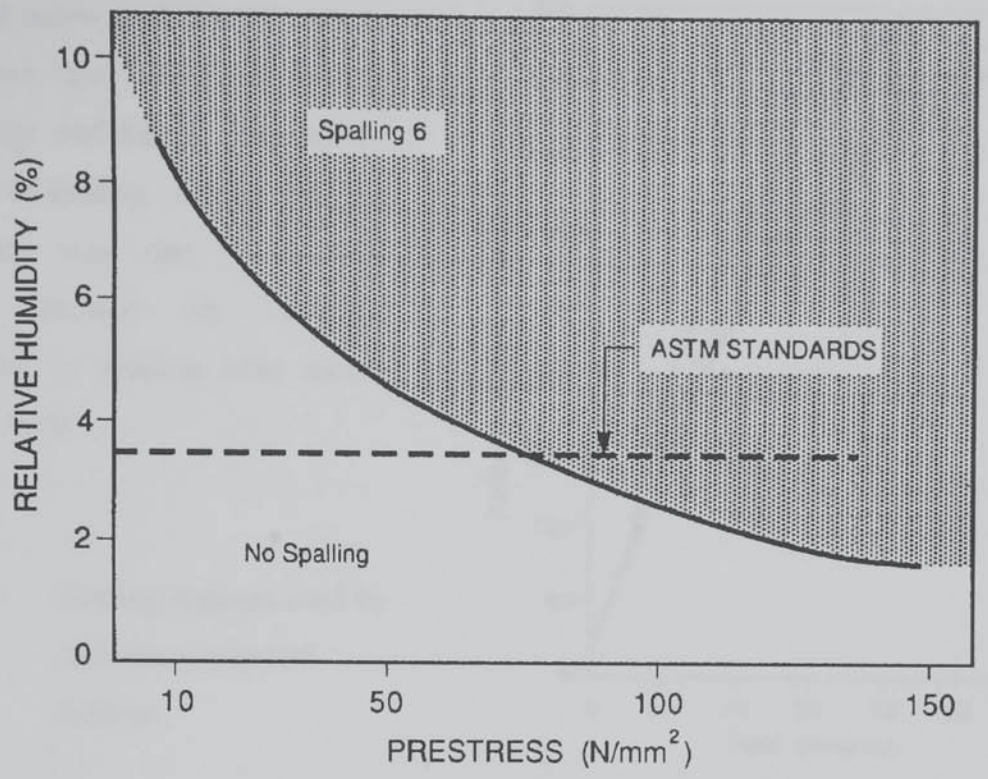

Figure 2.8 Safe spalling envelope (after Christiaanse *et al.*, 1972)

2.4.4 AKHTARUZZAMAN AND SULLIVAN, IMPERIAL COLLEGE, LONDON, 1970

Akhtaruzzaman and Sullivan (1970) studied the influence of curing, age and rate of heating on the weight loss of specimen concrete beams. The loss in weight was recorded as being due to evaporation of water from within the specimen and/or the loss of concrete due to spalling.

Their tests revealed that evaporation takes place in two distinct phases at temperatures of approximately 110 and 175°C. Heating 50 x 75 x 840 mm long beam specimens in accordance with relatively moderate heating regimes shown in Figure 2.9, Akhtarruzaman and Sullivan encountered explosive spalling. The spalling occurred when the concrete temperature was in the range of 165 to 200°C, i.e. during the second stage of moisture evaporation from the concrete's gel pores.

Akhtarruzaman and Sullivan's results, summarised below in Table 2.3, clearly demonstrated the effect of curing, specimen age and heating rate on the occurrence of spalling. One of their key observations was that water-cured specimens showed an increased susceptibility to spalling over moist-cured specimens.

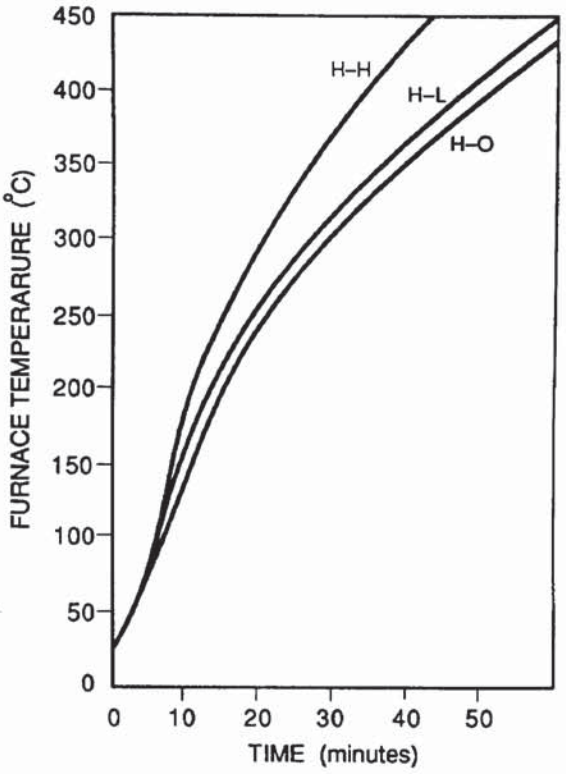

Figure 2.9 Heating regimes used by Akhtarruzaman and Sullivan

Heating Rate	Curing	Upper Age limit (days)	Furnace temp. (°C)	Concrete temp. (°C)
H - H	under water	28	380	166
	under sacking	10	421	198
H - L	under water	10	390	175
	under sacking	3	378	165
H - O	under water	18	380	166
	under sacking	5	378	165

Table 2.3 Summary of the test results of Akhtarruzaman and Sullivan (1970)

They developed a model of spalling which considers the concrete as a hollow sphere, under an internal pressure due to expanding water vapour. The model, which will be discussed in detail in Chapter 3, suggested that spalling was possible only for concretes younger than a certain critical age. Beyond this critical age, moisture contents were too low to allow development of the pressures necessary for spalling. The critical age was considered to depend on the curing conditions and the rate of heating.

2.4.5 ZHUKOV, RUSSIA, 1975

Zhukov (1975) developed a theory of spalling based on the behaviour of heated concrete as observed in a series of 35 tests on reinforced concrete slabs. Zhukov observed that dense concretes showed an increased susceptibility to spalling over normal weight concretes. He also observed an increased tendency of concretes with higher moisture contents to spall.

One of Zhukov's most important findings was the observation that concrete with low water to cement ratios (and thus having higher strengths and lower porosities) showed an increased susceptibility towards spalling than concretes with a higher w/c ratio. This observation has a significant impact on many of the theoretical explanations of the phenomenon of spalling discussed in Chapter 3.

2.4.6 SERTMEHEMETOGLU, KINGS COLLEGE, LONDON, 1977

During an extensive series of tests, Sertmehemetoglu (1977) used a diaphragm and pressure transducer to measure the pore pressures generated on the unexposed face of a heated concrete specimen. The concrete was heated using a blow torch. Surface temperatures were not recorded but would appear to be about 700°C after 30 minutes. The maximum pore pressure recorded in all of his many tests was 2.1 N/mm^2. This is less than the tensile strength of the concrete, even at elevated temperatures, which was estimated as being around 3 N/mm^2.

2.4.7 COPIER, HOLLAND, 1979

Copier heated prism and slab elements in a furnace. He varied the compressive stress, the reinforcement and the moisture content of both normal and lightweight concretes. Specimens were heated from both one and both sides. His tests were essentially an extension of the earlier work of Meyer-Ottens (1972). Copier produced a graphical representation of the results of fire tests, which is reproduced here as Figure 2.10.

Figure 2.10. Experimental results of Copier (1979)

Copier concluded that moisture content is the most important factor in the determination of the likelihood of spalling. Other important factors include the presence of reinforcement and compressive stress. The actual amount of reinforcement or the magnitude of the stresses are of lesser importance.

2.5 MORE RECENT INVESTIGATIONS

2.5.1 HERTZ, DENMARK, 1984

While studying the performance of concrete made with silica-fume admixture, Hertz encountered violent explosion of his specimens. He was testing 100 x 200 mm concrete cylinders subject to a heating rate of 1°C per minute. The concrete was very dense (almost 2700 kg/m^3) and had compressive strengths of between 60 and 180 N/mm^2. The moisture content of the cylinders was approximately 3.2 % by weight.

The explosions blew the cylinder to pieces, with maximum particle sizes of less than one tenth

of the original volume of the cylinder. The first cylinder to explode did so at an oven temperature of 350°C. This cylinder had an expected compressive strength of 180 N/mm^2. Cylinders of lesser strength did not explode until higher temperatures were reached. Reduction of cylinder size by either 50 or 75% eliminated the explosions. Addition of steel fibre mesh reinforcement did not eliminate the explosions.

2.5.2 SHIRLEY *et al.*, UNITED STATES, 1987

Shirley *et al.* (1987) conducted a number of ISO 834:1987 standard fire resistance tests on high strength (max. 117 N/mm^2) concrete slabs. The slabs were tested for up to 4 hours, with tests taking place some 90 days after casting. The relative humidity within the specimens was 80%.

None of the slabs showed any surface distress or damage. The absence of spalling may be due to the small size of the slab specimens, i.e. 900 x 900 x 104 mm deep.

2.5.3 SANJAYAN AND STOCKS, AUSTRALIA, 1993

Sanjayan and Stocks (1993) compared the performance of ordinary strength (27 N/mm^2) and high strength (105 N/mm^2) in the standard ISO 834:1987 fire resistance test. Their test specimens were 2500 x 1200 mm concrete T-beams. They were tested 105 days after casting, at which stage the moisture contents were 4.0%, by weight, for the normal strength concrete and 4.6%, by weight, for the high strength concrete.

The normal strength concrete beam suffered no damage during the fire test. The high strength concrete, on the other hand, suffered from severe explosive spalling 18 minutes into the test. Concrete from the flange of the beam was dislodged. The furnace temperature was 715°C. and the temperature of the concrete 25 mm beneath the surface was 128° C. Spalling continued to eject smaller pieces of concrete until 40 minutes into the test, at which stage the test ceased.

One interesting aside to the work of Sanjayan and Stocks was that the depth of cover to the steel reinforcement was varied over the length of the T-beam tested, with values of 25, 50 and 75 mm.

Spalling occurred in the area of the flange with 75mm cover. However, no firm conclusions may be drawn regarding the importance of cover depth, as spalling did not take place on the web, which also had 75mm cover. The absence of spalling could be due to increased cracking on the lower face of the web due to deformation.

2.5.4 JUMPANNEN, FINLAND, 1989

Jumpannen conducted an experimental investigation of the properties of high strength concrete at elevated temperatures. The concrete studied was made with quartzite aggregates and had compressive strengths ranging from 50 to 110 N/mm^2. The higher strength concretes showed a greater loss of strength at elevated temperature.

On heating cylindrical concrete specimens (8 mm diameter, 40 mm length) at 2°C per minute, no spalling took place. On heating at 32° C per minute, only slight spalling occurred, probably a form of aggregate splitting. This was not changed by heating under load. However, increasing the specimen size (100 x 100 x 400 mm prisms) resulted in explosive spalling of all high strength specimens on heating under load.

Jumpannen also studied ultra-high strength concretes, with compressive strengths ranging from 190 to 240 N/mm^2. The concrete specimens were 40 x 40 x 160 mm prisms and had moisture contents ranging from 2.3 to 3.0 % (by weight). On exposure to ISO 834:1987 standard heating conditions, the concretes exploded after 7 minutes, i.e. surface temperatures of 310°C. Interestingly, the concrete continued exploding, so that after 8 minutes of testing the specimen was completely destroyed. Reducing the rate of heating to less than 1° C per minute alleviated spalling.

Spalling, when it occurred, always did so in the temperature range 300 to 350°C, regardless of the rate of heating. This is a similar phenomenom to that observed by Akhtarruzaman and Sullivan (1970), who observed that spalling when it took place, did so at temperatures of 375 to 425°C.

2.6 OVERALL CONCLUSIONS

It is clear from the preceding review of many years of experimental investigation into the behaviour of concrete at elevated temperature, that there are many discrepancies and contradictions in observed effects. For example, the influence of age of a concrete on its susceptibility to spalling has been subject of conflicting reports. Malhotra (1972) suggested that ageing increased the susceptibility of concretes to spalling and presented sound evidence to this effect. However, Christiaanse *et al.* (1972), Akhtarruzaman and Sullivan (1970) and Copier (1979) presented experimental evidence to suggest that concrete reaches a critical age, after which it will not spall.

It is likely that many of the apparent contradictions associated with spalling are due to the variety of definitions and classifications of spalling that have been used over the years. Explosive spalling, surface spalling and destructive spalling are terms which have been used by various researchers, for the same mechanism. It is quite possible, even likely, that there are a number of different mechanisms of spalling. The conditions favourable to one mechanism may not necessarily suit another. The lack of clear definition of spalling types, thus, may be responsible for some of the apparently contradictory behaviour described.

After reviewing his test records in some detail, it is considered more than likely that Morris (1972) was referring to a form of sloughing-off, when he suggested that age increased susceptibility to spalling, thus explaining the contradiction with Meyer-Ottens (1972). However, experience from full-scale fire tests carried out by the Fire Research Station by Bullock (1990, personal communication) indicates that concrete held in an indoor environment for over 20 years old is capable of violent explosive spalling.

Despite the apparent contradictions, it is clear that any mechanism suggested to explain the explosive spalling of concrete must account for the following observed behaviour;

(i) Given suitable environmental conditions, in terms of load and thermal attack, all concrete can display the capacity for spalling (Morris, 1972, personal commmunication)

(ii) Thinner concrete sections are more susceptible to spalling than thick sections (Ashton and

Davey,1953; Hanneman and Thomas, 1959; Meyer-Ottens, 1972)

(iii) Applied loads increase the susceptibility of concrete members to spalling (Meyer-Ottens, 1972; Copier, 1979; Morris, 1972, personal communication)

(iv) Water-cured concrete specimens are particularly susceptible to spalling (Akhtarruzaman and Sullivan, 1970)

(v) High strength concrete has an increased susceptibility to spalling (Hertz, 1984; Sanjayan and Stocks, 1993; Jumpannen 1993)

(vi) Explosive spalling occurs within the first 40 minutes of heating to the standard BS 476:Part 8:1972 fire resistance testing regime (Malhotra, 1972). Spalling has been observed for concretes exposed to heating environments of 350 to 715° C.

(vii) For a given set of conditions, explosive spalling is less likely for concretes with moisture contents less than 3% by weight (Meyer-Ottens, 1972; Christiaanse *et al.*, 1972)

(viii) The expansion of a concrete gives a measure of its likehood to spalling. Concrete that has its thermal expansion restrained is more likely to spall. By corollary, concrete with a low thermal expansion is less likely to spall (Morris, 1972, personal communication)

(ix) The rate of heating influences the occurrence of spalling. However, when spalling does occur it does so within a consistent temperature range, regardless of heating rate, (Jumpannen, 1993; Akhtarruzaman and Sullivan, 1970).

CHAPTER 3. THEORIES TO EXPLAIN EXPLOSIVE SPALLING OF CONCRETE IN FIRES

3.1 INTRODUCTION

Following the early experimental work of Gary (1916), Endell (1929) carried out tests on the change of length and structure of concrete made with a variety of aggregates. He proposed that spalling could be attributed to the sudden volume change of the quartzitic components of aggregates at elevated temperatures. Bottke (1931) also attributed spalling to the bursting effect of temperature induced stresses which were a consequence of differential thermal expansion over the cross-section of heated concrete. He suggested that such bursting stresses were exacerbated by differential expansion between the concrete and reinforcing steel.

Hassenjaeger (1935), in his PhD thesis to the University of Braunschweig, Germany, summarised the experimental data available at that time and concluded that spalling could be explained by;

(i) rapid heating of concrete
(ii) thermally induced stresses exceeding the tensile strength
(iii) sudden changes in the structure and volume of the aggregate
(iv) bursting pressures caused by the liberation of water vapour and gases from the aggregates and the hardened cement paste.

It may be seen that the reasons suggested by Hassenjaeger to explain explosive spalling may be grouped into two categories, i.e. the effects of thermal stresses (i - iii) and the effects of high pore pressures (iv) within the concrete. The mechanisms of spalling proposed since his pioneering work in 1935 have generally fallen into one or other of these two categories. Thus it is convenient to discuss more recent work under the two headings;

(i) spalling due to thermal stresses
(ii) spalling due to pore pressures

3.2 SPALLING DUE TO THERMAL STRESSES

3.2.1 SAITO (1965)

Saito (1965) considered spalling to be a manifestation of compression failure at the heated face of the concrete. He proposed that spalling occurred when the surface compressive stresses generated by a non-uniform temperature distribution across the concrete section exceeded the compressive strength of the concrete.

Saito suggested that thermal stresses are generated within the cross-section of a heated concrete specimen due to the formation of temperature gradients. These temperature gradients will be influenced by the nature of heating at the concrete surface, the thermal properties of the concrete itself and, of course, time. Figure 3.1 gives the typical profile of a temperature distribution within a concrete slab, heated for 60 minutes in accordance with the BS 476:Part 20:1987 standard heating regime. Every point within the cross-section will be subject to a thermal deformation, which is proportional to its temperature. Saito suggested that the thermal deformation $\alpha\theta$, consisted of a longitudinal thermal expansion δ, a curvature $1/\rho$, and a thermal strain ϵ, as illustrated in Figure 3.2.

The temperature profile across the concrete section induces compressive stresses close to the heated surface, due to restrained thermal deformation. These stresses are counterbalanced across the section by tensile stresses in the cooler interior regions. Compressive stresses are generated at both the heated and unexposed faces, while tensile stresses develop in the central depths of the section. Saito suggested that spalling was a result of the surface compressive stresses exceeding the strength of the concrete.

In general, the strength of concrete is reduced at elevated temperatures, thus increasing its susceptibility to spalling. Overall, however, the susceptibility of a concrete to spalling is reduced with continued heating because of the reduction of its temperature gradients. Saito used elastic analysis to calculate the maximum compressive stresses that may be developed at the surface of a heated concrete. He predicted that spalling takes place when the thermally induced compressive stresses exceed the compressive strength of the concrete.

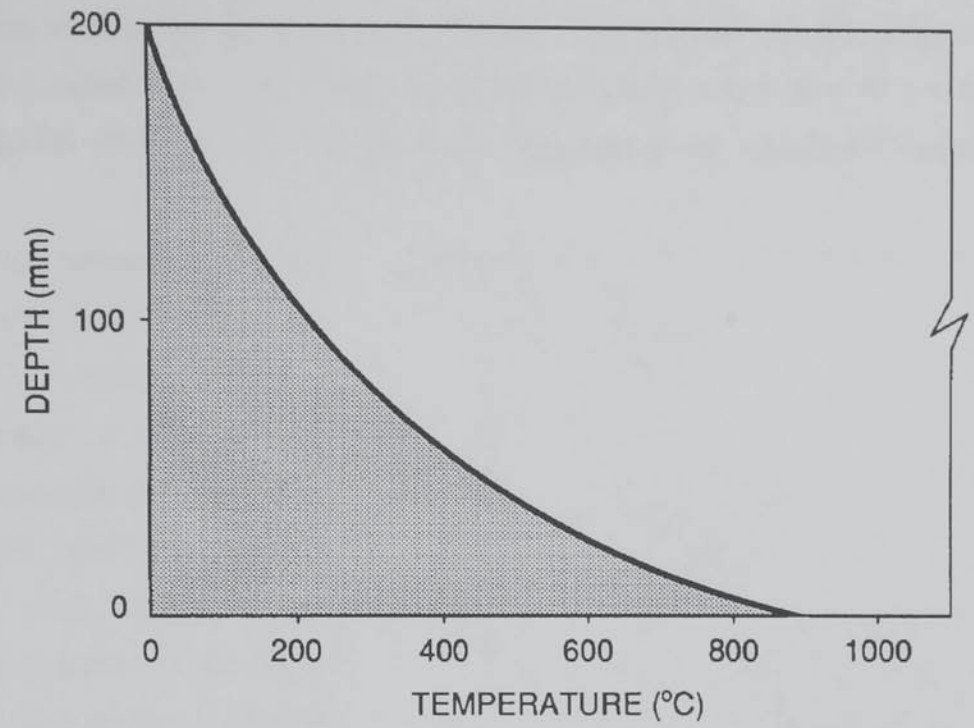

Figure 3.1 Typical temperature distribution in concrete heated for 60 minutes to BS476 Part 20.1985

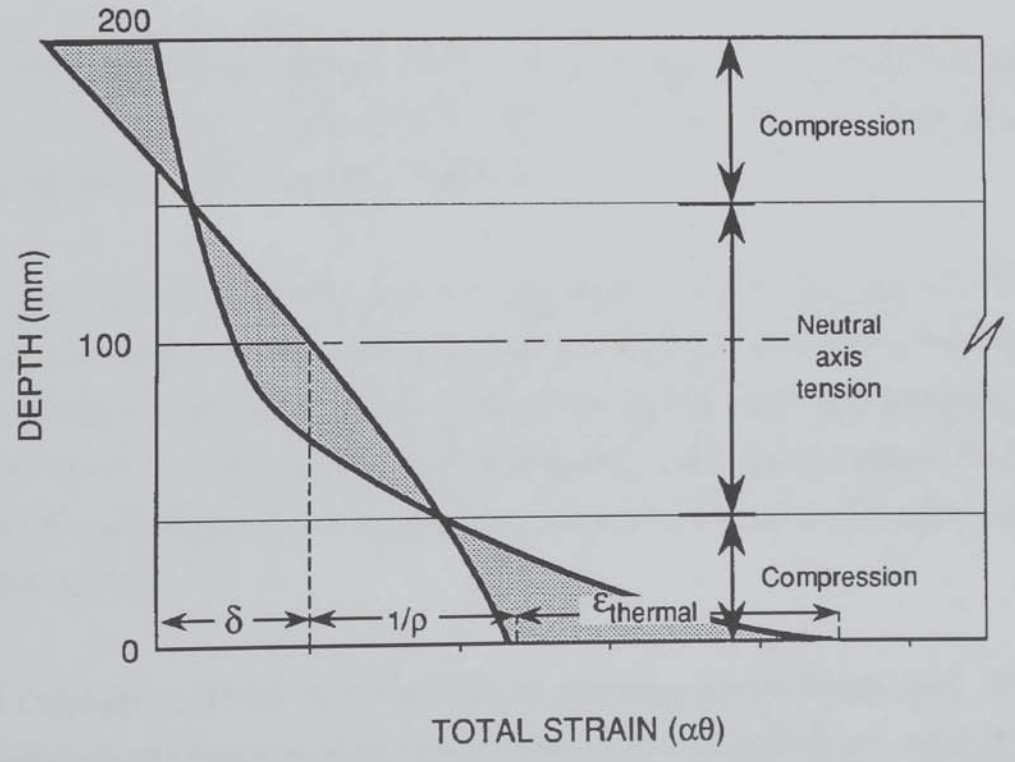

Figure 3.2 Resulting thermal strain in heated concrete

As the temperature gradients change with time, so do the thermal stresses. Thus, Saito predicted that the maximum surface stresses would increase with time, up to some point after heating has started, from whence they would begin to decrease. His prediction may be explained by study of Figure 3.3, which shows the change of temperature gradient with time for a concrete slab heated to the BS 476:Part 20:1987 standard heating regime (Saito would have used similar).

The maximum temperature gradient occurs some depth beneath the heated surface, typically within the first 30 minutes of test, although both time and depth are functions of the thermal properties of the concrete. Saito suggested that should the concrete be capable of sustaining the maximum thermal stress, then spalling will not occur.

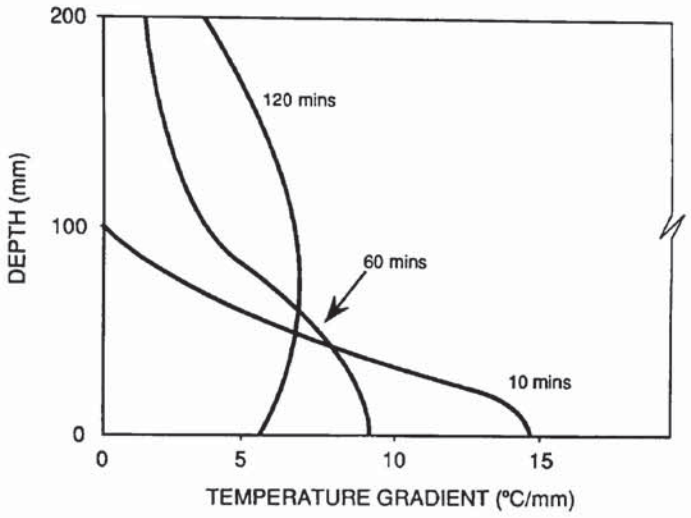

Figure 3.3 Variation of temperature gradient with depth at different times during heating

Thus, his theory suggested that spalling would take place within the first 30 minutes of a standard BS 476:Part 20:1987 (or equivalent) fire resistance test. This prediction correlates with the experimental observations discussed in Chapter 2.

In some cases, the surface compression may be augmented by load or prestress. These load stresses are super-imposed upon any thermal stresses that may be developed on heating. Thus, imposition of load or prestress reduces the magnitude of the thermal stresses necessary to cause compressive failure at the heated surface. In this manner Saito's theory explained the observed relationship between application of compressive stresses (load or pre-stress) and the increased likelihood of spalling.

This fact had been confirmed in several different test programmes (Nisugi *et al.*,1959; Ehm 1966). Saito's theory appeared to be further validated by some subsequent work of England (1971). England demonstrated that the time to the onset of spalling could be delayed by

imposition of load, due to its reduction of the compressive stress in the extreme fibres.

Saito explained the increased susceptibility of concretes with a high moisture content to spalling solely in terms of increased temperature gradients. Particularly severe thermal gradients may be set in concretes with high moisture contents due to the absorption of applied heat by the water vaporising in the central core without an increase in temperature. However, it is more likely that the presence of moisture will increase the thermal conductivity of the concrete, thus reducing the temperature gradients in the early stages of heating.

Ehm (1966) endorsed Saito's theory but also suggested that bursting stresses created by heated steel reinforcement had an important role. In retrospect, this seems unlikely to be the case, as the bursting stresses created by expanding steel, later quantified by Dougill (1971), generally have a relatively small magnitude.

Rickenstorf (1970) regarded spalling as a particular form of surface cracking. He described surface spalling cracks as cleavage cracks. Whereas moisture has no role in typical surface crack dynamics, it is dominant in the formation of cleavage cracks. He suggested that spalling was due to local stresses at discontinuities such as cracks, voids and poorly compacted zones exceeding the tensile strength of the concrete.

One serious shortcoming of Saito's theory is its inability to explain the reduced occurrence of spalling in thicker sections. As illustrated in Figure 3.4, Saito's theory suggested the opposite should be the case as compressive stresses in thick members will always be larger than those in thinner members. Subsequently, experiments have shown that spalling is less likely to occur in thicker members (Meyer-Ottens, 1972). This shortcoming was later addressed by Dougill (1972a).

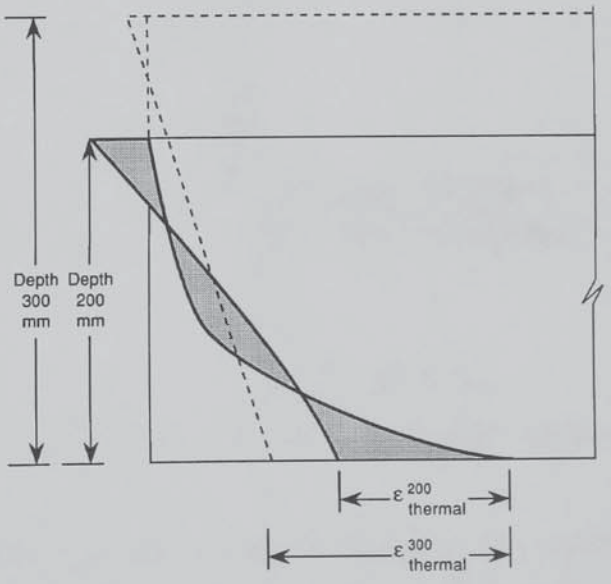

Figure3.4 Increased susceptibility of thicker sections to spalling

3.2.2 DOUGILL (1972)

Dougill (1972a) recognised the usefulness of Saito's theory and enhanced it by incorporating a more realistic view of the mode of failure. In doing so, Dougill was able to use the same basic theory to explain the observed behaviour of thick sections.

Dougill suggested that heating a plane concrete panel was directly analogous to subjecting it to a BS 1881:Part 4:1970 tensile splitting test in a stiff testing machine. The test is designed to assess the tensile strength of a concrete by subjecting it to a compressive loading. Shortly, after heating has commenced, the interior of the panel will be in tension, with the material near the surfaces in compression. Dougill realised that such a stress distribution is similar to that encountered during a splitting test. Figure 3.5 shows the analogous stress distributions. The analogy is complicated by the fact that the relative size of each stress zone changes with time.

Figure 3.5 Analogous stress fields induced by heating and splitting forces (Dougill, 1972a)

Dougill suggested that explosive spalling in a fire is a similar mode of failure to that which occurs when concrete specimens fail violently on testing in a flexible testing machine at load levels only slightly greater than those corresponding to peak stress. One of the reasons for the sudden violent failure is the presence of a strain softening region in the stress-strain curve.

The stress-strain curve has a negative slope in this region. Hognestad *et al.* (1955) observed particularly sudden failure when the slope of the descending part of the stress-strain curve equals the slope of the testing machine curve. It is possible that such a situation could exist between the cooler tensile zones of the section and the edge compression zones at some point after heating commences.

Dougill's model explains why thick members do not suffer the same instability as thinner members simply in terms of the proportions of stiffness across the section. The cooler zone provides stiff restraint to counterbalance surface stiffness losses to maintain the overall stiffness of the member. In terms of the testing machine analogy, thick members may be viewed as stiff testing machines.

Dougill's model predicts several observed characteristics of spalling. It explains how higher heating rates promote spalling by the fact that the rate of application of stress influences the shape of the descending branch of the stress-strain curve. Higher loading rates produce steeper slopes of strain-softening. The occurrence of spalling within the first 30 minutes of fire test was explained by several factors. Firstly, the thermal gradients have peaked. Secondly, with the passage of time, thermal creep will tend to relieve the stresses that have been developed. Finally, the slope of the descending branch of the stress-strain curve is reduced at elevated temperatures.

Dougill's theory may also explain the subsequently observed increased susceptibility of high strength concrete to spalling (Jumpannen, 1993). High strength concretes are more brittle and have a steeper descending characteristic. The same, however, applies to concretes made with lightweight aggregates which are not noted for their susceptibility to spalling.

3.2.3 CONCLUSIONS ON SPALLING DUE TO THERMAL STRESSES

Although, Dougill's theory is more realistic than Saito's (1965), it still does not explain several observed characteristics of spalling. It fails to explain the perceived role of moisture in spalling and the absence of spalling in concrete members with moisture contents less than 3%, as found later by Meyer-Ottens (1972). However, this may not necessarily be a limitation on his explanation as the effect of moisture on spalling is by no means certain.

In addition, tests by Akhtaruzzaman and Sullivan (1970) showed that spalling occurred much more frequently with water-cured rather than moist-cured concrete specimens. Water-cured specimens have more complete hydration at the surface and hence are better able to cope with any imposed thermal stresses. Dougill's theory, thus, would suggest that water-curing should reduce the likelihood of spalling, which is the opposite to that observed.

3.3 SPALLING DUE TO HIGH PORE PRESSURES

Many researchers have suggested that moisture content plays a significant role in the phenomenon of spalling. Several possible mechanisms have been advanced to explain the influence of moisture and are generally founded on the fundamental premise that on heating concrete, pressures are developed within its water-containing pores. These pore pressures impose bursting stresses on the concrete. A range of simple mechanisms has been proposed to explain the development of pore pressure in heated concrete and the resultant bursting stresses.

3.3.1 THEORY OF MOISTURE CLOG SPALLING

Shorter and Harmathy (1965) proposed that spalling was possible as a result of two completely different mechanisms. The first mechanism which they described as thermal spalling is a similar mechanism to that put forward by Saito (1965). However, they proposed that spalling may be the result of a completely different phenomenon called *"moisture clog"* spalling.

They explained that when a concrete slab is exposed to fire, desorption of its constituent moisture is initiated in a thin layer close to its heated surface. A major portion of the released vapours travel into the colder depths of the concrete, where they are cooled and condensed back to liquid. With further heating, the dry zone gradually gets thicker. In time, a fully saturated layer, which Harmathy called "*the moisture clog*" may develop some distance from the exposed face. A well defined front forms between the dry and the saturated layers. Further desorption may take place from the interfacial plane, causing the moisture clog in effect to migrate into the concrete. The model is illustrated in Figure 3.6.

Continued heating at the concrete's surface gives rise to the development of severe thermal gradients across the dry layer. When the temperature of the moisture clog reaches 100°C, the pore water vapourises and attempts to move into the cooler depths of the concrete section.

However, the water vapour leaving the moisture clog may be prevented from travelling to the cooler depths by the fact that the pores are saturated. Consequently, the vapour is acted upon by opposing forces of temperature and pressure gradients. The direction in which the vapour moves depends on the magnitude of each force. Thus, rate of heating and concrete permeability are vital parameters.

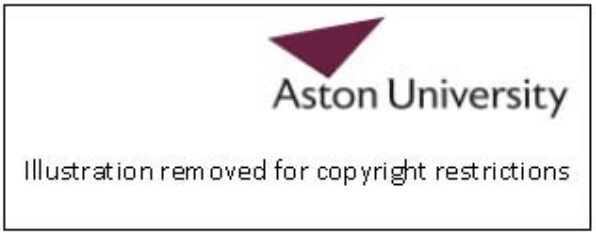

Figure 3.6 Shorter and Harmathy's (1965) model for spalling failure of concrete

As the temperature rises, the rate of heat flow increases through the dry layer. Assuming that the saturation and permeability of concrete are such that the water vapour cannot travel away from the heated surface, the vapour is forced across the dry layer against the thermal gradient. This

causes a build up of pore pressure. As the temperature rises, the pore pressures in the dry zone close to the moisture clog interface are built up, with vapours being trapped between the conflicting influences of high pressure and high temperature. Spalling is deemed to take place when the pore pressure exceeds the tensile strength of the concrete.

Shorter and Harmathy derived an expression for the likelihood of spalling, based on the model shown in Figure 3.6. They calculated the speed at which the moisture clog will travel into the slab under the action of a heat flux. They then predicted the speed at which the drying front moves into the slab under the action of the pressure gradient. They suggested that when the drying front moves faster than the moisture clog, pore pressures are generated at the interface which lead to explosive spalling. Shorter and Harmathy proposed that the rate at which the moisture clog moves under the heat flux V_h is governed by the rate at which evaporation takes place and may be given by;

$$V_h = \frac{q}{Q.\rho_w}.\frac{1}{\epsilon} \tag{3.1}$$

where;

Q = heat of vapourisation of water

ρ_w = density of water

ϵ = porosity of concrete

q = incident heat flux to surface of concrete, where

$$q = \frac{h\ (\theta_f - \theta_s)}{1 + \frac{h\ l}{\lambda}} \tag{3.2}$$

h = coefficient of heat transfer at surface of concrete

l = depth of moisture clog beneath surface

λ = thermal diffusivity of concrete

θ_f = temperature of fire

θ_s = temperature of concrete's surface

The rate at which the moisture clog moves under the pressure gradient V_p was derived from D'Arcy's Law of flow;

$$V_p = \frac{k}{\eta_w}\left(\frac{P_l - P_{atm}}{D}\right) \tag{3.3}$$

where;

k	=	permeability of concrete
η_w	=	viscosity of water
P_l	=	pressure of interfacial layer
P_{atm}	=	atmospheric pressure
D	=	width of moisture clog

Shorter and Harmathy suggested that the condition for build up of pore pressure is $V_h > V_p$, with the failure condition being $(P_l - P_{atm}) = \sigma_{strength}$, where $\sigma_{strength}$ is the tensile strength of the concrete. They concluded that the fractional pore saturation necessary for spalling was;

$$\frac{\phi}{\epsilon} > \frac{1}{1 + \left(\frac{A}{\epsilon\ k\ \sigma_{strength}}\right)\left(\frac{\lambda}{\lambda + h\ l}\right)} \tag{3.4}$$

where;

$$A = \frac{\delta l\ \eta_w\ h(\theta_f - \theta_s)}{Q\ \rho_w} \tag{3.5}$$

ϕ	=	moisture content
δl	=	change in depth of moisture clog

Shorter and Harmathy used Equation 3.4 to produce a spalling liability curve for a concrete with tensile strength of 1.7 N/mm^2 and porosity of 0.3. The curve is reproduced here as Figure 3.7. In theory, similar curves could be produced for a wide range of concretes. The usefulness of such an exercise is limited by the need to use material properties of which there are little data at elevated temperatures.

In addition, the usefulness of a design chart such as Figure 3.7 is limited by the fact that it is in terms of relative pore saturation. The relative pore saturation may only be converted to a usable

parameter such as relative humidity by use of the material's sorption relationship. Such information is not readily available at elevated temperatures.

The theory of Shorter and Harmathy suggests that even at full pore saturations, no spalling will occur if the permeability is sufficiently high. Similarly, at very low permeabilities explosive spalling is almost guaranteed. They suggested a threshold permeability in the order of 10^{-9} m/s. For concretes with a permeability less than this threshold, Harmathy suggested that spalling will inevitably take place. However, the threshold is quite high. Neville (1981) suggested that 5 days after casting, concrete with a water/cement ratio of 0.7 will be less permeable than Harmathy's limit. Indeed, the permeability of most concretes will be less than 10^{-9} m/s and thus his theory suggests that most all concretes should spall on heating. Clearly this is not the case.

Sertmehemetoglu (1977) suggested a modification to Harmathy's model. He proposed that before the pressures build up that a significant proportion of the concrete's moisture may leave the clog through the dry zone. Thus, he suggested that a reduction in the moisture content of the clog increases the rate of movement of the interfacial layer. Sertmehemetoglu determined the velocity of vapour from the clog to the surface as V_s where;

$$V_s = \frac{k_{vapour}}{\eta_{vapour}} \cdot \frac{(P_l - P_{atm})}{l} \qquad (3.6)$$

where k_{vapour} = vapour permeability of concrete.

For any degree of pore saturation α, he defined the condition for failure as;

$$(\alpha - 1)\ V_h - V_p > V_s \qquad (3.7)$$

Sertmehemetoglu combined Equations 3.6 and 3.7 with Shorter and Harmathy's Equation 3.5 to suggest a new governing equation for the occurrence of explosive spalling;

$$\frac{l\ V_s^2}{V_s + V_h}\left(\frac{\phi}{\epsilon - \phi}\right) - \frac{l\ V_h\ V_s}{V_h - V_s} > \frac{k_w}{\eta_w}\ \sigma_{strength} \qquad (3.8)$$

Sertmehemetoglu produced a design nomogram to express this relationship for concrete with tensile strengths of 1.73 and 3.5 N/mm^2 which is also shown in Figure 3.7. His analysis suggested that the susceptibility of a concrete to spalling is solely a function of its permeability, within typical ranges of moisture content (2 to 5% by wt.) and permeability (10^{-9} to 10^{-11} m/s).

Sertmehemetoglu suggested that the increased susceptibility of concretes with a high moisture content to spalling may be due not to the moisture *per se*, but rather to the reduced permeability which may result from more complete hydration in the presence of excess water. The influence of load on the occurrence of spalling may also be explained in terms of permeability. Imposed compression loads act against the development of tension cracks that result from heating, thus maintaining the permeability at a lower level than would be the case with unloaded specimens. However, imposed loads which impart flexure, for example in the lower flange of a beam, promote cracking at the heated face, which will alleviate pore pressures and hence reduce the probability of explosive spalling, as observed by England (1971).

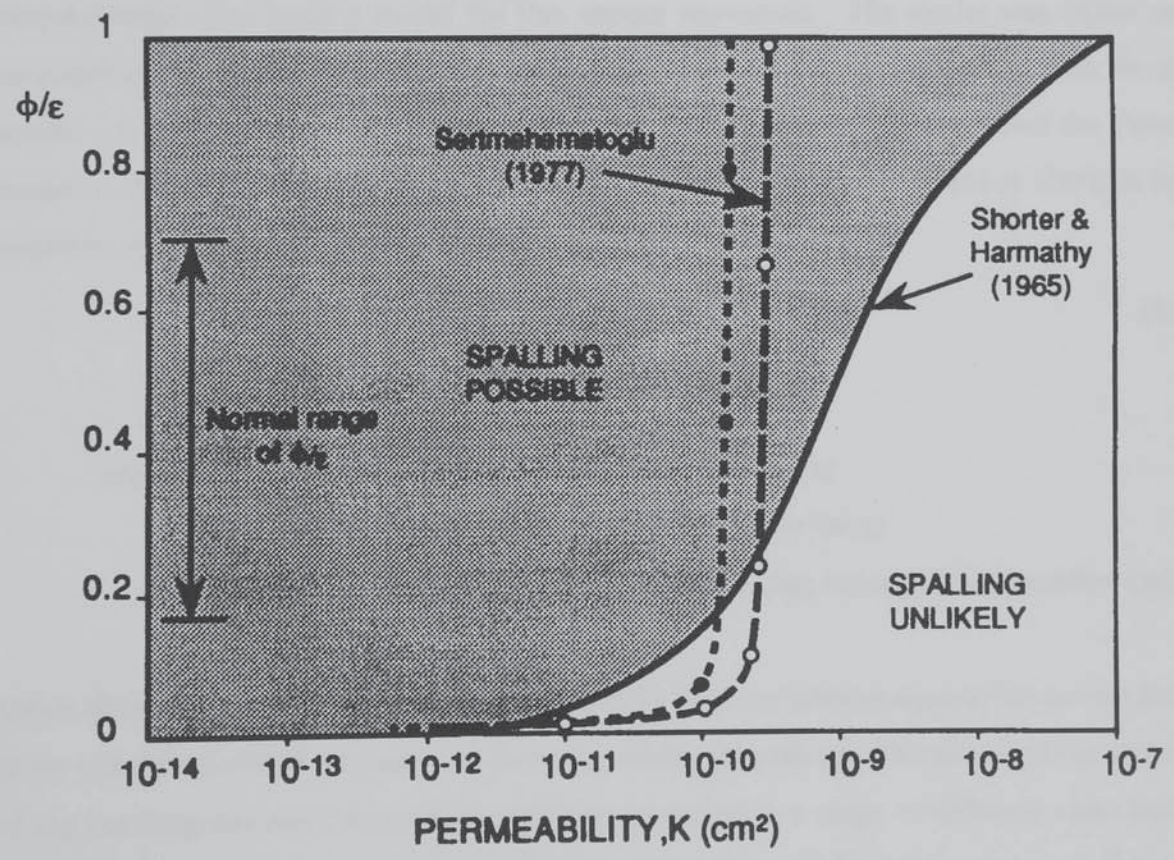

Figure 3.7 Spalling liability curve based on moisture clog model

3.3.2 SPALLING DUE TO VAPOUR DRAG FORCES

While, Shorter and Harmathy proposed that the bursting stresses, which caused spalling, were a result of static pore pressure at the moisture clog/dry zone interface, Meyer-Ottens (1972) in his PhD Thesis at Technical University of Braunschweig, Germany suggested that the bursting stresses were a result of drag forces generated by the water vapour escaping from the moisture clog to the heated surface. Meyer-Ottens proposed that friction between the outflowing vapour and the pore walls effectively subjected the concrete to a tensile stress. When this stress exceeded the tensile strength of the concrete, spalling occurred.

Meyer-Ottens assumed that the moisture clog moved by vapourisation. He related the location of the moisture clog at any instant in time to the 100°C isotherm. The build up of pore pressure predicted by Shorter and Harmathy was recognised by Meyer-Ottens, but instead of driving the moisture clog into the concrete, he assumed it forced vapour towards the heated surface.

Meyer-Ottens produced a model for this vapour movement. His model was based on the assumption that vapour flow through a porous system may be represented by flow through a bundle of capillary tubes. He assumed that such flow was laminar and applied the Poiseuille Equation. Finally, he produced an expression for the bursting stress generated at 100°C in heated concrete, $\sigma_{burst,100}$;

$$\sigma_{burst,100} = 7.16\ \phi\ V_{100}\ l \qquad (3.9)$$

where; ϕ = moisture content (% by weight)
V_{100} = velocity of the 100°C contour (m/s)
l = flow length , i.e. depth of clog beneath heated surface (m)

Meyer-Ottens suggested that a comparison of these bursting stresses against the tensile strength of the concrete provided a measure of the susceptibility to spalling. He calculated the magnitude of the bursting stresses that could possibly be generated in a range of different concretes. He observed that the stresses increased with depth, to a maximum at 60 mm, as shown in Figure 3.8. The bursting stresses are nearly zero by 120 mm. Meyer-Ottens suggested that spalling of specimens with thicknesses in the order of 120 mm is unlikely. Experimental observations

reported in Chapter 2 confirms that thicker specimens are less likely to spall.

Meyer-Ottens theory suggested that the moisture clog does not get saturated but that pressures develop which drive vapour towards the heated surface. This assumption has since been brought into question by the work of Bažant and Thonguhthai (1979), who predicted the development of the moisture clog in heated concrete, using a finite element solution to the equations of state for temperature and pressure within a heated concrete.

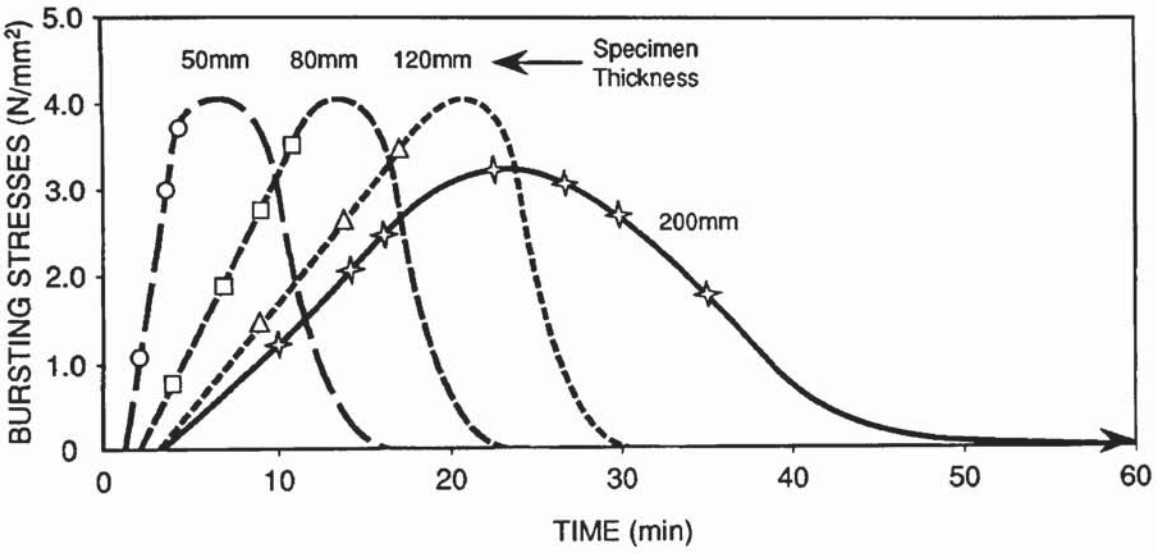

Figure 3.8 Bursting stresses predicted in heated concrete (after Meyer-Ottens, 1972)

A further doubt is cast over Meyer-Ottens' theory by the role of the movement of the 100°C isotherm. The theory suggests that the faster the contour moves, the greater the pore pressures developed. However, examining Figure 3.9, which shows the relationship between the velocity of the isotherm and a concrete's moisture content, there is a clear suggestion that drier concrete should suffer from higher splitting pressures. This predicted behaviour contradicts Meyer-Ottens' own experimental observations on the reduced incidence of spalling amongst drier concretes.

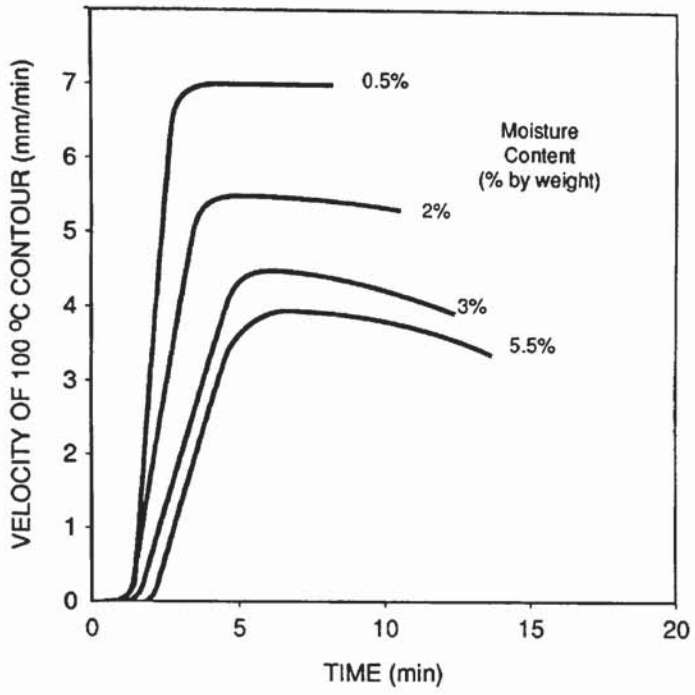

Figure 3.9 Relationship between velocity of 100°C isotherm and moisture content

3.3.3 NUMERICAL MODELLING OF PORE PRESSURES DEVELOPMENT IN HEATED CONCRETE

The development of pore pressures within heated concrete is principally governed by the ease with which moisture may travel through the concrete. As Shorter and Harmathy (1965) explained, where moisture may flow easily throughout a concrete there is little opportunity for the development of pore pressure. Thus pore pressure development is related both to the amount of water within the concrete and the nature of the pores through which it flows.

3.3.3.1 Nature of pores in concrete

Cement paste is a porous solid that contains unhydrated cement particles, cement gel (i.e. hydrates of cement compounds such as C_3S (Alite), C_2S (Belite), C_3A and C_4AF) and some minor components. The paste consists of two different types of pores called gel pores and capillary pores.

3.3.3.1.1 Capillary pores

Capillary pores represent that part of the gross cement paste volume, which have not been filled by the products of hydration. Their size ranges from approximately 200Å and water molecules may pass easily through them. Thus, capillary pores are important in determining the permeability of hardened concrete. The amount of capillary pores reduces as hydration proceeds.

The rate of reduction is governed by the water/cement ratio of the cement paste. For pastes with a water/cement ratio greater than 0.38, there will always be some capillary pores present, even after 100% completion of the hydration process.

Capillary pores vary in size and shape and form an inter-connected system, randomly distributed throughout the cement paste. Generally, however, the connecting pores are of much smaller dimensions as the growth of the gel particles fills the pore space. With an increase in the water/cement ratio above 0.7, there is reduced potential for the gel particles to develop sufficiently to block all of the capillaries and such pastes will be highly porous.

3.3.3.1.2 Gel pores

Cement gel has been shown capable of holding large quantities of evaporable water and thus is highly porous. Gel pores form a network of inter-connected interstitial spaces between the gel particles.

Gel pores are much smaller than capillary pores and are generally of sizes in the order of 15 to 20Å. Thus, gel pores are only about 5 times larger than the diameter of the water molecule. this fact dictates the nature of moisture transport through gel pores, which is by a completely different mechanism to that which takes place in capillaries. The volume of gel pores is approximately 28% of the total gel volume. The gel porosity is governed by the type and fineness of the cement itself, and is relatively independent of the water/cement ratio of the paste.

3.3.3.2 Water in cement paste

The amount of water present in cement paste depends on the ambient humidity. Capillary pores in particular, because of their relatively large size, contain levels of moisture that are related to the relative humidity. At relative humidities below about 45%, the capillaries are emptied of free water. There are several different types of water present within a cement paste.

Free: Water held in capillary pores. It moves with relative ease through the concrete

Adsorbed: Water held in the gel pores. It may either be held at the surfaces of the gel particles by Van der Waal forces or, alternatively, may be held within the sheets of tobermorite gel and in such cases often referred to as inter-layer water

Combined: Water chemically combined within the hydrates of the cement gel particles

The different types of water within cement paste are shown in Figure 3.10. Although it is unclear what percentage of each type of water exists within a paste, it appears that both adsorbed water and inter-layer water have similar energies of binding and may thus be viewed in a similar manner.

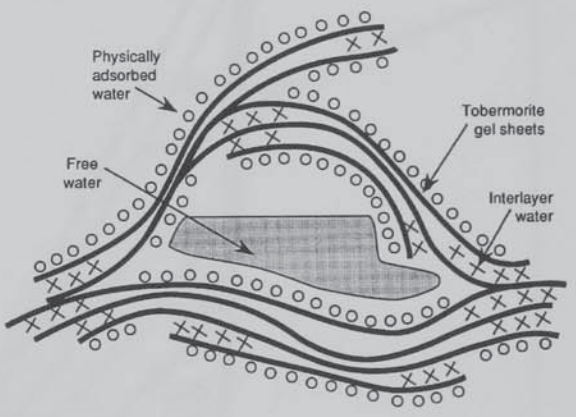

Figure 3.10 Types of water in cement paste

The simplest distinction of the water components may be made by dividing them into categories of evaporable (at 105°C) and non-evaporable. Such a categorisation is by definition imprecise, however, as it depends on the vapour pressure. In addition, heating increases hydration and thus increases the percentage of water held in chemical combination.

Akhtarruzaman and Sullivan (1970) showed that on heating concrete shows an increased loss in

mass at two distinct temperatures levels, i.e. 105 and 175° C. They concluded that free water was removed at 105°C while adsorbed gel water and also possibly some combined water was removed at 175°C.

The quantity of moisture w in the liquid phase of a cement paste is related to its equilibrium vapour pressure P_v by a relationship known as the '*Equilibrium Sorption*'. This relationship is temperature dependent and when measured for a particular temperature is referred to as the '*Sorption Isotherm*'. Some sorption isotherms of concrete are shown in Figure 3.11.

For convenience, the equilibrium vapour pressure may be expressed as a fraction of the relative humidity of the environment P_v^o. The equilibrium sorption relationship is quite difficult to determine through experiment but it may be predicted. The equilibrium sorption relations is a function of the maximum amount of moisture that the cement paste may hold (its porosity n), the maximum amount of adsorbed water that the paste may hold (its specific surface S) and the affinity between the pore surface and the water molecule (as measured by the constant C in the Brunaeur-Emmett-Teller Equation). Given values for n, S and C, an estimate of the equilibrium sorption relation can be made for any material.

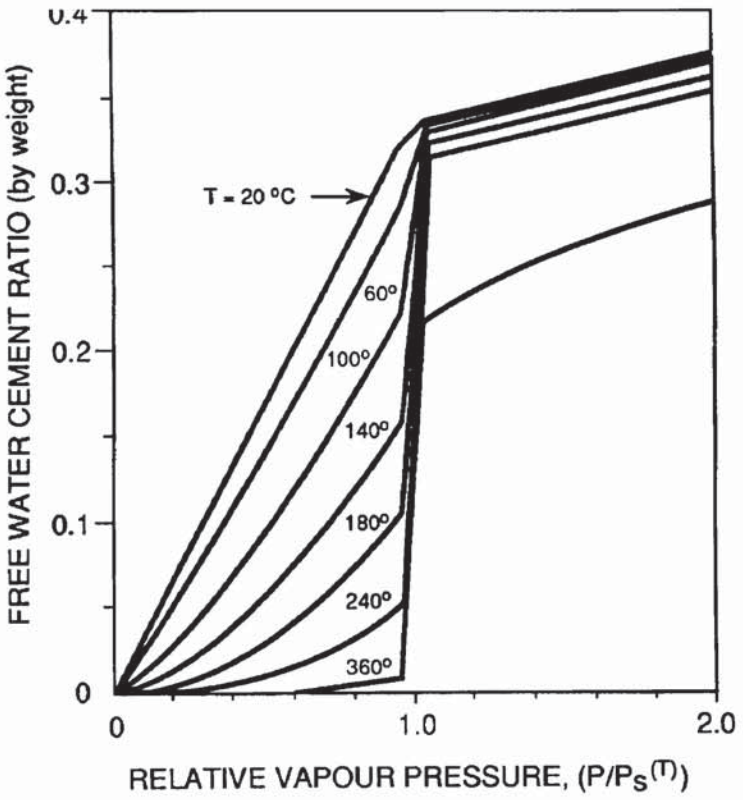

Figure 3.11 Sorption relation of hydrated cement paste (after Bažant and Thonguthai, 1979).

3.3.3.3 Movement of water in heated concrete

Several different theories to explain the movement of moisture within concrete have been offered over the years, namely Theories of Diffusion, Capillary Flow and Evaporation-Condensation.

3.3.3.3.1 Diffusion theory

The movement of water through porous media by diffusion was first proposed by Lewis (1921). The principle assumption is that the moisture flux η is proportional to the gradient in moisture concentration w. This may be stated more rigorously as;

$$\eta = - \rho_w \chi \frac{\delta w}{\delta x} \tag{3.10}$$

where;

x	=	distance
χ	=	coefficient of diffusion
ρ_w	=	density of water

Combining Equation 3.10 with the Continuity Equation;

$$\rho_w \frac{\delta w}{\delta t} + \frac{\delta \eta}{\delta x} = 0 \tag{3.11}$$

gives Fick's Second Law of Diffusion;

$$\frac{\delta w}{\delta t} = \chi \frac{\delta^2 w}{\delta x^2} \tag{3.12}$$

Although mathematically elegant and directly analogous to Fourier's Law for heat flow, Fick's Second Law of Diffusion was found by Mc Cready *et al.* (1940) to be a poor indicator of moisture flow within porous media and an improved explanation was sought.

3.3.3.3.2 Capillary flow theory

The capillary flow theory modifies the diffusion theory in that it considers the moisture flux η to be proportional to the gradient of the total moisture potential ϕ and not simply the gradient of moisture content. Thus capillary flow may be regarded as a special case of D'Arcy's Equation and may be stated mathematically as;

$$\eta = - \rho_w \kappa \frac{\delta \phi}{\delta x} \tag{3.13}$$

where κ is the capillary conductivity which is a function of moisture concentration w. The total moisture potential is the summation of the chemical and capillary potentials of the water within the concrete. The chemical potential is measured by Gibb's Free energy for water ζ and the capillary potential ψ. Combining Equation 3.13 with the Continuity Equation 3.11 above allows the horizontal flow of moisture may be described by;

$$\frac{\delta w}{\delta t} = \frac{\delta}{\delta x} \left(\chi' \frac{\delta w}{\delta x} \right) \tag{3.14}$$

where; χ' = coefficient of capillary diffusion, defined by $\kappa(\delta \psi / \delta w)$

w = moisture concentration

t = time

It is clear that Equation 3.14 represents a special case of Fick's Second Law of Diffusion, with the diffusion coefficient depending on the moisture content. However, Equation 3.14 is only applicable to transport in the pendular state, i.e. where moisture forms continuous threads through the porous medium. At an early stage, heated concrete departs from this model of behaviour and enters the funicular state, where discrete beads of water form in its pore structure. A different mechanism for moisture transport is then involved.

3.3.3.3.3 Evaporation - Condensation Theory

In a closed system, moisture moves in the opposite direction to the temperature gradient, i.e. from hot to cold. The evaporation-condensation theory has been developed to explain such behaviour.

It assumes that liquid water is immobile and that moisture can only move through the concrete as a vapour. Thus, the theory suggests that water is heated, vaporises to steam, moves under pressure gradients to cooler regions of the concrete, loses heat in transit and as a result condenses back to water.

The governing equations have been derived by Harmathy (1969b) for moisture flow through a one-dimensional slab (of thickness l) heated on its surface and are presented below in Equation 3.15. The governing equations were derived by combining Fick's Law of Diffusion, Fourier's Law of Heat Flow, D'Arcy's Law of Convective Mass Transport and the Equations of Conservation of Energy, Momentum and Continuity.

The governing equations are;

$$A_k\frac{\delta^2\varphi}{\delta x^2} + B_k\frac{\delta^2 p}{\delta x^2} + C_k\frac{\delta^2 T}{\delta x^2} + D_k\left(\frac{\delta\varphi}{\delta x}\right)^2 + E_k\left(\frac{\delta p}{\delta x}\right)^2 + F_k\left(\frac{\delta T}{\delta x}\right)^2 + G_k\frac{\delta\varphi}{\delta x}\frac{\delta p}{\delta x} + H_k\frac{\delta\varphi}{\delta x}\frac{\delta T}{\delta x} + J_k\frac{\delta p}{\delta x}\frac{\delta T}{\delta x} = K_k\frac{\delta\varphi}{\delta t} + L_k\frac{\delta p}{\delta t} + M_k\frac{\delta T}{\delta t} \quad (3.15)$$

where;

x	=	distance from the heated surface
p	=	pore pressure
T	=	absolute temperature
φ	=	mole fraction of water vapour in the gaseous phase
k	=	1,2,3
$A_k...L_k$	=	experimentally determined functions of state variables p and T

3.3.3.4 Numerical models of pore pressure in heated concrete

Numerical solutions to these governing equations have been developed for a range of different boundary conditions by Bažant and Thonguthai (1979), Ahmed and Huang (1990) and Harada and Terai (1991).

Bažant and Thonguthai (1979) solved Equation 3.15 numerically using a finite element technique. They considered the variation of both the equilibrium sorption relation and concrete permeability with temperature. They validated their model against the experimental observations on mass loss of heated concrete recorded by Chapman (1976), as opposed to direct pore pressure measurements.

Bažant and Thonguthai's prediction for temperature and pore pressure rise are given in Figure 3.12 for a 200 mm thick concrete slab heated at 80°C per minute for a concrete with permeability 10^{-12} m/s, saturation water content 100 kg/m^3, water/cement ratio 0.5 and conductivity 1.7 J/m s°C.

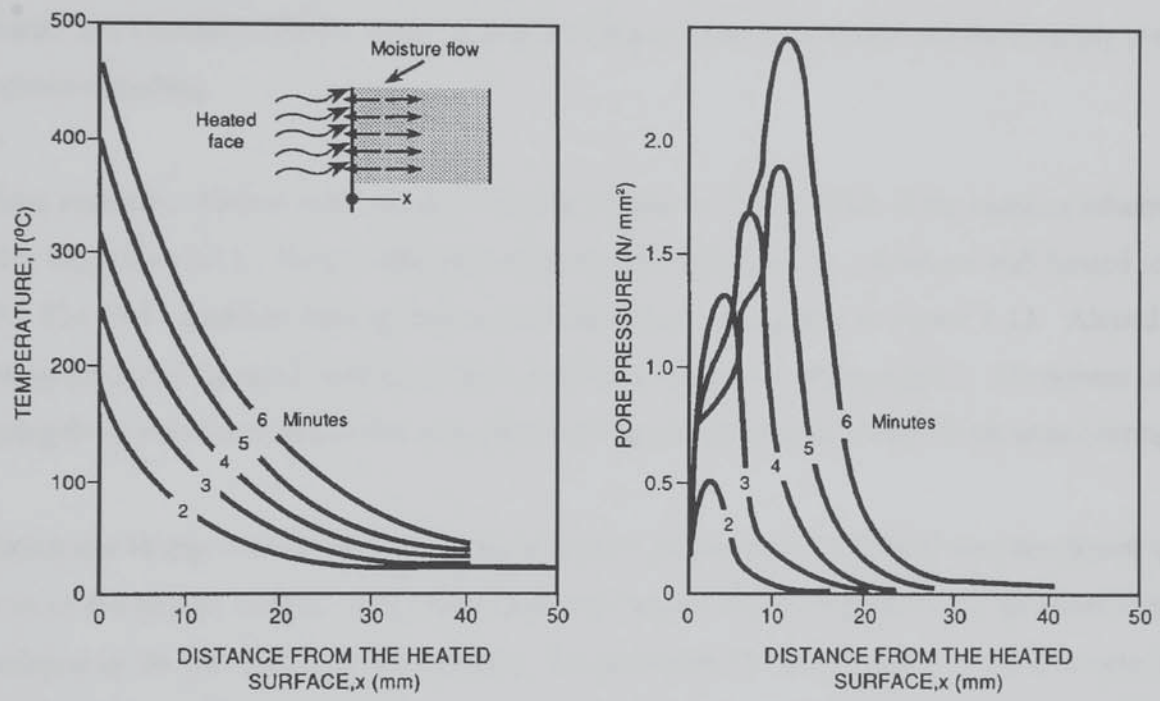

Figure 3.12 Temperatures and pore pressures predicted in a heated concrete slab (after Bažant and Thonguthai, 1979)

Figure 3.12 shows that pore pressures may rise to more than 2.0 N/mm^2 after a mere 6 minutes of heating. The maximum pore pressure occurred at a depth of about 15 mm. These pore pressures are substantially higher than had been previously predicted by Bažant and Thonguthai (1978) for concretes heated at slower rates. The results shown in Figure 3.12 were considered particularly significant as they represented the first time that researchers had either measured or modelled pore pressures in open concrete that were numerically similar to the tensile strength of

ordinary concrete, particularly at elevated temperatures. Bažant and Thonguthai (1979) also noted, somewhat surprisingly, that the pore pressures developed were only slightly less than those developed within sealed concrete specimens.

Bažant and Thonguthai explained that the movement of moisture was dictated by two competing influences, i.e. the pressure and temperature gradients. The pressure gradient attempts to drive the water within the concrete towards the heated surface, whereas the temperature gradient attempts to move the water into the cooler depths of the concrete. Close to the surface and within the drying zone, the pressure gradient dominates and pore pressures are relieved to the atmosphere. Further into the concrete, however, the temperature gradient begins to dominate and Bažant and Thonguthai recognised this region as akin to the 'moisture clog' first described by Shorter and Harmathy (1965). Thus, it could be argued that their model can successfully predict explosive spalling.

More recently, Ahmed and Huang (1990) have used a fully implicit finite element scheme to solve Equations 3.11. They predicted pore pressures developed in a concrete slab heated to the ISO 834:1987 standard heating regime and their results are given in Figure 3.13. Ahmed and Huang predicted the rapid build-up of pore pressures across the drying region. Movement of the drying front into the depth of the slab alleviates the pressures after about 60 minutes heating.

Ahmed and Huang observed that the maximum pore pressure of 0.4 N/mm^2 was developed quite close to the heated surface. They attributed this fact to the development of a 'moisture clog' as predicted by Shorter and Harmathy (1965). By increasing the permeability of the concrete, they found that the maximum pore pressures were reduced as shown in Figure 3.14. They suggested that fully saturated concrete could be free of explosive spalling, if it were sufficiently permeable.

Harada and Terai (1991) also modelled the development of pore pressures in heated concrete walls subjected to the standard ISO 834:1987 heating regime. They predicted a maximum pore pressure of 0.13 N/mm^2. This pressure was achieved after 30 minutes heating and remained static despite further heating. They attempted to validate their model against experimental behaviour but their attempts were limited by practical difficulties in measuring pore pressure.

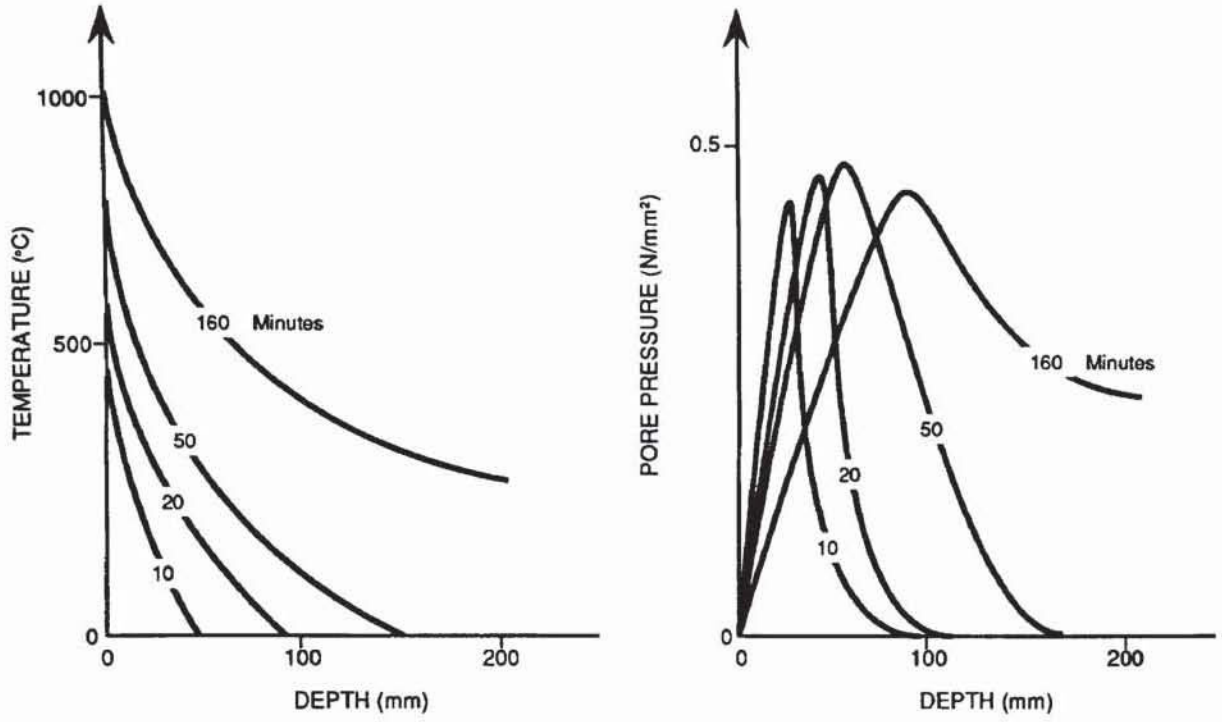

Figure 3.13 Temperature and pore pressure predicted in a heated slab (after Ahmed and Huang, 1990)

Figure 3.14 Influence of permeability on maximum pore pressure (Ahmed and Huang, 1990)

The maximum pressures predicted by different researchers vary enormously despite the fact that they were all modelling essentially similar situations. There is clearly a need for experimental work to verify the accuracy of the different models proposed.

3.3.4 MEASUREMENT OF PORE PRESSURE IN HEATED CONCRETE

Nekrasov *et al.* (1967) was one of the first researchers to attempt to measure the pore pressure in heated concrete. He cast a number of 2mm copper pipes into large blocks of refractory concrete and using a manometer recorded the pressure development on gradual heating to 800° C Nekrasov did not encounter any spalling or failure of the concrete and observed a maximum pore pressure of 0.2 N/mm^2 which was reached after many hours of heating at a relatively slow rate.

Bremer (1967) independently adopted a similar methodology to Nekrasov, using the apparatus shown in Figure 3.15 and observing the relationship between pore pressure and temperature shown in Figure 3.16. Bremer found that the pressures observed were rarely more than 40% of the saturated steam pressure.

Figure 3.15 Measurement device used by Bremer (1967)

Figure 3.16 Pore pressures recorded by Bremer (1967)

Thelanderson (1974) used a similar approach in the examination of concrete specimens, subjected to transient heat and torsional loading. He studied concrete rods of 1500 x 150 x 150 mm, made with quartzite aggregate concrete (water/cement ratio 0.55). At heating rates of 4 and 8°C per minute, maximum pore pressures of 0.5 and 0.65 N/mm^2 were recorded respectively and explosive spalling encountered. The temperature and pressure history recorded is given in Figure 3.17.

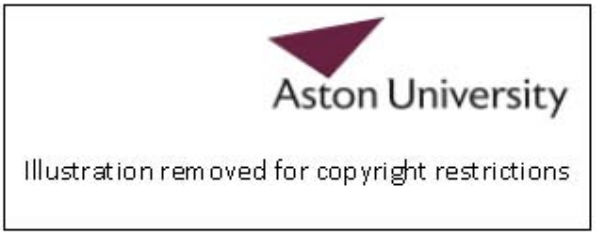

Figure 3.17 Pore pressure and temperature results achieved by Thelanderson (1974)

It is unclear how pressures of these orders could cause explosive failure of the mortar, which could be expected to have a tensile strength in the region of 2 N/mm^2. However, Thelanderson had used the simplistic liquid filled tube measurement techniques of Nekrasov *et al.* (1967) and Bremer (1967) and thus the values that he recorded must be regarded more for their relative rather than absolute magnitudes. It is significant that concrete heated at 2°C per minute did not explode.

Chapman (1976) examined the pore pressures developed in sealed concrete specimens in considering the use of concrete as a lining material in nuclear reactor vessels. His measurements showed that heating fully sealed concrete could generate pressure well in excess of the saturation vapour pressure of steam, as shown in Figure 3.18. Chapman found that the magnitude of the pore pressures developed was influenced by the initial ratio of the volume of liquid to gas within the concrete pores. Thus, he confirmed the validity of Shorter and Harmathy's (1965) consideration of pore saturation in their governing equation for spalling, i.e. Equation 3.4.

Figure 3.18 The pore pressures recorded by Chapman (1976)

England *et al.* (1991) adopted the same approach as Chapman had in the study of the same problem. They confirmed that heating sealed concrete specimens could generate pore pressures of up to 10 N/mm^2. Their results confirmed that moisture migrates away from the heated surface

and causes the maximum build-up of pressure in more remote areas of the concrete.

Sertmehemetoglu (1977) carried out a major study of explosive spalling, which included measurement of pore pressures. He heated concrete specimens from one side only and measured the pressure developed at the unexposed face, by sealing it within a diaphragm which included a pressure transducer. In effect his specimens were sealed, although Sertmehemetoglu suggested that the diaphragm had a similar effect to the existence of a 'moisture clog', predicted by Shorter and Harmathy (1965).

Sertemehemetoglu recorded the variation of these pressures with thickness of the concrete specimen, which he considered equal to the depth of the 'moisture clog' and found that they increased with depth up to a maximum value of some 2 N/mm^2 at a depth of 100 mm. Neither the pressure recorded nor its related depth correlate particularly well with observations of explosive spalling in practice. Sertmehemetoglu proposed a mechanism for spalling that correlated with his experimental results. His ideas will be discussed further in Section 3.6.2.

The studies of Chapman (1976), Sertmehemetoglu (1977) and England *et al.* (1991) have concentrated on sealed or semi-sealed concrete specimens, where measurement of pore pressures is relatively easy. However, such conditions do not accurately reflect typical concrete members on exposure to fire environments. Nekrasov (1967), Bremer (1967) and Thelanderson (1974) attempted to record pore pressures in more realistic situations and the early measurement difficulties that they encountered exist to this day.

As mentioned in Section 3.3.3.4 recent work in Japan of Harada and Terai (1991) has confirmed the continued difficulties associated with the measurement of pore pressure in open concrete members. Harada and Terai used an embedded tube, filled with silicone oil and connected to a transducer. While some pressures were recorded in the early stages of test, evaporation of the oil and pressure release by cracking of the concrete prevented further measurements.

3.3.5 MECHANISM FOR SPALLING AT OBSERVED PORE PRESSURE LEVELS

Sections 3.3.3 and 3.3.4 have made it clear that practical measurement and numerical models

both show that pore pressures in heated concrete are generally less than concrete's tensile strength. Akhtaruzzaman and Sullivan (1970) proposed a model of spalling which explained how such relatively low pore pressures could cause bursting failure. Their model considered concrete as a hollow sphere containing free water and steam, as shown in Figure 3.19. The volume of the sphere was related to the summation of the entire void space within the concrete. The thickness of the shell of the sphere was determined using the concept of an 'equivalent mass' of hydrated cement gel.

Figure 3.19 Model used by Akhtarruzaman and Sullivan (1970)

Akhtarruzaman and Sullivan's model was based on the fundamental premise that application of heat generated an internal steam pressure within a concrete. This steam pressure may in turn generate hoop stresses within the sphere. The internal steam pressure was found simply using the mean concrete temperature and the known relationship between the temperature and the saturation vapour pressure of steam (e.g. Rogers and Mayhew, 1991). The internal steam pressure was converted to hoop stress using thin cylinder analysis. The model predicted spalling when hoop stresses exceed the tensile strength of the concrete.

Although the model's use of saturation vapour pressures is quite simplistic, it does overcome many of the difficulties associated with calculating the actual pore pressures within a heated concrete. These include lack of knowledge of the exact size and locations of the gel pores and the onset of cracking.

The model explains the observed influences of moisture content and age on explosive spalling.

In addition, their model was used successfully to explain the explosive spalling of a large number of concrete specimens observed in their experimental programme. They observed that spalling occurred in the temperature range of 165 to 198°C. The saturated vapour pressure of steam in this temperature range is between 0.6 to 1.4 N/mm^2. Even allowing for some loss in tensile strength at elevated temperatures, such pressures appear insufficient to cause failure of the concrete. It is clear that the usefulness of Akhtarruzaman and Sullivan's model was its ability to explain how such relatively low pressures may cause explosive spalling.

There remains, however, uncertainty regarding the thickness of the gel pore shell and its variation with temperature. Furthermore, subsequent experimental work (Harada and Terai, 1991) and numerical modelling (Bažant and Thonguthai, 1979, Ahmed and Huang, 1990) have shown that the pore pressures developed in concrete remain well below the saturation vapour pressure.

In addition, the model does not adequately explain some observed experimental behaviour. For example, wet cured specimens are more dense and strong near the surface than moist cured specimens. Thus, they should be better able to resist the pore pressures generated by heating and be in turn less susceptible to spalling. The opposite is in fact the case, with Akhtarruzaman and Sullivan themselves observing that water curing increased the susceptibility to splitting.

3.4 SPALLING DUE TO COMBINED THERMAL STRESS AND PORE PRESSURES

3.4.1 SUPER-IMPOSITION OF STRESSES

Zhukov (1975) in what was then the U.S.S.R. proposed that the stresses developed within a heated concrete member may be superimposed upon each other and their summation compared to the material strength of concrete. He considered that the stresses acting could be categorised as load induced stresses σ_l, thermal stresses σ_t and pore pressures σ_p, as shown in Figure 3.20.

The stresses acting on a slab heated on one face are;

x - direction: pore pressure

y - direction: stresses due to applied load
and restrained thermal expansion

z - direction: stresses due to restrained thermal expansion

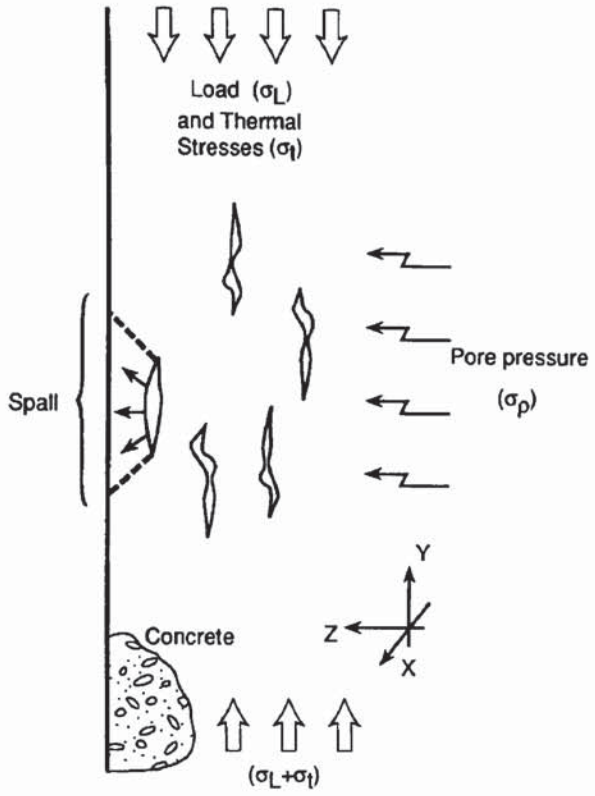

Figure 3.20 Stresses acting in heated concrete (after Zhukov, 1975)

Zhukov used basic elastic theory to quantify the total strain in the x-direction ϵ_x as;

$$\epsilon_x = \frac{1}{E}\left\{\sigma_p - \nu(\sigma_l + 2\sigma_t)\right\} \tag{3.16}$$

The strain energy density in the x direction W_x, is the area under the stress-strain curve (taken as linear) and is given by;

$$W_x = \frac{\sigma_p}{2\,E}\left\{\sigma_p - \nu(\sigma_l + 2\sigma_t)\right\} \tag{3.17}$$

This may be equated with the strain energy necessary to cause failure (or rupture) of the concrete W_{fail}, where;

$$W_{fail} = \frac{1}{2} \cdot \sigma_{rupture} \cdot \frac{\sigma_{rupture}}{E} \qquad (3.18)$$

If it is assumed that Young's Modulus of Elasticity is the same both in tension and compression, then Equations 3.17 and 3.18 above may be compared, thus giving the governing equation for bursting failure as;

$$\sigma^2_{rupture} = \sigma_p^2 + \nu \ \sigma_p \ (\ \sigma_l + 2\sigma_t \ ) \qquad (3.19)$$

Since the stresses due to temperature and imposed load may be calculated, Zhukov devoted much effort to calculating the stresses imposed by pore pressure. In a manner broadly similar to Meyer-Ottens (1972), Zhukov developed a model of the outflowing vapour and calculated the tensile stresses generated by the drag forces of the outflowing vapours.

Zhukov predicted that stresses of up to 15 N/mm^2 could be generated in a heavy (dense) concrete with a moisture content of 8%. For lightweight concrete of the same moisture level, he predicted a bursting stress of 1.6 N/mm^2 . These values are relatively large, explaining how relatively small pore pressures could generate stresses in excess of the concrete tensile strength. Zhukov indicated that his spalling predictions had been verified on tests on 35 concrete slabs, although no further details or references were given.

His theory, however, seems flawed. The consideration of the concrete pores as tubes carrying moisture from the clog would suggest that for flow to occur, the pressure at the open end of the tube may not be greater than that at the clogged end. Thus, it is difficult to believe that relatively small pore pressures at the clog will generate such large drag stresses. Despite the apparent limitations of his pore pressure model, the manner in which Zhukov suggested the superimposition of the different stresses appears useful and will be taken further in later chapters.

More recently, Zhukov (1994) has updated his methods for forecasting the brittle spalling failure of heated concrete. His new approach combined his earlier model of combined thermal and moisture imposed stresses (Zhukov, 1975) with fundamental cracking theory and was based

largely on experimentally determined correlations.

Zhukov (1994) proposed that the tendency of a concrete to explosive spalling may be given by a parameter K_{spall}, which considers thermal and pore pressure stresses from heated steam within the concrete. He proposed that pore pressure stresses were proportional to the moisture content m, the temperature difference between the heated surface and the failure zone $\Delta\theta$, and a structural parameter P, which he considered to be of a similar nature to permeability.

He proposed that the thermally induced stresses are governed by $\Delta\theta$, the coefficient of expansion α, and the Modulus of elasticity E. Zhukov assumed that $\Delta\theta$ may be reasonably approximated by the reciprocal of the thermal conductivity k. He assumed that neither density nor specific heat capacity vary amongst concretes. In fact, this assumption is not as limiting as it might appear (Connolly *et al.*, 1994).

Zhukov presented the tendency for spalling to occur as the ratio between the imposed thermal and pressure stresses and the coefficient of stress intensity K_{stress} for concrete. Over a heated area of concrete A the susceptibility to spalling is given by;

$$K_{spall} = f\left(\frac{\alpha\ E\ \Delta\theta\ P\ A\ m}{K_{stress}\ k}\right) \tag{3.20}$$

With the exception of the parameter P, the other variables in Equation 3.20 are properties of the concrete and its environment. Zhukov derived an experimental relationship between the structural parameter P and concrete porosity. Thus he was able to use Equation 3.20 to quantify the susceptibility of different concretes to spalling. The results of his analysis are presented in Table 3.1. High values of K_{spall} indicate increased susceptibility to spalling.

Table 3.1 also includes critical moisture contents which represent the limiting value above which spalling is likely. Zhukov calculated these critical moisture content by assuming that K_{fail} had a constant value of 6.3, regardless of the nature of the concrete.

Concrete	Porosity	P (mm^{-2})	K_{spall}	m_{crit} (%)
Normal-weight with granite aggregate	0.10	0.1	1	3
Light-weight with ceramsite aggregate	0.15	0.07	0.7	6
Light-weight with siliceous aggregate	0.15	0.1	1.7	2

Table 3.1. Susceptibility of different concretes to spalling (after Zhukov,1994)

Thus, he gives the critical moisture content m_{crit} as;

$$m_{crit} = \frac{6.3\ K_{spall}\ k}{P\ \alpha\ E} \tag{3.21}$$

Zhukov suggested that if a concrete has a working moisture content less than its critical value, then brittle spalling failure is likely after 5 to 10 minutes heating. This appears to be unsually early in the heating process as explosive spalling is generally observed between 20 and 40 minutes after the commencement of heating (Malhotra, 1972). In retrospect, it appears possible that Zhukov may have been considering a severe form of aggregate splitting.

The values for the critical moisture contents predicted by Zhukov are quite low and suggest that explosive spalling appears likely in most situations, which is generally not the case.

Zhukov considered applied compressive stresses by super-imposing them on the numerator in Equation 3.20. By such means, he predicted the relationship between susceptibility to spalling, concrete moisture content and applied stress. The predicted behaviour of normal-weight concrete made with coarse granite aggregates is given in Figure 3.21.

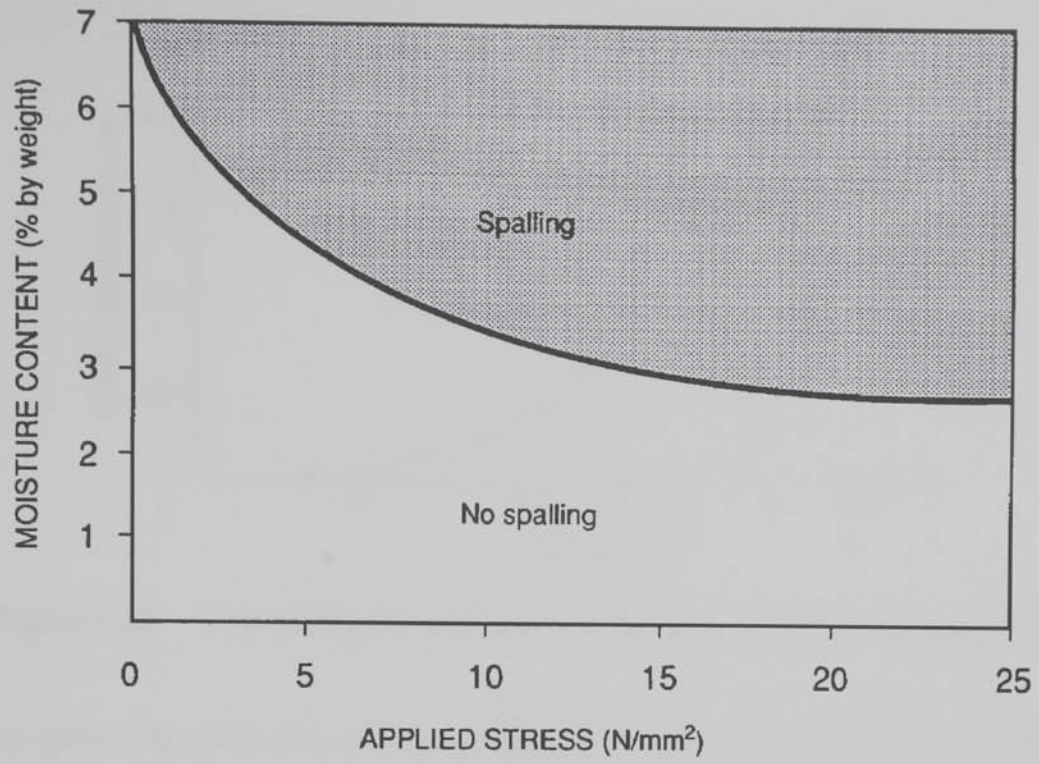

Figure 3.21 Spalling envelope for typical concrete (after Zhukov, 1994)

3.4.2 COMBINED EFFECTS OF LOAD INDUCED CRACKING AND PORE PRESSURES

Sertmehemetoglu (1977) carried out a comprehensive study on the mechanism of spalling for his PhD thesis at Kings College, where he attempted to measure the pore pressures that developed in heated concrete after the formation of a moisture clog. Sertmehemetoglu heated concrete specimens from one side and measured the magnitude of the pore pressures developed on the unexposed face using a diaphragm and a pressure transducer. An example of some of the measurements taken are shown in Figure 3.22.

The recorded pressures are generally similar to those that have been suggested by others (Thelanderson 1974; Ahmed and Huang 1990), although it was the first time that an increase of maximum pressure with depth of specimen was actually measured. Such an increase was predicted by the moisture clog theory of Shorter and Harmathy (1965).

Figure 3.22 Experimental pore pressure observations of Sertmehemetoglu (1977)

The magnitude of the pore pressures measured by Sertmehemetoglu cast significant doubts on the credibility of the spalling mechanisms proposed by Shorter and Harmathy (1965), Meyer-Ottens (1972) and Zhukov (1975). The doubts centre on the fact that the maximum pore pressure recorded by Sertmehemetoglu was 2.1 N/mm^2, which even allowing for temperature effects is less than the tensile strength of concrete, which will have typical values in the order of 3 N/mm^2. Sertmehemetoglu's readings indicated that pore pressures alone do not cause spalling.

To explain the difference between the measured pressures and those necessary to cause spalling Sertmehemetoglu proposed a mechanism for spalling, which expanded on some earlier ideas of Dougill (1971). Dougill had noted that heating concrete specimens subjects the region of the heated face to compressive stresses, causing a system of cracks to develop parallel to the heated face. The existence of such cracks had been previously confirmed by Hsu (1963). As the temperature rises, Sertmehemetoglu proposed that the cracks fill with vapour produced by the desorption of pore water. The vapour pressure in the cracks, subjects the concrete to forces normal to the direction of heating, thus creating the bursting pressures necessary for spalling.

Sertmehemetoglu artificially generated cracks parallel to the heated face by casting discs at various depths within concrete specimens. He then measured the magnitude of mechanically applied bursting stresses necessary to cause rupture of the concrete's surface. Sertmehemetoglu found that the bursting stresses required depended on the crack size and depth, but observed that

stresses of the magnitude of previously measured pore pressures were sufficient. A sample of his results are shown in Figure 3.23.

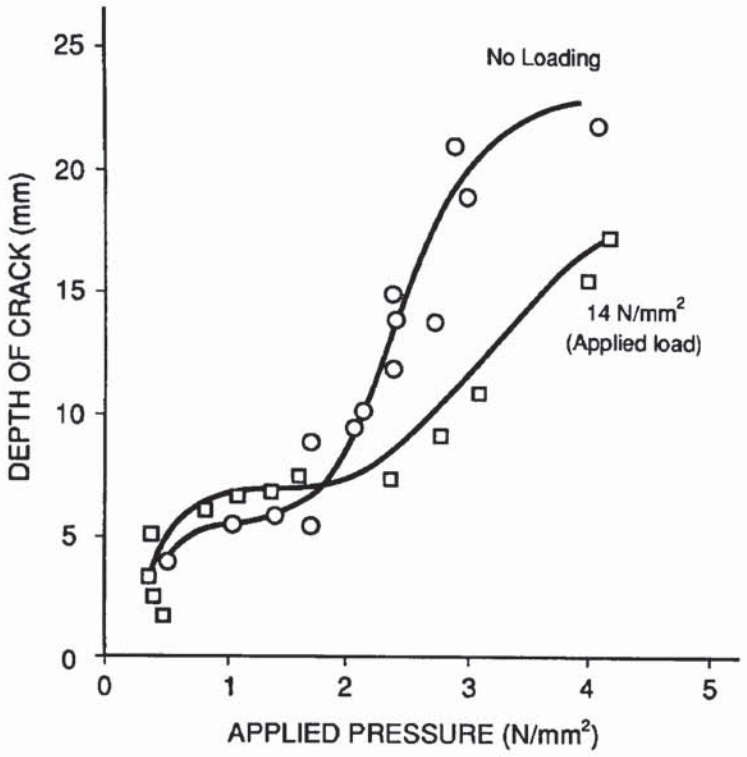

Figure 3.23 Variation of rupture pressure imposed on 50mm diameter crack with depth from surface (after Sertmehemetoglu,1977)

This Figure shows clearly for unloaded concrete specimens that bursting pressures of 2.1 N/mm^2 at depths up to 10mm may be capable of causing surface rupture. Thus Sertmehemetoglu identified a mechanism by which observed pore pressures could cause failure and spalling of concrete.

Setmehemetoglu proposed that biaxial compression, by increasing the development of primary cracks parallel to the heated face, promoted the occurrence spalling. However, this contradicts his experimental observation that the pressures necessary to cause failure increase on application of biaxial load. This suggests that spalling is less likely in the presence of biaxial load, although the effect appears only significant for depths beyond 10 mm.

3.5 OVERALL CONCLUSIONS ON SUGGESTED MECHANISMS OF EXPLOSIVE SPALLING

To date, the majority of mechanisms proposed to explain explosive spalling suggest it is due to either thermal stresses (Saito, 1965; Dougill,1972a) or vapour stresses (Shorter and Harmathy, 1965; Meyer-Ottens, 1972; Akhtarruzaman and Sullivan, 1970).

Predicting spalling based on thermal stresses would have the merit of simplicity, as reasonable estimates may be made of their magnitude using fundamental elastic theory. Furthermore, non-linear constitutive models for concrete have been investigated for many years and accurate models for predicting thermal stresses developed. However, experimental observations of the susceptibility of water-cured, low moisture, high strength and thick concrete specimens contradict the theory.

The generation of pore pressure in the heated concrete is difficult to predict. A range of models have been examined which range in complexity from simple use of Steam Tables (Rogers and Mayhew, 1991) to full solution of the equations of state using finite element analysis (Bažant and Thonguthai, 1979). The majority of such models predict pore pressure levels which are substantially less than the tensile strength of concrete.

Akhtarruzaman and Sullivan (1970) have shown that the tensile strength of the concrete is the correct parameter against which to compare pore pressure. The limited experimental data available (Thelanderson, 1974) have confirmed that pore pressures are seldom of a similar magnitude to material strength. Thus it would appear unlikely that explosive spalling was purely a result of excessive pore pressure within concrete.

Sertmehemetoglu (1977) suggested that spalling resulted from the combined effects of pore pressure and thermally induced biaxial load. The effect of load was simply to create planes of weakness parallel to the heated face of the concrete. He demonstrated that the action of relatively small pore pressures from within such planes could initiate spalling.

However, his theory did not account for the influence of compressive stress in a rigorous manner. Although, biaxial compression promoted cracking, it substantially increased the pressures

necessary to burst concrete. Furthermore, the increased susceptibility of water-cured concrete to spalling was not explained.

Considering the theoretical models put forward by various researchers and described in this Chapter, together with a review of information provided by the experimental programmes reported in Chapter 2 suggests that both thermal stresses and pore pressure stresses need to be present for spalling to occur. It is possible that spalling could be explained by a theory which considers all of the stresses acting within heated concrete.

Adopting a similar approach to Zhukov (1977), it is reasonable to suggest that at any instant in time, the probability of explosive spalling occurring *P(spalling)* may be given by;

$$P(spalling) = \frac{f\,(\sigma_{pore}\ ,\ \sigma_{thermal}\ ,\ \sigma_{load}\ )}{g\ (\sigma_{strength})} \qquad (3.22)$$

where;

σ_{pore} = pore pressure

$\sigma_{thermal}$ = thermal stress

σ_{load} = load induced stresses

$\sigma_{strength}$ = tensile strength of concrete

$f(..)$ = function combining action effects

$g(..)$ = function determining material reaction.

A programme of experimental work was put in hand both to verify the validity in concept of Equation 3.22 and also to quantify the functions $f(..)$ and $g(..)$. The experimental work will be discussed fully in Chapters 4 to 7 and Equation 3.22 evaluated in Chapter 8.

CHAPTER 4. INITIAL EXPERIMENTAL WORK

4.1 INTRODUCTION

A review of the experimental investigations that have been undertaken by previous researchers on the spalling of concrete has been reported in Chapter 2. A number of possible mechanisms for spalling of heated concrete have been discussed in Chapters 3. This Chapter outlines an initial programme of experimental work that was undertaken with the following objectives;

(i) to observe the explosive spalling of heated concrete under controlled conditions

(ii) to determine in an empirical manner the effect on explosive spalling of;

- (a) aggregate type
- (b) concrete strength
- (c) concrete age
- (d) restraint

(iii) to identify a test apparatus and procedure that would be suitable for use in a more detailed subsequent study

This initial experimental work was viewed as a pilot study and was intended simply as a means of developing a "feel" or intuitive understanding for the types of conditions which promoted explosive spalling. No effort was made to conduct a detailed investigation of the interaction between these conditions. It was planned that such interactions would be the subject of a more comprehensive investigation at a later stage.

4.2 PILOT STUDY OF HEATED CONCRETE SLABS

4.2.1 TEST SPECIMEN

The concrete specimens tested were 300 x 300 x 30 mm thick concrete slabs. The slabs had 3 thermocouples cast within them i.e. one at each surface and another at mid-depth. In a simplistic

attempt to measure pore pressure (based on the approach of Nekrasov *et al.*, 1967), a number of specimens had a pair of 3 mm diameter copper pipes cast within them at depths of 10 and 20 mm.

The specimens were tested within a purpose designed mild steel container as shown in Figure 4.1. The container was built of dimensions slightly less than those of the concrete test specimens. In this manner, the specimens were wedged into the steel container to provide a reasonable seal around their edges. This seal was improved by application of a silicone based sealant to the joint between the slab and the sides of the container.

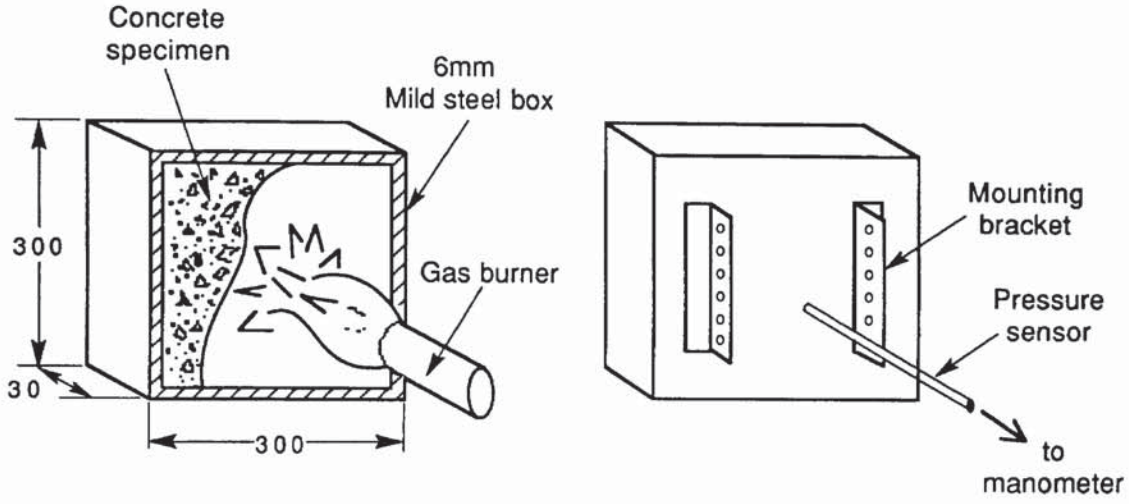

Figure 4.1 Purpose designed mild steel test specimen container

The rear of the steel container opened into a mild steel pipe of diameter 5 mm. The pressure developed between the rear of the specimen and the enclosing steel container was observed by connecting this pipe to a manometer The pipe also served as a means of ducting thermocouple wires from the specimen to the data logging facility.

4.2.2 SOURCES OF HEAT

Three different sources of heat were examined in the pilot study namely;

(i) a 1 m^3 gas-fired furnace heated to the standard BS 476:Pt.20:1987 heating regime

(ii) a gas-fired radiant panel imparting a total heat flux 100 kW/m^2 to the specimen

(iii) direct flame impingement from gas-fired burners

Each heat source induced a different temperature response within the concrete specimens. The different rates of surface temperature rise are given in Figure 4.2 (measured in a typical Gravel aggregate concrete).

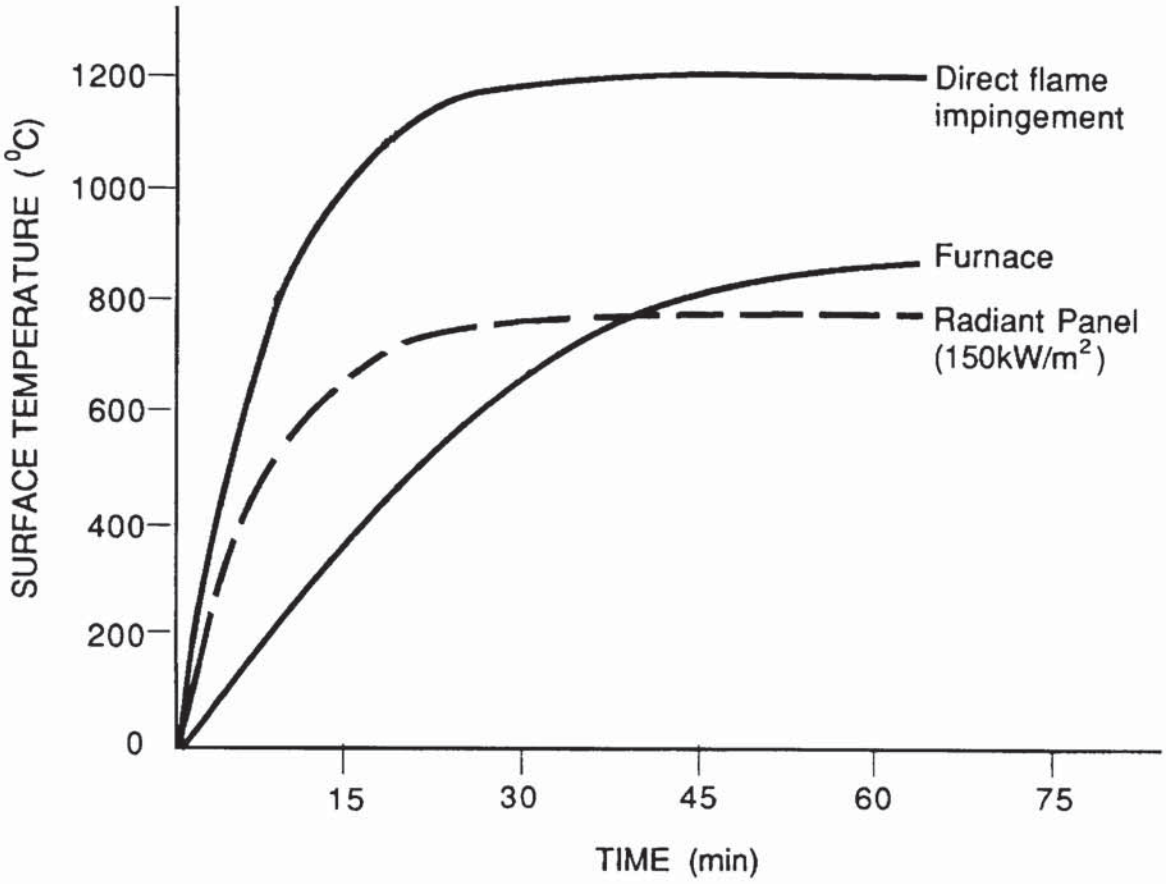

Figure 4.2 Surface heating rates of concrete exposed to several different heating sources

A number of specimens were subjected to the BS 476:Part 20:1987 heating regime within a 1 m^3 gas-fired furnace. Although, such standardised exposure had the attraction of being an established and widely recognised heating regime, thus allowing comparison to be made with a vast database of fire test results, it had several practical disadvantages. These included difficulties in observing the progress of the test and the condition of the concrete's surface.

Similar problems arose in trying to listen for the sound of aggregate's splitting or popping from the surface. A further disadvantage was the fact that hot furnace gases totally surrounded the test specimen, which meant that the specimen holder and thermocouple cable passing from the specimen had to be protected from heat. In addition, measurement of pressure between the concrete and its container was impossible within a furnace environment.

The gas-fired radiant panel proved a reliable heat source. The total heat flux incident on the test specimen was measured using a Gardon heat flux meter and a replacement technique. The test specimen was exposed to a total heat flux of 100 kW/m^2, which is representative of heat flux levels encountered in real fires (Bullock, 1990, personal communication). Radiant panels have been used for many years at the Fire Research Station and are consistent and repeatable sources of heat. The fact that the unexposed face remained relatively cool facilitated instrumentation.

The exposure of test specimens to direct flame impingement provided the most severe thermal assault, with the flames having properties of high temperature and momentum. It was estimated that the flame temperatures were in the order of 1000°C. However, direct flame impingement heating was difficult to replicate on a regular basis. This was primarily due to the fact that the heating was controlled by adjusting the flow of gas to the burners, which unfortunately relied on a coarse and poorly calibrated valve. Such difficulties were exacerbated by use of the burners to perform unrelated fire tests in the periods between spalling investigations.

4.2.3 TEST OBSERVATIONS AND RESULTS

Although, the furnace and the gas-fired burners provided some useful comparative data, the majority of the pilot study was undertaken using the gas-fired radiant panel. As spalling has generally been observed within the first 30 minutes of a standard fire resistance test (Malhotra, 1984), it was considered reasonable to run the exploratory tests for 45 minutes.

The measurement of pore pressure was not particularly successful. High temperatures caused melting of the plastic tube between the specimen container and the manometer. In addition, problems were caused by the condensation of water vapour within the tube causing a blockage. In a number of tests a slight but noticeable increase in the pressure was recorded behind the specimen some time after heating had commenced, but measurements were generally unreliable.

Some aggregate spalling was observed and this will be discussed in detail in Chapter 9. Some surface crazing, cracking and disintegration was also observed in some specimens. The cracking was most severe among the lower strength concretes.

4.2.3.1 Effect of aggregate type

An investigation was made of the susceptibility to spalling of concretes made with different aggregates. The aggregates assessed were;

(i) Thames Valley Gravel, Kingsmead Quarry
(ii) Crushed Granite, Mount Sorrell Quarry
(iii) Lytag, Boral Ltd.

In all cases concrete was made using siliceous gravel sand (St. Albans quarry). The maximum aggregate size used was 10mm. The concretes were designed in accordance with Building Research Establishment guidance (1988) to give 28 day compressive strengths of 20, 40 and 60 N/mm^2. Although there was some variation in the measured 28 day strengths, they were quite small and were not considered further.

The concrete specimens were cast using purpose designed moulds and vibrated using a poker vibrator. The concrete was cured under damp hessian sacking for 2 days, demoulded and then stored under polythene sheet within the laboratory until testing some 28 days after casting.

No explosive spalling was encountered in any of the concretes examined regardless of the heat source used. Concrete made with Thames Valley Gravel, which had been considered by Malhotra (1984) to be particularly susceptible to spalling, showed a similar resistance to spalling as both the Lytag and Granite aggregate concretes.

4.2.3.2 Effect of concrete strength

Concrete with 28 day compressive strengths of 20, 40 and 60 N/mm^2 were exposed to heat 28 days after casting. No explosive spalling was encountered regardless of the heat source used.

4.2.3.3 Effect of concrete age

Concrete made with Thames Valley Gravel aggregate was tested at 4, 7 and 28 days after casting. The compressive strengths were measured by the Building Research Establishment's Concrete Testing Laboratory on the day of test as 26.5, 35.5 and 48.0 N/mm^2 respectively. The moisture contents of the specimens were also measured at the ages of 4, 7 and 28 days and mean values of 6.2%, 4.6% and 2.8% (by mass) were recorded respectively.

It was observed that aggregate splitting was more severe amongst younger concrete specimens. Furthermore, the younger specimens were more friable and distressed after heating probably as a result of their inferior strength. However, all specimens showed a similar resistance to explosive spalling and no surface failure was observed in any case.

Heating tests were subsequently repeated on concrete specimens some 3, 6, 12 and 24 months after casting. Although some useful observations were made regarding aggregate splitting, no explosive spalling was observed in any of the tests undertaken.

4.2.3.4 Effect of restraint

It has been suggested that imposed stresses or edge restraint such as pre-stress may increase the susceptibility of concrete to spalling (Meyer-Ottens, 1972). It was observed during the initial pilot tests that the test specimens bowed significantly on heating. This bowing opened up cracks in the heated surface and appeared capable of alleviating the thermal stresses that might have been developing. Accordingly, a number of tests were carried out on specimens to which a range of different restraining forces had been applied.

A number of 28 day old concrete specimens made with Gravel aggregate were heated after being clamped between 2 no. steel channel sections, which were held together with 12 mm diameter studding and tensioned using a torque wrench to 30 kNm.

A number of specimens of increased thickness were manufactured so that they would effectively restrain themselves. Other specimens were manufactured with an increased surface area of 500

x 500 mm and were exposed to heating over their central 300 x 300 mm. The surrounding concrete perimeter was protected from heat by a ceramic fibre blanket and reflective tin foil.

Three specimens were provided with restraint by casting 9 no. mild steel reinforcing bars (diameter 6 mm) at mid-depth within the concrete specimen. This proved a successful means of preventing thermal bowing. The restraint provided to the concrete specimens in the manner described above did not make any discernable difference in the observed susceptibility of the concrete to spalling. As in previous tests, no explosive spalling was encountered. While restricting thermal bowing did reduce the incidence of surface cracking, somewhat unexpectedly it had little influence on the occurrence of spalling. The concrete specimens were not sufficiently restrained so as to prevent thermal expansion and further work was considered necessary to consider the effects of more substantial restraint.

4.3 FURTHER AD-HOC EXPERIMENTS ON HEATED CONCRETE SLABS

4.3.1 IMPERMEABLE MEMBRANE

Shorter and Harmathy's (1965) prediction of a 'moisture clog' within heated concrete has been widely accepted as a reasonable explanation for explosive spalling. Their theory suggested that moisture may move from the heated face into the depths of a concrete, which will become saturated and effectively impermeable. They suggested that the bursting pressures which cause spalling develop at this impermeable layer called the 'moisture clog'.

A number of ad-hoc exploratory tests were undertaken with impermeable membranes cast into the concrete. The idea was to artificially create (or at least hasten the creation) of the moisture clog. In the first instance polythene membranes were cast into the concrete at a range of different depths (10, 15 and 20 mm). The fact that polythene melts at elevated temperatures was not considered a problem as the membrane was intended to restrict the passage of liquid water at temperatures well below 100°C. However, some membranes made of a tin-foil were also used.

The membranes did not successfully encourage the development of a moisture clog which

initiated spalling. While some water did migrate towards the membrane, the water simply moved laterally and escaped with relative ease from the edges of the test specimens. Thus the pore pressures were effectively alleviated rather than magnified. In addition, the membrane surface acted as a plane of weakness within the concrete specimen and with the occurrence of cracking near the edges, in many cases the tests specimens simply disintegrated. No explosive spalling was observed in any of the 6 specimens tested.

4.3.2 HEATING ON BOTH FACES

It had been observed in many of the initial pilot tests that water escaped through the rear of the specimen. It was thought possible that the escape of this water may alleviate pore pressure, hence explaining the complete absence of spalling in all of the pilot tests. Accordingly, several tests were carried out on C40 Gravel aggregate concrete specimens with heating applied from both sides. Although most of these tests were carried out using the gas-fired furnace, in some cases two sided heating was achieved in front of the radiant panel by positioning the specimen orthogonally to the panel.

Water persisted in escaping from the specimen despite the two sided heating. Water was observed flowing (as a liquid) to the heated surface from whence it vaporised. Such water flows tended to be local to isolated areas of the concrete surface and clearly coincided with cracks. No explosive spalling was encountered in any of the 6 tests undertaken. It was observed that the disintegration and cracking of specimens was significantly increased compared to that observed for one-sided heating tests. This is explained by the increased concrete temperatures associated with two-sided heating.

4.3.3 POORLY COMPACTED SPECIMENS

A small number of tests were carried out on concrete specimens that had not been adequately compacted. These specimens showed no inclination towards explosive spalling.

4.4 DISCUSSION OF INITIAL TEST RESULTS

An extensive array of concrete specimens had been tested without the slightest trace of explosive spalling. Concrete made with aggregates considered susceptible to spalling were heated at rates that were far more severe than the BS 476:Part 20:1987 standard heating regime. Dense concretes with strengths up to 60 N/mm^2 were heated at rates of over 50°C per minute without showing any surface distress. Concrete with micro-silica admixture, old concrete cubes from previous research programmes, even commercial concrete paving slabs were all subjected to severe heating regimes in the search for explosive spalling. In total over 45 exploratory tests were conducted on concrete specimens, many of which a review of the literature (Chapter 3) had suggested would spall explosively. In fact, not one single specimen did.

A clear trend of cracking behaviour was observed in all tests. The stresses, induced by heating the concrete, quickly exceeded the material's tensile strength and most specimens cracked as shown in Plate 4.1. It is possible that cracking not only allowed any pore pressures that had developed to be relieved but also may have alleviated thermal stresses.

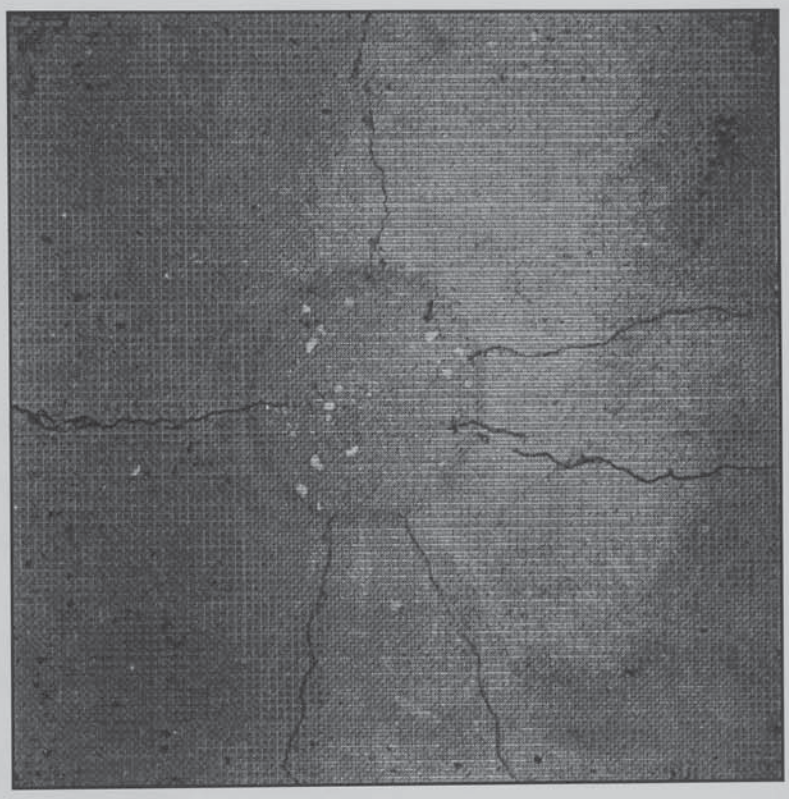

Plate 4.1 Typical crack patterns in heated specimen

Dougill (1971) experienced a similar lack of success in inducing concrete to spall. It appears that his programme of fire tests and the pilot experiments reported in this Chapter were both missing one vital ingredient necessary for spalling, namely restraint. Accordingly further tests were planned to include the effects of restraint.

4.5 EXPLORATORY TESTS ON RESTRAINED CONCRETE DISCS

4.5.1 TEST SPECIMEN

A series of tests were carried out on concrete cast directly into mild steel tubing. The concrete examined had 28 day compressive strength of 40 N/mm^2 and was made with Thames Valley Gravel aggregate. The concrete was cast directly into mild steel tubing with an internal diameter of 150 mm and a wall thickness 6 mm. A number of concrete specimens were prepared with thicknesses ranging from 20 to 200 mm.

The idea behind the tests was that the steel tube would provide a quantifiable level of restraint to the concrete specimens. Although initially the principal variable studied was the thickness of the specimen, it was planned that the effect of differing levels of restraint could be examined by varying the wall thickness of the steel tubing.

4.5.2 SOURCES OF HEAT

The steel tubing was kept cool in order to maximise the edge restraint. Accordingly, a small high intensity gas burner was used to heat the concrete, primarily on the grounds that it could apply high levels of heat accurately as shown in Figure 4.3.

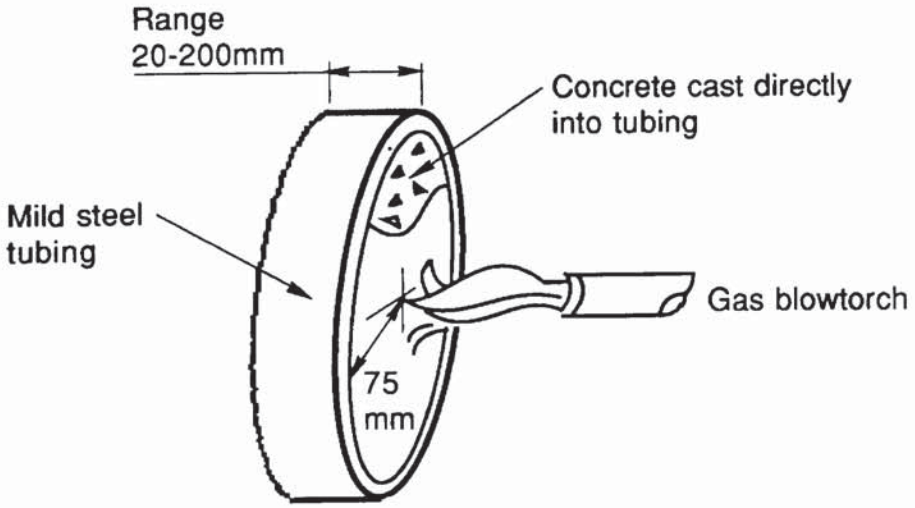

Figure 4.3 Apparatus for heating restrained concrete specimens

It was not the first time that such a heating source had been used in the study of spalling. Sertmehemetoglu (1977) used a similar approach. Edge restraint was further enhanced, by concentrating the heating at the centre of the concrete specimen, thus affording the heated areas additional restraint from the cooler concrete perimeter. As in the pilot tests, the duration of heating was 45 minutes.

4.5.3 TEST OBSERVATIONS AND RESULTS

The results of these tests provided the first major step towards meeting the objectives of the experimental programme, in that explosive spalling was induced in concrete specimens. Although the concrete heated was the exactly similar to that used in over 45 pilot tests, the provision of restraint had clearly effected the propensity of the concrete to spalling. However, it must noted that explosive spalling occurred only under the conditions shown in Table 4.1.

Depth (mm)	One sided heating	Two sided heating
20	Surface Spalling	Explosive spalling
30	No spalling	Explosive spalling
50	No spalling	No spalling
100	No spalling	No spalling
200	No spalling	No spalling

Table 4.1 Results of tests on restrained concrete specimens

There was obviously some other effect involved whereby the thicker concrete specimens did not develop the stresses necessary for spalling. The apparent resistance of thick sections to spalling had been previously noted by Meyer-Ottens (1972). However, as reported in Chapter 3 the models of pore pressure development in locally heated concrete, e.g. Bažant and Thonguthai (1979), do not implicitly recognise the importance of specimen thickness within their analysis.

4.6 CONCLUSIONS

The tests on the restrained concrete discs were very useful and confirmed two important facts;

(1) the edge restraint imposed on concrete influences its susceptibility to spalling

(2) an increase in the thickness of a concrete specimen alleviates spalling

Somewhat excited by this, the first encounter with explosive spalling, it was decided to pursue such tests further, but to abandon plans to cast the concrete in tube sections of varying thicknesses. This decision was taken because of uncertainty regarding the level of restraint afforded to the concrete, both from the relatively cool concrete perimeter and the steel tube itself. Furthermore, the steel tube was discarded because it prohibited the sensible application of load to the concrete specimen. A review of spalling theories detailed in Chapter 3 indicated that external loading was too important to be disregarded. Accordingly, it was proposed to replace the steel tube with a purpose designed loading rig, which could load concrete to quantifiable levels.

Thus, the pilot tests were successful in meeting two of the initial objectives. Explosive spalling had been induced in heated concrete and a clear direction found for further research. The pilot tests allowed the nature of the test specimen to be decided upon and the functions required of future test apparatus were clarified.

The primary function of the test apparatus was to create the conditions necessary for explosive spalling, which have been broadly quantified by the pilot tests as restraint. However, further work would require that both heating and restraining forces be applied in a strictly controlled and quantifiable manner. Thus, a very important requirement of the test apparatus was that it allow all the stresses acting on the concrete to be quantified. This means that the test apparatus had to be designed in such a manner that the load, thermal restraint and internal pore pressures developed within the concrete test specimens can be accurately measured.

CHAPTER 5. EXPERIMENTAL INVESTIGATION OF THE EFFECTS OF SIMULTANEOUS HEATING AND LOADING ON CONCRETE

5.1 INTRODUCTION

A review of the literature reported in Chapter 3 has concluded that the probability of occurrence of spalling *P(spalling)* may be represented as;

$$P(spalling) = \frac{f\,(\sigma_{pore}\ ,\ \sigma_{thermal}\ ,\ \sigma_{load}\ )}{g\ (\sigma_{strength})} \qquad (5.1)$$

The pilot experiments reported in Chapter 4 suggested that the functions f (..) and g (..) are weighted in favour of the thermal and load induced stresses rather than pore pressure. The objectives of the more detailed programme of experimental work, reported in this Chapter, were to verify the validity in concept of Equation 5.1 and to attempt to evaluate the functions f (..) and g (..).

In order to achieve these objectives a structured programme of experimental work was required, where the terms σ_{pore} , σ_{load} , $\sigma_{thermal}$ and $\sigma_{strength}$ were each varied in a quantifiable manner and the effect on *P(spalling)* monitored.

5.2 DESIGN OF HEATING AND LOADING TEST APPARATUS

5.2.1 TEST SPECIMEN

The test specimen was a 150 mm diameter concrete cylinder of depth 100 mm. The specimen was cast using standard cast-iron moulds, which were readily available because of their use for casting specimens for tensile splitting tests to BS 1881:Part 117:1983. The moulds were fitted with purpose-built spacers to enable test specimens of the correct depth to be cast, while still allowing two smooth faces to be achieved.

5.2.2 SPECIFICATION AND DESIGN OF TEST APPARATUS

5.2.2.1 Design function

The test apparatus was designed to provide uniformly distributed loading over the circumferential surface of cylindrical test specimens. The loading had to be measurable throughout its range to a maximum value of 80 N/mm^2. The test specimen was to be heated at such a rate that its surface temperature increased by 5° C per minute. The temperature fields and pore pressures developed within the concrete had to be measurable as did the restraint to thermal expansion.

5.2.2.2 Original design

In the first instance it was decided to mount the specimen within a loading frame. The specimen was contained within accurately machined loading shoes, which imparted a uniform load over its circumferential surface area. The load was to be transmitted from the loading frame to the shoes, via steel loading arms, which were fitted with facilities for measuring the loads transmitted. The loading stresses were to be generated by hydraulic rams within the loading arms. The original test apparatus is shown in Plate 5.1.

The steel loading frame, the loading arms, all connection details and the loading shoes were designed in accordance with BS 5950:Part 1:1990. The structural design calculations are given in Appendix I. The loading shoes were accurately machined to achieve a near perfect fit between the concrete specimen and the shoes. This relatively expensive exercise was undertaken to minimise local stress concentrations. The loading arms and shoes were supported and aligned using a super-structure of steel studding.

The load was applied by hydraulic rams in both the vertical and horizontal direction. The magnitude of the applied load was measured using a load cell. Both rams were supplied from the same hydraulic pump and acted equally in both directions.

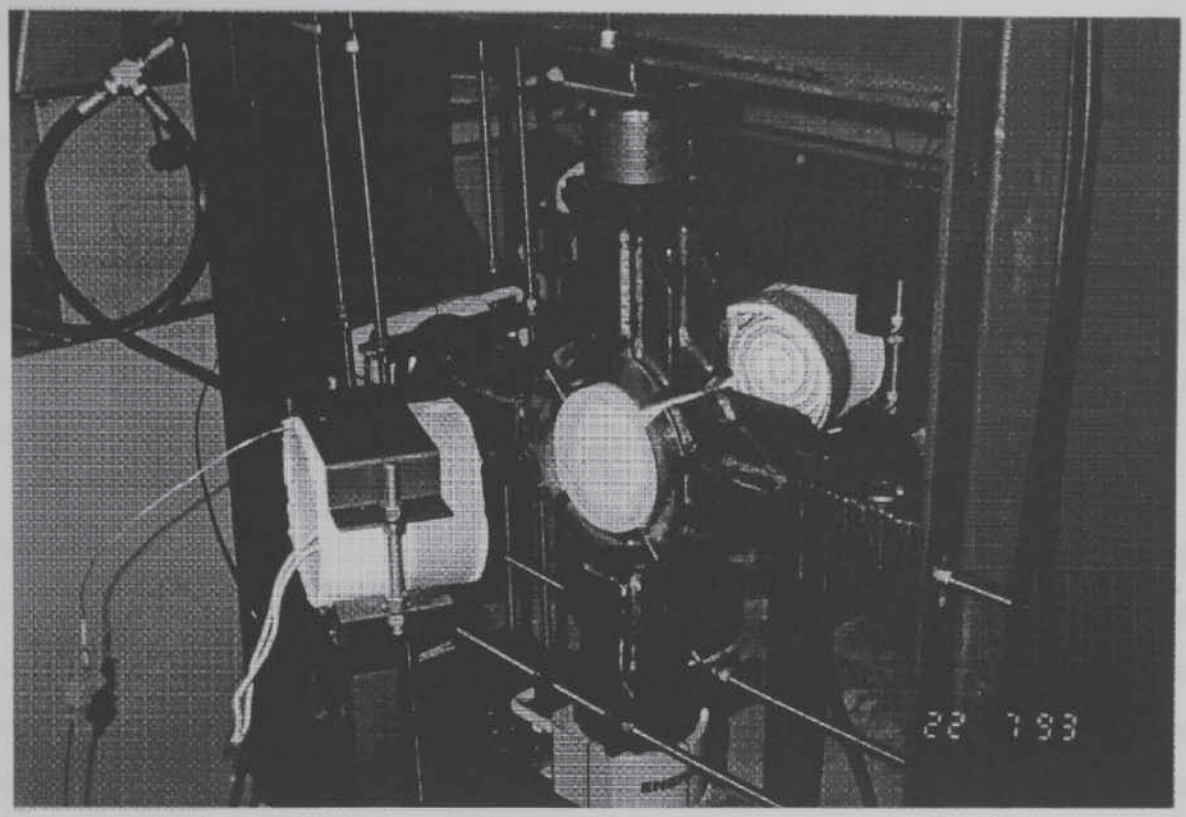

Plate 5.1 Heating and loading test apparatus

Pore pressures were measured by casting a hollow ceramic tube into the test specimen. This tube was then connected to a pressure transducer. Pore pressure measurement will be discussed fully in Section 5.3.3.3.

After conducting some commissioning tests, an unforeseen problem was encountered with the test apparatus, namely lateral instability. Due to the size of the test specimen and the span of the loading arms slight eccentricities in alignment across either of the loading arms resulted in lateral movement and instability at high load levels. Although, in theory such instability should not have occurred, practical limitations in alignment accuracies meant that it did.

Every effort was made to enhance and improve the alignment procedures. The loading arms were plumbed vertically in line. A framework of steel rods and bars were clamped onto the rig to provide a measurement datum against which all items within the test apparatus could be accurately positioned. The measures to improve specimen alignment were reasonably successful. However improvements only succeeded in deferring the onset of instability to increasingly high loads. At the load levels examined, discrepancies in alignment of less than 0.5 mm could cause instabilities and regular alignment to within such a tight tolerance was beyond the test procedure

originally envisaged.

To overcome the problem, side plates were fitted to the loading shoes so that at high load levels lateral movement would be prevented. In effect the test apparatus was made rigid in the lateral direction, while remaining pinned in the plane of application of load. The modified loading shoes and connections are shown in Figure 5.1. The success of the modification relied on a very close machined fit between the connection from the load arm to shoe. The central alignment of the shoe on the pin was guaranteed by using spacer plates and a "letter-box" approach.

The modified and laterally rigid test apparatus was successful up to a point. However, as with the alignment improvements, the new connections succeeded only in deferring the onset of lateral instability. When instability did occur, the side plates proved inadequate and the welds between the side plates and the connector were simply torn apart, albeit in a gradual manner. As a result there were two options, namely strengthening the side plates or the redesigning the test apparatus. It was decided to adopt the latter option.

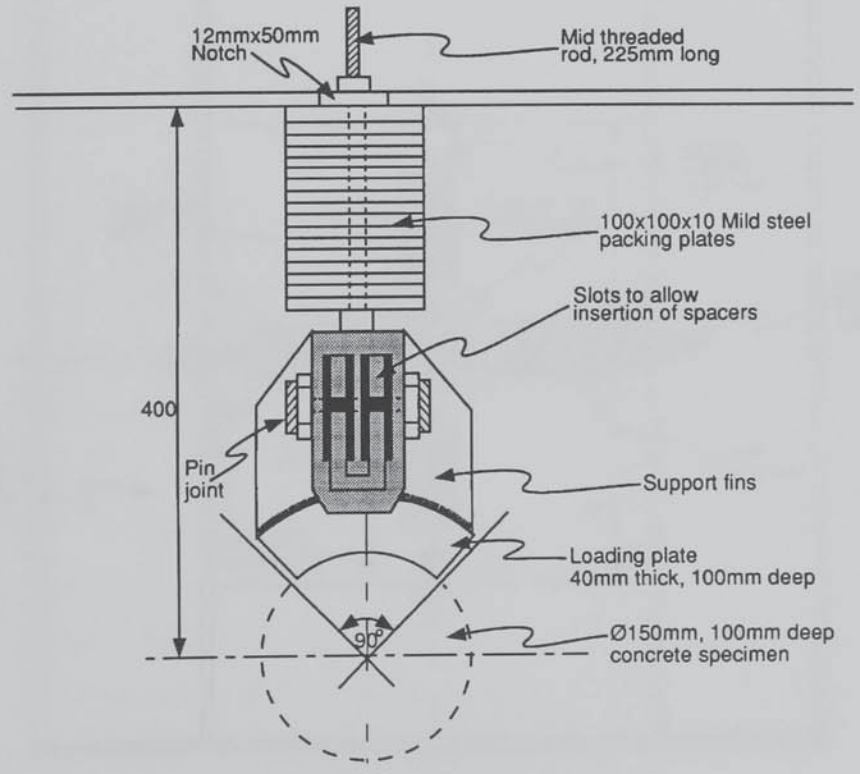

Figure 5.1 Design of laterally rigid connection between loading arms and shoes

5.2.2.3 Improved design

The test apparatus was redesigned to include a change in the connections between the loading arms and loading shoes. All in-plane and lateral flexibility was removed from the joints. It was decided that the risk of slightly non-uniform application of load through a rigid connection outweighed the problems of lateral instability. The lateral stability of the test apparatus and more particularly of the test specimen was considered to be fundamentally important. The safety risks associated with the release of suppressed lateral instability under conditions of high imposed load and thermal restraint, outweighed all other concerns from the design viewpoint.

The connections were redesigned as rigid in all directions and an improved test apparatus constructed as shown in Figure 5.2. This simplified the entire test procedure and made placing, positioning and general alignment of the test specimen much easier. It was hoped that careful alignment would reduce the possibility of non-uniform loading to the test specimen.

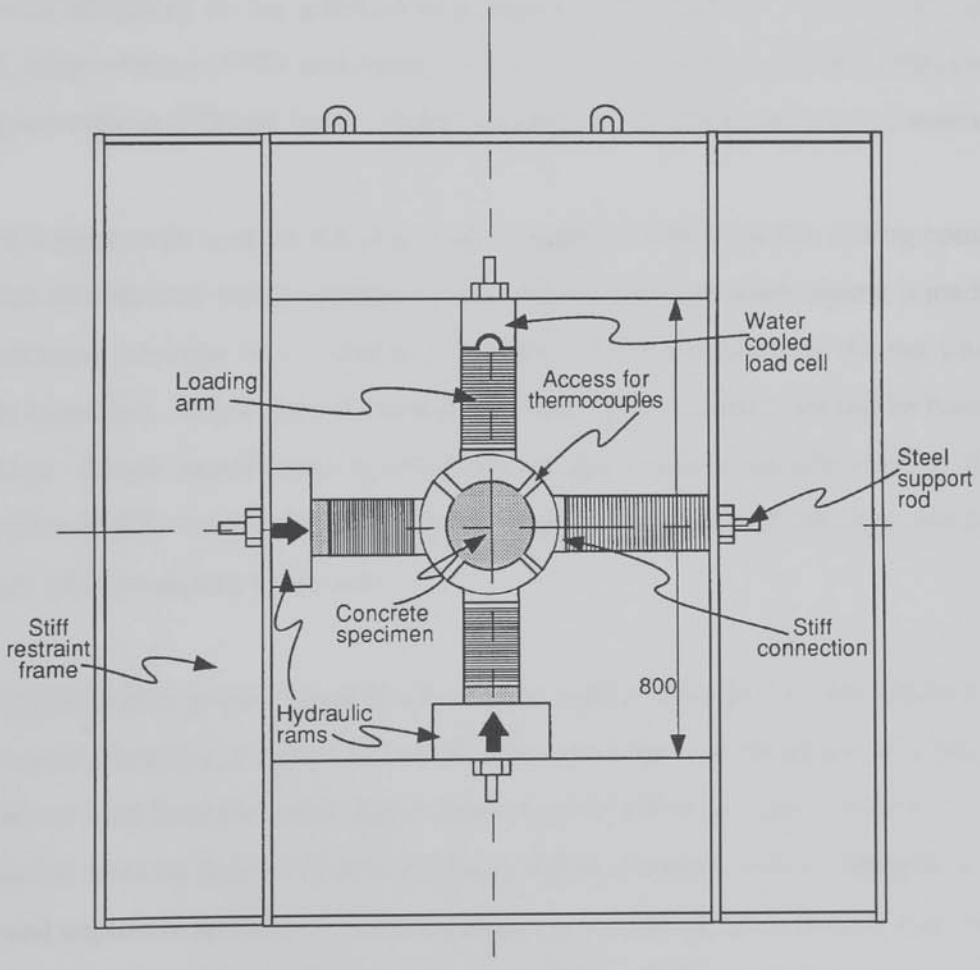

Figure 5.2 Improved test apparatus

5.2.3 SOURCE OF HEATING

5.2.3.1 Design Criteria

The design criterion for the heating source included;

(i) provision of adequate heating levels
(ii) safety in use
(iii) maintenance of visibility of the test specimen
(iv) robustness on exposure to exploding concrete

or

easily and inexpensively repaired or replaced

While the majority of these requirements were straightforward and indeed obvious, further thought was necessary on the question of adequate heating levels. As has been discussed in Chapter 2, Meyer-Ottens (1972) and Austin *et al.* (1992) observed completely different behaviour by heating concrete at different rates. Higher heating rates represented a more severe condition.

At a more fundamental level, it has long been recognised within the fire testing community that specification of a heating regime simply in terms of a time-temperature regime is inadequate. As the temperature response of a concrete specimen will be governed by the net total heat flux incident to its surface, proper specification of the heating environment should be based on a heat flux criterion. Simple specification of a time-temperature regime considers neither the variation in emissivities of different heat sources nor the variation in surface emissivities and heat transfer coefficients of the concrete specimen.

Thus, it was decided to specify target levels of total incident heat flux to the concrete specimens, both for correctness and to allow the work to be reproduced as necessary at a later date. The target levels of total heat flux were decided based on information from real fires, as examined in large scale fire tests by Bullock (1990, personal communication) and summarised in Figure 5.3. He observed explosive spalling of concrete panels in these tests and hence it may be concluded that such heat flux levels impose a reasonably severe thermal assault on the concrete. The design heat fluxes were thus chosen as total incident heat flux levels of 80, 110 and 140 kW/m^2.

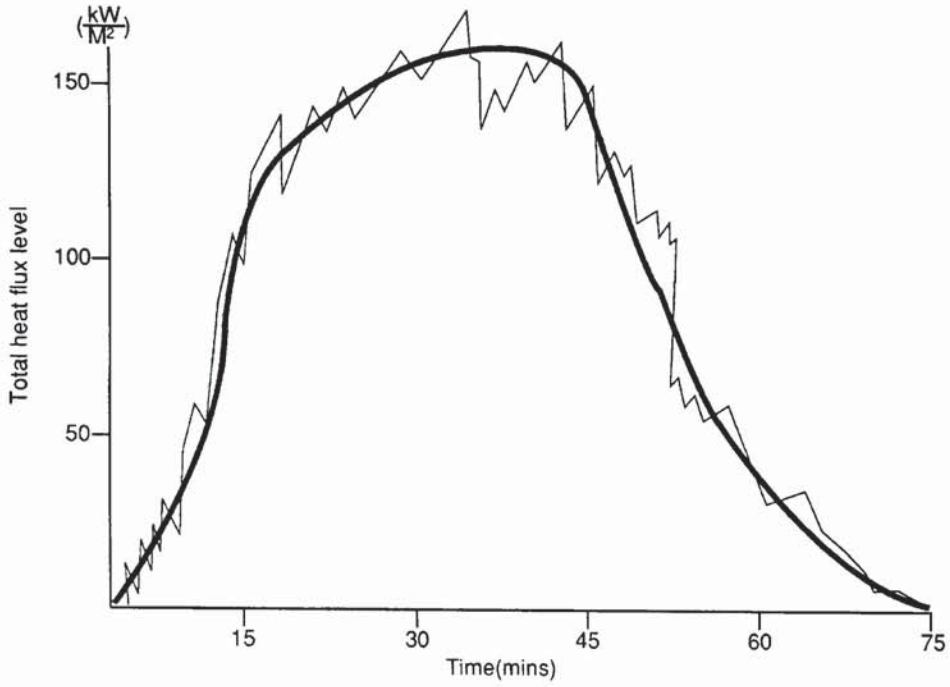

Figure 5.3 Heat fluxes recorded in real fires (after Bullock, 1991, personal communication)

5.2.3.2 Electrical heating

As had been investigated in the exploratory pilot tests, a range of heating sources were available. These ranged from a 1 m^3 gas-fired fire resistance test furnace to a gas-fired blow torch. It was decided that the sensible choice of heat source would be one which could be applied locally to the test specimen without heating the rest of the test apparatus. This would avoid the need for protection to the steelwork and would make test measurements and data capture far easier.

As the tests were investigating a surface phenomenon, the test specimen had to be always visible during heating. Thus, it was decided to use a form of radiation heating from either a gas or electrical source. As gas burners required some associated infra-structure, it was decided to use an electrical radiative heat source on the grounds of simplicity.

It was quite difficult to locate an electrical radiating panel capable of providing the requisite quantity of heat without large operating currents. The choice of heating panels was further reduced by the explosive and violent nature of spalling, which meant that the heaters had to be either substantially robust or alternatively easily (and inexpensively) replaceable.

An appropriate high resistance heating element was sourced from Kanthal Electrical Ltd. The heating elements were capable of producing heat flux levels of some 150 kW/m^2. The heaters were relatively inexpensive and were designed to withstand temperatures of some 1400°C. The heating wire was sufficiently flexible to be coiled in a tight circle of radius 4 mm.

A number of purpose designed heating discs were constructed for this research programme by Kanthal. The coiled heating wire was laid in increasing circles within a ceramic backing disc of diameter 150mm. The heating disc was placed directly opposite to the test specimen and the heating conditions monitored to ensure that they met the design criterion. In fact, they did not.

The difficulty was that in order to view the concrete the heating discs had to be a reasonable distance from the surface. This allowed most of the generated heat to escape to the surrounding atmosphere by convection. The problem was solved by constructing a purpose-designed enclosure around the heating disc to reduce losses. The enclosure essentially formed a miniature furnace with the concrete specimen making up one wall. The heating device is shown in Figure 5.4.

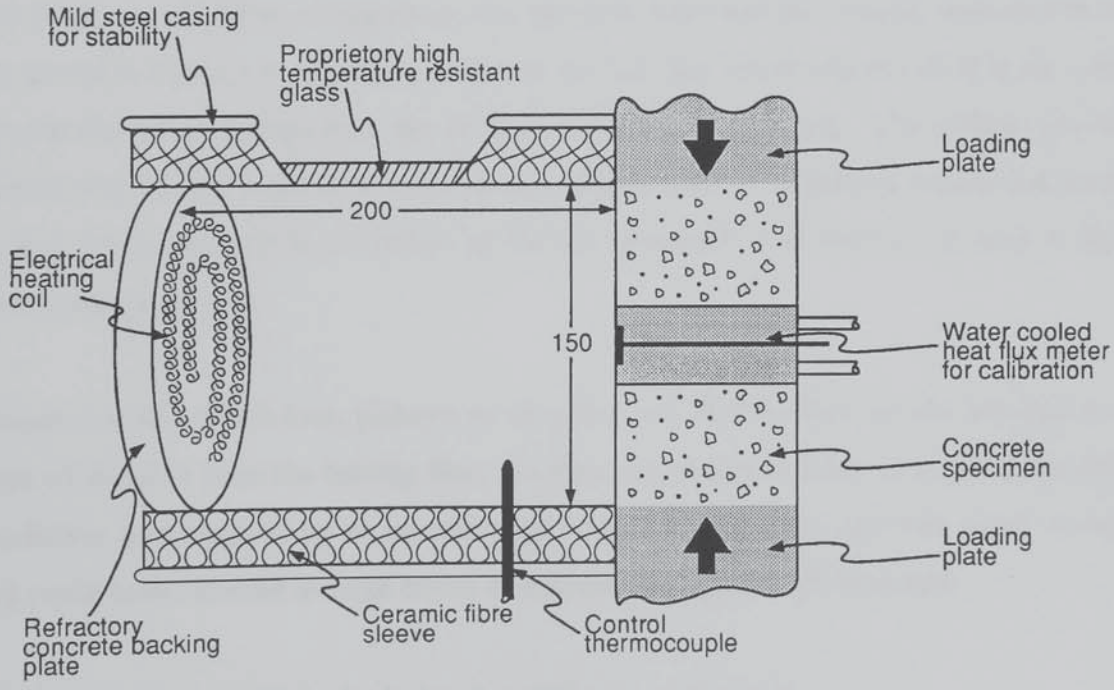

Figure 5.4 Heating enclosure (with calibration arrangement)

The heating enclosure was lined with a ceramic fibre insulating material to minimise conduction heat losses. The design requirement of specimen visibility was met by incorporating a window into the heating enclosure. The window was sealed with a proprietary fire resisting glass which was capable of sustaining exposure to temperatures of up to 1200°C.

5.2.3.3 Calibration of heat source

The total heat flux levels produced by the heating discs were recorded using a Gardon heat flux meter. The heat flux meter was manufactured by Medtherm and had been recently calibrated by the Building Research Establishment Radiometer Calibration Service. A heat flux meter measures the total incident heat flux falling on its surface, i.e. both radiative and convective heat flux.

As the heat flux within the heating enclosure had a large convective component, it was significantly affected by the heat balance within the enclosure. Thus, it was necessary to calibrate each heating enclosure that was eventually used during the experimental programme.

Accordingly, a calibration arrangement was set up to represent the heating enclosure in its end use as shown in Figure 5.4. It may be seen that the heat flux meter was mounted in the centre of a concrete disc with its measuring face flush with the concrete surface. The calibrating concrete specimen was, in fact, a remnant from the exploratory tests on restrained concrete discs and as such had the same material properties as the test specimens that were to be used in the later experimental programme.

Although initially it had been planned to vary the heat flux incident on the test specimen by varying its distance from the heating disc, this idea was abandoned due to its poor repeatability. As radiation is attenuated by an inverse square law with distance, relatively small positioning errors could have resulted in large errors in incident heat flux to the specimen.

Three measurements were made during the calibration procedure;

(i) total incident heat flux on calibration plane

(ii) power flow to electrical heating disc

(iii) temperature within the heating enclosure

As the test apparatus consisted of two heating enclosures, the calibration exercise was carried out twice. However, both heating enclosures performed reasonably similarly. In the subsequent experimental programme the heating enclosures were recalibrated after any change had occurred in their operation. This happened several times when explosive spalling necessitated replacement of a heating disc.

The pattern of behaviour observed during the calibration exercise was that for any particular electrical power setting, an equilibrium heat balance was set up and both the temperature within the heating enclosure and the total heat flux incident upon the test specimen stabilised at constant levels. In general, equilibrium was achieved within approximately 10 minutes. The development of heat flux to the specimen versus electrical power input is given in Figure 5.5. This Figure allowed power settings to be chosen against which the development of total heat flux and enclosure temperature could be monitored. These were compared to the target heat flux levels of 80, 110 and 140 kW/m^2 and adjustments made to the power settings until the targets were met. The power settings were noted and their full calibration curves recorded as shown in Figure 5.6.

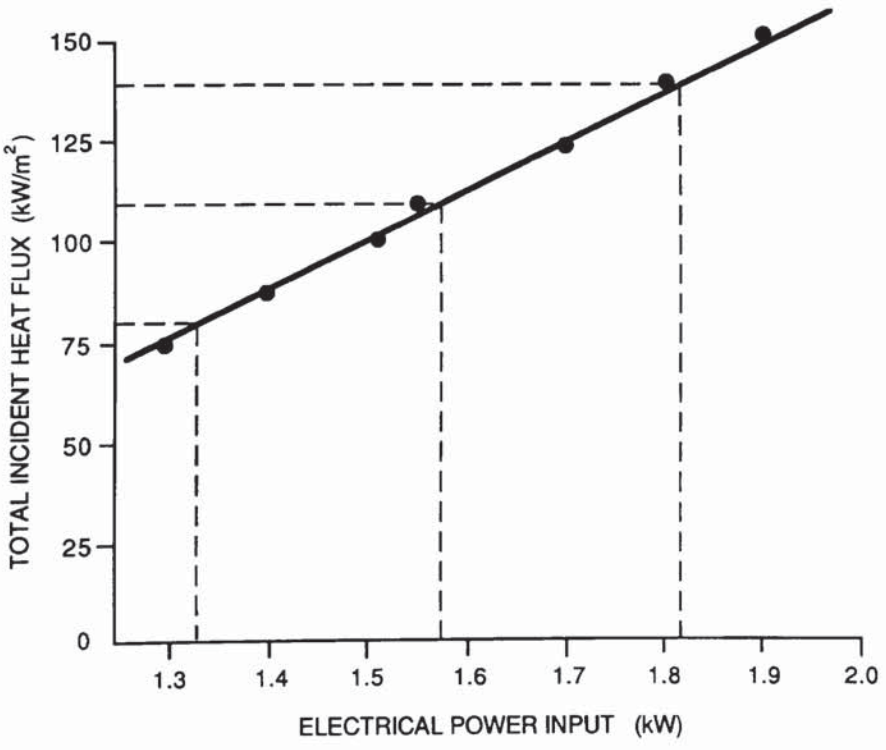

Figure 5.5 Total incident heat flux to the calibration element versus input electrical power

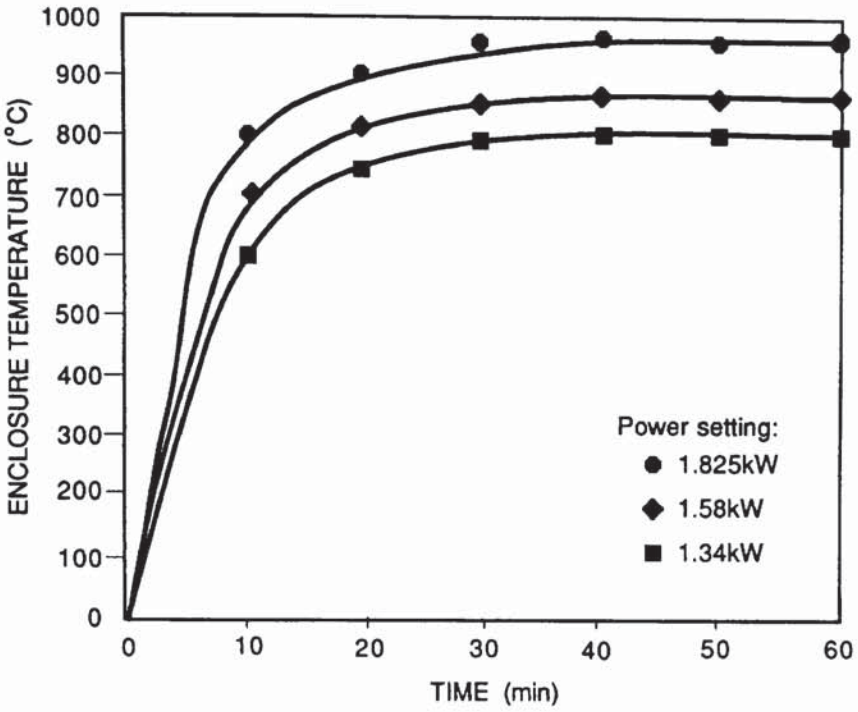

Figure 5.6 Calibration curves for heating enclosures

It may be observed that the heating regimes do not appear to generate significantly different temperature regimes within the heating enclosures. However, the different power levels resulted in a significant change in the intensity of the heating coils. Given that the principle mode of heat transfer is radiation, the various power levels resulted in quite different surface temperatures in the concrete specimens. This point is illustrated in Chapter 6, where the actual specimen temperatures are presented and discussed.

5.3 TEST PROCEDURE

5.3.1 CONCRETE MIX DESIGN

The concrete specimens all had the same fundamental mix design. Every effort was made to make the concrete mix representative of that which might be encountered as typical of concreting practice in the United Kingdom. The mix proportions, which were arrived at using Building Research Establishment (1988) guidance, are given in Table 5.1.

MIX DESIGN DETAILS	**TARGET FREE W/C 0.50**	**TARGET FREE W/C 0.40**	**TARGET FREE W/C 0.30**	**EXTRA SAND MIX**	**MICRO-SILICA MIX**
OPC (kg)	8.410	10.510	14.010	12.859	11.350
MICROSILICA (kg)	-	-	-	-	2.522
20-10mm (kg)	21.642	21.642	21.642	22.453	25.969
10-5mm (kg)	10.698	10.698	10.698	11.226	12.836
SAND (kg)	13.135	10.841	5.707	18.135	13.009
TOTAL WATER (kg)	4.950	4.950	4.922	5.939	5.941
FREE WATER (kg)	4.121	4.099	4.203	5.049	4.953
ACTUAL FREE w/c	0.49	0.39	0.30	0.39	0.39
CONPLAST 211 (kg)	-	-	0.068	-	0.045
SLUMP (mm)	40	40	40	40	40
DENSITY (kg/m^3)	2362	2372	2386	2360	2350
Aggregate / Cement	5.41	4.11	2.72	4.49	4.11
% FINES	28.9	25.1	15.0	31.4	25.1
CEMENT CONTENT (kg/m^3)	338	425	587	430	421

Table 5.1 Concrete Mix Design

The coarse Thames Valley aggregate was from the Kingsmead Quarry. A petrographic examination of the Gravel was undertaken by the Building Research Establishment's Petrographic Analysis Unit and the results are given in Table 5.2. The fine aggregate was siliceous gravel sand from Smallford Quarry, St. Albans, Hertfordshire.

Mineral	**Percentage**
Quartzite	5.2
Flint	93.5
Sandstone	0.7
Limestone	0.6

Table 5.2 Petrographic Profile of Thames Valley Aggregate

5.3.2 PRODUCTION OF TEST SPECIMENS

5.3.2.1 Casting of test specimens

All concrete test specimens for this research programme were produced by the Building Research Establishment Concrete Laboratory under strict quality conditions. The specimens were cast in batches to allow for scheduling of the test programme. A batch consisted of a range of specimens types. Obviously the majority of the batch was made up of cylindrical test specimens. One third of these specimens had thermocouples fitted. In order to allow measurement of pore pressure, 20% of test specimens were fitted with hollow ceramic tubes as described in Section 5.3.3.3

For quality control purposes 2 no.100 x 100 x 100 mm concrete cubes were cast for determination of the concrete's 28 day crushing strength. In addition, 2 no.300 x 150 mm concrete cylinders were cast to measure the 28 day splitting strength of the concrete as measured by BS 1881:Part 117:1983.

Two 100 x 150 mm concrete cylinders were cast in each batch. These were identical to the test specimens in every way except for the fact that one surface was not smooth. This allowed them to be cast in the end of standard moulds used for tensile splitting test specimens. These samples were kept in the same environment as the test specimens and were used for the determination of the specimen's moisture content immediately prior to testing.

5.3.2.2 Curing and conditioning of test specimens

After casting, the concrete specimens were immediately cured under damp sacking. The specimens were demoulded after 24 hours and placed under water at 20°C. Water-curing was chosen, as Akhtarruzaman and Sullivan (1970) had suggested that water-curing increased the susceptibility of concrete to spalling.

The specimens were removed from water after 14 days and were placed in a conditioning room under conditions of constant temperature (20±2°C) and relative humidity (50±20%). Some 28 days after casting the specimens were tested. Those specimens which could not be tested

immediately at 28 days were sealed in polythene bags within the conditioning room, until the first opportunity at which they could be tested.

The standard cubes and cylinders for compression and splitting testing were all tested some 28 days after casting. These tests were carried out by the Materials Testing Section at the Building Research Establishment and the results are presented in Chapter 6.

5.3.3 Test measurements

5.3.3.1 Temperature

The temperature was recorded throughout the depth of the concrete specimens using Chromel-Alumel (Type K) thermocouples. The thermocouples were made using bare wires (gauge 20) welded together at the heated junction. The thermocouples were cast into one surface of the concrete and at depths of 5, 10, 15, 30, 50, 70, 85, 90 and 95 mm. Thus an almost symmetrical thermocouple array was put in place and symmetry was used to give a basic check on the gross accuracy of the measurements.

The placing of the thermocouples within the concrete was undertaken using a purpose built template as shown in Figure 5.7. Reasonably accurate positioning of the thermocouple wires within the template was achieved by clamping the wires across the flanges of the specimen mould.

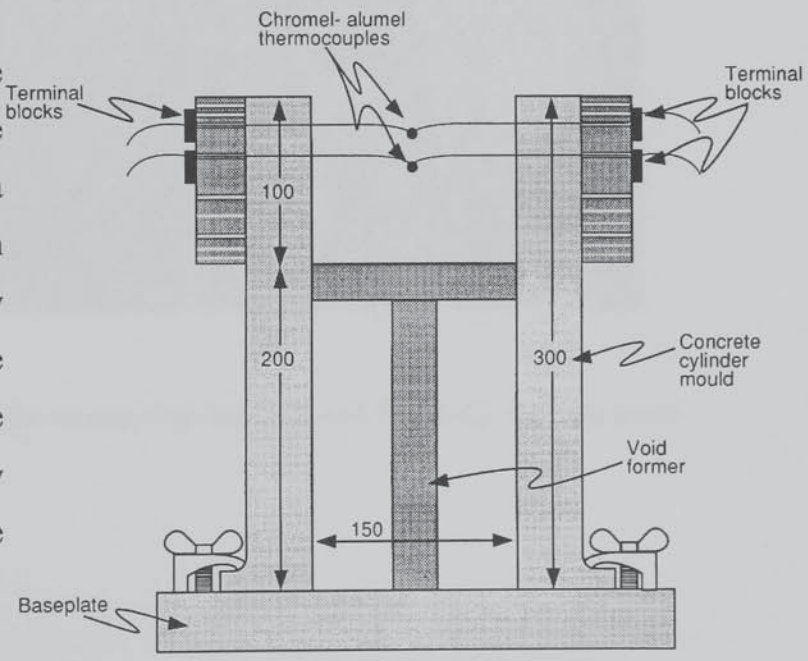

Figure 5.7 Specimen mould and thermocouple template

5.3.3.2 Restraint and imposed load

The load imposed upon the specimen and the restraint to thermal expansion developed within the loading arms were recorded using an Elliot C60 load cell, as shown in Plate 5.3. The load cell had a working range of 500kN. The load cell was calibrated by the Building Research Establishment's Instrumentation Laboratory. It was calibrated together with the connection plates and fixings that were used in the test apparatus.

A secondary check on the magnitude of the loads imposed on the specimens was given by monitoring the pressure within the hydraulic system to the loading rams which was directly related to the stress applied to the test specimen. This provided a useful check on the gross accuracy of the load measurement during the period of the test.

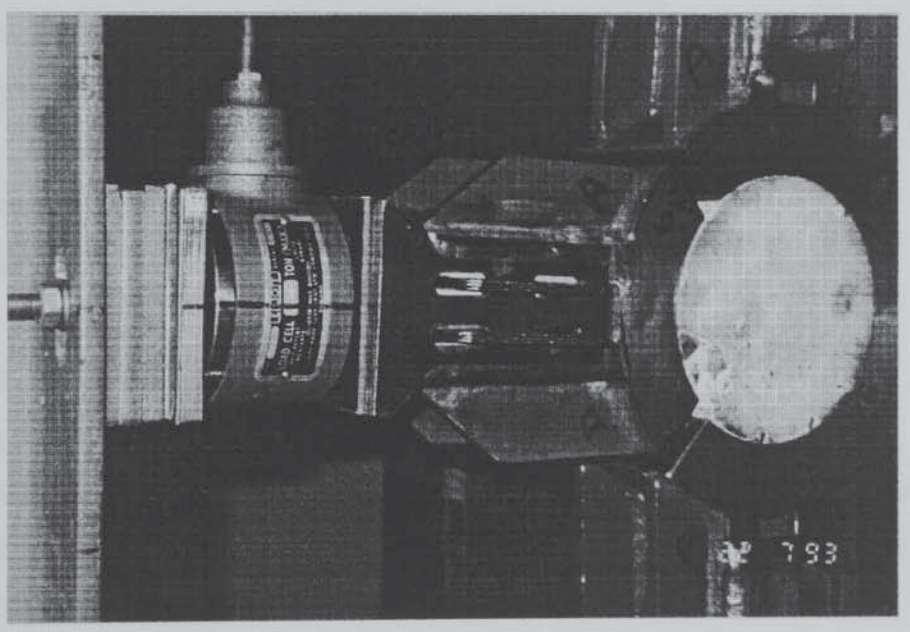

Plate 5.2 Load cell for monitoring imposed and thermally induced loads

5.3.3.3 Pore pressure

The pore pressure developed within the heated concrete was measured using a modification of the technique used by Bremer (1967), Nekrasov *et al.* (1967) and Harada and Terai (1991). Two ceramic tubes were cast into the concrete specimen at one third and two third depths. The tubes

had an outer diameter of 8 mm and each contained 2 no. 2 mm holes. These holes transmitted the pore pressure. In early tests, the end of the ceramic tubes within the concrete, were fitted with 10 mm of cylindrical porous polyurethane foam. The foam provided a pore of known volume at the end of the tube in which pressures could develop and also prohibited the cement paste from blocking the measuring tube. The measuring technique is illustrated in Figure 5.8.

However, an improved technique was devised and employed in the majority of the tests which involved sealing the holes in the tube using well-fitting wire. The tube could be cast into the concrete without the foam as the wire kept the holes clear. Several hours after the concrete had been cast and it was relatively stiff, a void was created at the end of the tube by withdrawing the tube by 5 mm. The wire was also retracted at this stage.

The ceramic tube was connected to a pressure transducer, via a length of copper tube and some compression fittings. The pressure transducer was capable of reading pressures up to 10 N/mm^2. Its output was connected to a Schlumberger data logging device to give on-line data capture. The transducer was kept within its operational temperature limits by water cooling.

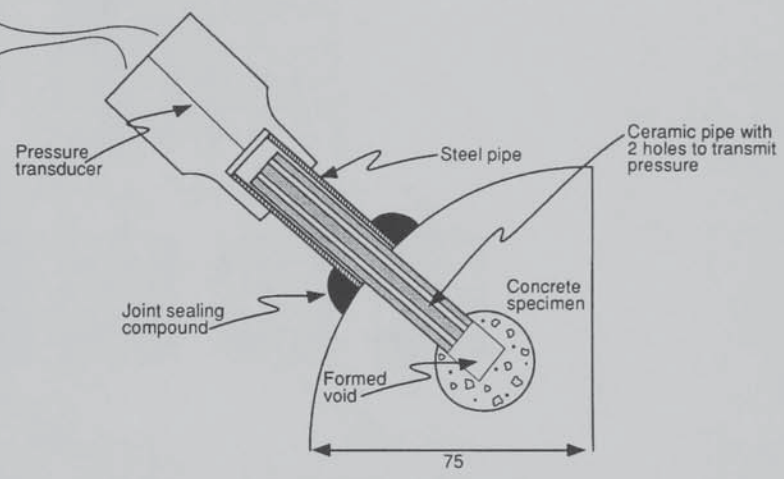

Figure 5.8 Arrangement for measuring pore pressure developed in heated concrete

5.3.3.4 Extent of spalling

The extent of spalling was measured by using a purpose built circular steel counting grid. The steel grill was placed over the test specimen, immediately after heating had ceased. The number of grid squares (10 x 10 mm) placed over concrete that was more than 50% damaged were counted. This figure expressed as a percentage of the total surface area provided a measure of the extent of spalling.

The depth of spalling was measured using a depth gauge. The depth of spalling was measured at the grid points and this allowed the volume of spalling to be calculated. In most cases, the simplest and most instructive measurements were the number of spalls, the surface area of the largest spall and the mean spalling depth.

5.4 DESIGN OF EXPERIMENTAL PROGRAMME

The influence of a range of variables on the occurrence of spalling were studied. The structures of the experimental programme is presented in Figure 5.9.

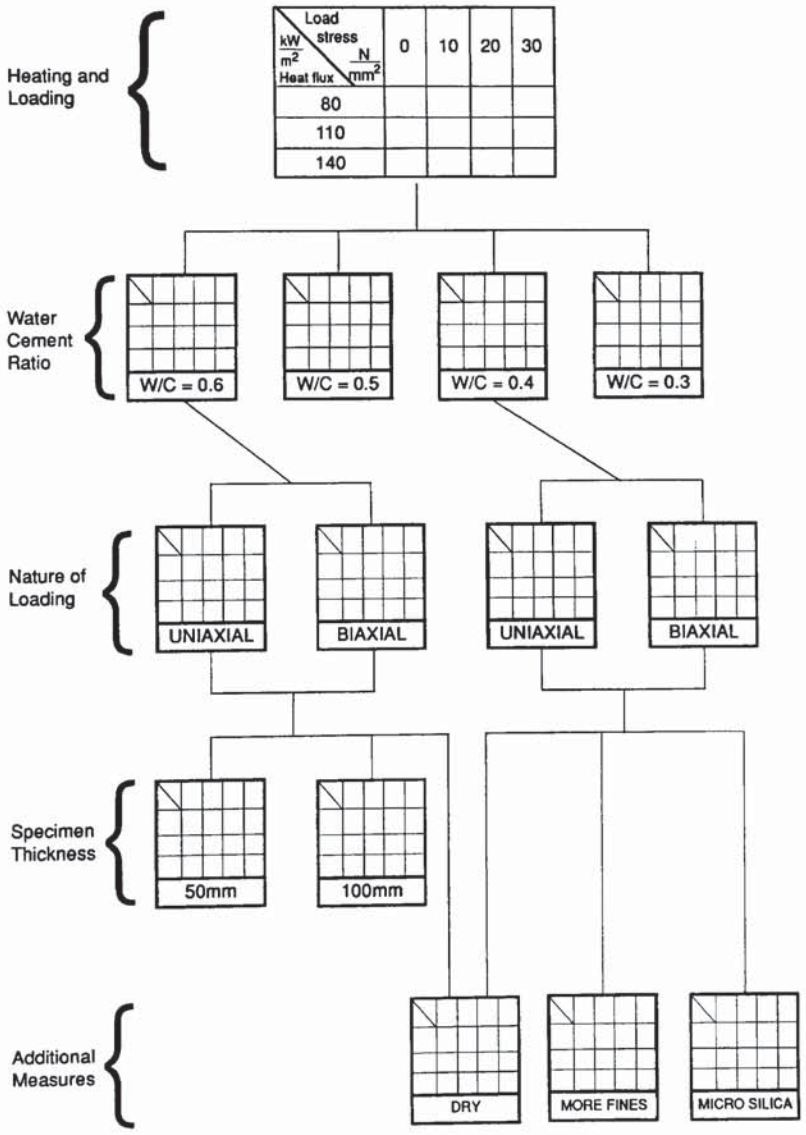

Figure 5.9 Structure of experimental programme

The final version of the heating and loading test facility is shown in Plate 5.4. The programme of structured tests detailed in Figure 5.9 was carried out using this rig. The details of the experimental data recorded are described in Chapter 6.

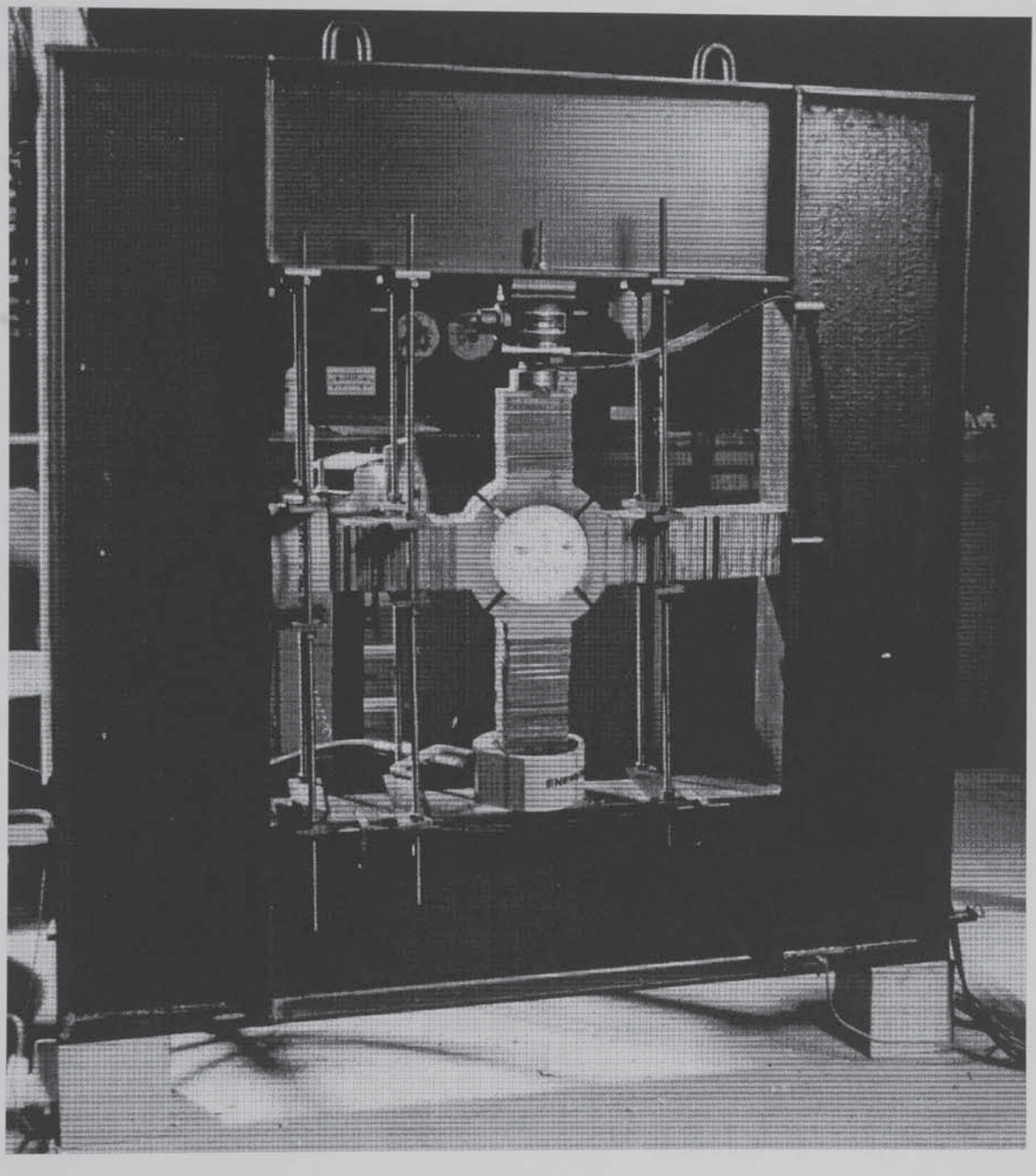

Plate 5.3 Final version of test rig

CHAPTER 6. RESULTS OF HEATING AND LOADING TESTS

6.1 OVERVIEW

The programme of experiments detailed in Figure 5.9 requires over 154 individual tests to be undertaken. Given the nature of spalling, it appears important to replicate each test several times thus further increasing the total number of tests required. However, by considering the choice of tests undertaken in a quasi-random manner, the total number of tests was reduced to just over 200. This permitted extensive repetition of some of the more critical tests.

Ideally, the test programme should have been planned using randomisation techniques, such as latin squares, to eliminate errors due to differences between specimens from different batches. However, the nature of the experiments did not lend themselves to such an approach. For example, if it were assumed that all the specimens within one batch were acceptably similar, the effects of differences between batches could be minimised by randomly distributing the specimens from one batch throughout each heating/loading test matrix (shown in Figure 5.9). However, as the specimens had to be tested 28 days after casting, all the specimens in one batch had to be tested on the same day. It was considered that more errors would be introduced by the necessary varying of heating and loading levels within a day's experiments than would be reduced by randomisation. Accordingly, priority was given to minimising the changes to the heater settings.

The differences between batches of specimens were kept to a minimum by the operation of a rigorous quality control regime (approved by NAMAS) within the Concrete Laboratory at the Building Research Establishment (BRE). Some limited randomising of samples was undertaken by allowing some tests dates to slip to the 29th and 30th day after casting.

6.2 MATERIAL PROPERTIES

6.2.1 MATERIAL STRENGTH

The test specimens were cast in batches of one dozen. In each batch two 150 x 150 mm cubes

and two 300 x 100 mm concrete cylinders were cast for the determination of the compressive and tensile splitting strengths of the concrete mix. The density of the concrete was also measured. The measured material properties are given in Table 6.1.

Sample Ref.	W/C Ratio	F_{cu} (N/mm^2)	$F_{cylinder}$ (N/mm^2)	ρ (kg/m^3)
A93/148	0.6	42.0	3.45	2360
A93/149	0.6	42.5	3.60	2360
A93/214	0.6	40.8	3.40	2355
A93/222	0.6	42.3	3.45	2355
A93/224	0.6	41.8	3.50	2360
A93/230	0.6	41.8	3.47	2355
A93/241	0.6	42.8	3.35	2355
A93/248	0.6	42.0	3.40	2360
A93/256	0.6	42.3	3.22	2355
A94/035	0.6	42.0	3.47	2350
A94/098	0.6	41.8	3.35	2355
A94/121	0.6	41.5	3.40	2355
A94/141	0.6	42.0	3.40	2355
A94/162	0.6	42.3	3.30	2350
A94/179	0.6	42.0	3.40	2355
A94/231	0.5	50.8	3.70	2365
A94/232	0.5	50.0	3.60	2365
A94/233	0.5	50.3	3.70	2365
A94/234	0.4	63.3	4.10	2385
A94/235	0.4	63.0	4.10	2385
A94/236	0.4	63.0	4.05	2385
A94/237	0.3	68.8	4.80	2390
A94/238	0.3	69.0	4.75	2390
A94/239	0.3	68.3	4.80	2390
A94/336	0.4	62.0	4.10	2385
A94/422	0.4	67.0	4.80	2369

Table 6.1 Measured properties of test specimens

The concrete cubes and cylinders were tested at the Concrete Testing Laboratory of the BRE. The compressive strength F_{cu} was determined in accordance with BS 1881: Part 116:1983, with the load being applied at 0.25 N/mm^2/s. The tensile splitting strength $F_{cylinder}$ was determined in accordance with BS 1881:Part 117:1983, with the load being applied at 0.03 N/mm^2/s. The density ρ of the concrete was measured in accordance with BS 1881:Part 114:1983.

6.2.2 RELATIONSHIP BETWEEN STRENGTH OF SPECIMEN WITHIN TEST RIG AND COMPRESSIVE STRENGTH

The factors considered in the design of the test rig for imposing multi-axial load on concrete specimens have been discussed in Chapter 5. The test rig transfers load to cylindrical concrete specimens through four curved loading shoes. Although load may be imposed on the specimen in one direction alone if required, such loading is not strictly uni-axial and is certainly not uni-axial in the same sense as the load applied in the standard compression test. Accordingly, the compressive strength of the concrete making up the test specimen does not directly represent the ability of the specimen to sustain loads within the test rig.

A series of commissioning tests were undertaken to ascertain the load levels that caused failure of the cylindrical concrete specimens in the test rig. Two series of tests were carried out, firstly with the loads applied in a single direction and secondly with loads applied in both axial directions. All loads were applied at a rate of 0.25 N/mm^2/s. The load was applied until the specimen failed, with failure being defined as inability to sustain further loads, which was signalled in practice by a sudden loss in the reaction afforded to the hydraulic rams.

The typical modes of failure observed are shown in Plate 6.1 and 6.2. Fracture of the specimen was observed both in the cement matrix and across aggregate particles. Failure was violent in most cases, but particularly when the specimens were loaded in both axes. In such cases, the failure plane was parallel to the unloaded face at a depth of roughly one quarter the specimen thickness. This correlates with some observations on failure modes of bi-axially loaded concrete specimens reported by Robinson (1967) and Sertmehemetoglu (1977).

It is recognised that the loads imposed on the cylindrical specimens are not strictly speaking bi-

axial as the loading shoes (or platens) were in contact with the specimen in the third dimension. As the loading shoes were not fitted with any special brushes or friction reducing devices, the loading was to some extent tri-axial. The tri-axial effect was increased by restrained thermal expansion when the specimens were heated.

The failure stresses recorded for the specimens when loaded in one and both axes are given in Figure 6.1 and these data give some measure of the behaviour of the concrete specimens within this particular test rig at ambient temperature. The information contained in Figure 6.1 will be used in Chapter 8 in the evaluation of the behaviour of the concrete specimens during the heating and loading tests.

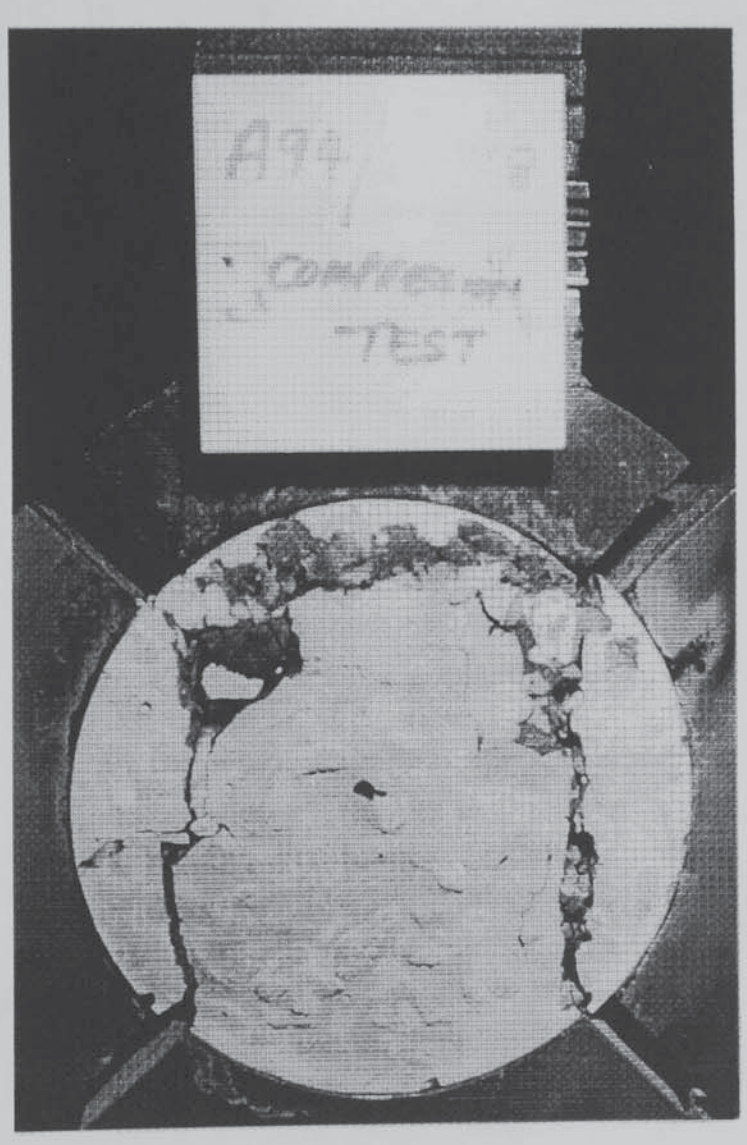

Plate 6.1 Failure modes of concrete specimens in test rig at ambient temperatures loaded in a single vertical direction

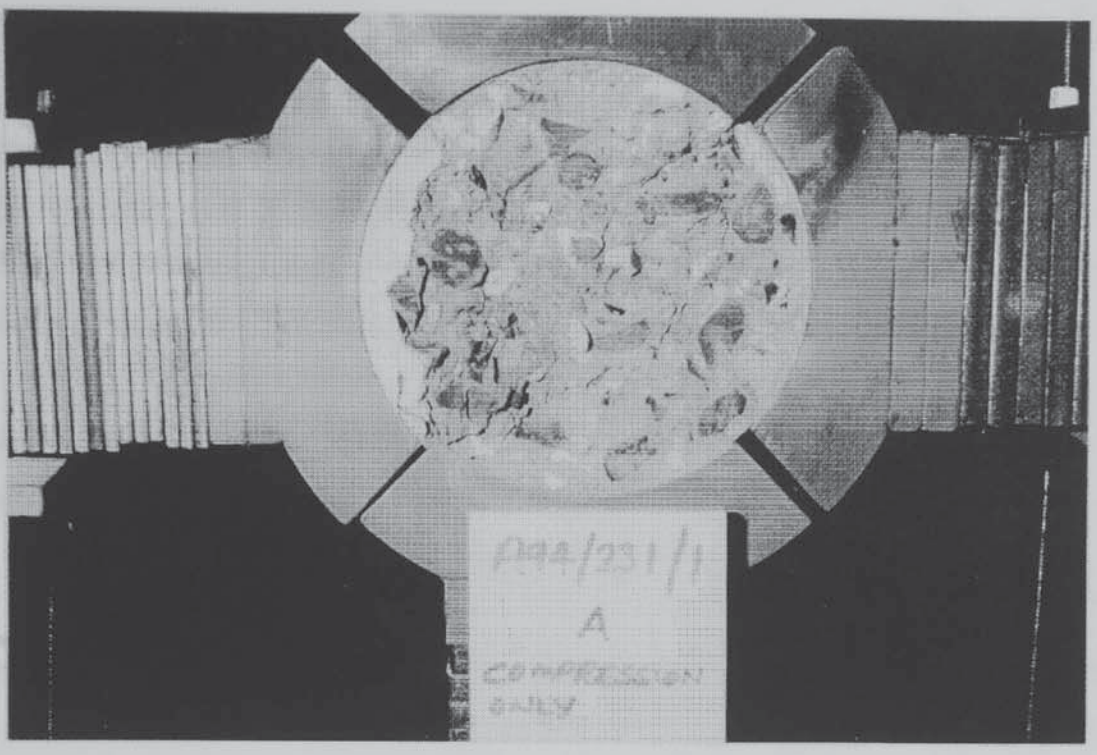

Plate 6.2 Failure modes of concrete specimens in test rig at ambient temperatures loaded in both vertical and horizontal directions

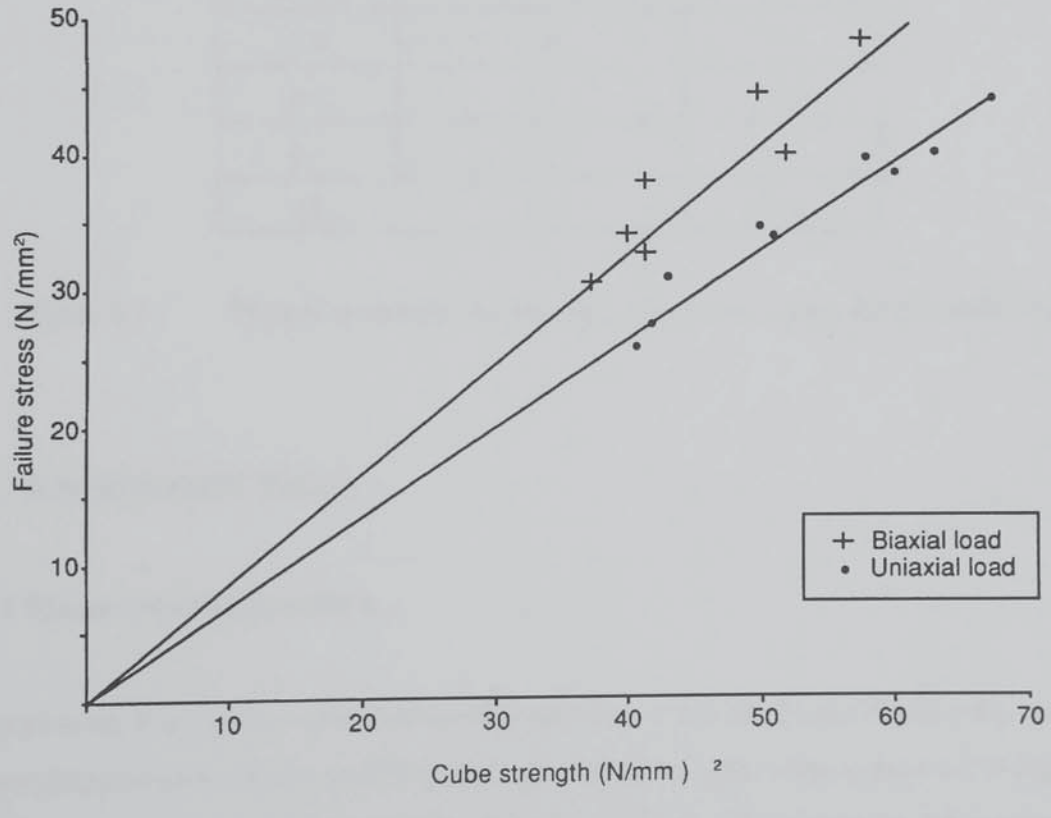

Figure 6.1 Relationship between failure stress (applied in test rig) and compressive strength

6.2.3 MOISTURE CONTENT AND ABSORPTION

Within each batch of specimens, two cylindrical specimens of dimensions similar to those specimens, which were subsequently tested under conditions of heating and loading, were set aside for determination of moisture content and absorption. The moisture content was measured after drying the specimens at 105°C until the mass became constant (generally within 48 hours).

The absorption of each specimen was measured by submerging the oven-dried specimens (after cooling) in water for 48 hours and observing the percentage increase in mass (saturated surface dried condition). The results give a measure of the specimen's pore volume.

These properties were measured for each batch of specimens when they came available for heat and load testing, generally 28 days after casting. Some typical measured values are given in Table 6.2 and their magnitude appears quite reasonable.

W/C Ratio	**Moisture Content** (% by weight)	**Absorption** (% by weight)
0.6	5.1	7.9
0.5	4.7	7.2
0.4	4.5	6.7
0.3	4.2	6.2

Table 6.2 Typical moisture content and absorption values for concretes examined

6.2.4 MICROSTRUCTURE

6.2.4.1 Measurement procedure

Information on the size and distribution of pores within the specimens was determined using a mercury intrusion porosimetry (MIP) technique. Intrusion tests were carried out using standard apparatus, in this case a *Micromeritics Poresizer Model 9310* made by Micromeritics Ltd. Dunstable, Bedfordshire.

The concrete specimen was broken down with a hammer and chisel until material of a suitable size (approximately 5 mm cubes) could be selected from the interior. Samples containing obviously large aggregate particles were rejected. The samples were treated with propan-2-ol solvent to displace any contained water and then evacuated over several days to completely remove the solvent.

A weighed quantity of sample (generally about 5 g) was placed inside the chamber of a glass cell, or "Penetrometer", which has a glass capillary stem surrounded by a metal sheath. The Penetrometer was then placed within the Poresizer and evacuated to 50 microns to remove residual moisture and gases. The Penetrometer chamber and capillary were then filled with mercury and pressure gradually applied up to 200 N/mm^2, so as to force the mercury into the pores of the sample.

The volume of mercury intruded to the sample was measured by the change in capacitance of a cylindrical coaxial capacitor formed by the outer metallic sheath around the Penetrometer stem and the inner capillary of mercury which was reduced as mercury was forced into the pores of the sample. The pore radius was calculated using the Washburn Equation after assuming a contact angle of 117° between the mercury and the pores, based on the work of Winslow and Diamond (1970).

6.2.4.2 Results

The results of the MIP tests are summarised in Table 6.3. A complete description of the pore size distribution is presented in Figure 6.2, which shows the relationship between pore volume V and the pore diameter (to a logarithmic scale). However, a more meaningful picture of the pore size distribution is given in Figure 6.3 which shows the variation of $(dV/dlogR)$ with R. This Figure shows the rate of change of the data presented in Figure 6.2 and allows superior visualisation of pore size distribution.

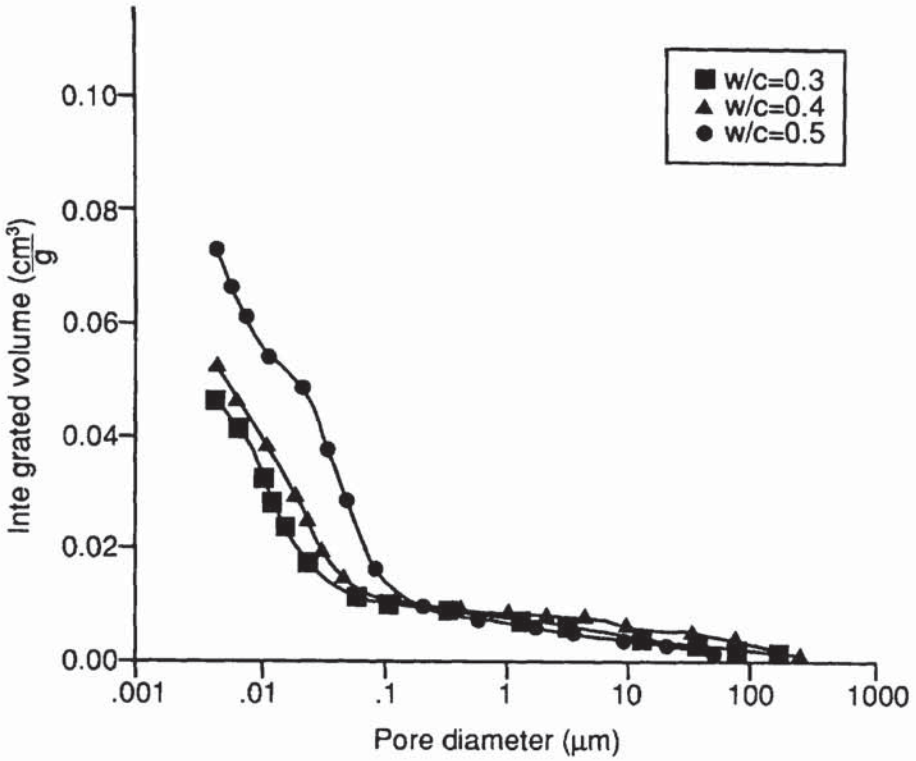

Figure 6.2 Variation of intruded pore volume with pore diameter

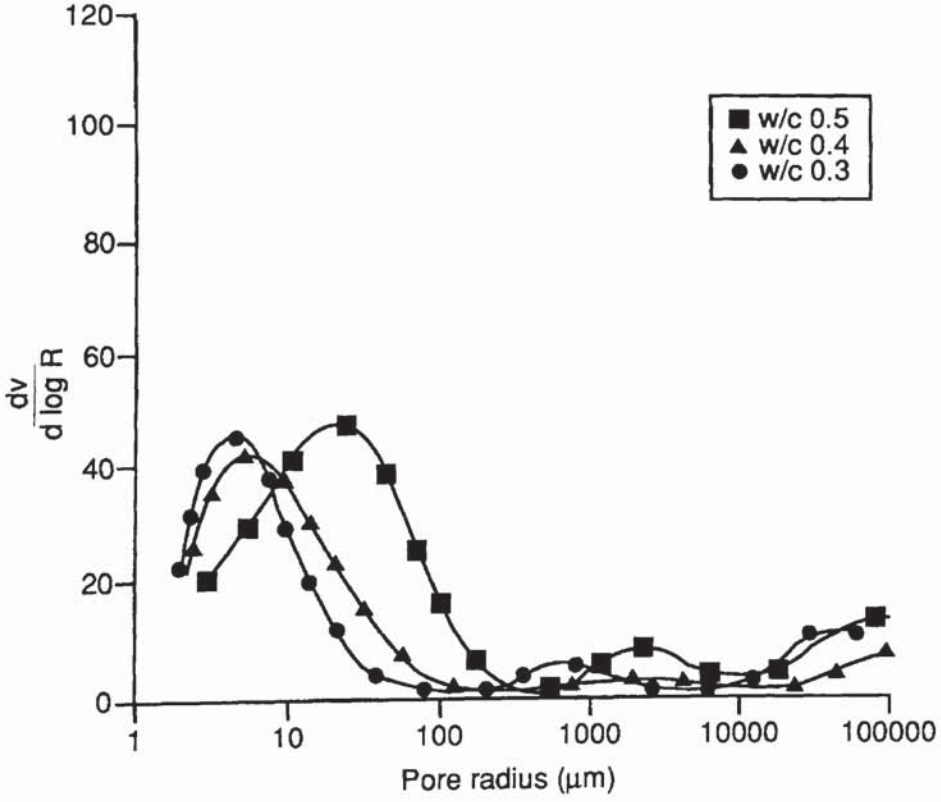

Figure 6.3 Pore size distribution

Water / Cement Ratio	Intrusion vol. (cm^3/g)	Total pore area (m^2/g)	Mean pore radius (μm)	Bulk density (g/cm^3)	% Capillary
0.3	0.0467	13.5510	0.0069	0.7125	14.4778
0.4	0.0533	14.9814	0.0071	0.7196	16.6961
0.5	0.0735	17.2119	0.0086	0.7146	22.8842
0.6	0.0968	17.4339	0.0111	0.7419	31.2884

Table 6.3 Summary of results of MIP tests

6.3 TEMPERATURE PROFILES

6.3.1 HEATING CONDITIONS

The factors influencing the design of the electrical heating enclosure were discussed in Section 5.2.3. Based on information on the heat flux levels encountered in real fires, target heat flux levels of 80, 110 and 140 kW/m^2 were set. These levels were achieved by calibrating the electrical power input to the heating coils to reference output heat flux levels.

The specimens were heated in a similar manner on both sides. The temperatures within the heating enclosure under different heat flux conditions are presented in Figure 6.4. The gas temperatures are generally higher than the standard fire resistance heating curve (BS 476:Part20:1987) over the first 10 minutes. An imposed heat flux of 140 kW/m^2 represents a more severe exposure than the standard fire resistance heating curve at all times.

The severity of heating is probably best judged by comparing the temperatures at the heated concrete surface under the different heating regimes, as shown in Figure 6.5. These surface temperatures provide a better measure of imposed heat flux as the emissivity of the heaters was directly related to the input electrical power.

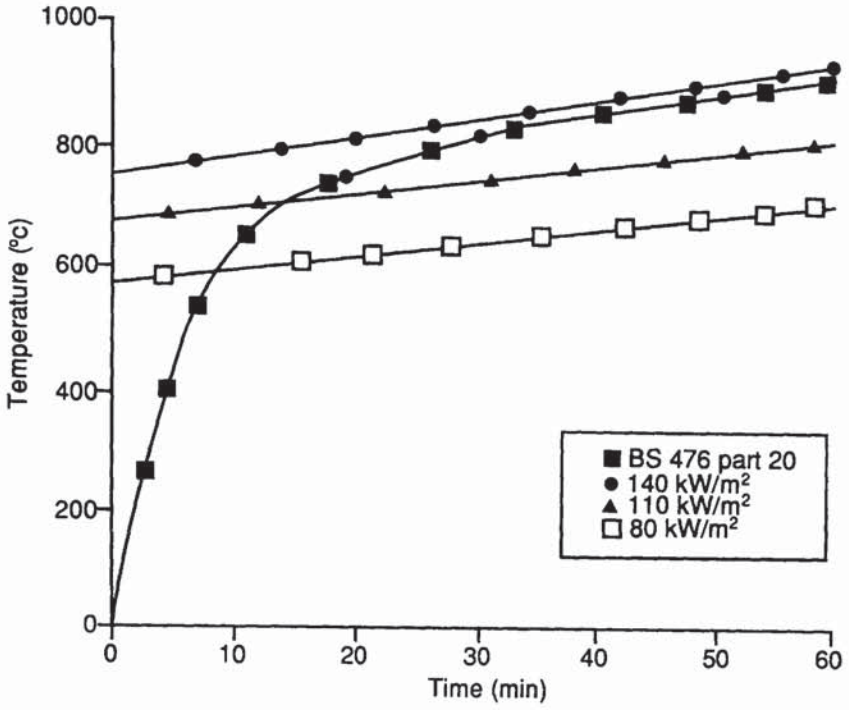

Figure 6.4 Gas temperatures within heating enclosure

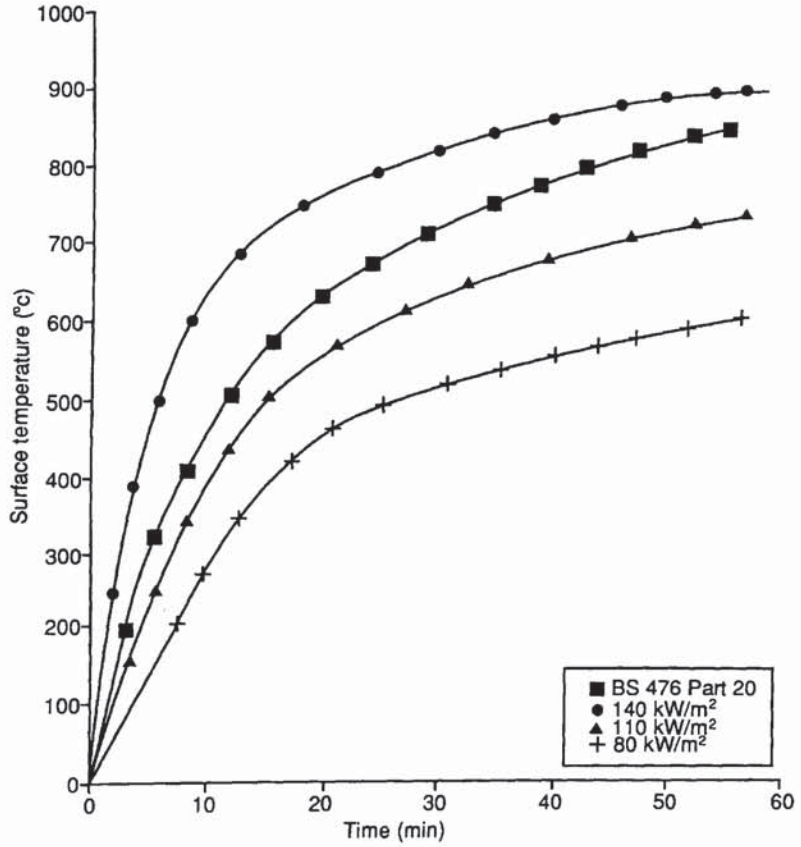

Figure 6.5 Surface temperatures of concrete specimens exposed to various heat flux levels

6.3.2 TEMPERATURE FIELDS DEVELOPED WITHIN TEST SPECIMENS

Some typical temperature profiles induced within the 28 day old concrete specimens (w/c = 0.6) at different times during heating are shown in Figures 6.6, 6.7 and 6.8. The temperature profiles shown in these Figures are based on the temperatures measured at discrete points in actual test specimens. For simplicity, a linear interpolation has been assumed between the measurement points. The fact that temperature distributions in heated concrete more typically take a parabolic form is accounted for by the distribution of thermocouples across the specimen.

Thermocouples were only actually placed in 25% of the test specimens, but the temperature profiles observed appeared sufficiently consistent to allow extrapolation to the remaining specimens. Temperatures were also observed in concrete specimens with different w/c ratios and the values recorded will be used in any subsequent analysis. A typical example of the temperature-time history at different depths beneath a concrete surface subjected to 140 kW/m^2 is given in Figure 6.9 for information.

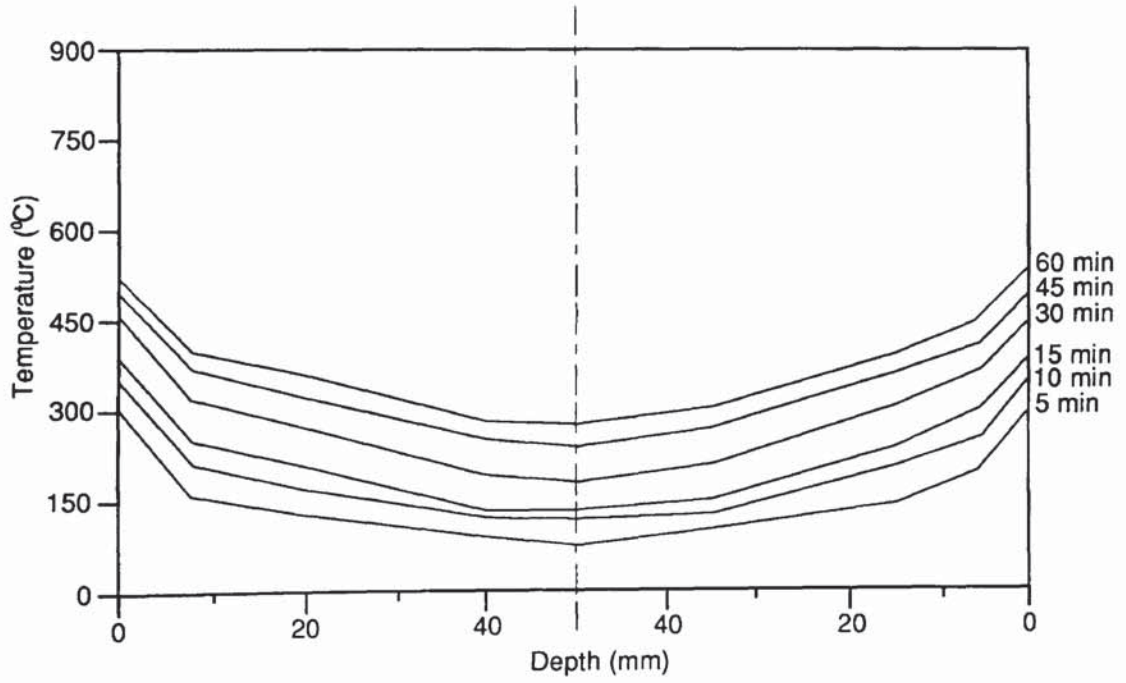

Figure 6.6 Temperature profile across test specimen on exposure to 80 kW/m^2

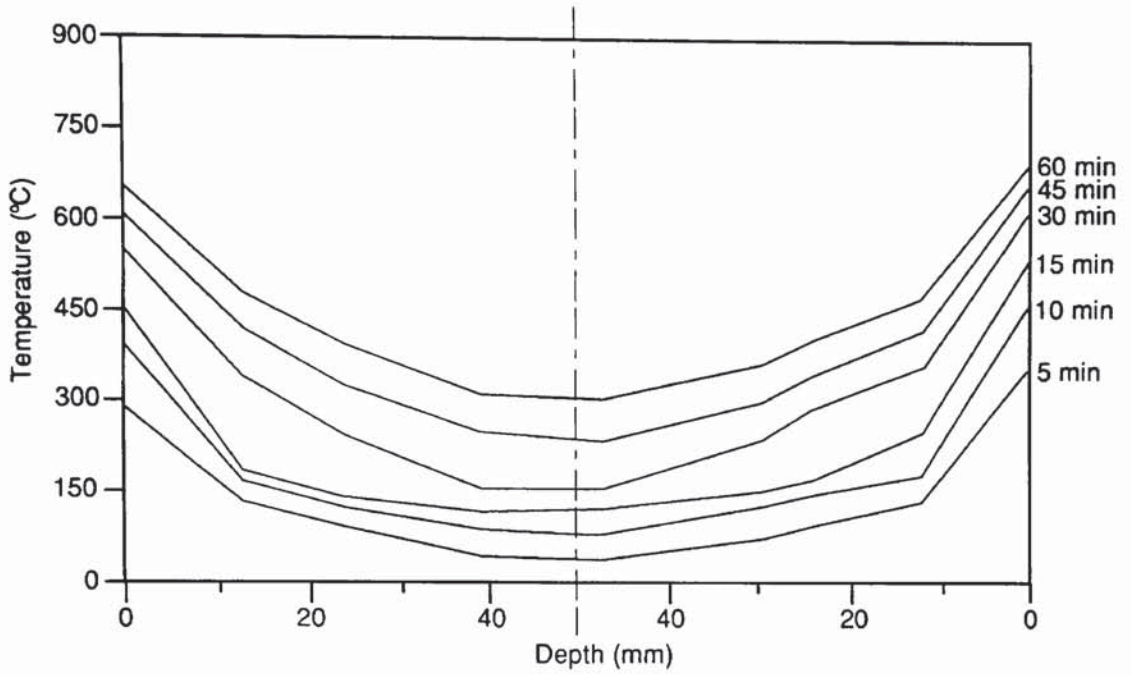

Figure 6.7 Temperature profile across test specimen on exposure to 110 kW/m^2

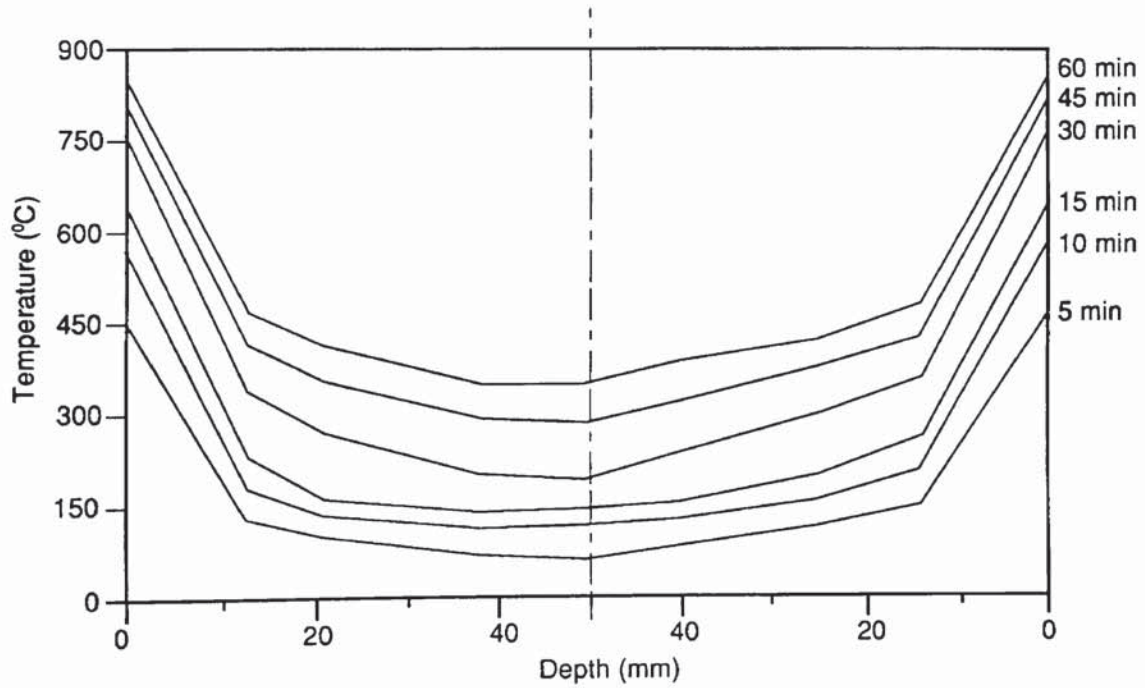

Figure 6.8 Temperature profile across test specimen on exposure to 140 kW/m^2

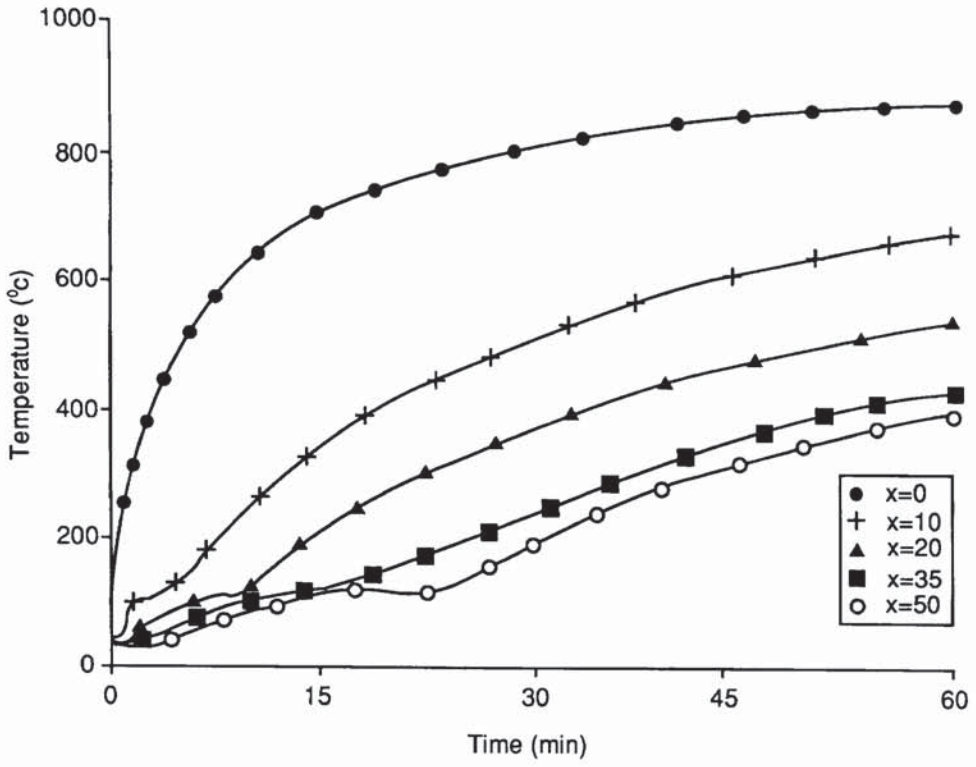

Figure 6.9 Temperature-time development at depths beneath heated surface (140 kW/m^2)

6.3.3 INFLUENCE OF APPLIED LOAD ON TEMPERATURES

The temperatures developed within a heated concrete specimen are governed by its thermal diffusivity, i.e. thermal conductivity over the product of specific heat capacity and density. In principle, the imposition of load should not have any effect on these properties, except for the rate of loss of density at elevated temperatures which is likely to be reduced in the presence of load. The independence of temperature response from imposed load is shown in Figure 6.10, which shows the development of surface temperatures under different loading conditions.

However, in the early stages of heating the presence of moisture has a significant effect on the temperature development. Similarly the presence of moisture is important in deciding the thermal response at the centre of the test specimen with moisture tending to migrate to the cooler central region of the test specimen as heating continues. The passage of moisture through the specimen is influenced by applied loads. On heating the permeability of concrete is increased by a number of mechanisms, one of which is the onset of cracking. Imposed load suppresses the development of cracks and thus hinders the reduction in permeability.

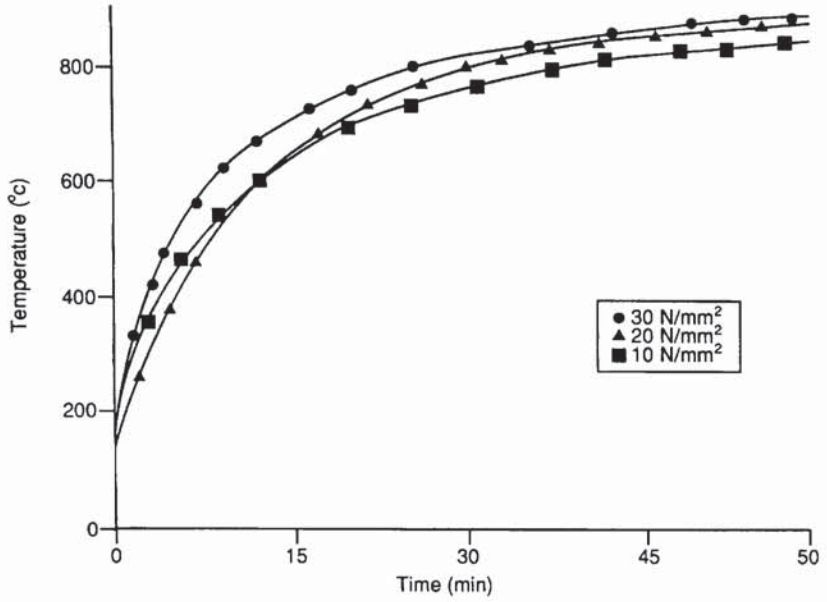

Figure 6.10 Surface temperature development under different loading conditions

The effect of imposed load on the temperature development at the centre of a concrete specimen is shown in Figure 6.11. It is clear from these data that imposed load inhibits moisture flow from the specimen. Thus moisture is present in the central region of the specimen for longer and temperatures are suppressed. When all the moisture has been removed the temperature rise continues at roughly the same rate regardless of load level, in a manner similar to the observed effects at the surface.

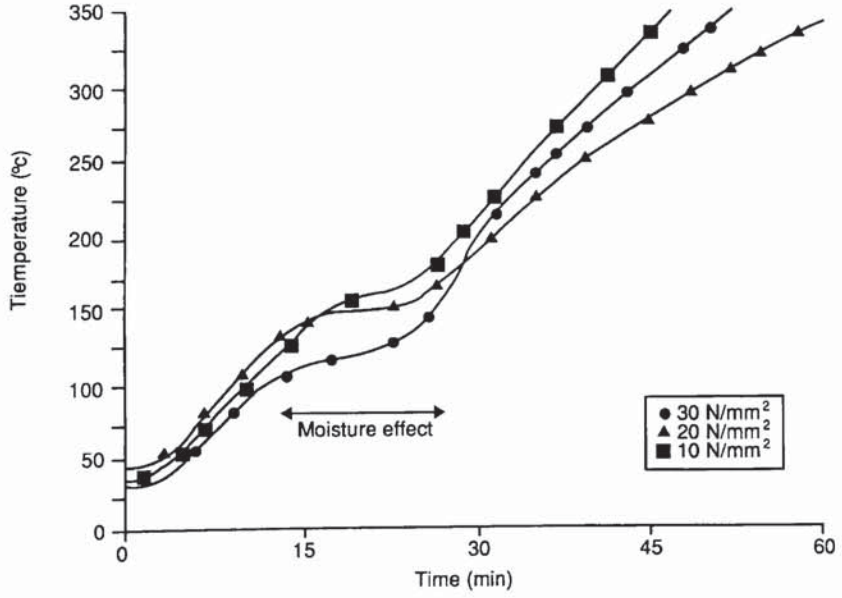

Figure 6.11 Temperature development in centre of concrete specimen under different loading conditions

The importance of imposed load to temperature development is thus related to the rate of change of position (velocity) of the vapour front (as manifested by the 100°C isotherm) away from the heated surface. Figure 6.11 clearly shows that an increase in the load imposed on the specimen reduces the velocity of the 100°C isotherm. This relevance of this effect will be discussed in Chapter 8.

6.4 THERMAL STRESSES

The deformation of concrete at elevated temperatures and the resultant thermal stresses that may be developed have been discussed in Chapter 3. In summary, thermal stresses may come from two sources;

(i) internal restraint to expansion (due to temperature gradients)
(ii) external restraint to thermal expansion of entire specimen (by some external load)

6.4.1 DEFORMATION OF TEST SPECIMEN

Concrete specimens, completely free of load, were subjected to heat flux levels of 140 kW/m^2 and their free deformation monitored through their depth. A typical example of the results is given in Figure 6.12. The concrete specimen has been heated from both sides, using the electrical radiant heaters described in Section 5.2.3, and thus the outer faces contract very early in the test, while the centre remains stable. As moisture is removed from the cement paste (generally between 5 and 10 minutes) expansion of the Gravel aggregate begins to dominate and the heated faces begin to expand.

Within a similar timescale, the temperature at the centre of the test specimen begins to increase and moisture is removed with an accompanying shrinkage. The stresses acting through the thickness of the specimen are a maximum during this stage of heating. After about 20 minutes the centre of the specimen begins to expand alleviating internal thermal stresses as temperature gradients are gradually reduced. The maximum difference in deformation between the centre of the specimen and the heated face occurs between 15 and 20 minutes after heating commenced.

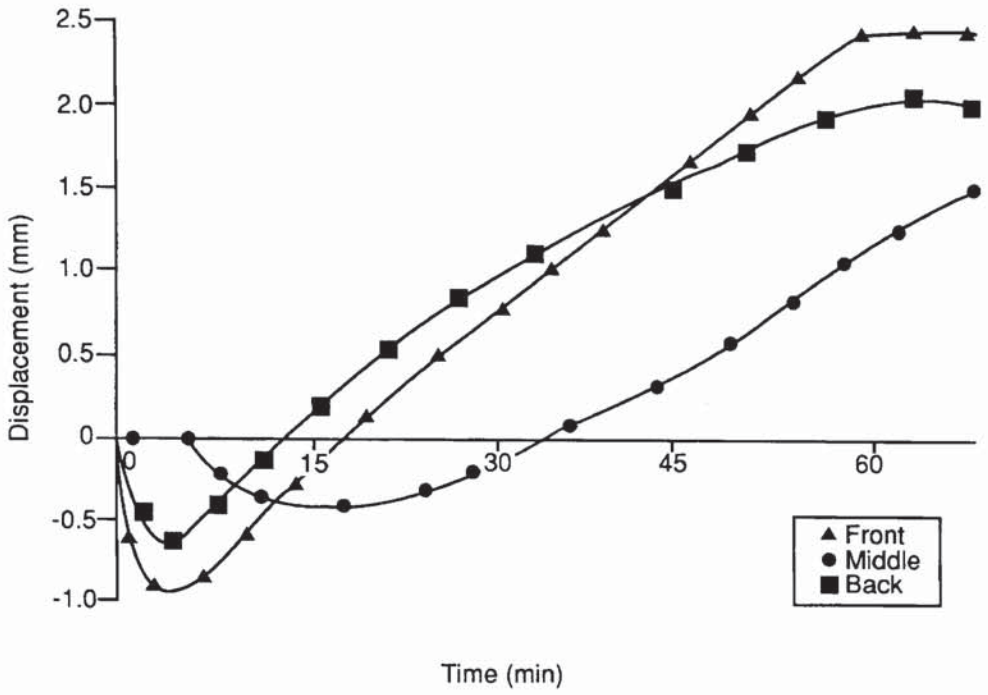

Figure 6.12 Thermal deformation across heated concrete cylinder

6.4.2 INFLUENCE OF APPLIED LOAD ON THERMAL STRESSES

When the specimen is acted upon by a load, free thermal expansion is prevented to an extent proportional to the magnitude of the loads acting. Within the test rig, the load cell is mounted in series with the loading arm to provide a continuous reading of the loads being transmitted to the specimen.

As the thermal deformations reported in Figure 6.12 suggest, the specimens contracted in the early stages of heating and as the hydraulic jacking system was not mechanically controlled to maintain a constant load, the loads on the specimen were slightly reduced. When this was observed, the load was manually reapplied to prevent it dropping below its initial level.

Thus, constant attention was required over the first 5 minutes of the test and manual jacking needed to keep the requisite load level. There was not as much need for jacking in the early stages of tests on higher strength concretes as the degree of initial contraction was quite small due to the reduced water/cement ratio.

The influence of external restraint on the thermal stresses developed in concrete specimens heated to 140 kW/m^2 is shown in Figure 6.13. This Figure shows that thermal stresses are highly dependent on the loads applied. Such behaviour has been reported previously by Anderberg and Thelandersson (1976). Figure 6.13 also shows that the magnitude of the stresses generated due to restrained thermal expansion were not very large and they would not be expected to cause a compressive failure of the specimens.

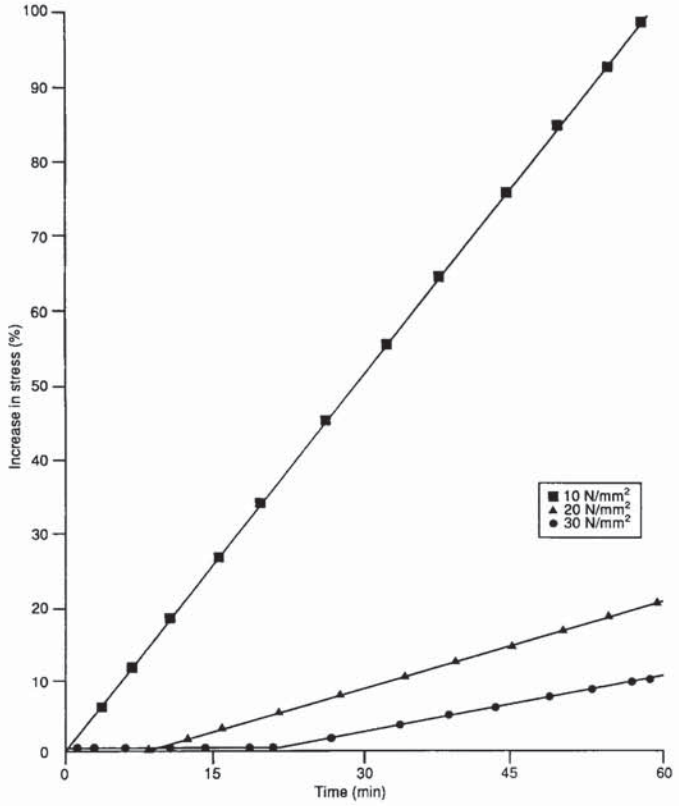

Figure 6.13 Effect of applied load on stresses due to restrained thermal expansion

6.5 PORE PRESSURE MEASUREMENTS

The attempts to measure pore pressures developed within the specimen were unsuccessful. The ceramic probe acted as a crack inducer within the surface of the specimen and caused the concrete to crack in a direction radial to the probe, as shown in Plate 6.3. These cracks must have extended over the entire depth of the probe as when they occurred pore pressure readings almost immediately dropped to zero. A number of different sealing systems were employed between the probe and the concrete with little success. As cracking failure occurred generally within the first 5 minutes of test, no useful data were obtained.

Similar problems have been previously encountered by Harada and Terai (1991) and no obvious solutions present themselves. The potential magnitude of the pore pressures and the effect that they might have on explosive spalling requires further consideration. It may be that some indirect means of measuring pore pressures will have to be considered, although the technique of monitoring mass loss used by Bažant and Thonguthai (1979) does not appear sufficiently reliable. The question of pore pressures will be considered in detail in Chapter 7.

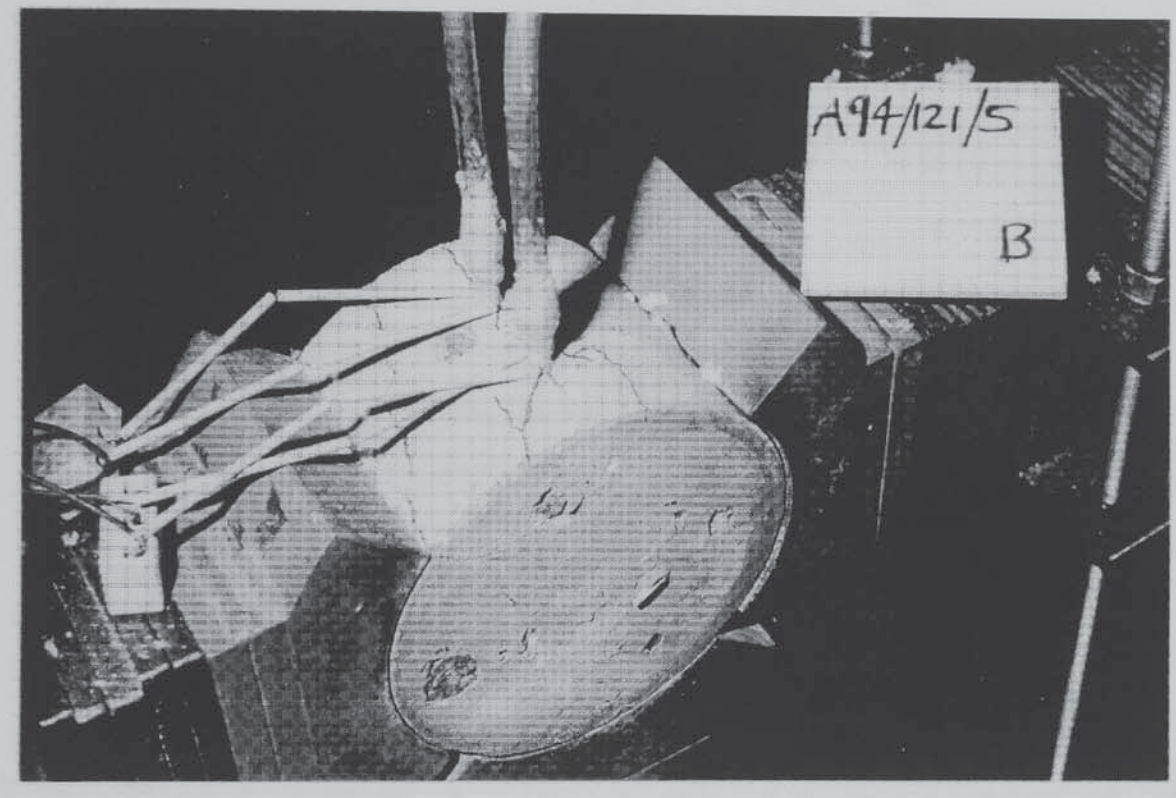

Plate 6.3 Pore pressure probes (with thermocouples) causing cracking of specimen

6.6 ULTRASONIC PULSE VELOCITY MEASUREMENTS

Standard equipment for measuring the longitudinal wave velocity in concrete was used to evaluate the extent of the damage caused to the test specimen by simultaneous application of load and heat. The time taken for a wave pulse to traverse the test specimen was measured across both its diameter and thickness, before and after heating. The increased time taken for the wave pulse to transmit through the specimen provided a measure of the extent of cracking that had occurred within it. Table 6.4 presents a summary of the data observed over the entire test series. Trends in behaviour have been highlighted by using a dimensionless *velocity factor* which relates the

reduced pulse velocity after heating to the datum pulse velocity measured before heating. The velocity factor varies with the mean specimen temperature.

W/C Ratio	Mean Specimen Temperature (°C)	Velocity factor	
		Thickness	Diameter
0.6	425	0.27	0.48
0.6	475	0.21	0.31
0.6	525	0.14	0.28
0.5	425	0.16	0.63
0.5	475	0.14	0.33
0.5	525	0.12	0.29
0.4	425	0.22	0.56
0.4	475	0.19	0.29
0.4	525	0.06	0.22
0.3	425	0.18	0.39
0.3	475	0.11	0.22
0.3	525	0.09	0.18

Table 6.4 Velocity factor recorded in ultrasonic pulse velocity readings

The pulse velocity measured from one face of the test specimen to the other was the most reliable and consistent reading at ambient temperatures. However, aggregate spalling and surface deterioration of the test specimens after heating significantly reduced the quality of these readings after the test. Hence, although pulse measurements across the diameter were somewhat inferior due to the difficulty in establishing consistent surface contact, they proved more reliable after heating due to the absence of surface damage.

The relationship between the reduction in pulse velocity and mean specimen temperature is shown in Figure 6.14. Ultrasonic pulse velocity provides a measure of the extent of cracking within the concrete specimen. Cracking generally results in a loss in concrete stiffness and a reduction in the modulus of elasticity. Therefore, although the data was available for a limited temperature range, it is interesting to note that the results show a reasonable correlation with observations on the reduction in modulus of elasticity recorded by Schneider (1985).

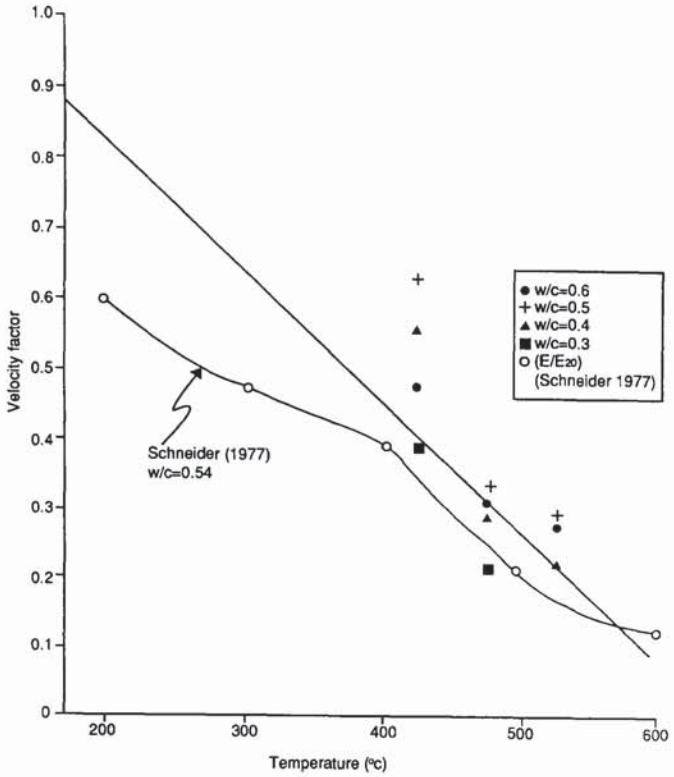

Figure 6.14 Relationship between reduction in pulse velocity and mean specimen temperature

6.7 SUMMARY OF RESULTS

6.7.1 OBSERVED BEHAVIOUR

A wide range of different behaviour was observed during the experimental programme. The most common form of heating damage was *aggregate spalling* (shown in Plate 6.4), which was observed in the vast majority of test specimens. A detailed study of the factors affecting *aggregate spalling* is made in Chapter 9. A more serious form of surface damage or *surface spalling* was observed in some specimens, although very infrequently. An example is shown in Plate 6.5. The factors contributing to *surface spalling* are discussed further in Chapter 7.

Explosive spalling was observed to occur either partially (shown in Plate 6.6) or completely (shown in Plate 6.7) over the heated concrete face. Explosive spalling removed typically 15 to 20 mm depths of the concrete. As shown in Plate 6.8, explosive spalling often caused damage to the heaters and in some cases to the test rig itself (Plate 6.9). In such cases the concrete specimens were completely destroyed (Plate 6.10).

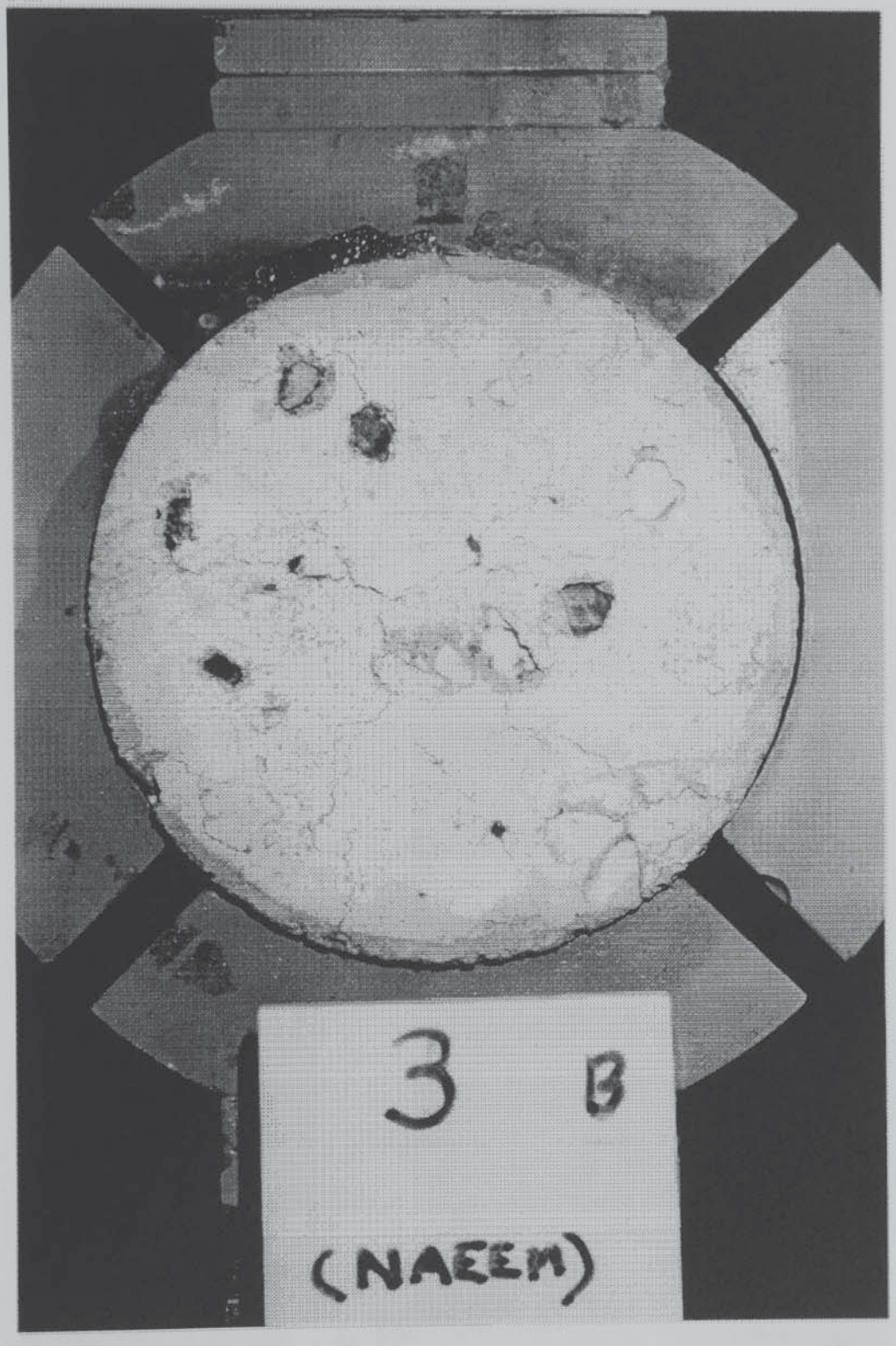

Plate 6.4 An example of aggregate spalling

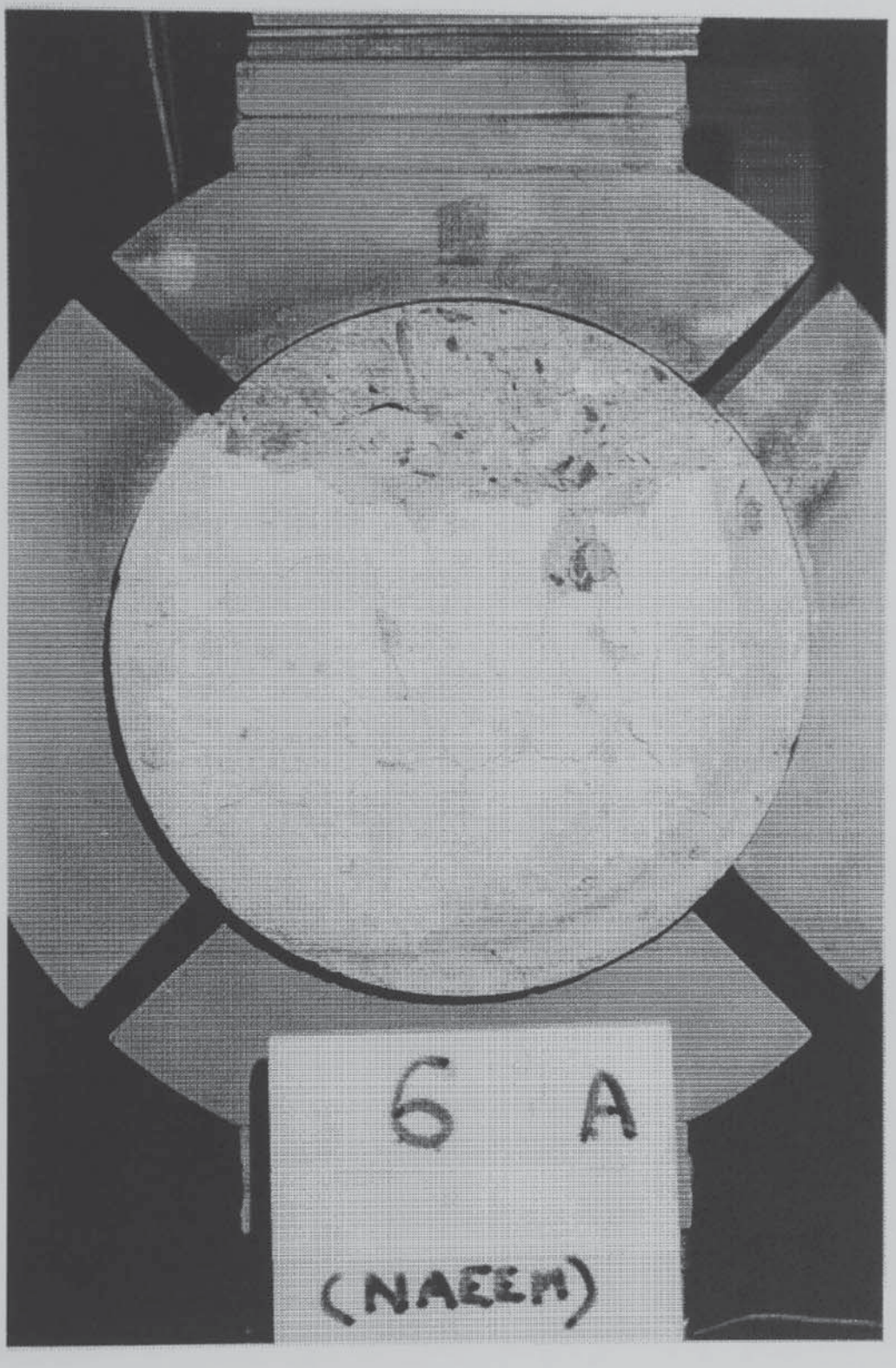

Plate 6.5 An example of surface spalling

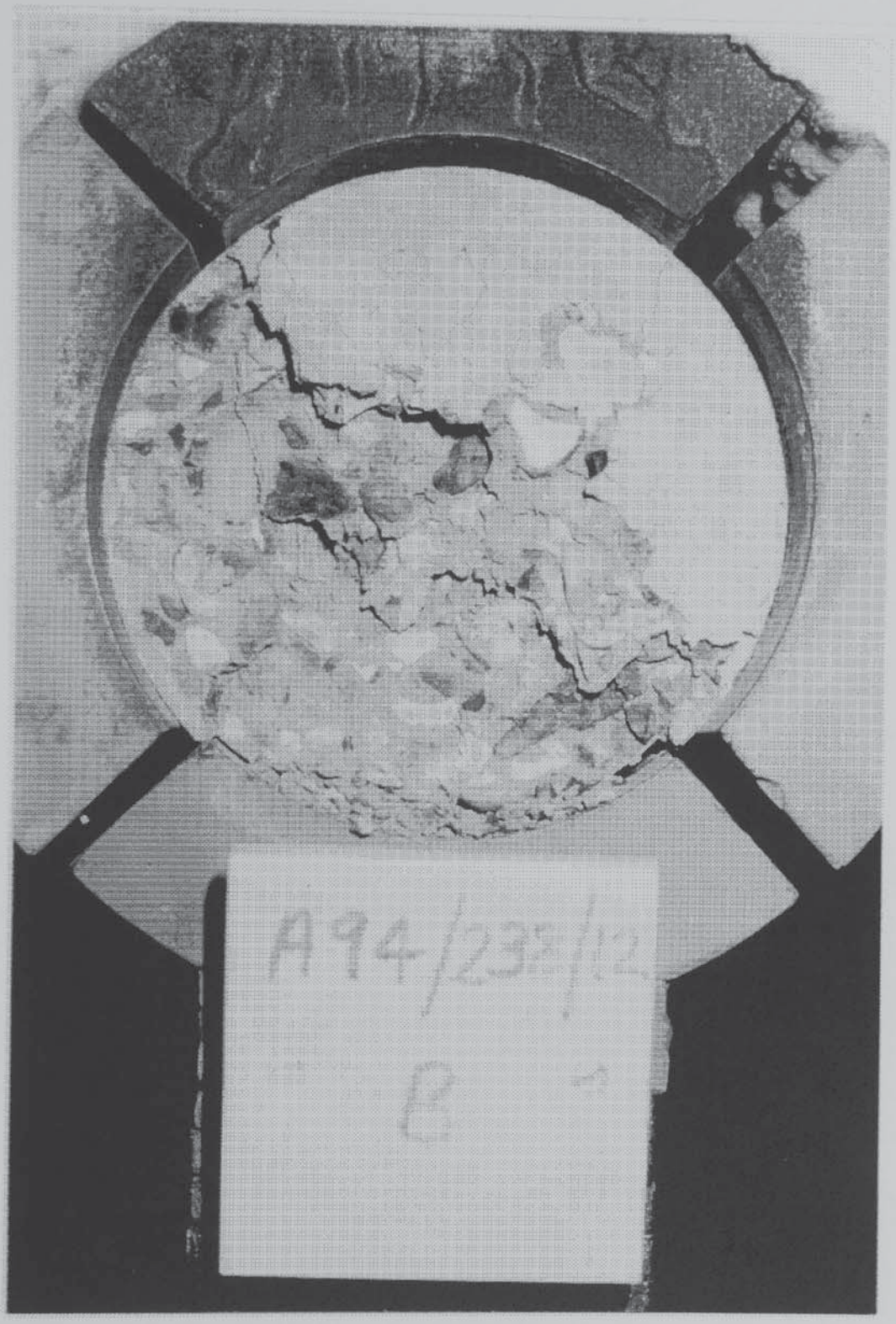

Plate 6.6 Partial explosive spalling

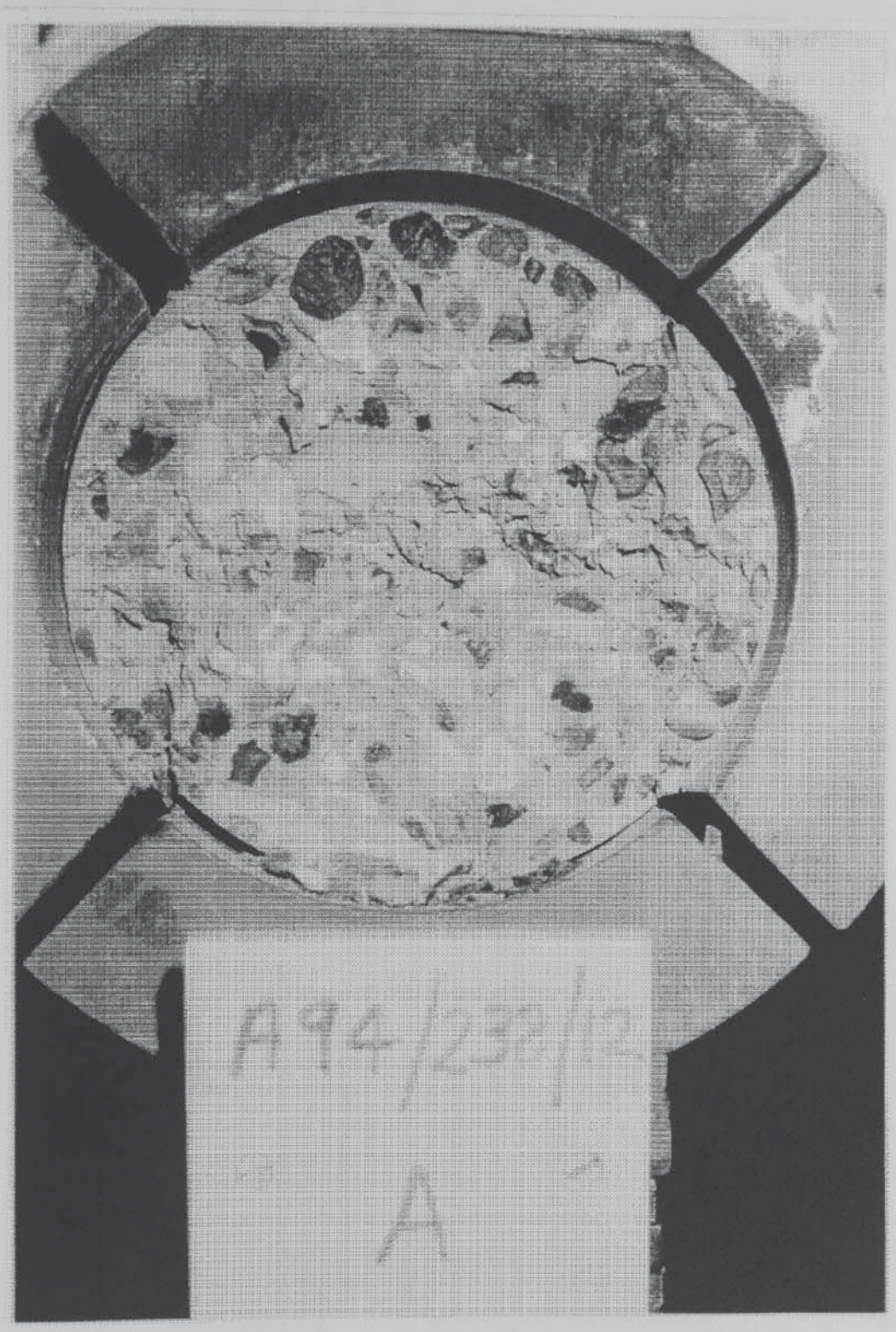

Plate 6.7 Explosive spalling over entire surface of specimen

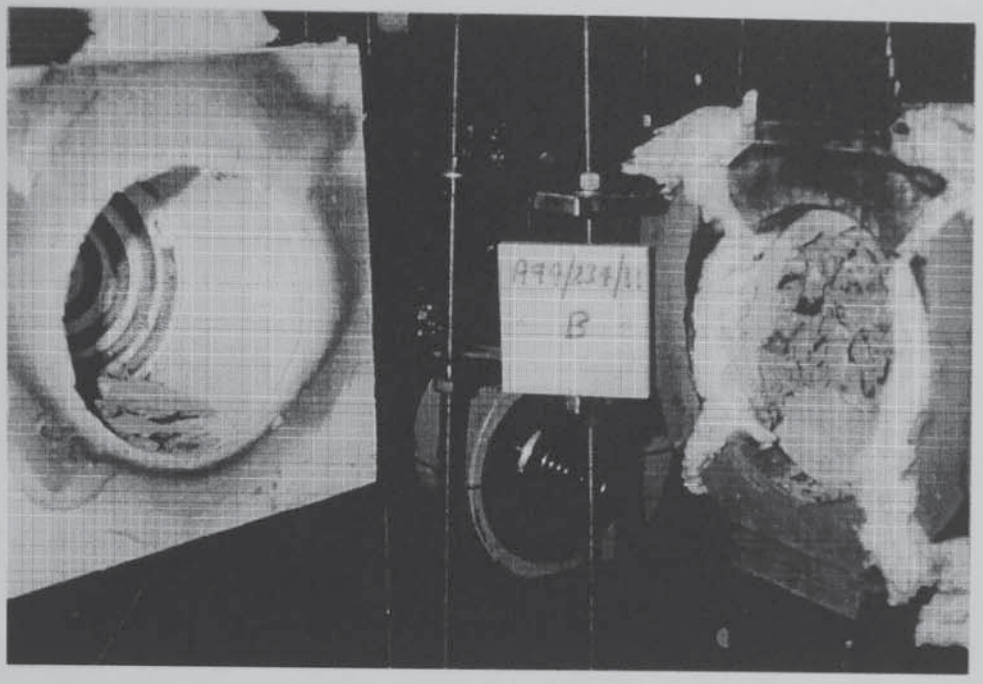

Plate 6.8 Violent explosive spalling damaging heaters

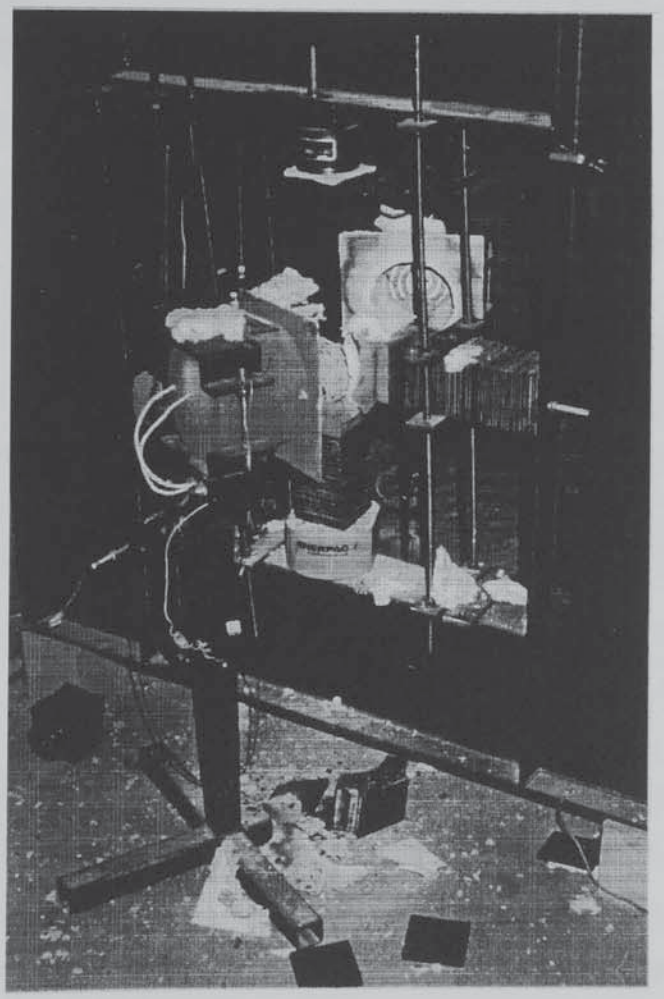

Plate 6.9 Violent explosive spalling damaging test rig

Plate 6.10 Complete destruction of concrete specimens by explosive spalling

6.7.2 THE EFFECT OF HEATING AND LOADING CONDITIONS ON SPALLING

The experimental results of heating and loading tests conducted on concrete specimens with a water/cement ratio of 0.6 are shown in Tables 6.5, 6.6 and 6.7 for heating conditions of 80, 110 and 140 kW/m^2 respectively. These data clearly show that increasing the rate of heating promotes the likelihood of explosive spalling, with the probability of explosive spalling under an applied load of 30 N/mm^2 increasing from 0.25 on exposure to 80 kW/m^2 up to a probability of 0.5 on exposure to 140 kW/m^2.

Furthermore, increasing the heating rate reduces the load levels at which spalling may take place with some specimens heated to 110 kW/m^2 failing at applied load stresses of 10 N/mm^2. This is a significant observation as the measured stress needed to crush the test specimen at ambient temperature is in the order of 35 N/mm^2. Failure at such low stress levels suggests that explosive spalling failure is not simply a manifestation of ordinary compression failure and other mechanisms are acting. The theoretical study reported in Chapter 3 concluded that these other mechanisms are related to thermal stress and pore pressure.

Reference	w/c Ratio	Heat (kW/m^2)	Load (N/mm^2)	Final Load (N/mm^2)	Notes
A93/241/2	0.6	80	0	0	-
A93/248/3	0.6	80	11.1	15.5	-
A93/162/12	0.6	80	10.3	15.4	-
A93/162/2	0.6	80	20.2	25.7	-
A93/162/11	0.6	80	20.3	23.7	-
A93/248/1	0.6	80	20.2	24.1	-
A93/256/3	0.6	80	30.1	31.7	-
A93/256/13	0.6	80	30.1	31.5	Spalling
A93/248/4	0.6	80	30.1	31.2	-
A93/141/11	0.6	80	30.2	32.2	-

Table 6.5 Experimental results (heating = 80 kW/m^2, w/c = 0.6)

Reference	w/c Ratio	Heat (kW/m^2)	Load (N/mm^2)	Final Load (N/mm^2)	Notes
A93/241/3	0.6	110	0	0	-
A93/256/4	0.6	110	10.4	17.1	-
A94/179/3	0.6	110	10.4	18.0	-
A94/098/1	0.6	110	20.1	22.9	-
A93/256/1	0.6	110	20.2	25.0	Spalling
A93/256/12	0.6	110	20.4	23.9	-
A94/035/12	0.6	110	30.0	32.2	Spalling
A93/256/2	0.6	110	30.0	32.4	-
A93/256/11	0.6	110	30.1	31.4	-
A93/256/6	0.6	110	30.1	31.9	-
A94/098/1	0.6	110	30.1	31.3	Spalling
A94/098/3	0.6	110	30.1	29.7	-
A94/141/1	0.6	110	30.1	32.4	-
A94/162/3	0.6	110	30.4	32.4	-

Table 6.6 Experimental results (heating = 110 kW/m^2, w/c = 0.6)

Reference	w/c Ratio	Heat (kW/m^2)	Load (N/mm^2)	Final Load (N/mm^2)	Notes
A93/230/1	0.6	140	0	0	-
A93/035/11	0.6	140	10.2	17.8	-
A93/241/1	0.6	140	10.4	16.6	-
A93/162/1	0.6	140	10.8	19.8	-
A93/224/11	0.6	140	15.2	22.6	-
A94/098/2	0.6	140	20.0	23.9	-
A94/141/12	0.6	140	20.1	25.6	-
A94/179/13	0.6	140	20.1	23.8	-
A94/141/2	0.6	140	20.2	26.1	-
A93/248/2	0.6	140	20.3	25.1	-
A93/248/6	0.6	140	20.3	23.5	Spalling
A93/248/5	0.6	140	20.3	23.5	-
A94/035/2	0.6	140	20.4	25.4	-
A93/224/4	0.6	140	20.3	25.9	-
A94/098/6	0.6	140	20.7	23.8	Spalling
A94/035/1	0.6	140	30.0	32.9	-
A93/256/5	0.6	140	30.0	32.4	Spalling
A94/035/4	0.6	140	30.0	32.7	Spalling
A93/248/11	0.6	140	30.1	32.5	Spalling
A94/121/6	0.6	140	30.1	31.2	-
A94/141/6	0.6	140	30.1	33.3	-
A94/162/6	0.6	140	30.1	32.5	Spalling
A94/141/3	0.6	140	30.1	31.0	-
A93/098/2	0.6	140	30.2	31.9	-
A93/035/5	0.6	140	30.3	32.6	Spalling

Table 6.7 Experimental results (heating = 140 kW/m^2, w/c = 0.6)

The experimental data reported in Tables 6.5, 6.6 and 6.7 demonstrate that there is a degree of probability associated with the occurrence of explosive spalling. For example, the data in Table 6.7 show that given nominally identical conditions some specimens spall while others do not. The applied load stresses, developed thermal stresses and presumably the developed pore

pressures would be expected to be similar for all these specimens yet the occurrence of spalling was not consistent. The role of probability in explosive spalling will be addressed in Chapter 8.

6.7.3 THE EFFECT OF WATER/CEMENT RATIO ON SPALLING

The behaviour observed in test specimens made with concretes of different water/cement ratios is presented in Tables 6.8, 6.9 and 6.10. When viewed together with the data in Table 6.7, these data show an increased susceptibility to explosive spalling amongst concretes with higher water/cement ratios.

Reference	w/c Ratio	Heat (kW/m^2)	Load (N/mm^2)	Final Load (N/mm^2)	Notes
A94/237/5	0.3	80	10.5	16.0	-
A94/237/7	0.3	80	30.3	31.9	Surface spalling
A94/237/4	0.3	110	30.4	33.1	Release* spalling
A94/237/11	0.3	140	5.4	9.7	Surface spalling
A94/237/3	0.3	140	10.3	16.9	-
A94/237/5	0.3	140	10.5	16.0	-
A94/237/2	0.3	140	20.5	25.5	Release* spalling
A94/273/2	0.3	140	25.0	27.8	-
A94/237/1	0.3	140	30.2	30.3	Surface spalling
A94/237/7	0.3	140	30.3	31.0	Surface spalling

(* Spalling on release of load after test)

Table 6.8 Experimental results (w/c = 0.3)

The behaviour reported in Table 6.8 contradicts the general perception that higher strength concretes are more vulnerable to explosive spalling (Hertz, 1984; Jumpannen, 1993). However, it must be remembered that this perception is founded on the effect that low water/cement ratios have in reducing permeability and hence increasing pore pressures. Should the magnitude of such pore pressures not be sufficient to cause explosive spalling, there is no reason why stronger concretes should not demonstrate increased resistance to spalling.

It is likely that the interaction between pore pressures and the other stresses acting decides the

behaviour of the test specimen. The nature and effect of any possible stress interactions will be discussed fully in Chapter 8.

Reference	w/c Ratio	Heat (kW/m^2)	Load (N/mm^2)	Final Load (N/mm^2)	Notes
A94/234/5	0.4	80	30.1	33.4	-
A94/234/3	0.4	110	30.0	33.0	Surface spalling
A94/234/4	0.4	140	10.4	19.7	-
A94/234/2	0.4	140	20.1	27.3	Release spalling
A94/234/1	0.4	140	30.2	30.7	Surface spalling

Table 6.9 Experimental results (w/c = 0.4)

Reference	w/c Ratio	Heat (kW/m^2)	Load (N/mm^2)	Final Load (N/mm^2)	Notes
A94/231/8	0.5	80	34.0	34.0	-
A94/231/7	0.5	110	38.3	37.7	-
A94/231/2	0.5	110	14.1	22.8	-
A94/231/4	0.5	140	27.3	29.8	-
A94/231/5	0.5	140	34.2	33.9	-
A94/231/3	0.5	80	40.0	42.2	Spalling

Table 6.10 Experimental results (w/c = 0.5)

6.7.4 THE EFFECT OF NATURE OF LOADING ON SPALLING

The performance of the concrete specimens loaded in one direction only is reported in Table 6.11. Comparing these data to the data in Table 6.8, it is immediately clear that specimens loaded in one direction are more susceptible to spalling. This can be explained in terms of the reduced resistance of uniaxially loaded specimens to crushing failure as described in Section 6.2.2. In the same manner as higher strength specimens appear to demonstrate more resistance to spalling, so too do the biaxially loaded (and in effect stronger) specimens.

Reference	w/c Ratio	Heat (kW/m^2)	Load (N/mm^2)	Final Load (N/mm^2)	Notes
A94/238/3	0.3	80	20.4	22.7	-
A94/238/7	0.3	80	35.1	34.9	-
A94/238/1	0.3	140	19.6	23.8	-
A94/238/5	0.3	140	34.7	35.6	-
A94/238/4	0.3	140	34.9	31.9	Spalling
A94/238/2	0.3	140	30.1	26.2	Release spalling
A94/235/1	0.4	140	10.4	19.6	-
A94/235/4	0.4	140	15.2	21.7	-
A94/235/7	0.4	140	20.0	21.6	Spalling
A94/235/2	0.4	140	20.1	26.1	-
A94/235/8	0.4	140	22.6	20.2	Release spalling
A94/235/5	0.4	140	20.1	17.0	-
A94/232/1	0.5	140	0	0	-
A94/232/2	0.5	140	10.4	19.8	-
A94/232/7	0.5	140	20.4	24.3	-
A94/232/4	0.5	140	20.5	27.2	-
A94/232/12	0.5	140	24.9	24.0	Spalling
A94/232/8	0.5	140	30.5	33.5	Spalling

Table 6.11 Experimental results for uniaxially loaded concrete specimens

This explanation is not enhanced however by the completely different modes of failure observed in the uniaxially loaded specimens at ambient and high temperatures. As discussed in Section 6.2.2, ambient uniaxial crushing caused very definite cracks parallel to the direction of loading.

However, the uniaxially loaded specimens failed at high temperatures in a manner very similar to the failure of biaxially loaded specimens, i.e. in planes parallel to the heated surface. The effect of the nature of the applied load is possibly linked to the orientation of the cracks which form within the specimen and their effect on the permeability of the specimen.

6.7.5 THE EFFECT OF SPECIMEN THICKNESS ON SPALLING

The behaviour of some 50 mm thick specimens when heated under the action of uniaxial and biaxial loads are presented in Tables 6.12 and 6.13 respectively.

Reference	w/c Ratio	Heat (kW/m^2)	Load (N/mm^2)	Final Load (N/mm^2)	Notes
A94/231/10	0.5	140	10.2	12.2	-
A94/231/12	0.5	140	10.2	12.6	Spalling
A94/232/11	0.5	140	10.6	12.8	Spalling
A94/232/12	0.5	140	18.0	20.8	Spalling
A94/236/11	0.4	140	18.2	10.8	Crushing
A94/237/10	0.3	140	20.0	21.4	Spalling

Table 6.12 Experimental results for uniaxially loaded 50 mm thick concrete specimens

Reference	w/c Ratio	Heat (kW/m^2)	Load (N/mm^2)	Final Load (N/mm^2)	Notes
A94/233/11	0.5	140	14.4	17.6	-
A94/233/12	0.5	140	14.0	17.4	-
A94/232/10	0.5	140	14.2	23.2	Spalling
A94/234/11	0.4	140	20.4	26.4	-
A94/234/12	0.4	140	25.0	23.0	Spalling
A94/236/12	0.4	140	18.2	0	Crushed
A94/237/11	0.3	140	10.8	19.4	-
A94/237/12	0.3	140	0	0	-
A94/238/10	0.3	140	6.6	16.0	-
A94/238/12	0.3	140	24.0	26.2	Spalling
A94/239/10	0.3	140	18.0	19.4	-
A94/239/12	0.3	140	16.2	18.4	-

Table 6.13 Experimental results for biaxially loaded 50 mm thick concrete specimens

On comparing the data in Table 6.12 and 6.13 to the equivalent data for thick specimens in Tables 6.8, 6.9 and 6.10, it appears that a reduction in specimen thickness promotes explosive spalling. This corroborates the experience of Meyer-Ottens (1972).

These data are also significant in that they demonstrate that the levels of load stress (and indeed thermally induced stress) pertaining at failure are generally less than those reported in Table 6.9 and 6.10. This behaviour suggests that the other stresses that influence failure, i.e. pore pressures, have a larger magnitude in thin specimens rather than thicker specimens.

One explanation for this fact may be Meyer-Ottens' proposal that the magnitude of pore pressure stresses is proportional to the velocity of the 100°C isotherm, which was observed to increase in thinner specimens. These issues will be discussed further in Chapters 7 and 8.

6.7.6 THE EFFECT OF MOISTURE CONTENT OF SPECIMENS ON SPALLING

The effect of different moisture contents on the susceptibility of specimens to spalling is shown by the data in Table 6.14.

These data show that some specimens with nominally zero free moisture were capable of spalling, while other specimens with quite high moisture levels did not spall. Specimens with a nominally 0% moisture content (by weight) were created by oven drying ordinary concrete specimens. Specimens with higher moisture contents but similar strength characteristics were created by soaking ordinary specimens for 48 hours under water.

These experimental data appear to represent the first time that oven dried concretes demonstrate the capacity for explosive spalling. This contradicts the theories of Meyer-Ottens (1972) and Christiaanse *et al.* (1972) who suggested that there is a lower threshold of moisture content beneath which spalling cannot occur. These important findings will be discussed in Chapter 8.

Reference	w/c Ratio	Heat (kW/m^2)	Moisture content	Load (N/mm^2)	Final Load (N/mm^2)	Notes
A94/231/9	0.5	140	0%	24.7	25	Spalling
A94/232/9	0.5	140	0%	30.1	25	Spalling
A94/234/8	0.4	140	0%	30.1	28.3	-
A94/236/11	0.4	140	0%	30.0	30.0	-
A94/239/11	0.3	140	0%	30.1	30.9	-
A94/239/5	0.3	140	0%	30.0	31.1	-
A93/224/4	0.6	140	6.4%	20.3	25.9	Sloughing
A93/162/3	0.6	110	6.4%	30.4	32.4	Sloughing
A94/141/11	0.5	140	6.1%	30.1	23.8	-
A94/179/13	0.5	140	6.0%	25.1	26.5	Spalling
A94/233/5	0.5	140	6.4%	30.1	30.7	Spalling

Table 6.14 Experimental observations for specimens with different moisture contents

6.7.7 MISCELLANEOUS EFFECTS

Heating and loading experiments were undertaken on concrete specimens (w/c = 0.4) which had microsilica added. In principle, microsilica enhances the strength of concrete and lowers its permeability and according to Jumpannen (1993) promotes the likelihood of spalling. In all the cases examined, however, no explosive spalling was observed. It was observed that the specimens containing microsilica were prone to surface spalling.

A batch of specimens was cast with the mix design slightly altered to increase the percentage fines by 5% to 45%. The water/cement ratio was maintained at 0.4. Although, no explosive spalling was observed in any of the heating and loading combinations studied, there was also an increased occurrence of surface spalling. The apparent susceptibility of these two different mixes to surface spalling is quite probably related to their permeability. The mechanisms of surface spalling will be discussed in Chapters 7 and 8.

CHAPTER 7. FURTHER INVESTIGATION OF ROLE OF PORE PRESSURES IN EXPLOSIVE SPALLING

7.1 INTRODUCTION

One of the principal limitations of the experimental results reported in Chapter 6 is the lack of information regarding the pore pressures generated within the heated concrete specimens. Accordingly, one major term in the generalised governing equation for spalling (Equation 3.22) remains unknown and this restricts the manner in which the experimental data reported in Chapter 6 can be evaluated.

This Chapter describes a programme of experiments undertaken to provide some measure of the pore pressures that could be developed in heated concrete specimens. The difference in approach between these new tests and those reported in Chapters 5 and 6 is that the new tests are carried out on small specimens. It is assumed that where specimens are small and thermally thin compared to the heat source, that both the load induced and thermally induced stresses within the specimen may be ignored. Equation 3.22 suggests that after effectively setting these other stresses to zero, then the stresses that cause spalling must result from pore pressures. By measuring the tensile strength of the concrete, an attempt can be made to quantify the magnitude of the pore pressures necessary to cause failure. Thus where heated specimens fail, predicted pore pressures can be related to the range of experimental conditions. It is hoped that by accurately measuring the conditions in the concrete specimens at failure, an empirical model may be developed to predict the pore pressures in heated concretes. Such a model could be used to evaluate the results from the experiments previously reported in Chapter 6.

A secondary objective of the experimental programme was to reproduce some of the spalling behaviour observed by other researchers when heating small concrete specimens. Sarvaranta *et al.* (1993) observed explosive spalling of 100 x 100 mm mortar specimens when subjected to a heat flux of 20 kW/m^2 under a cone calorimeter. Similar behaviour has been reported by Hertz (1984) and Jumpannen (1994), who both encountered violent and explosive spalling of 100 x 200 mm concrete cylinders heated at 1°C per minute. The experiments reported in this Chapter attempted to induce similar spalling behaviour.

7.2 TEST PROCEDURE

7.2.1 TEST SPECIMEN

By using relatively small test specimens, large numbers can be cast quickly and easily. Together with a straightforward test procedure this allowed study of the effect of a wide range of parameters on spalling such as the inclusion of different aggregates, polypropylene fibres and air entraining agents.

The test specimens examined were 75mm diameter x 20mm deep discs. The specimens were made with siliceous sand (St. Albans, Smallford Quarry), Ordinary Portland cement and had a range of water/cement ratios. Most of the specimens contained Thames Valley Gravel aggregate particles. Aggregates of equal size were selected and carefully placed in the specimen so that they touched its surface. The aggregate particles were placed as opposed to mixed into the mortar so that their depth from the heated surface would be exactly known. In addition, some specimens were cast incorporating Limestone aggregate, Lytag, polypropylene fibres and an air-entraining agent. The specimens were heated on one face and had thermocouples cast within them at the heated surface and also at mid-depth.

7.2.2 CURING AND CONDITIONING

The protocol for specimen manufacture, curing and conditioning is given in Table 7.1.

Day	Operation
0	casting then curing under damp sacking
1	demoulding then placement under water
7	conditioning at 20° C and 50%r.h.
14	sealing in polythene
28	testing

Table 7.1 Protocol for production of test specimens

7.2.3 EXPOSURE CONDITIONS

The test specimens were mounted horizontally on a non-combustible backing and heated using a radiant electrical heater, which was set at different heights above the specimen. This induced heating rates at the surface of the specimen ranging from 20 to 100°C/minute. The test apparatus is shown in Figure 7.1.

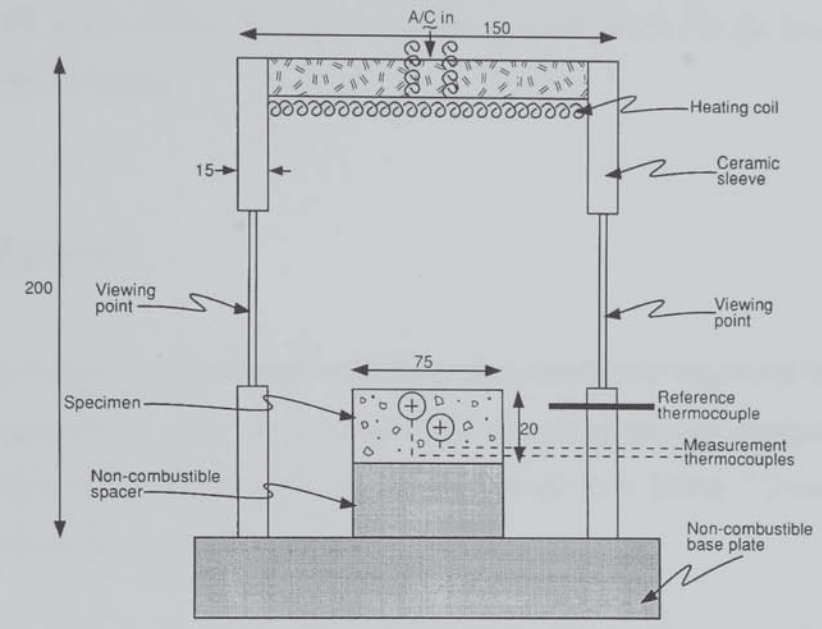

Figure 7.1 Apparatus for heating small test specimens

7.2.4 PARAMETERS INVESTIGATED

The effect of the following parameters on the occurrence of spalling was examined;

(i) Heating rate
(ii) Specimen age
(iii) Water/Cement ratio
(iv) Moisture Content
(v) Aggregate size
(vi) Aggregate type
(vii) Addition of polypropylene fibres
(viii) Addition of air-entraining agent

7.3 MATERIAL PROPERTIES

7.3.1 MOISTURE CONTENT

The specimens were cast in batches of 10 and the moisture content (by weight) of two specimens from each batch was measured after drying the specimens at 105° C until the mass became constant (generally within 48 hours). The results are given in Table 7.2 for Gravel concretes and Table 7.3 for other concretes.

7.3.2 ABSORPTION

The absorption of the same two specimens from each batch was measured by submerging the oven-dried specimens in water for 48 hours and observing the percentage increase in mass (saturated surface dry condition). The results are also given in Tables 7.2 and 7.3 and provide a measure of the specimen's pore volume.

Aggregate size		**20 mm**		**10 mm**		**5mm**		**Mortar**	
W/C Ratio	***Age*** (days)	Moisture Content (%)	Absorption (%)	Moisture Content (%)	Absorption (%)	Moisture Content (%)	Absorption (%)	Moisture Content (%)	Absorption (%)
0.4	*7*	6.4	6.7	6.7	7.2	6.9	7.8	6.1	9.0
	14	4.8	6.6	5.2	7.1	5.4	7.4	5.8	8.1
	28	4.5	6.5	4.7	6.9	5.3	7.5	5.5	7.8
0.5	*7*	5.6	8	7.5	8.7	7.8	9.6	7.0	10.7
	14	5	7.6	5.4	8.7	5.7	9.5	5.9	10.5
	28	3.9	7.3	5	8.3	5.6	9.5	5.2	9.9
0.6	*7*	8.7	10	7.6	10.3	7.8	10.9	8.2	12.9
	14	4.9	9	4.8	9.8	6.1	11.5	7.4	12.2
	28	4.1	7.9	4.6	10.1	5.7	11.2	6.4	11.4

Table 7.2 Moisture content and absorption values recorded for Gravel aggregate specimens

Specimen Type	W/C Ratio	Moisture Content (%)			Absorption (%)		
		7 days	*14 days*	*28 days*	*7 days*	*14 days*	*28 days*
Limestone	0.4	5.90	5.53	5.37	7.80	7.59	7.55
Thames Valley Gravel	0.4	5.82	5.68	5.19	7.72	7.66	7.31
Lytag	0.4	7.74	5.87	5.61	8.76	8.65	8.55
Gravel + air-entrainment	0.2	3.30	2.44	2.35	16.4	16.75	16.48
Gravel + Fibres	0.4	6.35	4.85	4.75	7.54	7.19	7.25

Table 7.3 Moisture content and absorption values recorded for other specimens

7.3.3 PORE STRUCTURE

Information on the size and distribution of pores within the specimens was determined using the same mercury intrusion porosimetry (MIP) technique as described in Chapter 6. The results of the MIP tests are summarised in Table 7.4. A complete description of the pore size distribution is presented in Figure 7.2 which shows the relationship between pore volume V and the pore diameter (to a logarithmic scale). However, a more meaningful picture of the pore size distribution is presented in Figures 7.3, 7.4 and 7.5 which plot ($dV/dlogR$) against R.

W / C Ratio	Age (days)	Intrusion vol. (cm^3/g)	Total pore area (m^2/g)	Mean pore radius (μm)	Bulk density (g/cm^3)	% Capillary
0.4	7	0.0679	15.9902	0.0085	0.7388	21.83
	14	0.0664	15.3741	0.0087	0.7386	21.36
	28	0.0620	13.5582	0.0092	0.7442	20.08
0.5	7	0.0861	20.6030	0.0084	0.7470	28.02
	14	0.0797	18.5255	0.0086	0.7303	25.33
	28	0.0793	16.0002	0.0099	0.7302	25.21
0.6	7	0.1081	20.2380	0.0107	0.7417	34.91
	14	0.1022	19.1575	0.0109	0.7241	32.22
	28	0.0968	17.4339	0.0111	0.7419	31.29

Table 7.4 Summary of results of MIP tests

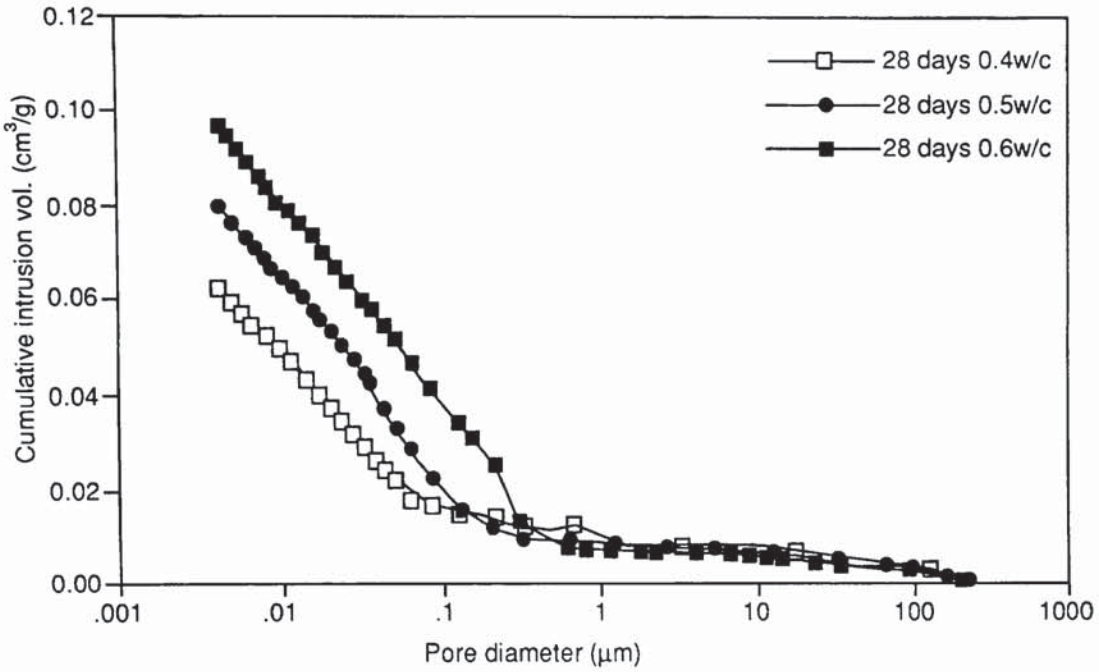

Figure 7.2 Variation of intruded pore volume with pore diameter

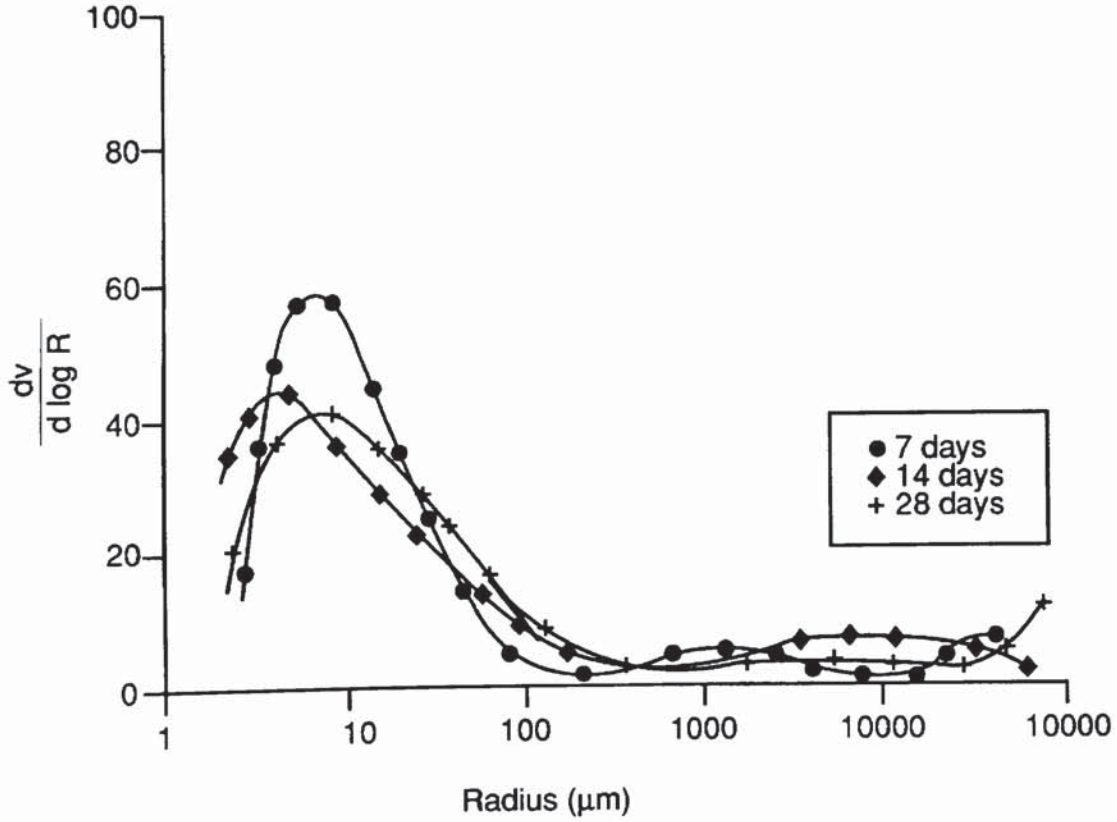

Figure 7.3 Pore size distribution (w/c = 0.4)

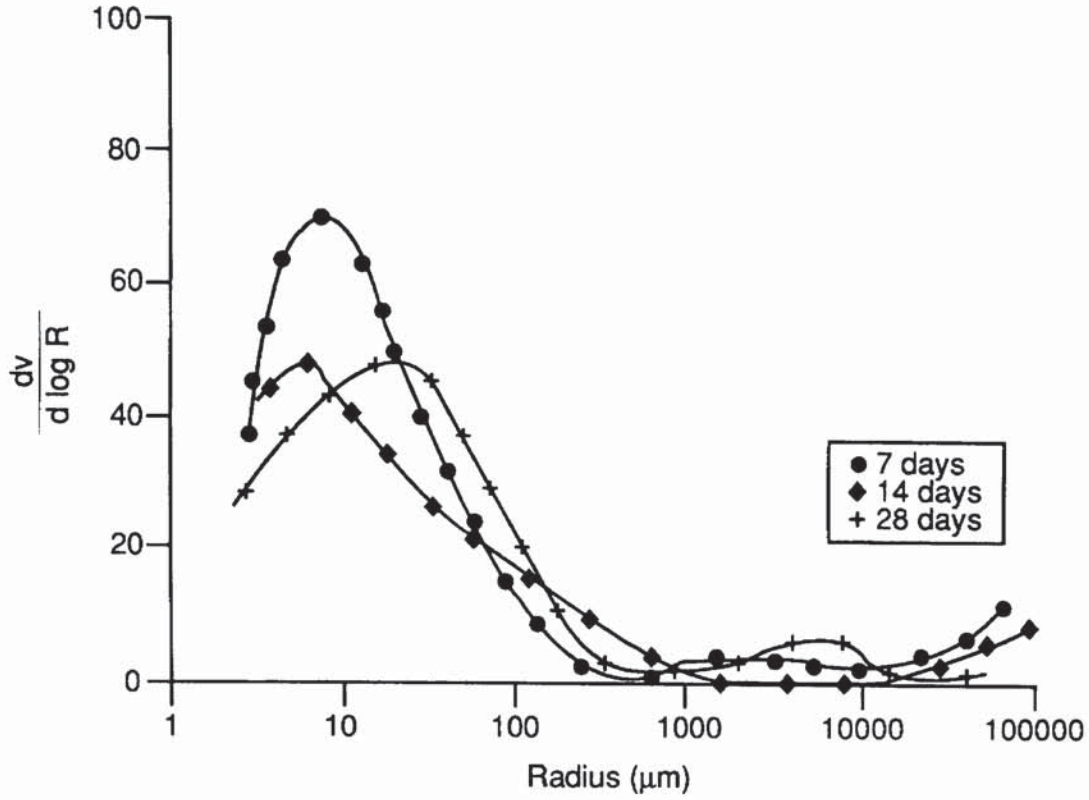

Figure 7.4 Pore size distribution (w/c = 0.5)

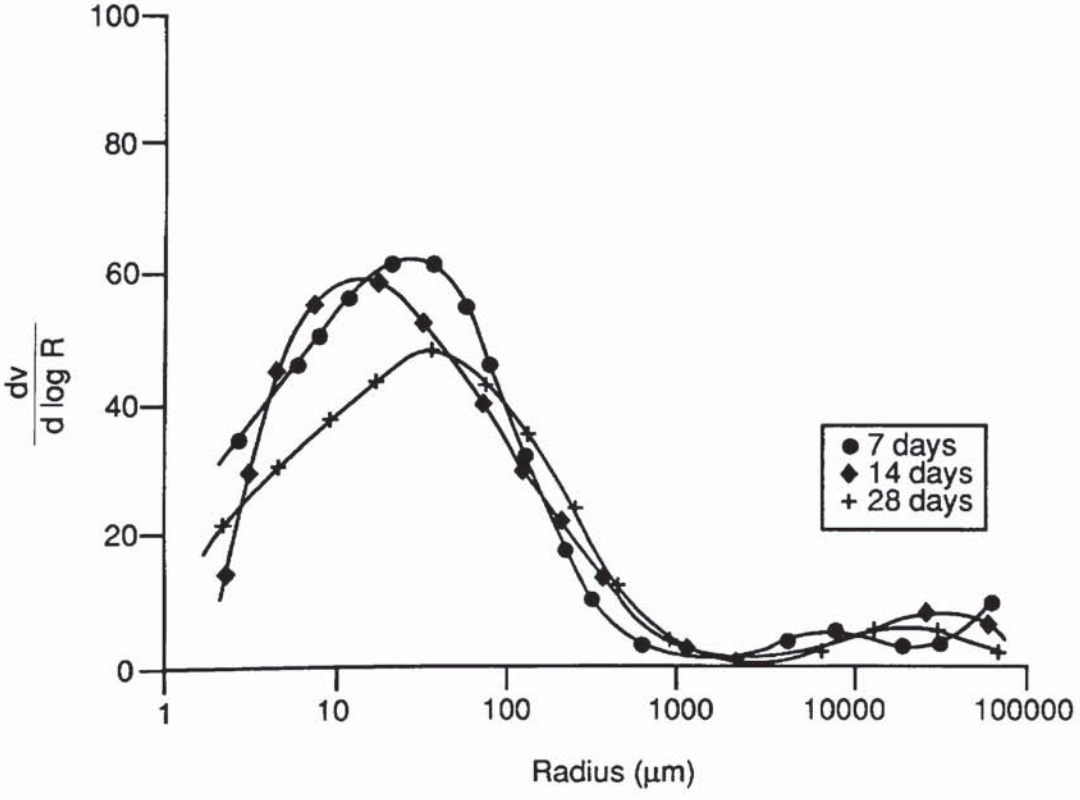

Figure 7.5 Pore size distribution (w/c = 0.6)

7.3.4 TENSILE STRENGTH

The direct tensile strength of the mortar specimens was determined by TBV Stanger Ltd., Elstree, Hertfordshire in accordance with the methodology described in BS 6319:Part 7:1985. Dumb-bell shaped mortar briquette specimens were subjected to a direct tensile load and their strength determined accordingly. The results are given in Table 7.5.

Water/Cement Ratio	Age (days)	Tensile Strength ($N/mm^{2)}$
0.4	7	4.3
	14	4.7
	28	4.9
0.5	7	3.6
	14	4.0
	28	4.2
0.6	7	2.1
	14	2.5
	28	2.8

Table 7.5 Tensile strength of mortar briquettes

7.4 EXPERIMENTAL RESULTS

7.4.1 TEMPERATURES

A typical example of the temperatures developed at the surface and centre of a heated specimen is given in Figure 7.6. This figure shows that although a temperature gradient does exist across the specimen, it is not very large. Accordingly the assumption that thermal stresses may be ignored appears reasonable. The temperature data recorded in each test can be used to calculate the velocity of the 100°C isotherm, which Meyer-Ottens (1972) suggested provides an important measure of the material's capacity to develop pore pressures.

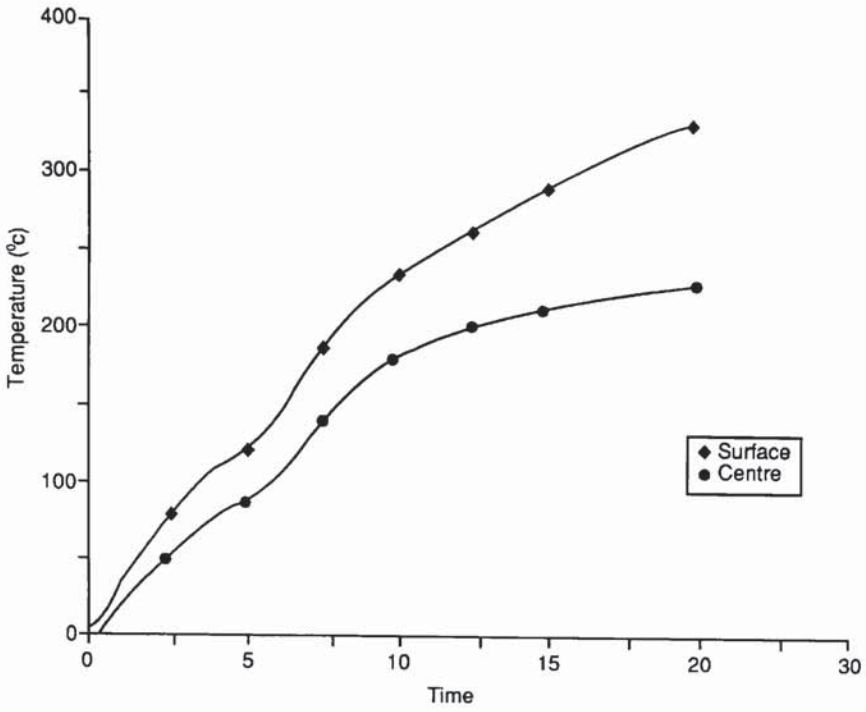

Figure 7.6 Temperatures developed in a typical mortar specimen

7.4.2 CATEGORISATION OF OBSERVED BEHAVIOUR

The response of the concrete specimens to the imposed heat flux may be classified into 4 categories as shown in Table 7.6. The observed failure modes are best described with the aid of photographs. Failures in Categories I and II are considered to be a form of explosive spalling for the purposes of further analysis. Category III failure (global cracking) appeared to relieve pore pressures and in all cases prevented subsequent Category I and II failures occurring.

Category	Description	Plate Ref.
I	Violent explosive failure of entire sample	Plate 7.1
II	Local failure of the specimen at its edge. Although explosive it is not as violent as Category I failure.	Plate 7.2
III	Failure of the specimen due to thermally induced cracking.	Plate 7.3
IV	No failure, only slight crazing at the surface	Plate 7.4

Table 7.6 Categorisation of failure modes

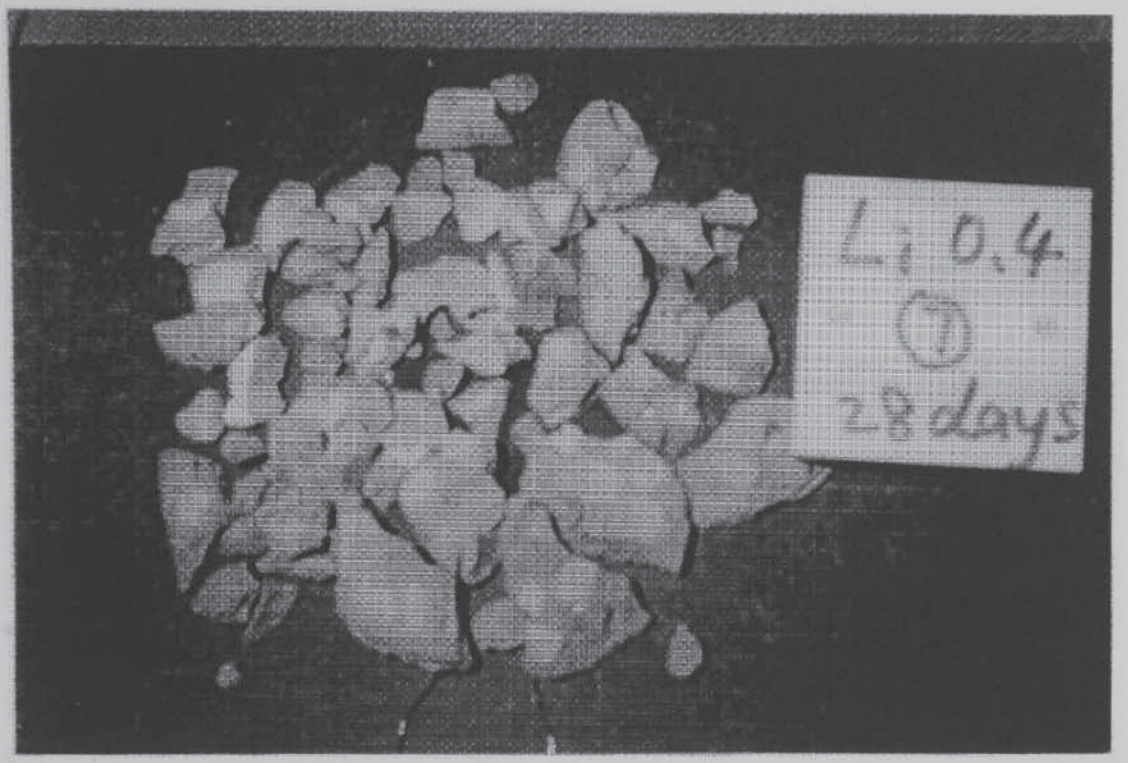

Plate 7.1 Example of Category I failure of Lytag concrete specimen

Plate 7.2 Example of Category II failure of Lytag concrete specimen

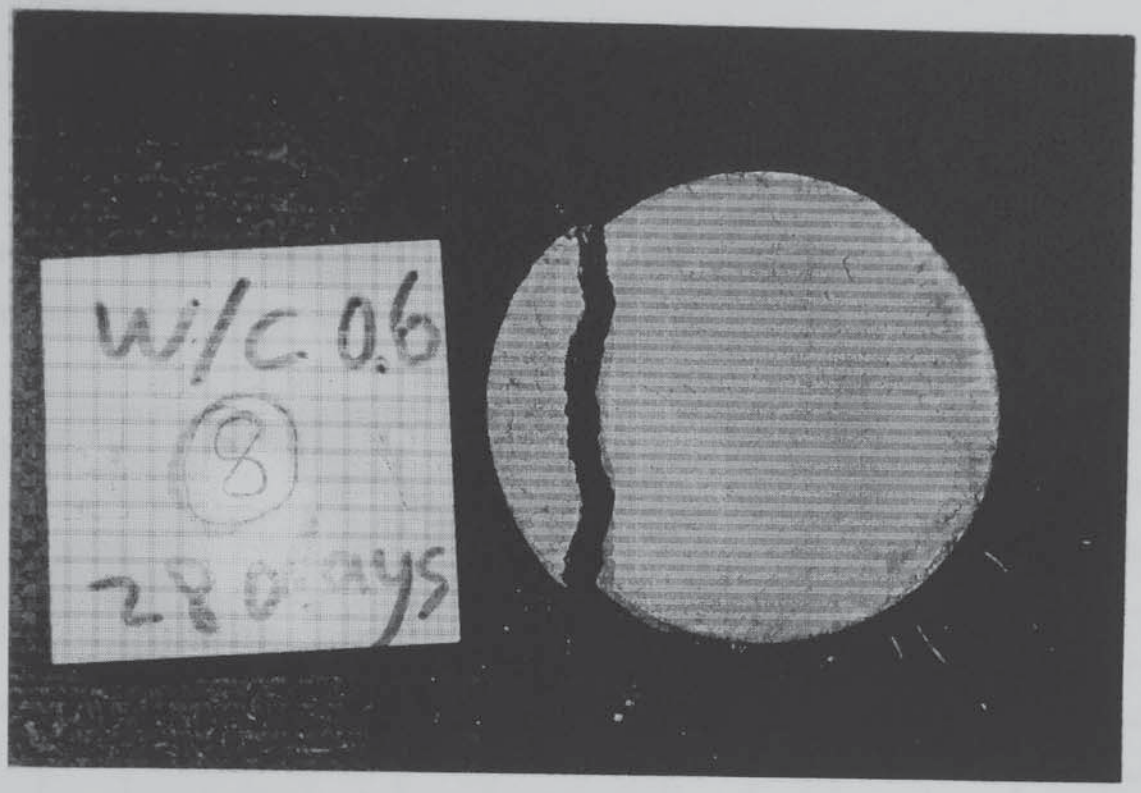

Plate 7.3 Example of Category III failure

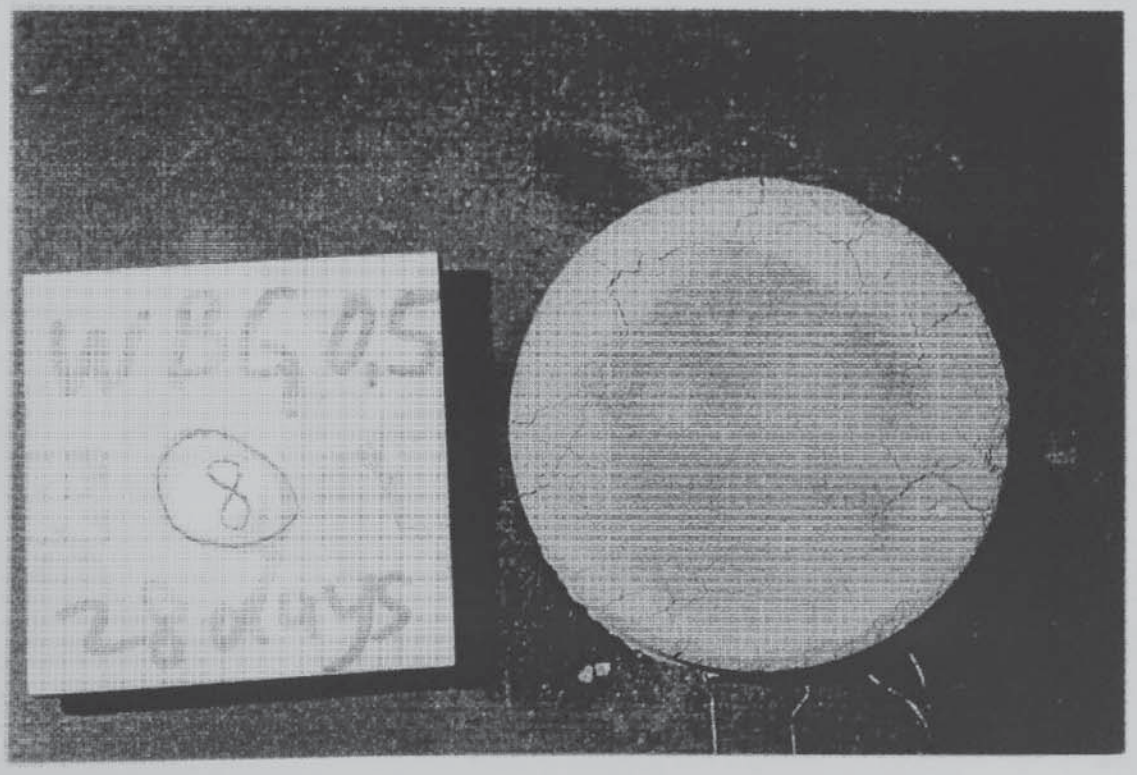

Plate 7.4 Example of Category IV

7.4.3 RESULTS OF HEATING TESTS

The results of the heating tests are summarised in Table 7.7 for Thames Valley Gravel specimens and in Table 7.8 for the other specimens. The heating rates referred to in these Tables relate to the rate of temperature rise actually measured at the surface of the specimen and therefore the heating rates vary somewhat from specimen to specimen. The failure temperature was also measured at the heated surface.

Agg. size		**20 mm**			**10 mm**			**5 mm**			**Mortar**		
Age days	w/c	Heat Rate (°C/s)	Fail Temp (°C)	Mode	Heat Rate (°C/s)	Fail Temp (°C)	Mode	Heat Rate (°C)	Fail Temp (°C/s)	Mode	Heat Rate (°C/s)	Fail Temp (°C)	Mode
7	0.4	0.4	246	I	0.4	288	I	0.4	303	I	0.4	343	II
		0.8	180	I	0.8	192	I	0.8	208	I	0.8	198	II
14		0.8	165	II	0.4	295	III	0.4	301	III	0.8	266	II
		1.0	179	II	0.8	159	II	0.7	208	I	1.3	137	II
28		1.3	-	IV	0.4	336	III	0.5	233	I	0.80	-	IV
		1.4	-	IV	0.8	255	I	0.8	245	I	1.0	159	II
7	0.5	0.4	230	I	0.4	-	IV	0.3	225	I	0.7	312	III
		0.8	221	I	0.8	233	I	0.8	229	I	1.0	154	I
14		0.4	-	IV	0.4	-	IV	0.3	-	IV	1.0	241	II
		0.8	-	IV	1.0	196	I	0.7	230	I	1.3	155	II
28		1.0	-	IV	0.7	298	I	0.5	343	III	0.7	343	III
		1.7	-	IV	1.3	385	III	1.0	375	I	1.3	-	IV
7	0.6	0.4	-	V	0.4	-	IV	0.3	-	V	0.4	-	IV
		0.8	196	II	0.8	-	IV	0.6	340	III	0.8	325	I
14		0.8	-	IV	1.2	-	IV	0.6	-	IV	0.8	363	III
		1.7	187	II	1.5	-	IV	1.3	203	II	1.5	216	II
28		0.8	-	IV	0.8	-	IV	1.0	-	IV	0.7	387	III
		1.5	216	II	1.5	-	IV	1.3	-	IV	1.4	-	IV

Table 7.7 Results of heating tests on Thames Valley Gravel specimens

Specimen Type	Limestone			Lytag			Gravel + Air entrainment			Gravel + Fibres		
Age (days)	Heat Rate (°C/s)	Fail Temp (°C)	Mode	Heat Rate (°C/s)	Fail Temp (°C)	Mode	Heat Rate (°C/s)	Fail Temp (°C)	Mode	Heat Rate (°C/s)	Fail Temp (°C)	Mode
7	0.3	234	I	0.3	203	I	0.3	-	IV	0.5	-	IV
	1.0	241	I	0.7	240	I	1.0	-	IV	1.1	-	IV
14	0.3	196	I	0.3	180	I	0.7	-	IV	0.7	-	IV
	0.5	188	I	0.7	200	I	1.0	-	IV	1.0	-	IV
28	0.3	-	I	0.3	253	I	0.7	-	IV	0.7	-	IV
	0.4	187	IV	0.7	273	I	1.0	-	IV	1.0	-	IV

Table 7.8 Results of heating tests on other specimens

7.5 INITIAL OBSERVATIONS FROM RESULTS

7.5.1 EFFECT OF HEATING RATE

The results of the experiments indicate that increasing the rate of surface heating promotes the likelihood of explosive spalling. Furthermore, increasing the heating rate reduces the temperature at which explosive failure occurs. An illustration of the form that the relation between heating rate and failure temperature might take is shown in Figure 7.7. When failure occurs at a lower temperature a higher tensile strength has been overcome and thus these observations confirm that higher heating rates result in higher pore pressures within the concrete

7.5.2 EFFECT OF SPECIMEN AGE

The propensity of the specimens to spalling is reduced with increased age. Although this may be due in part to the increased tensile strength available in older specimens, it is more likely influenced by the significant reduction in moisture content (and increased absorption) that accompanies age. The effects of age and moisture content are discussed separately in the following Sections.

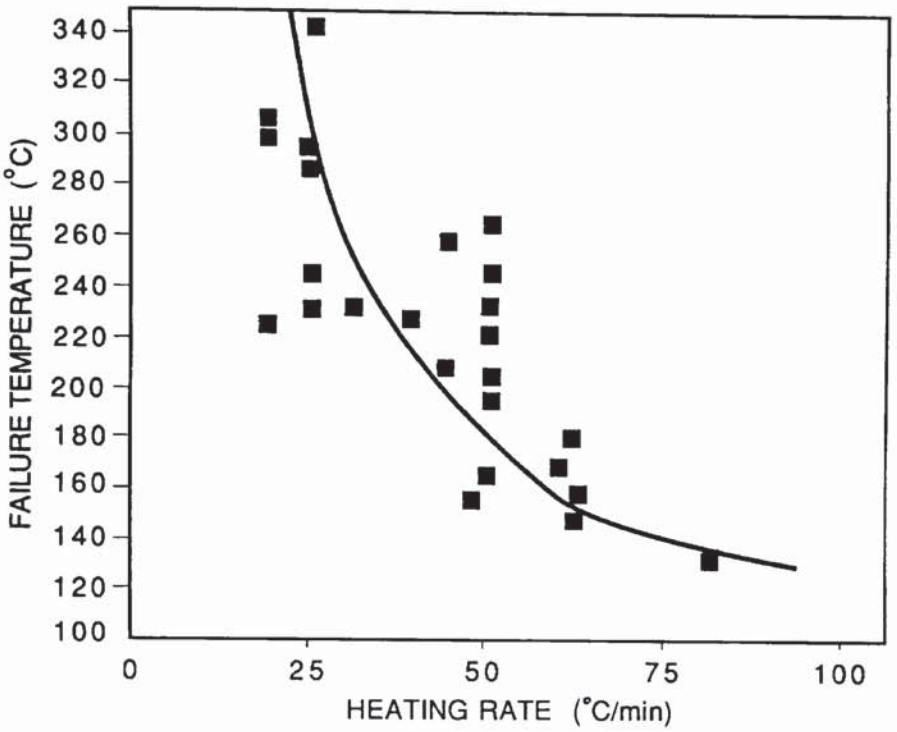

Figure 7.7 Relationship between rate of heating and failure temperature

7.5.3 EFFECT OF WATER/CEMENT RATIO

Although, the tensile strength of the specimens increased relatively slightly between 7 and 28 days, their propensity to spalling was significantly reduced over a similar timescale. The effect is not due only to the increased tensile strength, however, as specimens with lower w/c ratios (and consequently higher strengths) illustrated an increased susceptibility to spalling. Clearly, there are inter-related influences of moisture content, tensile strength and pore size distribution. It appears from the experimental data that tensile strength is of lesser importance than pore size distribution and consequently specimens with reduced w/c ratios are more susceptible to spalling.

It was also observed that the nature of the spalling was more violent in specimens with lower w/c ratios. This may be explained by the fact that larger pore pressures are necessary to cause failure of these higher strength specimens and consequently where failure occurs it is more violent because of the greater energy released. This correlates with behaviour reported by Hertz (1992) who observed that silica fume concretes reinforced with steel fibres (and thus having high tensile

strengths) exploded violently into very many small pieces when heated to certain levels. In effect, the superior tensile strength of the concrete can reduce its resistance to explosive spalling, as its permeability at higher temperatures is not increased by cracking and pore pressures continue to develop without relief.

7.5.4 EFFECT OF MOISTURE CONTENT

Representative samples from each batch of test specimens were examined for moisture content by drying them at 105°C and, as illustrated in Tables 7.2, moisture contents ranged from 5 to 10% by weight. All oven-dried specimens were subsequently heated in the test apparatus and monitored for spalling. Regardless of specimen age or aggregate type, no spalling was observed.

Although, bound water is still present at 105°C and Akhtarruzaman and Sullivan (1970) have shown that bound water can represent over 3 times the volume of free water, it would appear that in this case the absence of free water was sufficient to prevent spalling. This could be due to the fact that at the temperatures that the bound water becomes released (over 170°C), the cement gel breaks down and its capillaries increase in size, thus increasing permeability. Such a mechanism has been proposed by Bažant and Thonguthai (1978).

It is more useful, however, to view the behaviour in terms of the pore saturation. If a measure of the pore saturation is given by the ratio of the free moisture content to the absorption, the pore saturation becomes zero at moisture contents of zero. The experimental data suggest that the probability of explosive spalling also becomes zero in such cases. It may be concluded that the development of pore pressures is directly related to the pore saturation in the specimen.

7.5.5 EFFECT OF AGGREGATE SIZE

The test specimens were made of a cement/sand mortar. In some cases, aggregates were placed adjacent to and flush with the heated face to imitate a concrete surface but in a controlled manner. The effect of adding aggregate particles was to promote Category I failure with specimens containing larger aggregates being more susceptible to failure. This finding supports the general

perception that large aggregates are more likely to spall (Malhotra, 1984). Addition of large aggregates also reduced the time to explosive spalling of the specimens.

The experimental data show an increased susceptibility to spalling amongst the specimens containing 5 mm aggregates. This effect is probably due to a flaw in the test procedure, whereby specimens with 5 mm aggregate particles contained much more aggregate than specimens with larger aggregate particles. The aggregate cement ratio was not kept constant. The effect may also be related to the fact that the sand-cement matrix contains more saturated pores than the component aggregates and thus acts as the medium for pore pressure generation. Thus, the presence of aggregate has competing effects on spalling in that aggregates locally reduce the amount of pore pressure generating medium, i.e. mortar, but alternatively the presence of aggregate reduces the permeability of the concrete increasing pore pressures.

7.5.6 EFFECT OF AGGREGATE TYPE

Heating tests were undertaken on specimens containing Thames Valley Gravel, Cheddar Limestone and Lytag. Specimens made with Gravel were the most susceptible to spalling. Specimens containing Limestone behaved similarly to those containing Lytag, with the Lytag being if anything more susceptible to spalling.

The explosive spalling observed with the heated Lytag specimens was particularly violent in nature. In many cases, the explosive failure of the specimen was sufficient to damage the heater casing, as shown in Plate 7.5. The failure of the Lytag specimens was different from the others in that many aggregate particles themselves were split. In the Gravel and Limestone specimens, failure was limited to the mortar paste and bond around each aggregate particle. This suggests that pore pressures were actually created within the Lytag particles themselves. It may be concluded that where the saturation of the aggregate itself exceeds that of the cement matrix that the presence of aggregates at the heated surface promotes spalling.

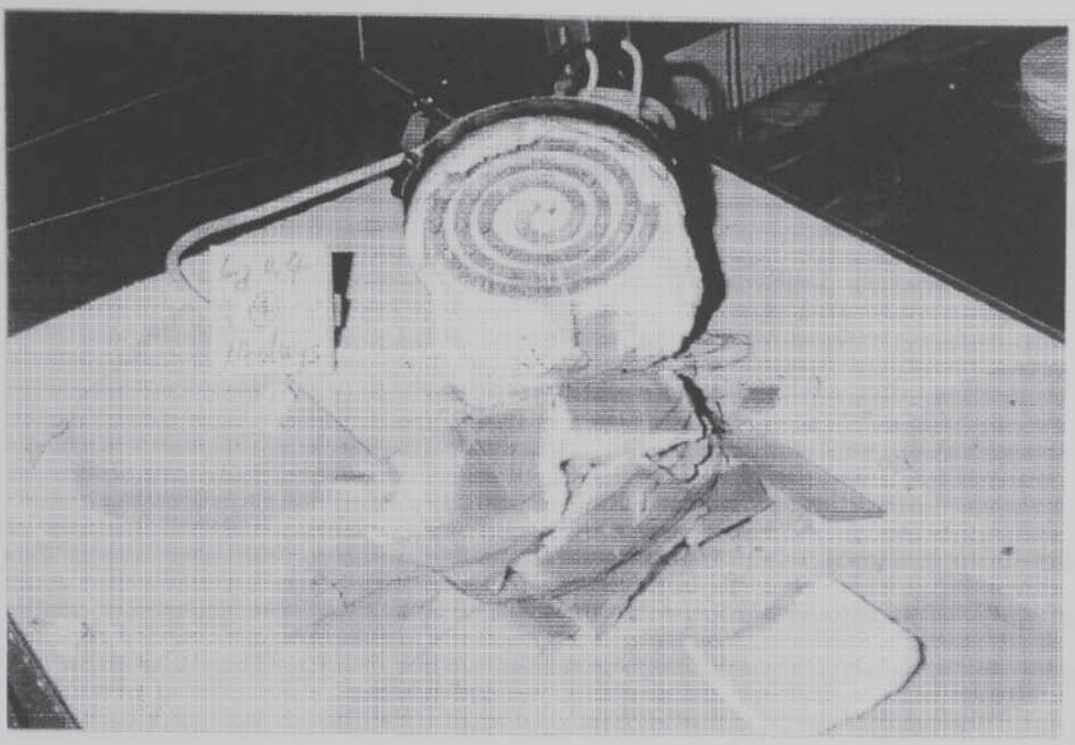

Plate 7.5 Destructive effect of explosive spalling on electrical heaters

Another factor that explains the inferior performance of the Lytag is its increased retention of tensile strength at elevated temperatures as reported by Zoldners (1960). Thus, the observed behaviour of Lytag corroborates the proposals made in Section 7.5.3 regarding the increased energy release in specimens with higher tensile strengths.

7.5.7 EFFECT OF INCLUSION OF POLYPROPYLENE FIBRES

The addition of 0.05 % (by weight) of polypropylene fibres into specimens with water/cement ratios of 0.4 and siliceous gravel aggregates of 10mm size completely eliminated the occurrence of spalling. Under heating conditions of 25°C per minute, 83% of similar specimens without fibres had failed explosively. Clearly, the addition of polypropylene fibres to concrete is an effective means of preventing explosive spalling. Similar conclusions have recently been reached by Diedrichs *et al.* (1994) based on their study of high strength concrete columns.

In the experiments reported in this Chapter, the temperatures at which spalling had occurred in the equivalent specimens without fibres ranged from 208 to 303°C. These temperatures are well in excess of the melting point of the polypropylene fibres. It is possible that the fibres prevent

build up of pore pressures by melting at high temperatures and thus increasing the permeability of the specimen and alleviating pore pressures. Further work is necessary to fully ascertain the effects that addition of polypropylene fibres has on the behaviour of concrete at high temperatures. The exact mechanism by which fibres appear to increase permeability cannot be determined based on the limited number of experiments undertaken for this Thesis.

7.5.8 EFFECT OF AIR-ENTRAINMENT

Specimens made using 10 mm Gravel aggregate and 0.125% (by weight) of an air-entraining agent were completely free of spalling regardless of the heating regime. The addition of the agent had the effect of reducing the moisture content and increasing the absorption value. In effect, air entrainment reduces the pore saturation within the specimen. As proposed in Section 7.5.4, susceptibility to spalling is directly related to pore saturation and accordingly air entrainment can be used to alleviate the pore pressures developed in heated concretes.

7.6 PORE PRESSURES DEVELOPED IN TEST SPECIMENS

7.6.1 UNDERLYING PRINCIPLES

As no instrumentation was cast within the test specimens, it is necessary to develop an indirect means of evaluating the pore pressures that might develop within the concrete on heating. The pore pressure developed within the concrete can be related to the tensile strength using a model based on that first proposed by Akhtarruzaman and Sullivan (1970). For those tests where explosive spalling occurred (Category I or II failure), it is assumed that the pore pressure is equal to that necessary to cause failure of a thin walled sphere under an internal bursting pressure. As shown in Figure 3.19, Akhtarruzaman and Sullivan suggested that concrete could be represented by an analogous hollow sphere. The thickness of the wall of the sphere is related to the volume of hydrated gel in the concrete and the volume of the sphere may be related to the volume of voids in the concrete.

Akhtarruzaman and Sullivan successfully used the model to predict the failure temperatures for

a range of different concretes but relied on several simplifying assumptions which cannot be justified in the light of information that has become available since their work. The most tenuous assumption made was that the pore pressure in the concrete at any given temperature was the vapour pressure of saturated steam at the same temperature. Subsequent work by Bažant and Thonguthai (1978) has shown this assumption to be incorrect.

The need for such an assumption is eliminated by adopting the following procedure for calculating the pore pressure developed in the heated concrete specimens at failure;

(i) calculation of radius of the model sphere
(ii) calculation of wall thickness of model sphere
(iii) determination of internal pressure necessary to generate a bursting stress in excess of the material's tensile strength (at failure temperature)

7.6.2 RADIUS OF MODEL SPHERE

Akhtarruzaman and Sullivan determined the radius of the model sphere from the total volume of voids within the prototype concrete. However, it is considered more suitable here to calculate the radius of the sphere from the amount of water available for generating pore pressures. Since, it is assumed based on the work of Akhtarruzaman (1973) that bound water is released from the cement gel at temperatures of approximately 175°C, and that spalling generally occurs at higher temperatures, the water available for pore pressure generation includes free water, absorbed gel water and water combined in hydrates. However, experience from the heating of oven-dried specimens has shown that it is the quantity of free water that dictates the susceptibility of a concrete to spalling and thus, the thickness of the wall of the model sphere may be given in terms of the free moisture content w_o as;

$$R_{sphere} = \sqrt[3]{\frac{3\ \rho_c\ V_s\ w_o}{4\ \rho_w\ \pi}} \qquad (7.1)$$

where;

V_s = volume of specimen ($157 \times 10^3\ mm^3$)

7.6.3 WALL THICKNESS OF MODEL SPHERE

The thickness of the wall of the model sphere is determined on the basis that the volume of the wall of the sphere is exactly equal to the volume of hydrated gel in the concrete. The volume of gel depends on the degree of hydration that has taken place, the w/c ratio and the mass of cement.

Sullivan (1970) suggested that at 28 days after casting, 20% of the total effective water goes into chemical combination with cement. Furthermore as 1g of cement combines chemically with 0.25g of water for complete hydration (Neville, 1981), the degree of hydration after 28 days h_{28} is given by;

$$h_{28} = \frac{0.2 \ w/c}{0.25} \tag{7.2}$$

where w/c is the effective water to cement ratio. The degree of hydration at any age h_{age} may be calculated from a knowledge of the relative strength of the concrete at that age F_{age} compared to the 28 day strength F_{28}. Thus;

$$h_{age} = \left(\frac{F_{age}}{F_{28}} \right) h_{28} \tag{7.3}$$

Neville provided a straightforward algorithm for calculation of the volume of the hydrated gel. He assumed that cement has a specific gravity of 3.15, that the non-evaporable water makes up 23% of the weight of the cement and that the volume of cement gel is equal to the volume of anhydrous cement and water less 0.254 times the volume of non-evaporable water. A further assumption that cement paste has a characteristic porosity of 28%, allows the volume of gel V_{Gel} to be quantified directly from the initial mass of cement M_{cement};

$$V_{gel} = 0.68 \ M_{cement} \ h_{age} \tag{7.4}$$

The thickness of the wall of the model sphere with such a volume may be calculated from simple geometry as;

$$T_{wall} = \sqrt[3]{\frac{3 \ V_{gel}}{4 \ \pi} + R_{sphere}^3} - R_{sphere} \tag{7.5}$$

7.6.4 INTERNAL PORE PRESSURE

It is assumed that explosive spalling occurs when the hoop stress generated in the (thin) walls of the model sphere reaches the tensile strength of the concrete. Thus, for specimens where spalling has been observed the pore pressure may be calculated by assuming that it is equal to the internal bursting pressure necessary to generate such a hoop stress. Thus;

$$P_{pore,fail} = \frac{(2\ R_{sphere}\ T_{wall} + T_{wall}^2)}{R_{sphere}^2} F_t(\theta) \qquad (7.6)$$

where;

$P_{pore,fail}$ = the pore pressure developed in the specimen at failure

$F_t(\theta)$ = the tensile strength of the specimen at failure which may be given as a function of temperature (after Thelandersson, 1971) by;

$$F_t(\theta) = F_t(20^oC)\ (1.12 - 0.0012\theta) \qquad (7.7)$$

$$\theta \geq 100^oC$$

7.6.5 CALCULATION OF PORE PRESSURES IN TEST SPECIMENS

Equations 7.1, 7.5 and 7.6 were used to calculate the dimensions of the model sphere and to calculate the pore pressures that existed at the moment of failure for the different mortar specimens examined. The variables of w/c ratio and age meant that in all some 9 data points were available. The failure temperatures of the different mortar specimens observed during the heating tests were presented in Table 7.7. Thus, the pore pressure acting at failure was calculated for each of the mortar specimens.

In order to avoid the need for calculating the dimensions of the model sphere in every case, the calculated pore pressures have been related directly to the initial tensile strength of the mortar (as given in Table 7.5). The empirical relationship is shown in Figure 7.8 and a good fit with the experimental data is achieved by the relationship;

$$P_{pore,fail} = 0.32\ e^{0.5\ F_t(20^oC)} \qquad (7.8)$$

This relationship may be used to calculate the pore pressure needed to cause failure of a heated specimen directly from its ambient temperature strength, without the need to use the model sphere routine. Equation 7.8 has been validated only for the test specimens studied in this programme.

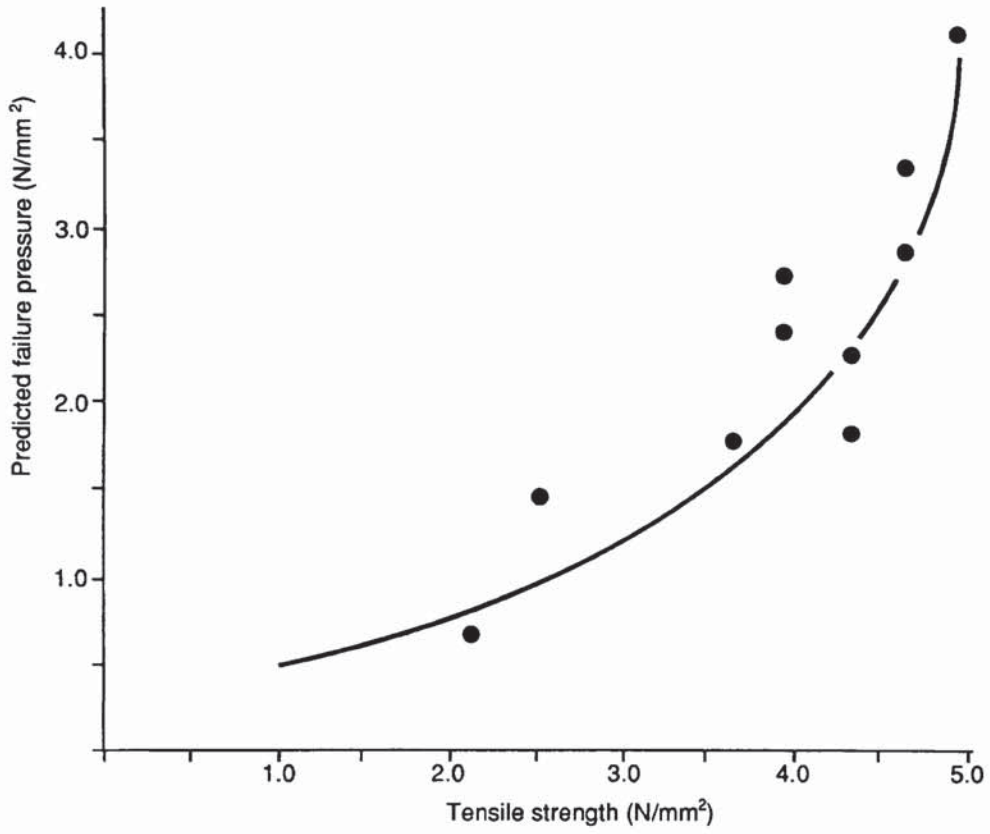

Figure 7.8 Relation between pore pressure at failure and initial tensile strength of mortar

7.8 CONCLUSION

For the small specimens examined, a model (Equation 7.8) has been developed to calculate the pore pressure needed to cause failure of concrete specimens as a function of their initial tensile strength. For larger specimens, the pore pressures will have to be considered together with both the thermal and load stresses before the likelihood of explosive spalling can be assessed. The means by which such assessment may be made is presented in Chapter 8.

CHAPTER 8. FURTHER CONSIDERATION OF RESULTS OF EXPERIMENTAL PROGRAMME

8.1 FRAMEWORK FOR CONSIDERING EXPLOSIVE SPALLING

A model of explosive spalling has been developed based on the scenario shown in Figure 8.1, which considers all the stresses acting on a heated concrete specimen and a reference system of axes *x*, *y* and *z*. Assuming that elastic theory is applicable, the strain in the x-direction may be described by;

$$\epsilon_x = \frac{1}{E}\left\{\sigma_x - \nu\ (\sigma_y + \sigma_z)\right\} \qquad (8.1)$$

where;

σ_x = stress acting in the *x* direction

σ_y = stress acting in the *y* direction

σ_z = stress acting in the *z* direction

ν = Poisson's Ratio

E = Modulus of Elasticity

The stresses acting in each orthogonal direction are summarised in Table 8.1. It is assumed that where the specimen is loaded in both directions, the stresses in the *y* and *z* directions are equal and where loading is uniaxial, only the stresses in the *z* direction are zero.

Direction	Stresses
x	Pore pressure stress σ_p (tensile)
y	Load stress σ_l (compressive) Thermal stress σ_t (compressive) Pore pressure stress σ_p (tensile)
z	Load stress σ_l (compressive) Thermal stress σ_t (compressive) Pore pressure stress σ_p (tensile)

Table 8.1 Stresses acting in heated specimen

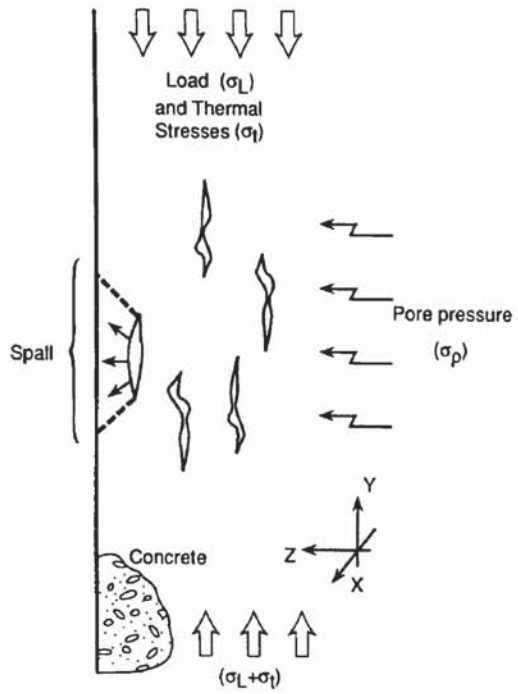

Figure 8.1 Stresses acting in heated concrete specimen

Applying the information from Table 8.1 to Equation 8.1, the total strain observed in a biaxially loaded specimen is given by;

$$\epsilon_x = \frac{1}{E}\left\{\sigma_p + 2\ \nu\ (\sigma_l + \sigma_t - \sigma_p)\right\} \tag{8.2}$$

The strain energy density in the x direction W_x may be described by;

$$W_x = \frac{1}{2}\ \sigma_x\ \epsilon_x \tag{8.3}$$

This must provide the work needed to cause failure of the concrete surface W_{fail} where;

$$W_{fail} = \frac{F_{tensile}^2}{2\ E} \tag{8.4}$$

Combining Equations 8.2, 8.3 and 8.4 gives a basic criterion for explosive spalling;

$$F_{tensile}^2 \leq (1 - 2\nu)\ \sigma_p^2 + 2\nu\ (\sigma_l + \sigma_t)\sigma_p \tag{8.5}$$

The form of Equation 8.5 correlates with many of the observations on explosive spalling reported in Chapters 2, 4 and 6. The equation accommodates the observed importance of pore pressure, yet explains the significant role played by applied load and restrained thermal expansion.

Equation 8.5 will be used as the fundamental basis for analysing the experimental data reported in Chapter 6. The necessary information on both load and thermal stresses is readily available for each individual test performed. However, the failure of the instrumentation to record pore pressures within the specimens means that an alternative approach has to be considered. The experimental work reported in Chapter 7 provides a basis for predicting the pore pressures necessary to cause failure of small mortar specimens. A more fundamental model of pore pressure development is needed at this stage if Equation 8.5 is to be used in the evaluation of the results of the heating and loading test programme.

8.2 DEVELOPMENT OF MODEL FOR PREDICTING PORE PRESSURE

8.2.1 BACKGROUND

As has been discussed in Chapter 3, a wide range of models have been developed over the years to predict the pore pressures developed in heated concrete. Such models are often quite complicated as it is a non-trivial task to determine the complete pore pressure response of a physically changing concrete matrix to the combined transport of moisture and heat.

Recognising the scope of the problem, the more modest objective of this Section is to ascertain what parameters affect the maximum pore pressure developed in heated concrete and furthermore to gain some insight into the relationship that might exist between these parameters. The parameter groupings recognised can then be correlated with the experimental data recorded during the small-scale heating tests reported in Chapter 7 and their application extended to the prediction of the maximum pore pressures developed the simultaneously heated and loaded concrete specimens.

8.2.2 THEORETICAL BASIS FOR PORE PRESSURE GENERATION

Given a control volume of concrete exposed to heating from one side, as shown in Figure 8.2, it may be assumed that the inflowing heat initiates the movement of any moisture within the concrete away from the heated surface by a process of evaporation-condensation. The rate at which such vaporisation takes place V_{vapour} is proportional to the rate at which heat enters the control volume.

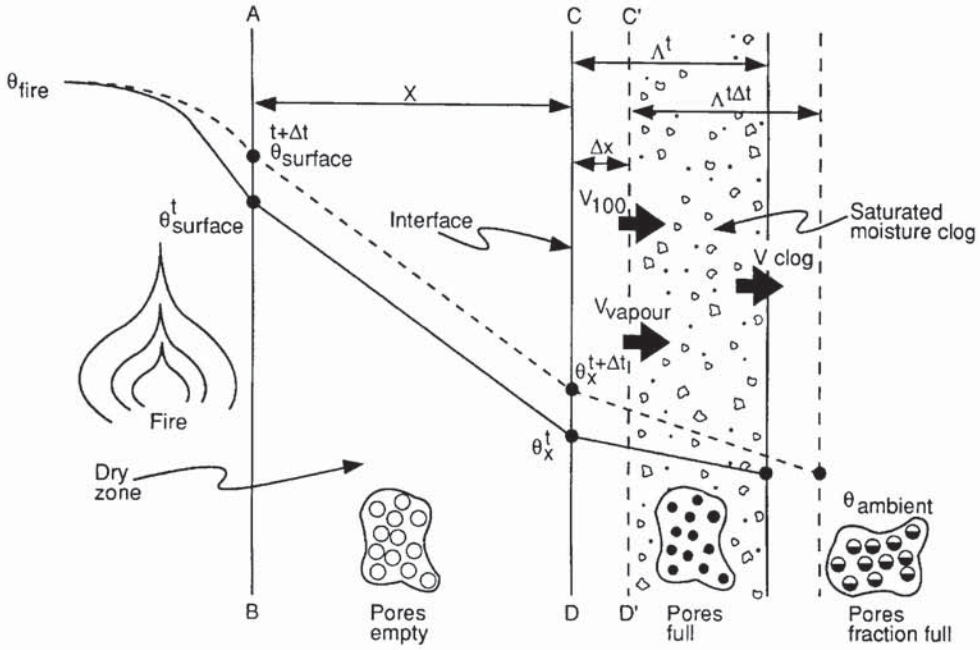

Figure 8.2 Model of heated concrete

However, the vaporised water does not simply move into the concrete. As Shorter and Harmathy (1965) described the inflowing moisture causes the pores some depth beneath the surface to become saturated and a moisture clog is set up. The moisture clog may itself move, but as Woodside and Kuzmak (1958) showed it will do so only under the influence of pressure. Such pressures are developed at the dry-zone to moisture clog interface by the restriction imposed on the evaporation-condensation process by the stagnant clog.

The rate at which the moisture clog moves V_{clog} is proportional to the pressure gradient acting across it. As increased vaporisation adds to the width of the moisture clog, more pressure is required to move it and thus in turn higher pore pressures develop at the interface. When these pressures become sufficient, they cause the clog to move. It is possible that spalling could be the

the result of the stresses induced by these pressures exceeding the tensile strength of the concrete.

In practice, the total movement of the clog may be monitored by observing the rate of change of position of the 100°C isotherm V_{100}. The total movement is related both to the vaporising force from the inflowing heat and the resistance effects of the concrete matrix, which may be regarded as a form of friction. Thus, it is proposed that;

$$V_{100} = V_{vapour} - V_{clog} \tag{9.6}$$

where; V_{100} = velocity of the 100°C isotherm
V_{vapour} = velocity of idealised vaporising front
V_{clog} = velocity of moisture clog

The moisture clog moves solely under the influence of the pressure gradient and given that the clog represents a fully saturated zone, D'Arcy's Law may be applied to give;

$$V_{clog} = \frac{K \ \Delta P \ \epsilon}{\eta \ \Lambda} \tag{9.7}$$

where; K = permeability of saturated concrete
ΔP = pressure differential across moisture clog
η = viscosity of moisture
Λ = width of moisture clog
ϵ = porosity of concrete

The width of the moisture clog Λ may be assumed to be directly related to its depth beneath the heated surface x as follows;

$$\Lambda = \frac{\phi}{1 - \phi} x \tag{9.8}$$

where ϕ is the degree of pore saturation. Assuming that the velocity of the clog is constant, (i.e. $x = V_{vapour} \cdot t$) and the pressure at the cooler side of the moisture clog is atmospheric, then Equations 8.6, 8.7 and 8.8 can be combined to give a basis for pore pressure development;

$$P_{pore} = \frac{\eta}{K \epsilon} \frac{\phi}{1 \phi} V_{vapour,\max} (V_{vapour} - V_{100}) t \qquad (8.9)$$

The characteristics of the velocity of the 100°C isotherm have been reported in Chapter 6 and also previously by Meyer-Ottens (1972) for different concretes. These data suggest that it is reasonable to assume that V_{100} achieves a constant value after about 5 minutes heating. Thus the maximum pore pressure $P_{pore,\ max}$ is governed by the maximum vaporisation velocity as follows;

$$P_{pore,\max} = \frac{\eta}{K \epsilon} \frac{\phi}{1 - \phi} V_{vapour,\max} (V_{vapour,\max} - V_{100}^{t^*}) t^* \qquad (8.10)$$

where; $V_{vapour,max}$ = maximum velocity of vaporisation front

t^* = time at which maximum vaporisation velocity is reached

$V^{t^*}_{100}$ = velocity of 100°C isotherm at time t*

While the velocity of the 100°C isotherm has to be observed experimentally, the maximum velocity that the vaporisation front might achieve can be predicted theoretically by considering the heat balance that exists within the heated control volume at any instant in time. Again, with reference to Figure 8.2, the fundamental balance (ignoring any heat losses) may be stated as;

$$q_{input} = q_{\theta} + q_{vapour} \qquad (8.11)$$

where; q_{input} = heat input into system ABC'D'

q_{θ} = heat used in raising temperature of ABCD

q_{vapour} = heat used in vaporising water in CC'DD'

Each term in Equation 8.11 may be evaluated individually. If it is assumed that the temperature gradient across the dry zone may be approximated as linear, then

$$q_{input} = \frac{k (\theta_s - \theta_x)}{x} \Delta t \qquad (8.12)$$

where; k = thermal conductivity of concrete

θ_s = temperature at surface of concrete

θ_x = temperature at dry zone to clog interface

x = depth of interface

Δt = time over which heat is input

The heat used in raising the temperature of ABCD is given by;

$$q_\theta = \rho_c \; x \; C \left(\frac{\theta_s^{t+\Delta t} + \theta_x^{t+\Delta t}}{2} - \frac{\theta_s^t + \theta_x^t}{2} \right) \tag{8.13}$$

where; ρ_c = density of concrete

C = specific heat capacity of concrete

Assuming that the rate of change of temperature at the interface is considerably less than the change at the heated surface, then Equation 8.13 may be simplified to;

$$q_\theta = \frac{\rho_C \; x \; C}{2} (\theta_s^{t+\Delta t} - \theta_s^t) \tag{8.14}$$

The heat required to vaporise the water in CC'DD' is given by;

$$q_{vapour} = \rho_w \; \phi \; \epsilon \; Q \; \Delta x \tag{8.15}$$

where; ρ_w = density of water

Q = specific heat of vaporisation of water at constant volume

Δx = change in depth of vaporisation front in time Δt

The governing heat balance equation (Equation 8.11) may now be re-assembled as;

$$\frac{k \; (\theta_s - \theta_x) \; \Delta t}{x} = \frac{\rho_c \; x \; C \; (\theta_s^{t+\Delta t} - \theta_s^t)}{2} + \rho_w \; \phi \; \epsilon \; Q \; \Delta x \tag{8.16}$$

The velocity of the vaporising front V^t_{vapour} at time t is defined as $\Delta x/\Delta t$ and is given by;

$$V^t_{vapour} = \frac{\Delta x}{\Delta t} = \frac{1}{\rho_w \; \phi \; \epsilon \; Q} \left(\frac{k \; (\theta_s - \theta_x)}{x} - \frac{\rho_c \; C \; x \; (\theta_s^{t+\Delta t} - \theta_s^t)}{2 \; \Delta t} \right) \tag{8.17}$$

A range of simplifying assumptions can be made to convert Equation 8.17 into a more useful form. A surface heating rate term m may be introduced, where;

$$m = \frac{\theta_s^{t+\Delta t} - \theta_s^t}{\Delta t} \tag{9.18}$$

By definition, the surface temperature θ_s may be described by the product $m.t.$ Furthermore the temperature at the dry zone-clog interface can be assumed to be 100°C. It is reasonable to assume that the vaporising front has similar characteristics to the 100°C isotherm and thus its velocity may be assumed to be constant some time after heating has commenced. Thus, the depth of the clog x at time t can be approximated from the mean velocity of the vapour front $V_{vapour,mean}$;

$$x = V_{vapour,mean}\, t \tag{9.19}$$

Given that the initial velocity of the vapour is zero ($V^{t=0}_{vapour} = 0$), $V_{vapour,mean}$ can be assumed equal to ($V^{t}_{vapour}/2$). Equation 8.19 may now be rewritten;

$$V^t_{vapour} = \sqrt{\frac{8\ k\ (mt - 100)}{(4\ \rho_w\ \phi\ \epsilon\ Q + \rho_c\ C\ m\ t)\ t}} \tag{9.20}$$

Equation 8.20 was differentiated with respect to time using mathematical computer sofware, allowing the time t^* at which V^t_{vapour} reaches its maximum value to be calculated;

$$t^* = \frac{10A + 100}{m} \tag{9.21}$$

where A is a dimensionless quantity which describes the physical condition of the concrete. In general, the relatively consistent nature of the material properties of concrete allow A to be assumed as a constant value of 18. This is demonstrated by the data given in Table 8.3. However, A is more fully given by;

$$A = \sqrt{100 + \frac{4\ \rho_w\ \phi\ \epsilon\ Q}{\rho_c\ C}} \tag{9.22}$$

The maximum velocity of the vaporisation front $V_{vapour,max}$ is calculated from Equations 8.20 and 8.21, giving;

$$V_{vapour,\max} = \left(\frac{1}{A + 10}\right)\sqrt{\frac{8\ k\ m}{\rho_c\ C}} \tag{8.23}$$

A complete pore pressure model has now been assembled. For any concrete heated by m °C per minute at its surface, once the rate of movement of the 100°C contour has been observed experimentally, Equations 8.10 together with 8.22 and 8.23 can be used to give a prediction for the maximum pore pressure that would be developed.

8.2.3 VALIDATION OF PORE PRESSURE MODEL

The pore pressures generated within the small test specimens described in Chapter 7 have been calculated using the model outlined in Section 8.2.2 (i.e. Equations 8.10, 8.22 and 8.23). In order to calculate the pore pressures developed within these specimens, the parameters required in the various equations have been allocated the values given in Table 8.2.

Material Property	Assumed Value
Viscosity (η)	10^{-3} N s / m^2
Porosity (ϵ)	recorded during MIP tests and given in Table 7.4
Saturation (ϕ)	assumed as (moisture content/absorption) from Table 7.2
Velocity of isotherm (V_{100})	assumed as time (in seconds) for thermocouple in centre of specimen to reach 100°C over depth (i.e. 0.01 m)
Density of water (ρ_w)	1000 kg/m^3
Density of concrete (ρ_c)	2200 kg/m^3
Heat of vaporisation (Q)	2.258 x 10^6 J/kg
Conductivity (k)	3 J / s m^2 °C
Heat capacity (C)	800 J / kg °C

Table 8.2 Material properties assumed when validating pore pressure model

The permeability of the concrete K has not been measured directly. However, Hughes (1985)

has suggested that permeability may be modelled by;

$$K = f\left(\frac{r^2}{n^2}\right) \tag{8.24}$$

where; f(..) = some empirically derived relationship
r = pore radius
n^2 = tortuosity factor (generally taken as 2.5)

A single value for pore radius called the mean pore radius R_{mean} provided a useful measure of the characteristics of each specimen, where;

$$R_{mean} = \frac{4\ V_{pore}}{A_{pore}} \tag{8.25}$$

where; V_{pore} = total volume of pores = total intrusion volume
A_{pore} = total pore area

The permeability of each specimen was calculated using Equation 8.24 and by assuming that a datum 28 day old mortar mix of w/c ratio 0.5 has a permeability of 6.1×10^{-15} m/s and a mean pore radius of 0.01 μm. Thus;

$$K = 6.1\left(\frac{R_{mean}}{0.01}\right)^2 . \ 10^{-15}$$

where R_{mean} is given by Equation 8.25 and measured in μm. The mean pore radius may easily be determined using mercury intrusion porosimetry. Values for R_{mean} are given for the different specimens in Table 7.4.

However, use of the mean pore radius in determining permeability does not account for the very significant effect of pore size distribution. For example, consider the flow in equal numbers of pores of radius 10 nm and 100 nm. Since the flow rate is proportional to the square of the pore radius, the flow in the 100 nm pores will be two orders of magnitude greater than that within the

10 nm pores. Thus the occurrence of relatively few large pores may dominate the overall permeability as opposed to very many smaller pores.

The pore pressure model described by Equation 8.10 has been applied to the small test specimen test data reported in Chapter 7 and the results of the relevant calculations are given in Table 8.3.

W/C Ratio	**Age** days	**m** °C/s	**ϕ**	**A**	**t*** Eq7.16	**$V_{vapour,max}$** ($x10^{-6}$) m/s	**$V_{100\,^{o}C}$** ($x10^{-6}$) m/s	**K** ($x10^{-15}$)m/s	**P_{pore}** N/mm²
0.6	7	1	0.64	19.6	291	125	72	7.38	1.33
0.6	14	2.2	0.63	18.9	130	19	98	7.25	1.78
0.5	7	1	0.65	18.3	285	129	81	4.30	2.72
0.5	14	1.2	0.56	16.8	221	151	67	4.51	3.16
0.5	14	2.1	0.57	16.9	130	197	95	4.51	3.07
0.4	7	0.2	0.68	17	1299	62	38	4.40	4.24
0.4	7	0.9	0.64	16.7	284	133	70	4.40	4.37
0.4	14	1.3	0.7	17.1	215	152	87	4.62	5.11
0.4	14	2.5	0.74	17.4	110	212	145	4.62	4.58
0.4	28	1.8	0.71	16.8	152	182	95	5.16	5.71

Table 8.3 Calculations to predict pore pressure using Equation 8.10

The relationship between these predicted pore pressures and those observed during the experiments (previously reported in Table 7.7) is given in Figure 8.3. The predicted pore pressures are consistently greater than those actually measured. This is not surprising given the assumption of zero heat loss made in the pore pressure model. Excellent correlation between the predicted and actual pore pressures can be achieved by placing a coefficient of 0.66 before the predicted pore pressures.

This coefficient may be taken directly into the permeability term by defining a new parameter, the effective permeability K_{eff}, which is the permeability which permits correlation with the experimental data, where;

$$K_{eff} = 1.5\ K \tag{8.27}$$

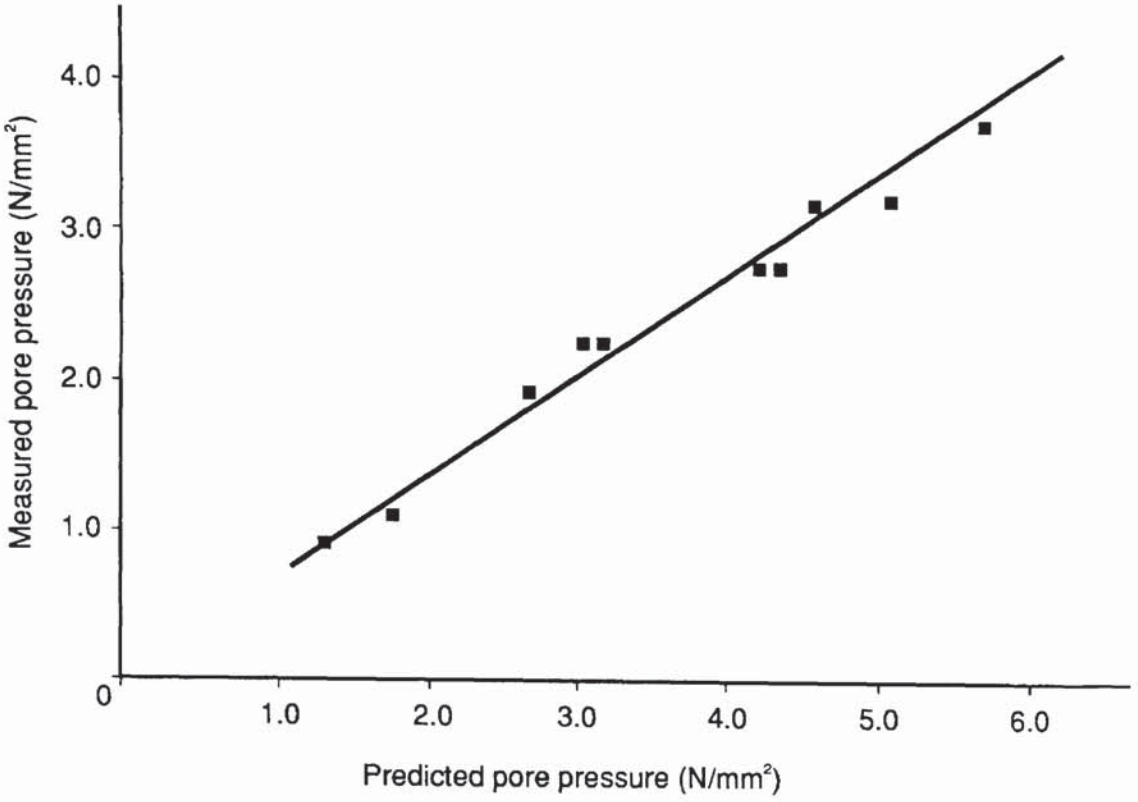

Figure 8.3 Predicted pore pressure versus observed pore pressure

In conclusion, the maximum pore pressure developed in a heated concrete may be described by;

$$P_{pore,\max} = \frac{\eta}{K_{eff}^2 \epsilon} \frac{\phi}{1 - \phi} V_{vapour,\max} (V_{vapour,\max} - V_{100}^{t^*}) t^* \qquad (8.28)$$

where t^* and $V_{vapour,\ max}$ are given in Equations 8.21 and 8.22 respectively.

8.2.4 SCOPE OF PORE PRESSURE MODEL

The explosive spalling encountered during the course of the small scale specimens test programme was extremely violent in nature. A number of electrical heaters were destroyed by the flying concrete projectiles. If reproduced at a larger scale, such explosive failure of concrete in fires could be a serious threat to structural stability.

PAGE MISSING IN ORIGINAL

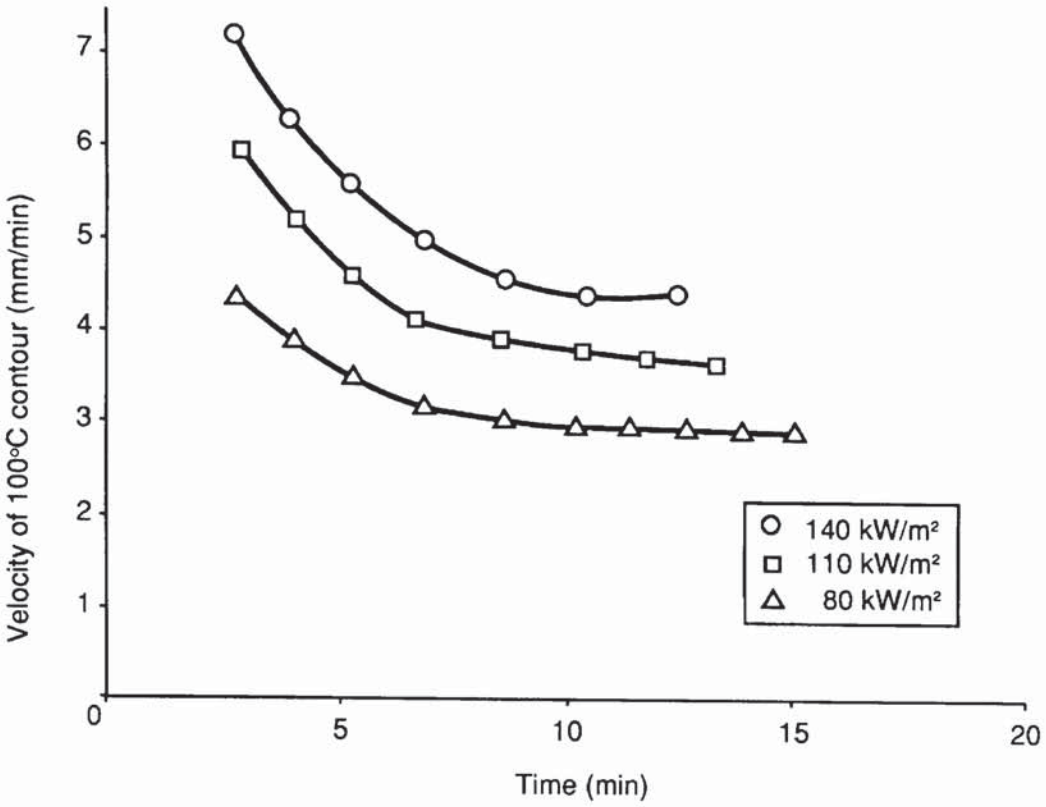

Figure 8.4 Velocity of 100°C isotherm

W/C Ratio	m °C/s	A	t_{max}	V_{max} ($x10^{-6}$) m/s	$V_{100\,^{o}C}$ ($x10^{-6}$) m/s	R_{mean} ($x10^{-9}$) m	K_{eff} ($x10^{-15}$) m/s	σ_{pore} N/mm²
0.3	0.45	14.9	553	99	60	0.0065	3.86	8.40
	0.57	14.9	436	111	63	0.0065	3.86	9.14
	0.72	14.9	346	125	68	0.0065	3.86	9.53
0.4	0.45	15.7	570	96	60	0.0071	4.61	5.26
	0.57	15.7	450	108	63	0.0071	4.61	5.84
	0.72	15.7	357	121	68	0.0071	4.61	6.12
0.5	0.45	17.1	602	91	60	0.0086	6.77	2.02
	0.57	17.1	475	102	63	0.0086	6.77	3.41
	0.72	17.1	376	115	68	0.0086	6.77	2.42
0.6	0.45	18.8	640	85	60	0.0111	11.27	0.69
	0.57	18.8	505	96	63	0.0111	11.27	0.84
	0.72	18.8	404	108	68	0.0111	11.27	0.89

Table 8.4 Predicted maximum pore pressure developed within test specimens

The pore pressures predicted by the model and reported in Table 8.4 appear to follow acceptable behaviour patterns, with pore pressures increasing in specimens with lower water/cement ratios and also in specimens subject to higher rates of surface heating. The pore pressures range from relatively small magnitudes among the more permeable concretes to much higher values for the higher strength concretes. The predicted values are in the same order as previous pore pressure predictions by Bažant and Thonguthai (1979) and Ahmed and Huang (1990).

Now that the magnitude of the pore pressures developed within the test specimens under the range of conditions examined have been quantified, some possible mechanisms for explosive spalling may be evaluated.

8.3 THE ROLE OF PROBABILITY

8.3.1 THE NEED TO CONSIDER PROBABILITY

A cursory look at the experimental data reported in Chapter 6 quickly illustrates the important role that probability plays in explosive spalling. There are many test scenarios where nominally similar specimens have been loaded to similar levels and heated to similar extents with completely different results. For example, Table 6.7 reports that 11 specimens were loaded to 30 N/mm^2 and heated under a flux of 140 kW/m^2. Although all specimens had similar (nominally identical) properties, only five specimens suffered explosive spalling.

One possible explanation for such behaviour is that explosive spalling is extremely sensitive both to permeability and tensile strength of concrete at elevated temperatures and both these properties are very sensitive to the manner in which heated concrete cracks. Cracking is strongly effected by material parameters (e.g. aggregate shape, aggregate surface roughness and distribution of aggregates) that are essentially random for each test specimen.

It appears pointless attempting to develop detailed hypotheses of the actual mechanisms of spalling where such non quantifiable effects have such a dominant influence. It is probably more fruitful to use Equation 8.5 as a means of grouping parameters which will allow an empirical model to be developed based on the extensive experimental data recorded. Thus;

$$P(spalling) \approx \frac{(1-2\nu)\sigma_p^2 + 2\nu(\sigma_l + \sigma_t)\sigma_p}{F_t^2} \leq 1 \qquad (8.29)$$

8.3.2 APPLICATION TO RESULTS OF HEATING AND LOADING TESTS

Equation 8.29 may be applied to the results of the heating and loading tests on the concrete specimens with water/cement ratios of 0.6 as reported in Chapter 6 (i.e. Tables 6.5, 6.6 and 6.7). The calculations are summarised in Table 8.5 and the results compared to the actually observed propensity of these specimens to explosive spalling.

Heat Flux (kW/m^2)	**Loading** (N/mm^2)	**P(spalling)** (observed)	$\sigma_l + \sigma_t$ (N/mm^2)	σ_p (N/mm^2)	F_t (N/mm^2)	**P(spalling)** Equation 8.29
80	0	0	0	0.69	3.40	0.02
	10	0	15.5			0.48
	20	0	24.5			0.75
	30	0.25	31.6			0.96
110	0	0	0	0.84		0.03
	10	0.5	17.5			0.66
	20	0	23.9			0.90
	30	0.25	31.7			{1.18}
140	0	0	0	0.89		0.03
	10	0	18.0			0.73
	20	0.18	22.4			0.90
	30	0.5	32.3			{1.28}

Table 8.5 Calculation of spalling factor (Equation 8.29) for w/c = 0.6 test specimens

The observed probability of explosive spalling is quite erratic. This can be explained not only by inherent chaotic influences but also possibly due to an inconsistency in the number of specimens tested under the various conditions. The probability of spalling predicted using Equation 8.29 is highly conservative in many cases. Accordingly, Equation 8.29 has been adapted to give a better fit with the experimental data;

$$P(spall) \leq 0.15 \left\{ \frac{\sigma_p (\sigma_l + \sigma_t + \sigma_p)}{F_t^2} \right\} \leq 1 \qquad (8.30)$$

Equation 8.30 applies only to concrete specimens with water/cement ratios of 0.6 and accordingly tensile strengths of 3.5 N/mm^2, as none of the other specimens demonstrated a tendency for explosive spalling when loaded biaxially.

8.4 MECHANISMS OF EXPLOSIVE SPALLING

It appears that the initial framework envisaged for explaining explosive spalling cannot comprehensively explain the observed experimental behaviour, which includes the fact that explosive spalling;

(a) was less frequent amongst higher strength concretes
(b) was observed in oven dried specimens
(c) was more frequent amongst specimens loaded uniaxially
(d) was more frequent amongst 50mm deep specimens than 100mm deep specimens
(e) was observed in higher strength specimens (w/c=0.3 and 0.4) on release of load

It is proposed that such behaviour can only be explained by reverting to the early proposals of Shorter and Harmathy (1965) that spalling was possible by either of two distinct mechanisms, namely excessive pore pressure or excessive thermally induced stress.

Many of the theories that have been proposed for explosive spalling and reviewed in Chapter 3 have been based on either the pore pressure or thermal stress approach. Thus, while individual theories based on one of the two mechanisms may have been conceptually correct, they failed to recognise the equally important role of the other mechanisms. Accepting that spalling may be a common consequence of different mechanisms explains many of the contradictory characteristics of spalling that have been observed by researchers over the years.

8.5 EXPLOSIVE SPALLING DUE TO PORE PRESSURES

8.5.1 MECHANISM FOR PORE PRESSURE SPALLING

The pore pressures predicted in the test specimens have been calculated in Table 8.4. At a glance, their magnitude suggests that explosive spalling should have taken place in most specimens. However, a closer look at the results in the context of the pore pressure model discussed in Chapter 7 explains the observed behaviour.

As pore pressure only occurs within the voids of a concrete, it cannot be compared directly to the tensile strength. In Chapter 7, it was suggested that a version of the failure criterion proposed by Akhtarruzaman and Sullivan (1970) can be used for explosive spalling. The failure model considers the concrete as a hollow thin walled sphere subject to an internal bursting pressure. The model was correlated against the experimental results of Akhtarruzaman and Sullivan and also those reported in Chapter 7. The pore pressures necessary to cause bursting failure σ_{fail} of the various concretes are calculated in Table 8.6 using the methodology (and symbols) explained in Section 7.6.

w/c ratio	ρ_c (kg/m^3)	w_o	h	V_{gel} (mm^3)	R_{sphere} (mm)	T_{wall} (mm)	σ_{fail}/F_t
0.3	2390	0.042	0.24	176,000	34.8	9.0	0.58
0.4	2385	0.047	0.32	167,000	36.2	8.2	0.50
0.5	2365	0.045	0.40	169,000	35.5	8.5	0.54
0.6	2355	0.051	0.48	157,000	37.0	7.5	0.47

Table 8.6 Calculation of pore pressure needed to cause bursting failure of concrete

Comparing these data with the pore pressures in the specimens suggests that certainly the specimens with water/cement ratios less than 0.5 should have suffered from explosive failure. However, it must be recalled that the failure model assumes that the hollow sphere has been subjected to internal pressures only. In the test rig, the specimens are loaded externally and such loads act against the bursting forces from the pore pressures.

For failure to occur, the following condition must be reached;

$$\sigma_{pore} \geq \sigma_{fail} + \sigma_{load} \tag{8.31}$$

Applying Equation 8.31, the maximum threshold load that may be applied before preventing explosive failure (under 140 kW/m^2) has been calculated as shown in Table 8.7.

w/c	F_t (N/mm^2)	σ_{pore} (N/mm^2)	σ_{fail} (N/mm^2)	**Threshold Load Stress** (N/mm^2)
0.3	4.8	9.53	2.78	6.7
0.4	4.1	6.12	2.05	4.1
0.5	3.7	3.70	2.00	1.7
0.6	3.4	3.40	1.60	1.8

Table 8.7 Calculation of threshold load stress

The data in Table 8.7 explain much of the observed behaviour. The very low values for threshold load stress necessary to overcome the developed pore pressures explains the absence of explosive spalling amongst the less permeable higher strength specimens. In addition, the data explain how the release of the imposed loads at the end of some tests precipitated explosive spalling of the higher strength specimens.

It is noteworthy that such load-release type explosive failure only occurred where the specimens had been loaded to a reasonably high level during the test (see data in Tables 6.8 and 6.9). This offers some explanation for the fact that the unloaded high strength specimens did not explode. It is proposed that the unloaded specimens did not explode because the pore pressures were relieved by the increase in material permeability during heating, for example by cracking. Thus, the maximum pore pressures predicted were never reached, as the permeability term in Equation 8.28 is increased at high temperatures.

The specimens that were loaded to high levels did not suffer the same degree of cracking as those loaded to a lesser degree (a fact confirmed from the ultrasonic pulse velocity measurements). Thus, once the applied load was released, a greater proportion of the predicted maximum pore

pressure was available to cause explosive spalling, explaining the observed behaviour.

It would be useful to undertake some further experiments where the specimen is loaded to levels immediately above and below the predicted threshold values given in Table 8.7. Such experiments could confirm the validity of the concept of a pore pressure spalling regime. The importance of specimen size in this respect would also benefit from further examination. It is unclear whether there is a maximum specimen size which may fail explosively due to pore pressures alone. If it is accepted that the spalling encountered during these tests on release of load was a form of pore pressure spalling, then concrete elements with thicknesses of up to 100mm may be vulnerable. This correlates somewhat with the findings of Hertz (1984) who reported explosive spalling of unloaded 300 x 100 mm concrete cylinders.

8.5.2 SURFACE SPALLING

Within larger specimens, pore pressure stresses may cause local failure of concrete near the heated surface. It is possible that particular conditions local to the concrete surface such as the presence of a number of larger aggregates or locally reduced permeability due to superior compaction and curing may result in high pore pressures. The consequence of such local build-up of pressures is likely to be surface spalling.

Although, the exact mechanism for surface spalling is unclear and has not been the subject of a specific experimental programme, it can possibly be visualised in the same terms as the pore pressure spalling. Considering the hollow sphere model, the restraint to internal bursting pressures will tend to zero at the exposed surface and thus failure is more likely.

Figure 8.5 also gives the failure envelope for explosive spalling of small specimens. If it is assumed that the criterion for surface spalling of large specimens are the same as those for explosive spalling for small specimens, then Figure 8.5 may be used as a predictor of surface spalling. Accordingly, the factors that influence surface spalling are the same as those discussed in Chapter 7 as being relevant to pore pressure development.

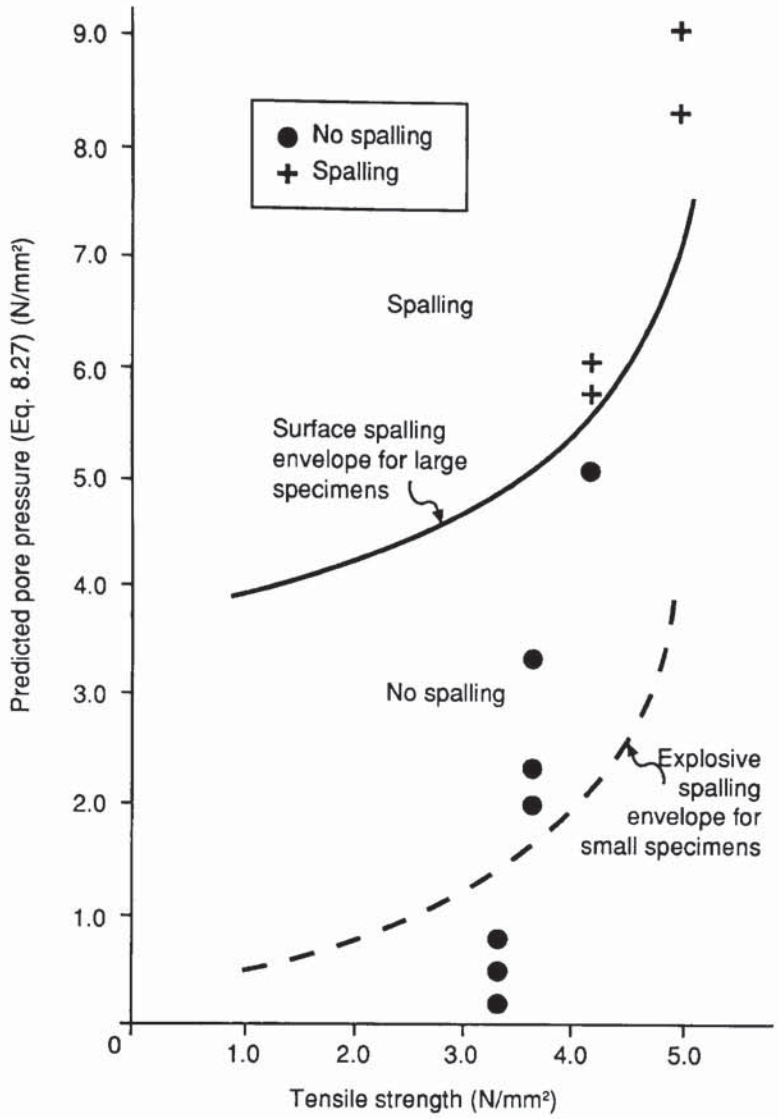

Figure 8.5 Chart for predicting the occurrence of surface spalling

It may be concluded from Figure 8.5 and the observations of previous researchers reported in Chapter 2 that the primary factors that affect surface spalling are;

(i) *Permeability*: Concretes become more susceptible to surface spalling with reduced permeability, i.e. reduced w/c ratio, increased hydration, more finely ground cement.

(ii) *Pore saturation*: Concretes become less susceptible to surface spalling with reduced levels of pore saturation, i.e. drying, air-entrainment or increased age

(iii) *Heating rate*: Heating rate is an important factor in deciding the occurrence of surface spalling, with increased heating leading to an increased likelihood of spalling

8.5.3 THE ROLE OF PERMEABILITY IN EXPLOSIVE SPALLING

The propensity of any concrete specimen to explosive spalling from pore pressures is governed by changes in its permeability at elevated temperatures. The permeability of concrete will change with an increase in temperature due to the action of several different mechanisms. The extent to which each mechanism influences the permeability change is governed by the degree of temperature change and the material properties of the concrete. The mechanisms that influence permeability can be summarised under the headings;

(i) Deterioration reactions
(ii) Differential thermal expansion of aggregate and paste
(iii) Thermal instability of aggregates
(iv) Microstructural changes
(v) Thermal stresses

8.5.3.1 Deterioration reactions

At elevated temperatures, concrete may suffer from material transformations and reactions, which adversely affect its structure. The evaporation of free water at 100°C is followed by the removal of chemically combined water (hydrate) at 175°C. The removal of this water dehydrates the cement gel in 2 stages; firstly the calcium silicate hydrates (in particular the layered CSH(I) structure) and then the calcium hydroxide. These dehydration reactions significantly reduce the binding capacity of the cement paste.

In addition, the aggregate particles themselves may undergo transformations at elevated temperatures. Siliceous aggregates, e.g. gravels, granites etc. undergo a physical transformation at 593°C, where the quartz constituents change from their α to β forms. Calcareous aggregates undergo a decarbonation reaction between 600 and 800°C, which because of the associated volume increase results in an increased permeability.

8.5.3.2 Differential thermal movement between aggregates and cement paste

At elevated temperatures, the thermal expansion of the individual components of concrete determines the overall response of the material. Like most materials, aggregates expand when heated, whereas cement paste contracts, due to removal of the water. The global deformation of concrete is decided by the ratio of aggregate to cement. Clearly the thermal incompatibility between the paste and the aggregate may lead to degradation of the concrete. The cement paste imposes a circumferential compressive stress on the aggregate particles.

The bond between the aggregate and the paste may fail due to shear stresses resulting from the incompatibility. This will significantly affect the permeability of the concrete mass. Failure of the aggregate-cement paste bond can provide a pathway for moisture movement through the concrete. The onset of degradation due to thermal incompatibility will be controlled by the coefficients of thermal expansion of the aggregate and the paste. While the material properties of aggregates suggest that almost all concretes will suffer from significant thermal incompatibility, its damaging effect is often greatly reduced by transient thermal creep.

8.5.3.3 Thermal stability of aggregates

Aggregate particles may split on exposure to heat as a result of the development of internal thermal stresses. Splitting of aggregate will tend to cause deterioration of the structure of the concrete. In addition, aggregate splitting is particularly important at the surface of concrete, where it is closely associated with the phenomenon of aggregate spalling. The thermal stability of aggregates will be addressed fully in Chapter 9.

8.5.3.4 Microstructural changes

Bažant and Thonguthai (1979) have proposed that permeability varies with temperature in the manner shown in Figure 8.6. Their data were achieved on the basis of evaluating the permeabilities necessary to ensure correlation between their numerical model for pore pressure

development and experimental results. However, although the large increase in permeability they predicted above 100°C is quite credible, it must be viewed with some caution as no actual measurements were made either of permeabilities or pore pressures, but simply rate of mass loss.

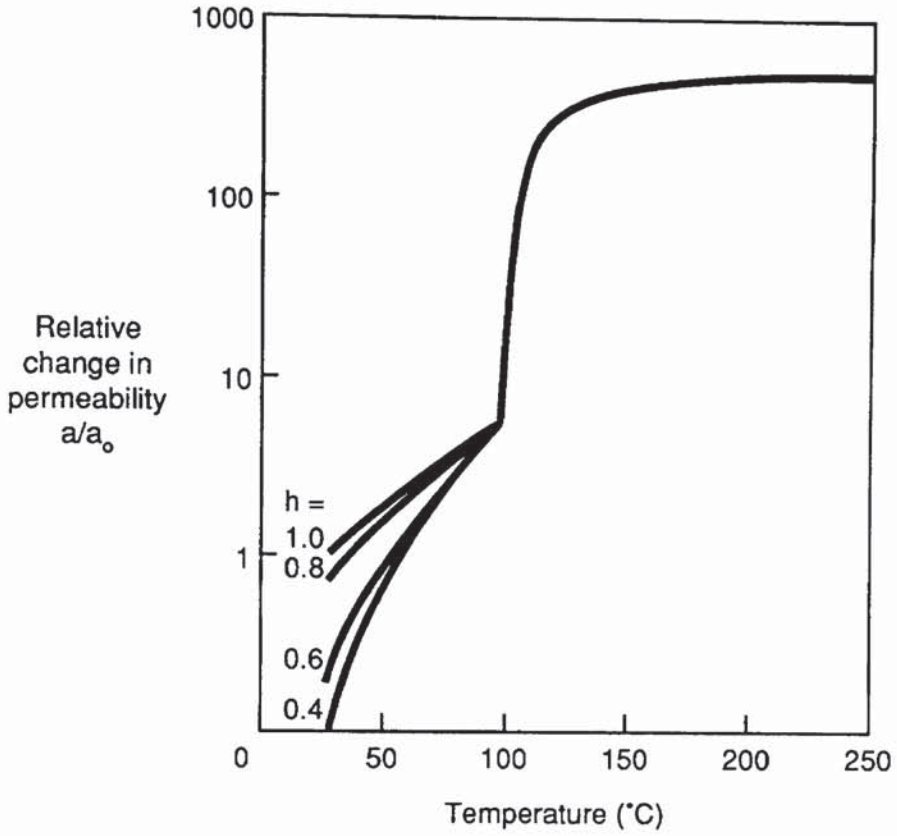

Figure 8.6 Variation of permeability with temperature (after Bažant and Thonguthai, 1979)

Some experimental work was undertaken by Jumpannen (1993), who produced details of the changing nature of the pore size distribution in high strength concretes at elevated temperatures. An example of her findings is given in Figure 8.7.

Assuming that the relationship between pore radius and permeability takes the form given previously in Equation 8.26, Jumpannen's data suggest that permeability increases substantially with increased temperatures. The pore size distribution was measured after gradually cooling the concrete to ambient temperature. The hatched area under the curve represents the porosity of the interfacial zone between the aggregate and the cement paste matrix, voids due to incomplete compaction and cracks due to shrinkage of the cement paste. The dotted area under the curves represent the capillary porosity.

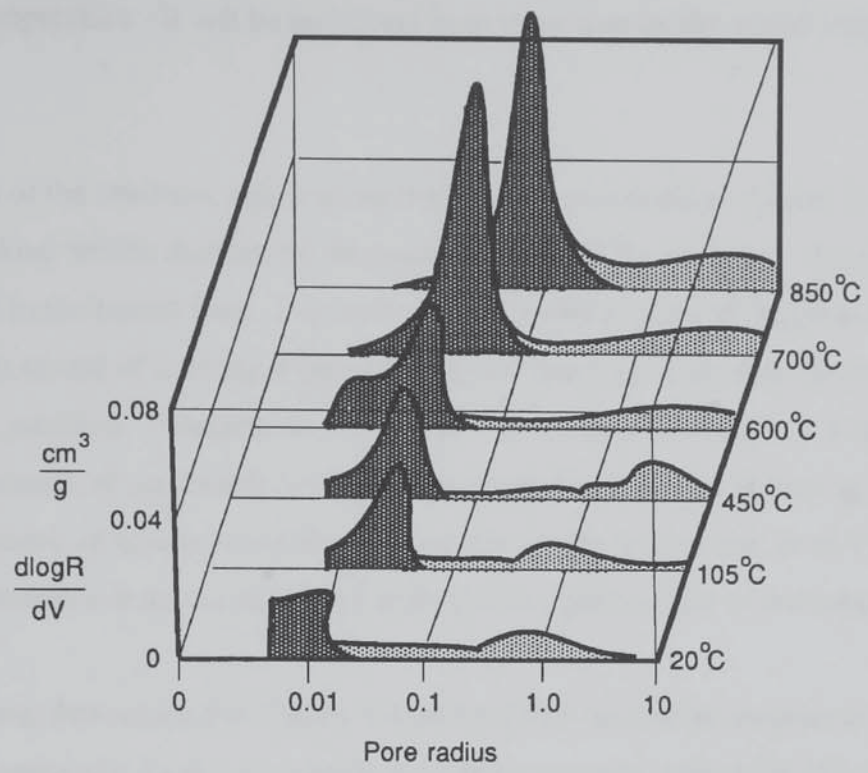

Figure 8.7 Changing pore size distribution at elevated temperatures (after Jumpannen, 1993)

Bažant and Thonguthai (1979) proposed that permeability can increase substantially, without similar increases in the total volume of pores by a mechanism whereby the necks within pores are gradually disintegrated at elevated temperatures. The validity of their proposed mechanism has not yet been confirmed practically. It is important that work is undertaken to this end as the mechanism proposed is effectively a form of "creep" which will allow relaxation of pore pressures at higher temperatures without cracking. This has consequences for the spalling behaviour of high strength (low permeability) concretes, as if the strength is sufficient to sustain the maximum pore pressure developed, then the subsequent stress relaxation at higher temperatures may alleviate spalling pressures.

8.5.3.5 Thermal stresses

The application of heat to a plane face of concrete generates temperature gradients through the depth of the section, perpendicular to the heated face. These gradients change with time, as the heating continues. The temperature gradients generate an associated thermal strain within the concrete. The hot outer layer of the concrete will endeavour to expand in proportion to any

increase in temperature. It will be restrained from expansion by the cooler central core of the concrete.

Some regions of the concrete, which are in tension, will eventually be subject to cracking. The onset of cracking will be dictated by the tensile strength of the concrete. Cracks will develop perpendicular to the heated face. The cracks will continue to grow in length as heat is applied. The maximum extent of cracking is governed by the thickness of the concrete member and the temperature gradients. Bearing in mind that the concrete member is 3-dimensional, an orthogonal network of cracks will develop perpendicular to the plane of heating. The existence of such a network of cracks was confirmed experimentally by Bascoul *et al.* (1989) Clearly, such crack patterns will have a significant impact on the permeability of the concrete section.

The experimental data reported in Chapter 6 confirmed that the thermal stresses in concretes with water/cement ratios of 0.3 and 0.4 are less than those in concretes with ratios of 0.5 and 0.6. This is because stronger concretes have a reduced degree of thermal deformation. Imposed loads tend to inhibit thermal expansion and tensile cracking. Thus, it would be expected that stronger concretes and those subjected to higher loads would suffer a reduced increase in permeability when heated.

8.5.4 THE ROLE OF MOISTURE CONTENT IN EXPLOSIVE SPALLING

The model for pore pressure development considers moisture content within the pore saturation factor. The sensitivity of pore pressure to pore saturation is shown in Figure 8.8, which is normalised against the arbitrary datum of 50% saturation giving a pore pressure of 1 N/mm^2. Figure 8.8 clearly explains why concretes with low moisture contents are substantially less susceptible to both surface and explosive spalling.

An additional consideration is the well established fact that the 100°C isotherm moves more slowly in specimens having a higher moisture content. Meyer-Ottens (1972) provided some information on the isotherm velocities which is reproduced here in Figure 8.9.

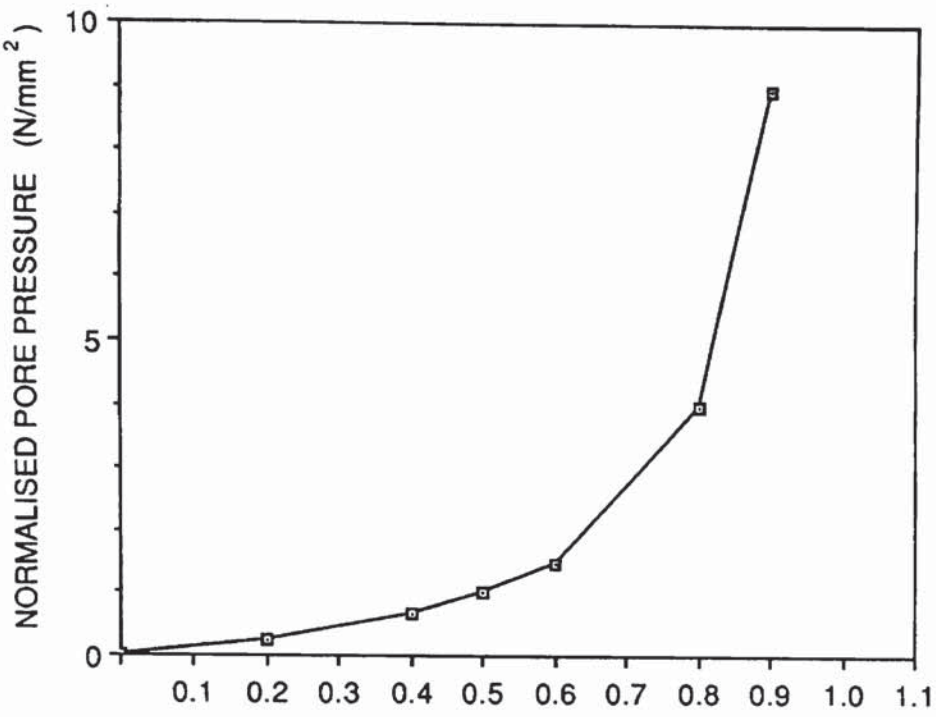

Figure 8.8 Effect of relative pore saturation on normalised pore pressure

When the 100°C isotherm moves more slowly, the model described by Equation 8.28 suggests that higher pore pressures are developed and consequently explosive spalling is more likely.

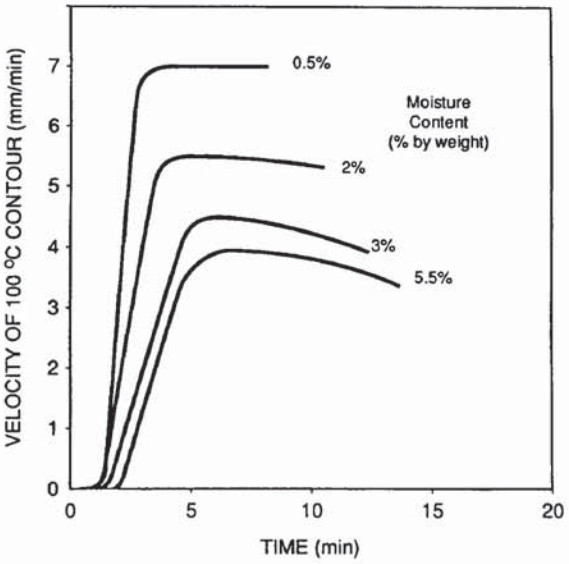

Figure 8.9 The effect of moisture content on velocity of 100°C isotherm

The experimental data reported in Table 6.14 has demonstrated that oven dried concrete specimens (with a nominally zero moisture content) are capable of explosive spalling when loaded uniaxially. This appears to cast some doubt on the concept of pore pressure spalling. It has been assumed that oven dry specimens have zero pore pressures based on the fact that none of the oven dried small specimens studied in Chapter 7 suffered any damage. This assumption may not necessarily be true.

In addition to free moisture, any "combined" moisture that is released on the dehydration of the cement gel could also available for pore pressure generation. Akhtarruzaman and Sullivan (1970) have demonstrated that combined water starts to be released from heated concrete at temperatures of around 175°C and may be up to three times the amount of free water. One possible explanation for the spalling of oven dry specimens is that the release of "combined" water causes the necessary pore pressures. It is more likely, however, that the spalling of oven dry specimens was related due to the thermal stress mechanism of spalling, which is discussed in Section 8.6.

8.6 EXPLOSIVE SPALLING DUE TO THERMAL STRESSES

8.6.1 MATERIAL RESISTANCE TO EXPLOSIVE SPALLING

It is unclear what is the most suitable measure of material resistance to explosive spalling. The use of tensile strength alone is clearly simplistic. As reported in Chapter 3, Sertmehemetoglu (1977) has previously shown the importance of depth D from the surface at which the maximum pore pressure occurs and the size of the cracks S in which the pressures develop. Such behaviour would suggest that material resistance to spalling is related to shear strength τ as opposed to tensile strength.

If the failure mode of the specimen were considered to be fundamentally rectangular in nature, the stress in the x direction needed to cause failure σ_x^{fail} would be;

$$\sigma_x^{fail} \geq \tau \frac{4\ D}{S} \tag{8.32}$$

If a more realistic conical failure mode is considered then depth and crack size become even more important, with the failure stress given by;

$$\sigma_x^{fail} \geq \tau \frac{8\sqrt{2}\ D\ (D + S)}{S^2} \tag{8.33}$$

Without information on the size and depth of cracks within the specimen Equations 8.32 and 8.33 have limited application. It is probably more useful to consider the resistance that the concrete

specimens have shown to compressive loads applied within the test rig. The data reported in Section 6.2.2 and presented in Figure 6.1 have been used to construct a failure envelope for specimens tested in the rig at ambient temperatures, as shown in Figure 8.10. Although, the data are limited to situations where one or other of the orthogonal loads are zero or both loads are equal to each other, previous work by Kupfer *et al.* (1969) and Kordina *et al.* (1984) suggest a likely form for the failure envelope. Figure 8.11 presents the likely effect that Kordina *et al.* proposed increased temperature would have on the failure envelope.

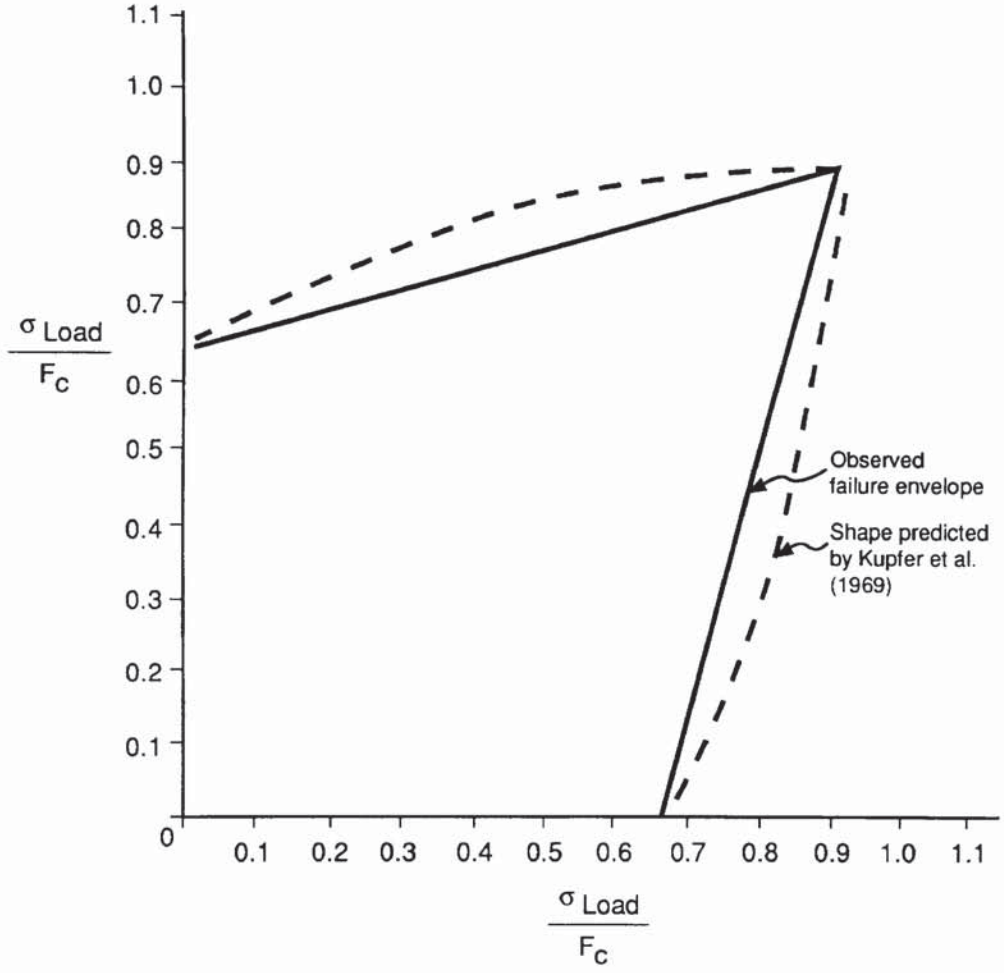

Figure 8.10 Failure envelope for test rig at ambient temperatures

8.6.2 STRESSES ACTING ON HEATED SPECIMENS

The experimental data presented in Chapter 6 may be analysed in the context of the failure envelope for concrete specimens within the testing rig. The loading ordinates on the stress plot may be noted directly from the sum of the thermal and load stress readings from the experimental

records and the pore pressures predicted in Table 8.4. As the pore pressure acts in an opposite direction to the applied stresses, the principle of effective stress may be applied. Accordingly, the net stress σ which is to be input as an ordinate on the failure envelope diagram is given by;

$$\sigma = \left(\frac{\sigma_1 + \sigma_t - \sigma_p}{F_c} \right) \tag{8.34}$$

The relevant experimental data is summarised in Table 8.8. As the exact nature of the failure envelope at elevated temperatures has not been quantified, temperature effects have been considered indirectly by imposing a reduction on the concrete compressive strength. The reduction factors are those suggested by Malhotra (1956) for stressed concretes made with siliceous Gravel aggregate. The compressive strength reduction factors have been calculated based on the mean specimen temperatures after 60 minutes, as given in Figures 6.7, 6.8 and 6.9.

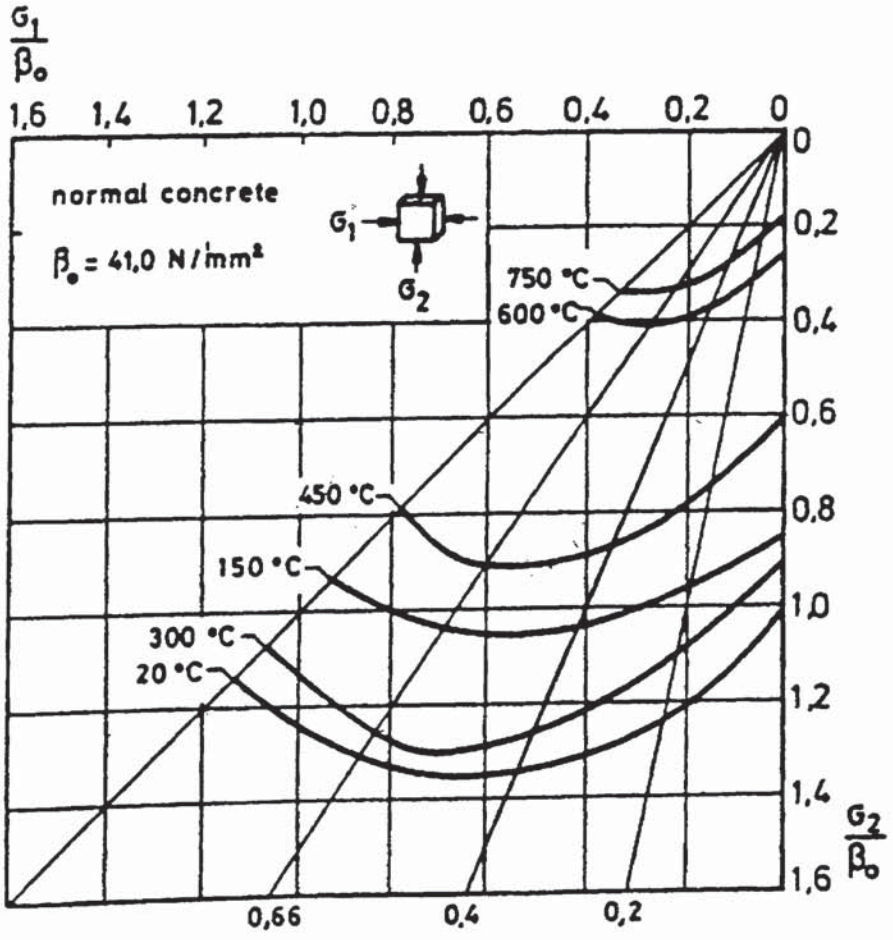

Figure 8.11 Effect of temperature on failure envelope (after Kordina *et al.*, 1984)

Heat Flux (kW/m^2)	$\sigma_l + \sigma_t$ (N/mm^2)	σ_p (N/mm^2)	F_c (N/mm^2)	σ	**Loading**	**Spalling**
80	0.0	0.69	35.7	-0.02	Biaxial	No
80	15.5	0.69	35.7	0.41	Biaxial	No
80	24.5	0.69	35.7	0.66	Biaxial	No
80	31.6	0.69	35.7	0.87	Biaxial	Yes
110	0.0	0.84	31.5	-0.03	Biaxial	No
110	17.5	0.84	31.5	0.53	Biaxial	No
110	23.9	0.84	31.5	0.73	Biaxial	Yes
110	31.7	0.84	31.5	0.97	Biaxial	Yes
140	0.0	0.89	29.4	-0.03	Biaxial	No
140	18.0	0.89	29.4	0.58	Biaxial	No
140	22.4	0.89	29.4	0.73	Biaxial	Yes
140	32.3	0.89	29.4	1.07	Biaxial	Yes
80	34.0	2.0	42.5	0.25	Biaxial	No
110	37.7	3.4	37.5	0.91	Biaxial	No
140	33.9	2.4	35.0	0.90	Biaxial	No
80	33.4	5.3	53.6	0.52	Biaxial	No
110	33.0	5.8	47.3	0.57	Biaxial	No
140	30.7	6.1	44.1	0.56	Biaxial	No
80	31.9	8.4	57.8	0.41	Biaxial	No
110	33.1	9.1	51.0	0.47	Biaxial	No
140	31.0	9.5	47.6	0.45	Biaxial	No
80	34.9	8.4	57.8	0.56	Uniaxial	No
140	35.6	9.1	47.6	0.45	Uniaxial	Yes
140	26.1	6.1	44.1	0.64	Uniaxial	Yes
140	24.9	2.4	35.0	0.89	Uniaxial	Yes
140	33.5	2.4	35.0	0.68	Uniaxial	Yes
140	30.1	0.0	44.1	0.71	Uniaxial	No
140	30.1	0.0	35.0	0.86	Uniaxial	Yes
140	31.1	0.0	47.6	0.65	Uniaxial	No

Table 8.8 Summary analysis of sample experimental data

8.6.3 CONCLUSIONS

The application of the data given in Table 8.8 is given in Figure 8.12. It is clear that by considering all the stresses acting on the specimen in the context of a material failure envelope provides some explanation for the observed spalling behaviour. Furthermore, it explains the beneficial effects of higher material strength and increased pore pressures. The mechanism proposed also explains how spalling of oven dried specimens may take place and the role of the nature of the loading.

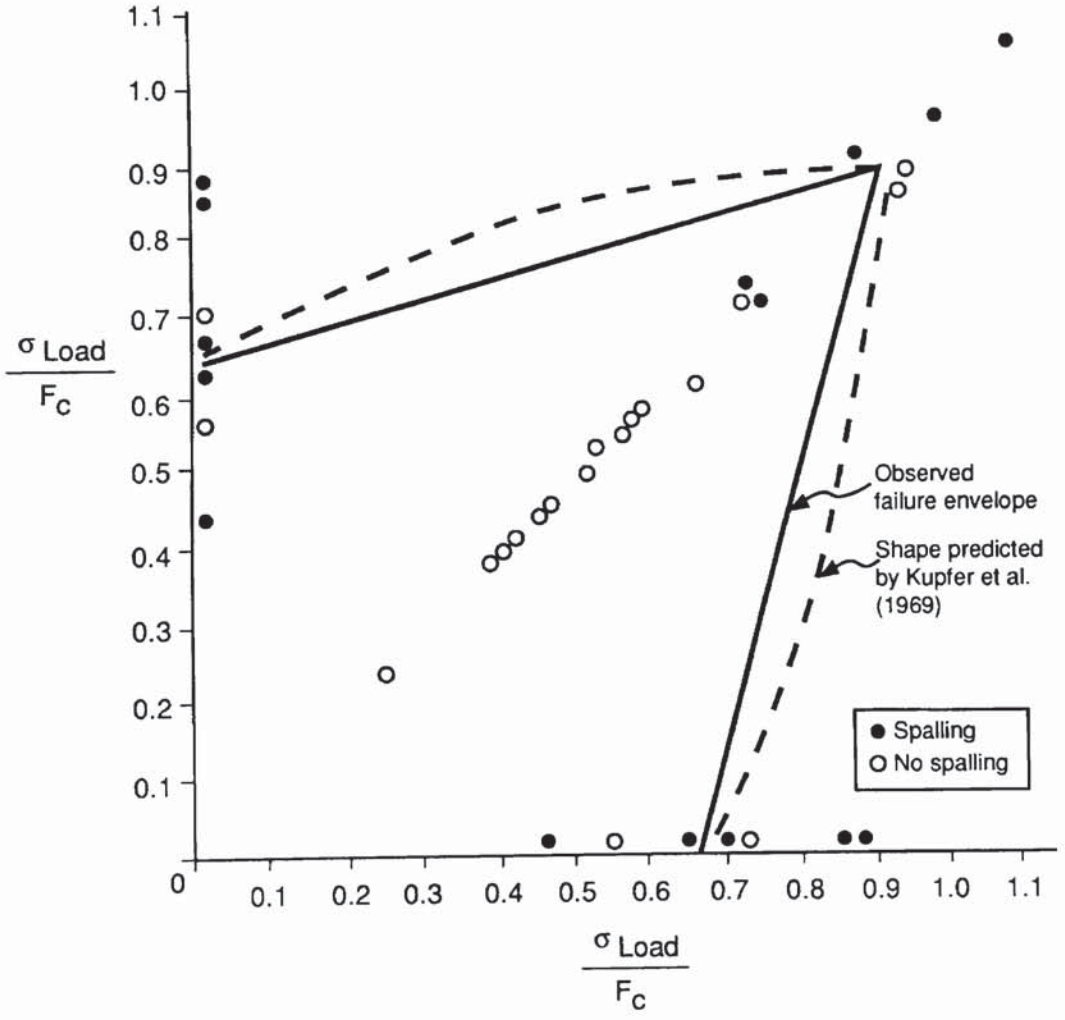

Figure 8.12 Experimentally observed stresses acting on heated specimens

8.7 INFLUENCE OF VARIOUS PARAMETERS ON EXPLOSIVE SPALLING

8.7.1 THE INFLUENCE OF HEATING AND LOADING CONDITIONS

The experimental data have shown that the heating and loading regime to which a concrete member is subjected is important in determining its susceptibility to explosive spalling. The factors which increase the thermal or load stresses acting on a concrete member increase its propensity to thermal stress spalling. Applied load reduces the susceptibility of a concrete to pore pressure spalling. However, as pore pressures can be overcome by relatively small loads (as calculated in Table 8.7), the dominant effect of load will be to increase stress levels and similarly increase the likelihood of spalling.

The nature of the loading is also important, with the effective increase in material strength associated with biaxial loading acting to reduce a concrete specimen's susceptibility to spalling. Sertmehemetoglu (1977) observed similarly improved performance from biaxially loaded concrete specimens. He found that biaxially loaded concrete slabs required larger internal bursting pressures to cause failure than the equivalent specimens loaded uniaxially.

The design of the test rig is also important in this context. The application of load directly through steel plates meant that the specimens were restrained by friction in the axis orthogonal to heating. This restraint was available to counteract the spalling forces within the specimen. The magnitude of such restraint was not quantified and by necessity it has been neglected within the consideration of explosive spalling. This simplification greatly restricts the understanding of the stress states within the heated specimens. It is recommended that any future work should either consider the forces acting in all three dimensions or alternatively use some form of friction free loading mechanism.

8.7.2 THE ROLE OF WATER / CEMENT RATIO IN EXPLOSIVE SPALLING

The experimental data regarding the influence of water cement ratio on the occurrence of spalling was reported in Section 6.7.4. These data demonstrated that concrete with reduced water/cement

ratios were less susceptible to explosive spalling under the conditions examined. In fact, under conditions of biaxial loading none of the specimens having water/cement ratios less than 0.5 exhibited any signs of spalling. A number of these specimens did spall when examined under uniaxial load.

Concretes with reduced water/cement ratios are less permeable and thus capable of developing higher pore pressures on heating. However, given the heating rates and nature and size of the concrete specimens examined in this series of tests, the pore pressures were of a lesser significance than the thermal and load stresses and thus a reduced water/cement ratio was beneficial in reducing spalling. Clearly, during the tests on small specimens the pore pressures were dominant and a reduced water/cement ratio increased the likelihood of explosive spalling. Specimen size is important in determining which particular regime of pore pressure influence pertains and further work is necessary to this end.

8.7.3 THE ROLE OF SPECIMEN THICKNESS IN EXPLOSIVE SPALLING

The experimental data reported in Section 6.7.6 have demonstrated the increased susceptibility of thin specimens to spalling. Thin (50 mm) specimens suffered explosive spalling under much less severe loading conditions than thick (100 mm) specimens. Furthermore, specimens made with concrete of lower water/cement ratios demonstrated a much increased susceptibility to spalling. As specimen thickness does not influence its strength (except possibly from the effect of friction in the third dimension), the observed behaviour suggests that the role of pore pressure has become more dominant.

Meyer-Ottens (1972) observed that the velocity of the 100°C isotherm V_{100} is increased in thinner specimens. Observations on the temperature profiles in the 50 mm thick concrete specimens confirm his findings. The equation for development of pore pressure (Equation 8.28) suggests that increased values of V_{100} leads to reduced pore pressures and accordingly increased susceptibility to thermal stress spalling.

8.7.4 CORRELATION WITH OBSERVATIONS FROM PREVIOUS RESEARCH PROGRAMMES

The explanations for explosive spalling proposed in this Chapter correlate well with the observed behaviour of spalling as described in Chapter 2. It is worth examining the range of observed effects and explaining them within the context of the understanding of explosive spalling described in this Chapter.

(i) *Given suitable environmental conditions, in terms of load and thermal attack, all concretes display the capacity for spalling (Malhotra et al., 1972)*

The mechanisms for explosive spalling described in this Chapter makes it clear that no concrete is immune to explosive spalling. Given any particular combination of load, thermal stress and pore pressure any concrete can suffer thermal stress induced spalling. The nature of the concrete will, however, affect its susceptibility to pore pressure spalling as factors such as water/cement ratio will influence strength, permeability and thermal expansion.

(ii) *Thinner concrete sections are more susceptible to spalling than thick sections (Ashton and Davey,1953, Hanneman & Thoms, 1959, Meyer-Ottens, 1972)*

The experimental investigation of simultaneously heated and loaded concrete specimens has proven this observation to be accurate. The reasons have been discussed in Section 8.7.3.

(iii) *Applied loads increase the susceptibility of concrete members to spalling (Meyer-Ottens, 1972; Copier, 1979; Morris, 1972)*

Again this observation has been confirmed during the experimental programme reported in this Thesis and the role of load discussed in Section 8.7.1.

(iv) *Water-cured concrete specimens are particularly susceptible to spalling (Akhtarruzaman and Sullivan, 1973)*

Water cured specimens could be expected to be more susceptible to explosive spalling because of their reduced permeability and associated increased level of pore pressure development. However, because of their superior strength, water cured specimens would be expected to be more resistant to thermal stress induced spalling.

(v) *High strength concrete has an increased susceptibility to spalling (Hertz, 1984, Sanjayan and Stocks, 1993, Jumpannen 1993)*

High strength concrete is more susceptible to pore pressure induced explosive spalling because of its reduced permeability. Table 8.4 shows how higher strength concretes develop larger internal pore pressures when heated than their lower strength equivalents. However, the data from the heating and loading experimental programme has demonstrated that high strength concretes are less susceptible to thermal stress induced spalling.

(vi) *Explosive spalling occurs within the first 40 minutes of heating to the standard BS 476:Part 8:1972 fire resistance testing regime (Malhotra, 1972). Spalling has been observed for concretes exposed to heating environments of 350 to 715° C.*

The temperature at which explosive spalling is most likely to occur depends on the rate at which pore pressures and thermal stresses are increasing and material strength is decreasing. Spalling is likely to occur as soon as the balance between the bursting and resistance stresses moves in favour of the resistance stresses. Parameters such as water/cement ratio, coefficient of thermal expansion, aggregate type and age will be critical in determining the temperature at which spalling takes place.

(vii) *Explosive spalling is very unlikely for concretes with low moisture contents , say less than 3% by weight, (Meyer-Ottens, 1972, Christiaanse et al., 1972)*

Explosive spalling due to excessive pore pressures is unlikely in specimens with low moisture contents and accordingly low potential pore pressures. As pointed out in Equation 8.27 the critical parameter is the pore saturation. The pore saturation also affects the magnitude of the thermal expansion of heated concrete and thus influence the thermal stress term in Equation 8.30. The overall effect within the spalling framework is for reduced moisture content to cause reduced susceptibility to spalling. Although moisture content has little influence on thermal stress induced spalling, the fact that very few concrete structures are loaded to levels where the necessary failure stress state is reached makes such spalling a relatively rare (but not impossible) occurrence.

CHAPTER 9. AGGREGATE SPALLING

9.1 INTRODUCTION

Aggregate spalling is a reasonably mild form of spalling, where the aggregate particles near the surface split in a plane roughly parallel to the heated surface. Aggregate spalling occurs in the early stages of heating and may be considered as a form of thermal shock. It is often referred to as aggregate splitting or popping because the split aggregate is ejected from the surface of the concrete with a characteristic popping sound. In some instances, the split aggregate particle may be bonded to some adjacent mortar, thus leaving a conical coin-sized crater on the surface of the concrete such as is shown in Plate 9.1.

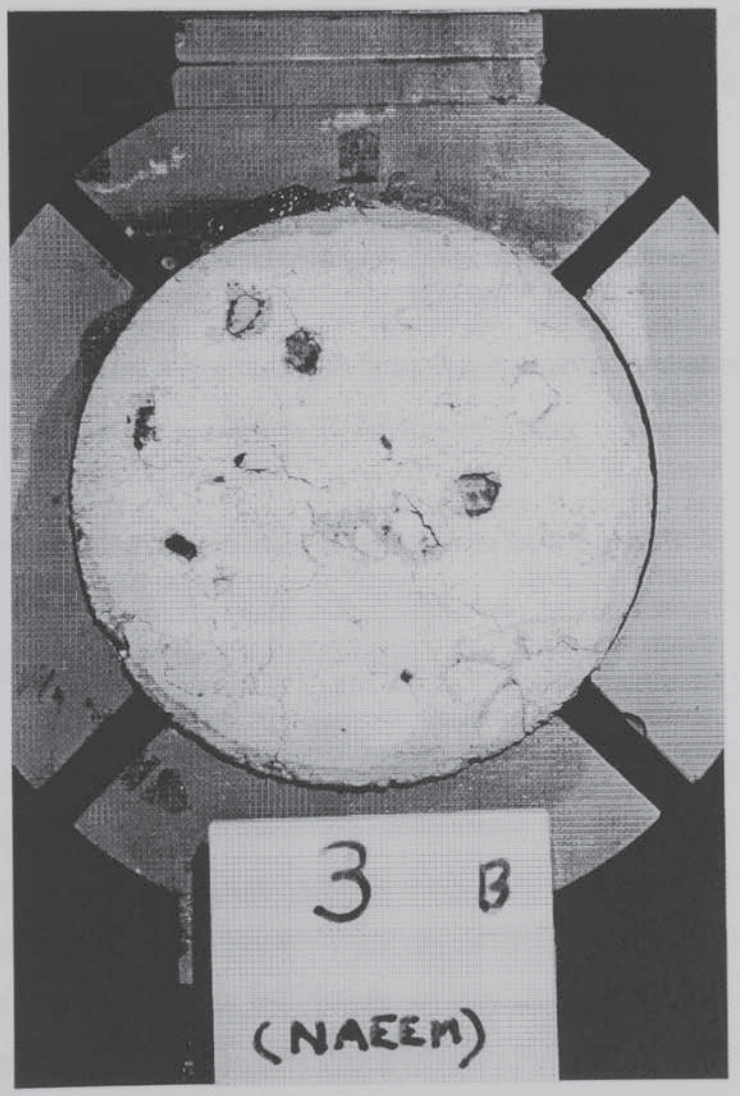

Plate 9.1. An example of aggregate splitting

Aggregate spalling is a very localised form of failure and has generally little consequence, other than causing cosmetic damage to the concrete. However, in some applications of concrete, aggregate spalling may be a matter of serious concern. Where concrete is repeatedly heated, for example, aggregate spalling may occur progressively causing the concrete surface to be continually eroded with each new application of heat. Examples of where such exposure conditions may be encountered include runway pavements used by military aircraft, fire fighting training facilities, fire resistance test furnaces and their associated specimen support frames.

To date, there has been relatively little research on aggregate spalling, probably because of its minimal effect on fire resistance and also possibly due to the fact that its occurrence appears to be limited to relatively few aggregate materials on exposure to the BS 476:Part 20:1987 standard fire resistance heating regime. An experimental programme undertaken by Meyer-Ottens (1972) together with a behavioural study of spalling by Malhotra (1984) provided some useful observations regarding aggregate splitting. These observations were based on experience gained while performing standard fire resistance tests and are thus limited to a single heating regime, i.e. BS 476:Part 20:1987 (or similar).

It was observed that;

(i) Certain aggregates were more susceptible to splitting than others (e.g. siliceous gravels were more susceptible than Limestones).

(ii) Man-made aggregates did not suffer from splitting.

(iii) Aggregate spalling ceased after a certain period of time.

Wu (1986) and Austin *et al.*(1992) studied aggregate spalling (which they simply referred to as spalling) with particular reference to concrete pavements used for military airfields. Concrete may be repeatedly exposed to very high temperature gases from the engines of vertical take-off and landing aircraft in these environments. Such high temperature exposure has been shown to result in widespread aggregate spalling which may not only cause damage to runway surfaces but may also produce projectiles of flying concrete which can damage aircraft engines.

The above studies have shown that given certain suitable heating conditions;

(i) All aggregates and concretes may suffer from spalling to some degree.

(ii) Concretes vary in their susceptibility to aggregate spalling, with concretes produced using man-made aggregates requiring particularly severe heating conditions before spalling.

(iii) Concrete made with larger sized aggregates are more susceptible to spalling than concrete made with small aggregates.

In their papers, both Wu and Austin *et al.* presented a ranking of concrete mixes with regard to their susceptibility to aggregate spalling. The usefulness of these rankings is limited by the fact that they concentrated on proprietory high temperature concretes made with artificial aggregates. Austin *et al.* reported that optimum performance was achieved by a concrete mix made using an artificial aggregate (Lytag) as both coarse and fines.

The objective of this Chapter is firstly to develop an understanding of the parameters that influence the susceptibility of individual aggregate particles to splitting when heated. Subsequently it is hoped to extend this understanding of the splitting of individual aggregates to develop a model for the spalling of aggregate within concrete.

9.2 THERMAL STABILITY OF INDIVIDUAL AGGREGATE PARTICLES

9.2.1 THEORIES TO EXPLAIN AGGREGATE SPLITTING

9.2.1.1 Aggregate splitting due to mineralogical content

Meyer-Ottens (1972) conducted an extensive series of fire tests on concrete building elements in Germany. He concluded that aggregate splitting was caused by the reaction to heat of the minerals within an aggregate particle. In general, Meyer-Ottens considered that splitting was due

to the release of water vapour within the aggregate, both from free water and water contained in hydrated minerals. He suggested that a less common causative fator of splitting may be the release of gases such as carbon dioxide and sulphur dioxide from the heated mineral compounds. The reasons suggested by Meyer-Ottens for the aggregate splitting are summarised in Table 9.1.

Aggregate Type	Chemical Composition	Reason for Splitting	Splitting Temperature °C
Sandstone	SiO_2 with FeOOH	Evolution of H_2O	260 to 350
Sandstone	SiO_2 with Fe_2O_3 & $CaCO_3$	Evolution of CO & CO_2	above 900
Flint	SiO_2, C, $CaCO_3$ & opaline bound H_2O	Evolution of H_2O, CO & CO_2	above 150 above 900
Weathered Feldspar	Kaolinite	Evolution of H_2O	390 to 450
Weathered Gneisses	Kaolinite	Evolution of H_2O	390 to 450
Barite	-	Evolution of SO_2	above 1100

Table 9.1. Reasons for aggregate splitting after Meyer-Ottens (1972)

Meyer-Ottens concluded that in order to suffer splitting, aggregates must be sufficiently dense so as to permit the development of internal splitting forces generated by the volume changes associated with the evolution of steam or gas on heating. He predicted that porous aggregates such as artificial man-made aggregates would not split regardless of the moisture contained within them.

This prediction was later discredited by Austin *et al.* (1992) who demonstrated that porous artificial aggregates such as Lytag could spall given suitable conditions. This highlighted the limitation imposed on Meyer-Otten's research by his use of heating regimes of relatively limited severity compared to those used by Austin *et al.* The heating regimes used by the different researchers are shown in Figure 9.1 thus illustrating the effect of rate of heating on aggregate behaviour.

In addition, Meyer-Otten's theory fails to account for the observed influence of aggregate size, which suggests that his theory does not adequately consider the thermal stresses acting within

heated aggregate particles.

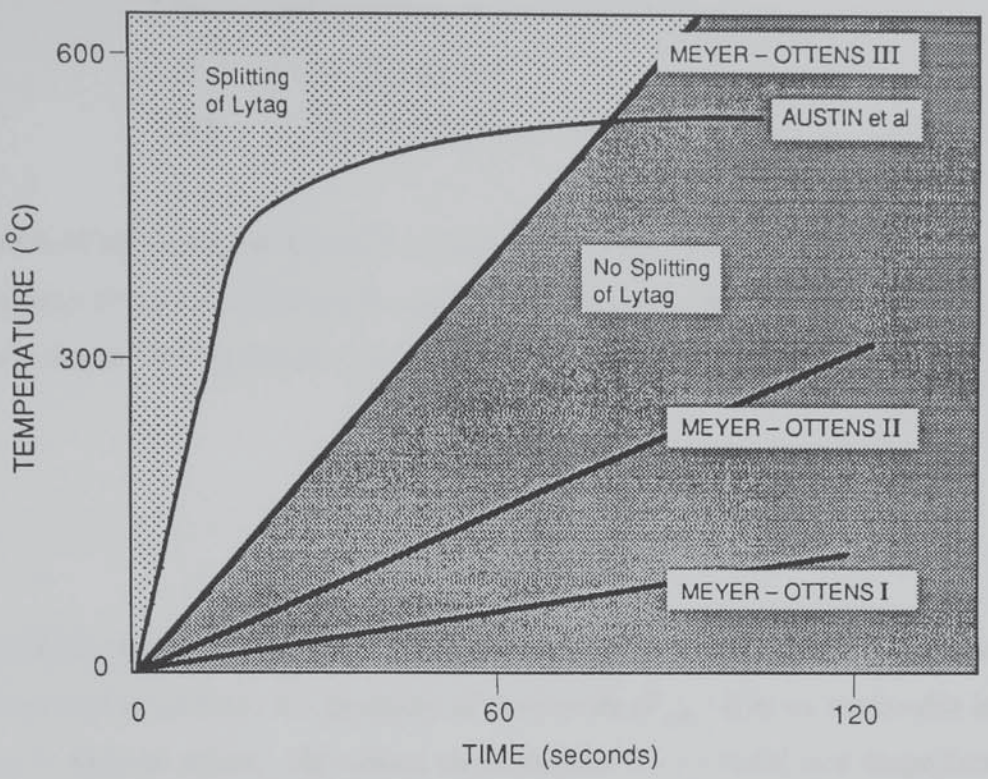

Figure 9.1. The heating regimes used by Meyer-Ottens (1972) and Austin *et al.* (1992)

9.2.1.2 Aggregate splitting due to thermally induced tensile stresses

When a particle of aggregate (which has been assumed in subsequent analysis as a homogeneous elastic sphere) is suddenly heated at its surface, tangential compression stresses of significant magnitude are developed at the heated surface. While no radial stresses exist at the surface, they gradually develop towards the centre of the aggregate particle, where they reach their maximum value. These radial stresses are tensile and tend to split the particle at its centre.

Grunberg (1925) calculated the magnitude of the surface compression and central tensile stresses (which are equal but opposite in nature) as;

$$\sigma_{max} = 0.38 \left(\frac{\alpha \ E}{1 - \nu} \right) \Delta\theta \qquad (9.1)$$

where; σ_{max} = maximum stresses in aggregate

E = Young's Modulus

α = Coefficient of Linear Expansion

ν = Poisson's Ratio

$\Delta\theta$ = temperature rise at surface

If the centre of an aggregate sphere is subjected to such radial tension and its ability to resist such stresses is described by its tensile strength F_{split} then the rise in surface temperature that is necessary to cause splitting failure $\Delta\theta_{fail}$ may be calculated directly from Equation 9.1;

$$\Delta\theta_{fail} = \left(\frac{1-\nu}{0.38}\right)\frac{F_{split}}{E\ \alpha} \qquad (9.2)$$

Manson (1952) studied the response of metallic materials to thermal shock for aeronautical applications and considered the grouping of properties $(F_{split} / E\alpha)$ as reasonable indicator of resistance to thermal shock. He viewed the multiplier $(1 - \nu / 0.38)$ as a shape factor. While Poisson's Ratio ν should also be considered within any thermal shock resistance factor, it may be ignored as it varies only slightly between different materials.

The thermal shock resistance factor described by Equation 9.2 assumes that surface temperature is immediately raised without any accompanied rise in internal temperature. This assumption may only be justified where surfaces are in near perfect thermal contact with their surroundings or alternatively where the material of the sphere is a very poor conductor.

Manson suggested that the Biot Modulus of a material must have a value greater than 5 for Equation 9.2 to be valid. The Biot Modulus is a parameter which relates the heat transfer coefficient at the surface of a material to its thermal diffusivity. Thermal diffusivity λ is the ratio between the conductivity k and the product of its specific heat capacity C and its density ρ. It gives a measure of the rate of temperature rise in a heated material. Aggregates generally have Biot Moduli values of less than 5 and accordingly thermal diffusivity must be considered within the thermal shock resistance factor.

Kent (1932) accounted for the thermal properties of the sphere by assuming it had its surface temperature raised by m°C per minute. He derived an expression for the maximum tensile stress

at the centre of the sphere which may be applied to an aggregate particle of radius R;

$$\sigma = \frac{E\ \alpha\ R^2\ m}{15(1-\nu)\ \lambda} \tag{9.3}$$

By rearranging Equation 9.3, the rate of heating resulting in aggregate splitting m_{fail} is given by;

$$m_{fail} = \frac{F_{split}\ \lambda}{E\alpha}\ \frac{15(1\ -\ \nu)}{R^2} \tag{9.4}$$

9.2.2 EXPERIMENTAL PROGRAMME

9.2.2.1 Objectives

An experimental programme was put in hand to evaluate the usefulness of Equations 9.2 and 9.4 in predicting the thermal stability of individual aggregate particles. This was achieved by studying the effect of the following parameters on the thermal stability of a range of aggregates;

(i) absolute surface temperature rise, $\Delta\theta$

(ii) rate of surface temperature rise, m

(iii) aggregate size, R

A secondary objective of the experiments was to observe the nature of aggregate splitting failure, together with the effect on splitting of the presence of moisture.

9.2.2.2 Procedure

A number of aggregates, typical of those used for the production of concrete in the United Kingdom, were heated in an oven and their behaviour was monitored. The aggregates studied are described in Table 9.2. A large number of tests were undertaken and the aggregates were exposed to constant oven temperatures of 100, 150, 200, 250,..., 800° C.

Aggregate Type	Source	Size (mm)
Crushed Granite	E.C.C.Croft Quarry	20 - 5
Rounded Gravel	Trent Valley	20 - 5
Crushed Gravel	Thames Valley	20 - 5
Crushed Greywacke	Ballybrane, N.Ireland	20 - 5
Crushed Limestone	Battscombe	20 - 5
Lytag	made by Boral Ltd.	14 - 5

Table 9.2. Aggregates investigated

The test procedure adopted was relatively straightforward. A batch of aggregate was sieved and samples gathered into groups according to size, i.e. 20-14 mm, 14-10 mm and 10-5mm. These samples were then placed in purpose designed perforated steel trays and their mass recorded. The sample trays were fitted with lids in order to contain any fractured pieces of aggregate.

The samples were placed in the oven set at the particular temperature of interest for 30 minutes. On removal, their mass was immediately recorded, with the change in mass being related to the moisture content of the aggregate. Then, the aggregate samples were sieved again and the percentage that had not suffered from a reduction in size noted. On correction for moisture content, this figure was recorded as the *% survival* of the sample. The values measured were averaged over a number of samples to give typical *% survival* values for each particular aggregate size and type. In some cases the *% survival* was effected by shrinkage rather than splitting of the aggregate. Close visual inspection of the aggregates showed where this had occurred and the test records were ammended to distinguish shrinkage from splitting.

Tests were carried out to determine the effect of temperature, rate of heating and aggregate size on thermal stability of a number of different aggregates. In order to ascertain the effect of moisture, tests were carried out on aggregates in oven dry and saturated surface dry conditions.

9.2.2.3 Results

The results of the oven tests on individual aggregate particles are given in Table 9.3. The aggregates were heated both in oven-dried (OD) and saturated surface-dried (SSD) conditions.

AGGREGATE SPLITTING (% SURVIVAL) WITH TEMPERATURE (°C.)										
AGGREGATE TYPE	**Condition**	**Size(mm)**	**100**	**200**	**300**	**400**	**500**	**600**	**700**	**800**
CRUSHED GRANITE	O.D.	20 - 14	100	100	100	100	100	100	100	100
		14 - 10	100	100	100	100	100	100	100	100
		10 - 5	100	100	100	100	100	100	100	100
	S.S.D	20 - 14	100	100	100	100	100	100	100	100
		14 - 10	100	100	100	100	100	100	100	100
		10 - 5	100	100	100	100	100	100	100	100
CRUSHED GRAVEL	O.D.	20 - 14	100	100	100	94	94	78	74	68
		14 - 10	100	100	100	100	94	86	82	85
		10 - 5	100	100	100	100	100	100	95	94
	S.S.D.	20 - 14	100	100	100	80	78	76	62	54
		14 - 10	100	100	100	76	69	75	75	74
		10 - 5	100	100	100	96	94	92	95	94
ROUNDED GRAVEL	O.D.	20 - 14	100	100	100	100	100	100	97	96
		14 - 10	100	100	100	100	100	100	100	100
		10 - 5	100	100	100	100	100	100	100	100
	S.S.D.	20 - 14	100	100	100	100	100	100	98	94
		14 - 10	100	100	100	100	100	100	98	97
		10 - 5	100	100	100	100	100	100	100	100
GREYWACKE	O.D.	20 - 14	100	100	100	100	100	100	100	100
		14 - 10	100	100	100	100	100	100	100	100
		10 - 5	100	100	100	100	100	100	100	100
	S.S.D.	20 - 14	100	100	100	96	89	77	50	36
		14 - 10	100	100	100	93	98	96	96	92
		10 - 5	100	100	100	100	100	100	100	97
CRUSHED LIMESTONE	O.D.	20 - 14	100	100	100	100	100	100	100	100
		14 - 10	100	100	100	100	100	100	100	100
		10 - 5	100	100	100	100	100	100	100	100
	S.S.D.	20 - 14	100	100	100	100	100	100	100	100
		14 - 10	100	100	100	100	100	100	100	100
		10 - 5	100	100	100	100	100	100	100	100
LYTAG	O.D.	20 - 14	100	100	100	100	100	100	100	100
		14 - 10	100	100	100	100	100	100	100	100
		10 - 5	100	100	100	100	100	100	100	100
	S.S.D.	20 - 14	100	100	100	100	100	100	100	100
		14 - 10	100	100	100	100	100	100	100	100
		10 - 5	100	100	100	100	100	100	100	100

Table 9.3. Summary of the results of aggregate splitting oven tests

9.2.3 MATERIAL PROPERTIES OF AGGREGATES

9.2.3.1 Mechanical properties of aggregates

In order to examine the validity of Equations 9.2 and 9.4, it is firstly necessary to ascertain values for the material properties required in both equations. In general, the mechanical properties of aggregates such as strength and Modulus of Elasticity depend on their composition, texture and structure. For example, low aggregate strengths may be due either to an inherent weakness in their constituent grains or their grains may be sufficienly strong but poorly knit together.

The compressive strength of aggregates typically has values in the order of 175 N/mm^2 which are considerably higher than the strength of concrete. This is important because the actual stresses at the points of inter-aggregate contact may subject individual aggregates to stresses well in excess of the nominally applied compressive stress to the concrete. However, material properties such as compressive strength and Modulus of Elasticity are rarely measured for aggregates with more easily measured properties such as the crushing value being adequate for most applications.

With data on the mechanical properties of aggregates at ambient temperature being limited, the data describing their mechanical performance at elevated temperatures are even more limited. Where such data are available, they are generally based on the results of geological studies of rocks. For example, Heuze (1983) provided much information on the high temperature properties of Granite, which he studied to model the movement of magmatic intrusions within the earth's crust. The usefulness of such geologically based data is limited by the fact that rocks contain planes of weakness. The presence of such planes within test specimens and furthermore their orientation relative to the testing apparatus have a marked effect on measured material properties. In addition, many rocks are significantly anisotropic, i.e. their material properties vary with direction. Typical examples include rocks containing calcite.

9.2.3.2 Thermal properties of aggregates

A reasonable amount of data are available for the coefficient of thermal expansion of rocks, e.g. Skinner (1966). However, the majority of such data have been recorded at what would be

considered from the fire viewpoint as low temperatures, i.e. less than 100°C. While the coefficient of thermal expansion of an aggregate may be taken as constant for small thermal changes, such an assumption is not valid for the extreme conditions encountered on exposure to very high temperatures. An example of this is the phase transition of quartzitic materials at 575° C, where the quartz changes from its α to β form, accompanied by a considerable increase in volume. A further increase in volume takes place at 1000°C on the formation of cristobalite. These types of reactions occur in many commonly used aggregates such as Gravel and Granite.

The thermal conductivity of aggregates is generally anisotropic and is effected by moisture content. Conductivity is the dominant thermal property of an aggregate, as specific heat capacity and density vary to a much lesser degree.

Based on a study of the literature, principally Marshall (1972), Orchard (1976), Heuze (1981), Neville (1981) and Collins (1989) estimates have been made for the thermal and mechanical properties required in Equations 9.2 and 9.4 for the range of aggregates examined in the oven tests. The properties assumed are given in Table 9.4. It is recognised that these data are generalised and cannot be unduly relied upon, with information on Gravel being particularly unreliable because of the large variety in possible sources. However, the data are representative of those which might be available to designers attempting to assess the susceptibility of aggregates to splitting. Thus, the data are considered adequate for the assessment of the models of aggregate splitting based on elastic theory.

Aggregate Type	**E** Gpa	σ_{comp} MPa	σ_{tens} MPa	ν	ρ kg/m^3	**k** W/mK	**C** J/kgK	λ mm^2/s	α x10^{-6}/K
Limestone	77.9	184	8.5	0.31	2700	3.23	845	1.4	4.4
Granite	66.0	246	13	0.23	2660	2.9	715	1.5	7.5
Lytag	38.9	89	4.7	0.31	830	0.26	1297	0.24	2.0
Greywacke	34.5	213	10.8	0.13	2240	1.79	711	1.1	11.6
Quartzite	68.0	170	7.5	0.30	2850	5.17	732	2.5	10.8

Table 9.4. Indicative estimates of aggregate properties

9.2.4 ASSESSMENT OF ELASTIC MODELS IN THE PREDICTION OF AGGREGATE SPLITTING

The usefulness of Equations 9.2 and 9.4 in assessing the thermal stability of aggregates may be evaluated by comparing their predictions of aggregate response to heat with the behaviour actually observed in the oven tests.

9.2.4.1 Evaluation of Equation 9.2

9.2.4.1.1 Predicted effect of temperature rise

The temperatures needed to cause splitting of different aggregates θ_{fail} were predicted using Equation 9.2 and the material properties in Table 9.4. The results are given in Table 9.5.

Aggregate	θ_{fail} °C
Limestone	45
Granite	53
Lytag	62
Greywacke	62
Quartzite	19

Table 9.5 Failure temperatures of different aggregates as predicted by Equation 9.2

9.2.4.1.2 Observed effect of temperature rise

It is immediately clear from Table 9.5 that Equation 9.2 predicts that all of the aggregates tested should have suffered splitting on exposure to the heating conditions in the oven. Clearly, the predicted failure temperatures are too low and Equation 9.2 is overly conservative.

The improved performance of aggregates in practice over the predicted behaviour could have been due to one or more reasons. Firstly, there is probably some degree of inaccuracy associated

with the basic material properties assumed. Furthermore the variation of these properties with temperature has not been considered. For example, the coefficient of thermal expansion or the stiffness of the aggregates may be reduced (or increased) at elevated temperatures.

Although the actual values of the failure temperatures predicted are clearly incorrect, the relative ranking of aggregate performance predicted by Equation 9.2 is reasonable. Equation 9.2 predicts that Quartzite is more susceptible to splitting than the other aggregates and indeed this was confirmed in the oven tests, where the Gravel containing 90% Quartzite proved most susceptible to splitting. It was noted during the tests that the splitting of the Gravel was generally concentrated on its Quartzitic constituents.

The observed splitting of the Gravel aggregate versus temperature is given in Figure 9.2. It is clear that *% survival* is not linearly related to temperature and an obvious change in behaviour takes places between 550 and 650°C corresponding to the α to β phase change. Figure 9.2 also shows the splitting of Greywacke at a range of temperatures and it also demonstrates a similar trend.

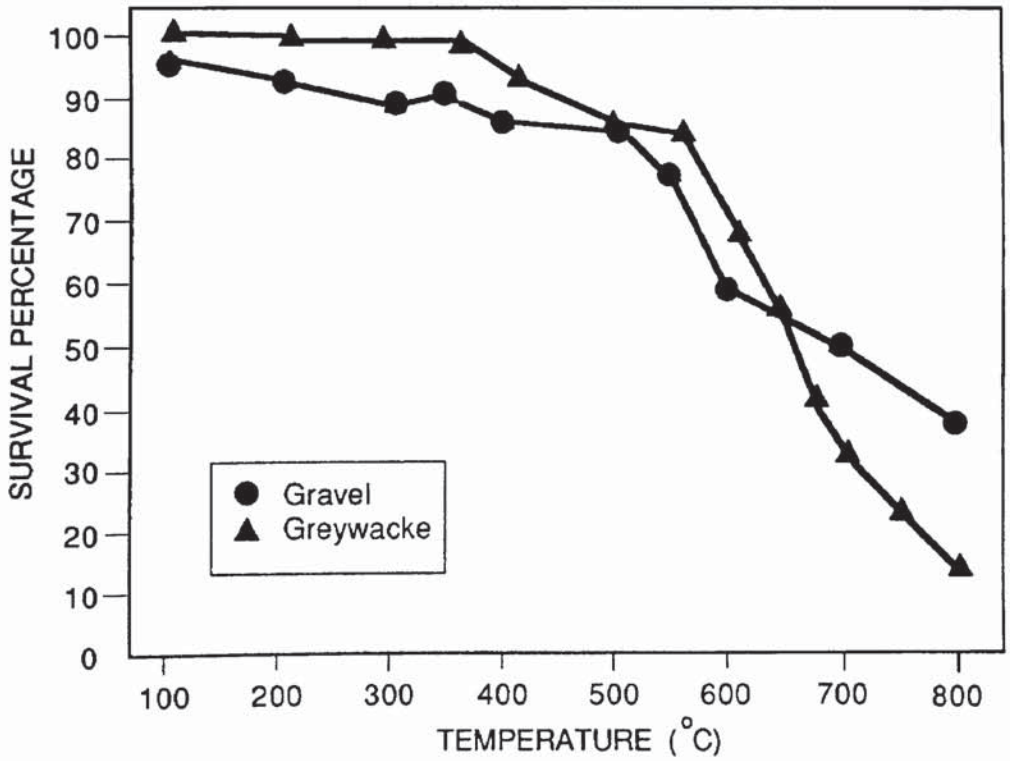

Figure 9.2. Variation of the extent of splitting with temperature

Figure 9.2 suggests that the coefficient of thermal expansion may not be assumed a constant. A full explanation of aggregate splitting clearly requires information on the temperature dependence of the coefficient of thermal exansion. The lack of such information makes a more comprehensive approach difficult.

However the relationship between aggregate splitting and temperature is not governed solely by the coefficient of expansion. The Granite, for example, also contained a Quartzitic component, yet did not suffer from any splitting or degradation up to temperatures of 800°C. Although, consideration of aggregate properties such as Modulus of Elasticity and tensile strength seems intiutively correct, the idealised elastic form of Equation 9.2 does not give a good fit with observed behaviour.

9.2.4.2 Evaluation of Equation 9.4

9.2.4.2.1 Predicted effect of heating rate

The rates of surface heating necessary to cause failure of aggregates m_{fail} may be calculated using Equation 9.4 and material properties from Table 9.4 and these m_{fail} values are given in Table 9.6.

Aggregate *size*	m_{fail} (°C/min)			
	20mm	*14mm*	*10mm*	*5mm*
Limestone	215	440	862	3447
Granite	272	554	1087	4350
Lytag	89	182	358	1429
Greywacke	233	476	933	3732
Quartzite	162	332	650	2599

Table 9.6 Rates of surface heating that result in splitting failure (after Equation 9.4)

9.2.4.2.2 Observed effect of heating rate

It was difficult to measure the actual rate of heating of the aggregate particles themselves. The

aggregates were of such a small size that the attachment of thermocouples to measure changes in surface temperature would have been difficult. There were also some practical difficulties associated with fixing thermocouples to aggregates.

Thus, in order to get an estimate of the likely thermal response of the aggregates to the oven environment, specialist computer software for thermal analysis was used. The surface heating rates of the aggregates were predicted using the software package THELMA, developed by Connolly and Kirby (1993) at the Building Research Establishment. The software solves, using a finite element numerical technique the relevant equations of heat conduction within the aggregate for the boundary conditions defined by the environment within the oven.

Use of thermal analysis sofware does, however, attract some degree of uncertainty. For example, the thermal properties of the aggregates have to be estimated from available tabulated data and such generalised data may not only be inappropriate to the individual aggregates studied, but also were derived at ambient rather than elevated temperatures. Furthermore, estimates have to be made of the boundary conditions input to the model to describe the heat transfer to the aggregate within the oven, i.e. convection factor and resultant emissivity. Thus, the usefulness of thermal modelling is not so much the prediction of heating rates but rather the calculation of the relative change in heating rate that accompanies an increase in oven temperature.

The surface heating rates predicted by THELMA are given in Table 9.7 based on temperature gradients calculated over the first 4 minutes.

Oven temp.		**100°C**	**200°C**	**400°C**	**800°C**
Normal weight	size 5mm	14	24	75	170
	size 14mm	5	14	30	100
Lytag	size 5mm	16	38	110	200
	size 14mm	8	18	45	140

Table 9.7 Rates of surface temperature rise (°C/min) of aggregates in oven environments

It may be seen from Table 9.7 that the rates of heating are reduced with time. The study of temperature gradients over the first 4 minutes is particularly relevant as it is within such a timescale that splitting has been observed. Comparison of the heating rates within the oven (Table 9.7) to the heating rates required for failure (Table 9.6) suggests that, with the exception of Lytag, none of the aggregates examined should have suffered any splitting but this was not the case. Equation 9.4 consistently predicts unrealistically high values for m_{fail} particularly for smaller aggregates. Equation 9.4 is completely inaccurate in its predictions of the performance of Lytag. However, Equation 9.4 successfully predicts that Quartzite is far more susceptible to splitting than Granite, Limestone or Greywacke.

The correlation in trend between the experimental observations and the behaviour predicted by Equation 9.4 was reasonable. However, there is very poor correlation in the actual values of m_{fail} and thus Equation 9.4 is of little value as a practical means of evaluating the thermal stability of aggregates.

9.2.4.3 Effect of aggregate size

The influence of aggregate size on the occurrence of splitting was determined by studying aggregates in a range of different sizes, i.e. 20-14mm, 14-10mm and 10-5mm. For practical reasons, no effort was made to test aggregates of a single size and in subsequent discussions a mean aggregate size has been assumed as representative of each batch.

The results of the tests on Thames Valley Gravel aggregate (presented in Figure 9.3) clearly show the influence of aggregate size, with the susceptibility to splitting reducing significantly with smaller aggregates. While some splitting was observed in the 10-5 mm grade Gravel, it was of a limited nature and the *% survival* never dropped beneath 94%.

The role of size is isolated in Figure 9.4, which shows the relationship between aggregate size and the *% survival* for a range of temperatures. At temperatures below the α to β Quartz transition, i.e. 575°C, the relationship between *% survival* and aggregate radius is approximately linear. Above the transition temperature, the relationship is best described by an inverse square which is predicted by Equation 9.4.

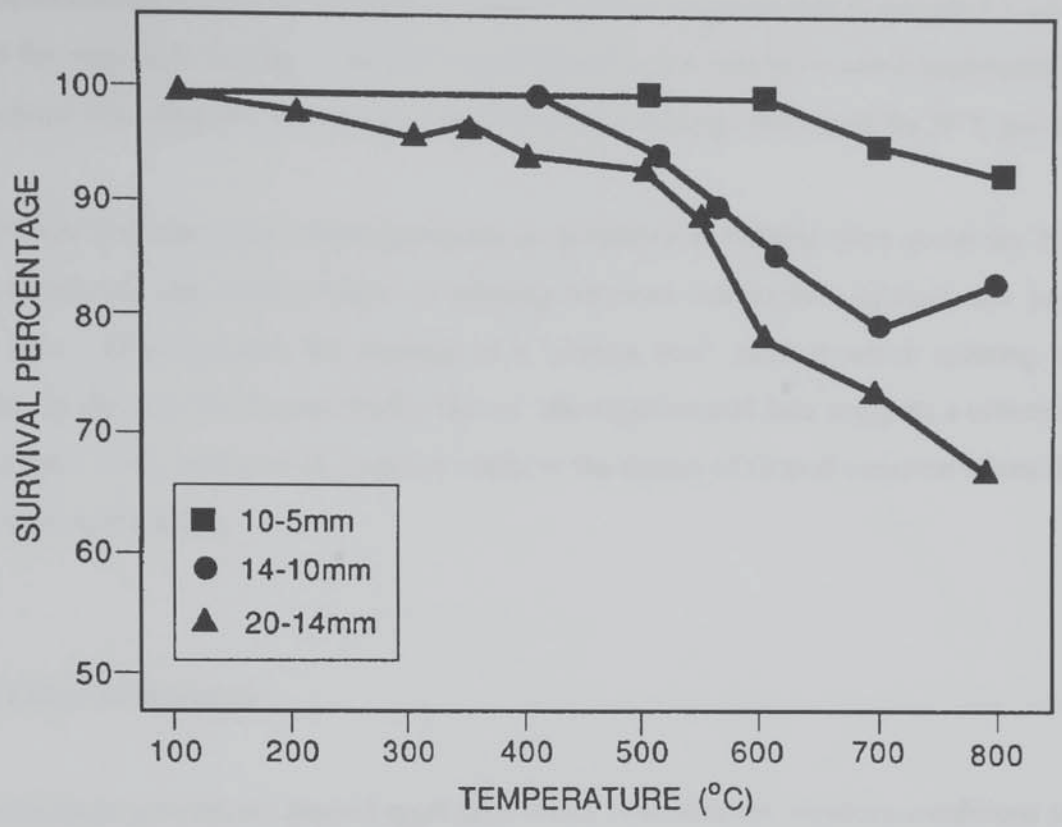

Figure 9.3. *% survival* of Thames Valley Gravel versus temperature for a range of sizes

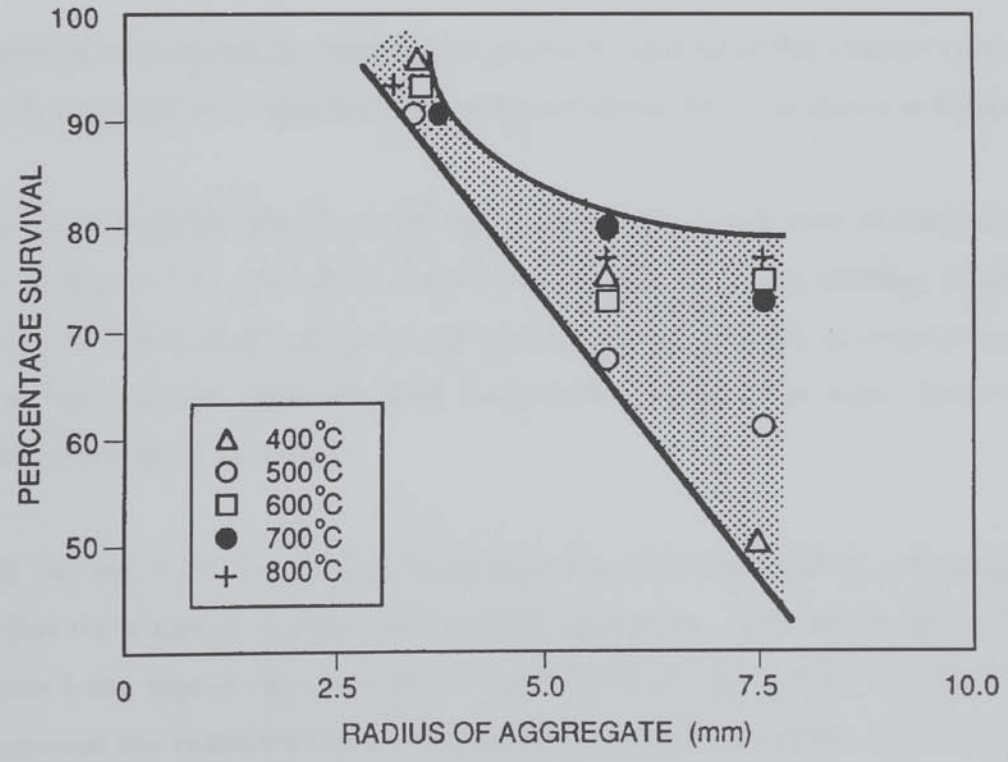

Figure 9.4. Relationship between aggregate size and *% survival*

These observations effectively confirms Manson's (1952) proposal that Equation 9.2 could not be used for very high heating rates, for which Equation 9.4 would be more appropriate. The experimental data suggests that a reasonable threshold heating rate would be 50°C per minute.

Figure 9.4 also indicates that when aggregates are subjected to heating rates above the 50°C per minute threshold, their susceptibility to splitting becomes independent of their size, beyond a certain size. This promotes the concept of a "critical size", beyond which splitting is more probable. In the case of Thames Valley Gravel, the experimental data suggests a critical size of about 12 mm. This information could be useful in the design of Gravel concrete mixes for high temperature applications.

9.2.4.4 Effect of moisture

The experimental programme studied aggregates under two different moisture conditions namely; *oven dried*, i.e. heated for 24 hours at 110° C, and *saturated surface dried*, i.e. immersed in water for 72 hours before being towelled dry at the surface.

The presence of moisture had a marked effect on the *% survival* of the Thames Valley Gravel increasing its susceptibility to splitting at temperatures above 300°C, as shown in Figure 9.5.

The influence of moisture was illustrated more dramatically in the case of Greywacke. As illustrated in Figure 9.6, oven dried Greywacke did not suffer any splitting regardless of temperature. However, Greywacke, containing moisture split violently at temperatures above 400°C. In fact, surface saturated dried Greywacke exhibited the most severe splitting encountered in the test programme.

Granite did not split at any temperature regardless of its moisture condition. However, it was observed that the saturated surface dried Granite was weaker, more friable and more easily crumbled after being exposed to temperatures over 600° C than dry Granite. Neither Limestone nor Lytag showed any reduction in their thermal stability with the presence of moisture.

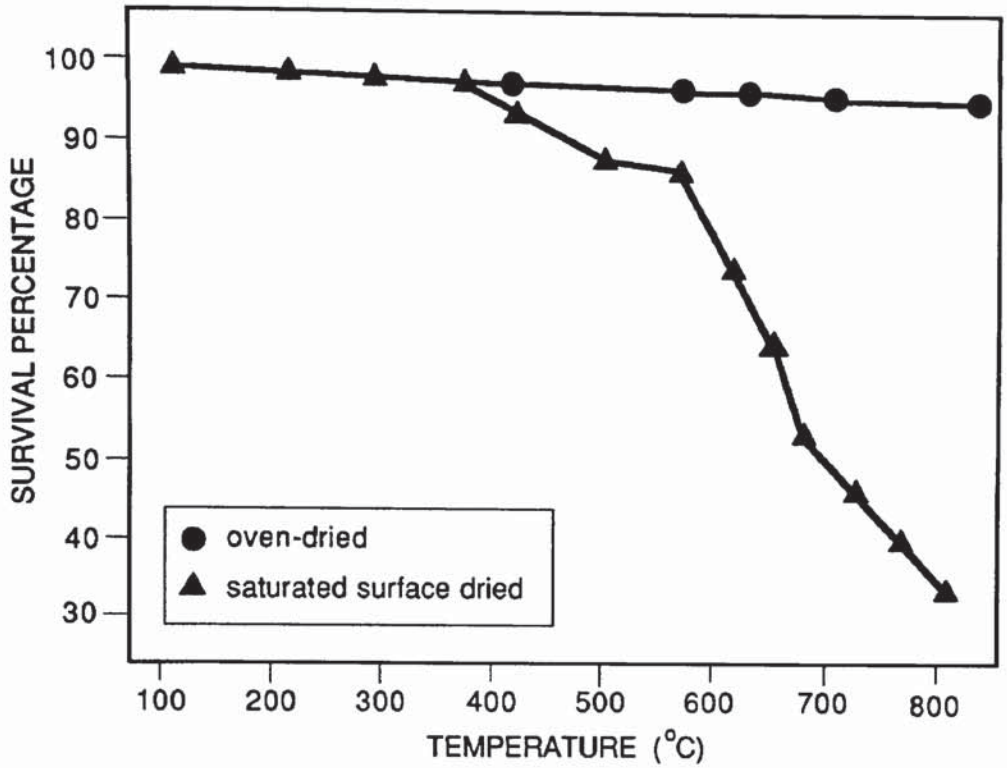

Figure 9.5. The influence of moisture on the splitting of Thames Valley Gravel

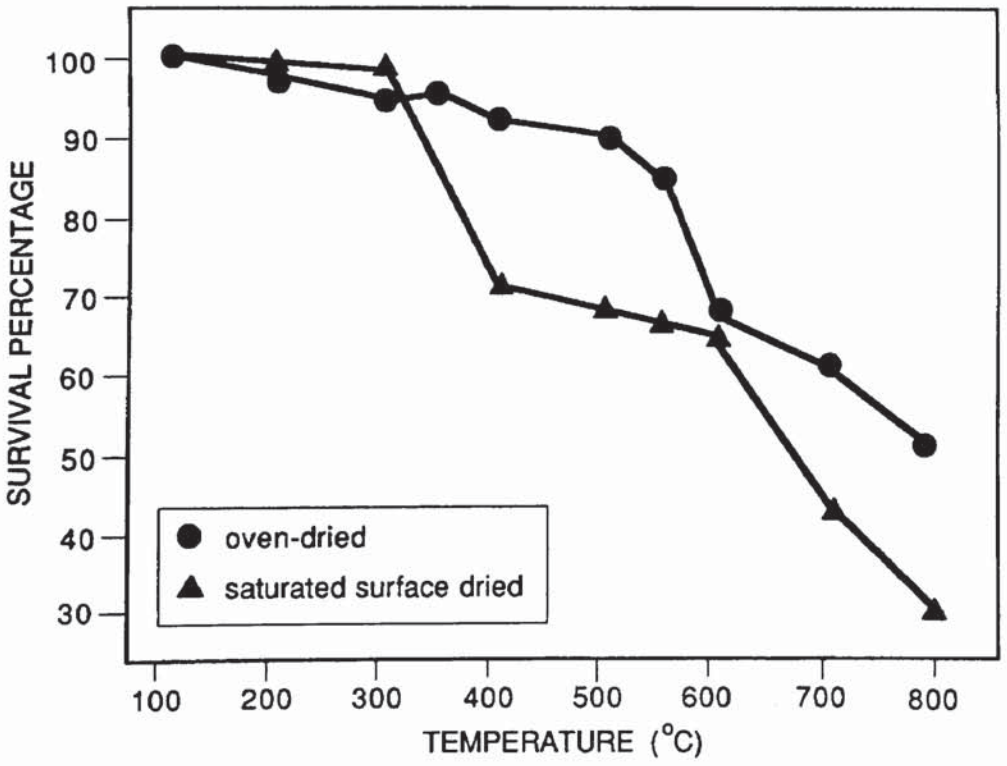

Figure 9.6. Influence of presence of moisture on the splitting of Greywacke

The reasons for the observed influence of moisture is unclear. Moisture increases the conductivity of aggregates, reduces thermal gradients and alleviates tensile stresses. Thus susceptibility to splitting should be reduced by the presence of moisture, as it effectively dampens the rate of surface heating. However, it was observed that moisture exacerbated splitting in the case of Gravel and introduced splitting to Greywacke, where it had not previously existed.

Some explanation for this behaviour has been offered by Meyer-Ottens (1972) as previously discussed in Section 9.2.1. He suggested that spalling was due to the expansion of vapour gases within the aggregate, whether they be evolved from free or chemically combined moisture and that aggregate splitting was a direct result of bursting stresses generated by internal steam pressures.

An evaluation of the moisture presence likely within the different aggregates seems to confirm his theory. A measure of the potential moisture content of an aggregate was its absorption value which is determined by measuring the difference between the mass of the aggregate in its oven-dried and saturated surface dried states. The ratio of the increase in mass to the mass of the dry sample, expressed as a percentage, is its absorption.

The Material's Section of the Building Research Establishment measured the absorption of the aggregates used in this experimental programme in accordance with the standard procedure laid down in BS 812:Part 2:1975 and the results are given in Table 9.8.

Aggregate	% absorption
Granite	3.1
Limestone	0.4
Gravel	1.6
Greywacke	3.0
Lytag	7.3

Table 9.8. Absorption of aggregates (as percentage of oven-dried mass)

The Greywacke had a relatively high absorption value. Thus, it is possible that the splitting observed in saturated Greywacke was a direct result of bursting stresses due to vapourisation of

moisture within it. Such bursting stresses may have been super-imposed on the thermally induced stresses, with their sum being sufficient to cause splitting at temperatures over 400°C.

Granite, which had similarly high absorption characteristics, may have been subjected to the same bursting mechanism. However, the higher tensile strength of Granite and its superior thermal stability (as measured in Section 9.2.4) could have been sufficient to resist the combined thermal and mechanical stresses. The Granite did show some signs of distress, however, and was friable and weak after heating. Limestone having similar mechanical properties to Granite had a much lower absorption value and thus did not suffer from the same moisture imposed bursting stessses.

The high absorption value recorded for Lytag suggests that there was plenty of water available to generate the bursting stresses necessary for splitting. In addition, its low tensile strength offered less resistance to these stresses. Despite both these facts, no splitting was observed. This may be due to the particularly low thermal stresses acting within the aggregate. However, more likely, is Meyer-Ottens' explanation that the porosity of Lytag was sufficiently high for moisture and steam to pass through it with relative ease. Whilst there may have been enough water in the Lytag to develop large bursting stresses, its high porosity ensured such stresses never materialised.

In conclusion, the experimental results have shown that caution needs to be exercised in applying any model for aggregate splitting to aggregates that contain reasonable amounts of moisture (i.e. absorption values above 3.0%). It appears that on heating, moisture generates internal bursting stresses, which when superimposed on thermal stresses may cause aggregate splitting.

9.3 NEW MODEL FOR PREDICTING THERMAL STABILITY OF AGGREGATES

Section 9.2 has clearly shown that simple elastic relationships such as Equations 9.2 and 9.4 are inadequate for predicting aggregate splitting. One reason for this may be the use of inappropriate data for the material properties of the aggregate. It is possible, however, that fundamental assumptions underpinning these Equations may be inapplicable and a completely new approach is necessary. The applicability of Equations 9.2 and 9.4 may be ascertained by studying the nature and mode of failure observed in practice and comparing it to that expected from the models.

9.3.1 OBSERVED MODE OF AGGREGATE SPLITTING FAILURE

It was observed that the aggregate particles failed from their surface inwards, rather than from their centre outwards. In addition, the failure planes were seen to be orientated tangentially to the aggregate's surface, as opposed to radially.

Plates 9.2 through 9.5 show a series of high speed photographs taken of the splitting of a 50 mm particle of Gravel aggregate. The aggregate was heated in the small-scale electrical heating enclosure described in Chapter 7 and was subjected to a heating rate of approximately 100°C per minute. Splitting started approximately 90 seconds after heating had commenced with the aggregate being completely destroyed after 240 seconds.

These Plates clearly show that the pattern of aggregate splitting is not consistent with the models of splitting based on tensile failure, but rather they suggested that aggregate splitting is a form of shear failure.

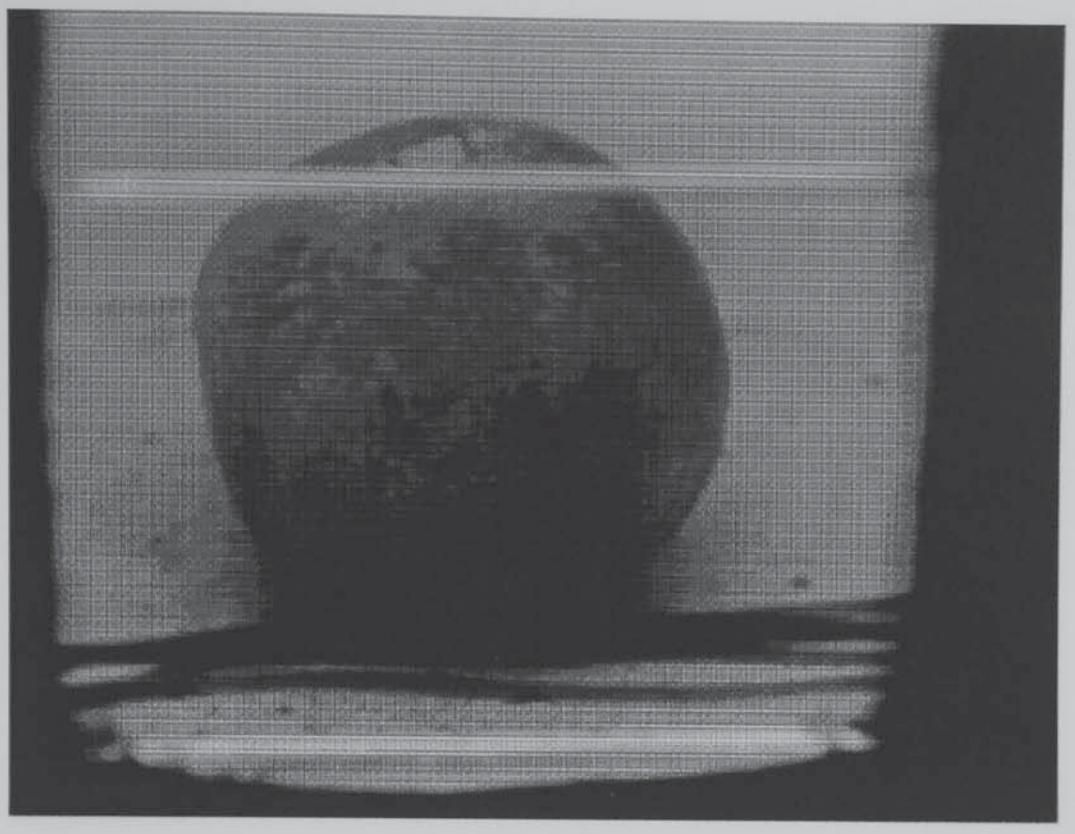

Plate 9.2. Early stages of aggregate under heating

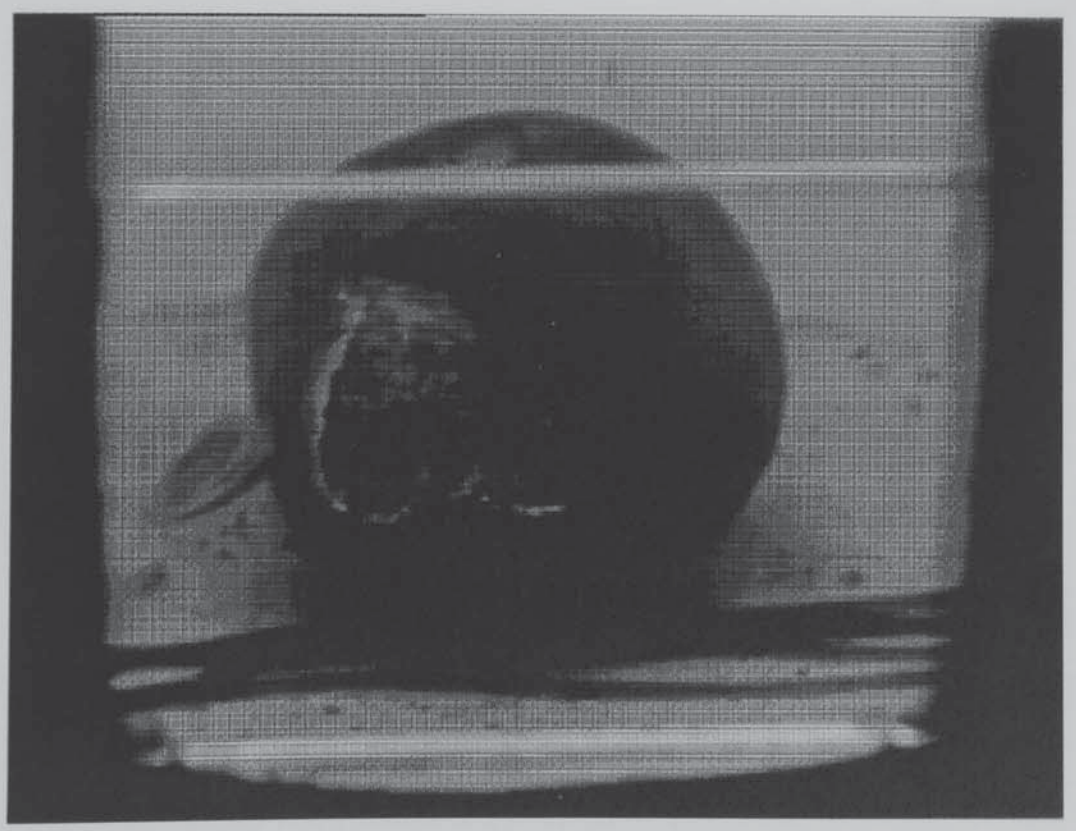

Plate 9.3 Early failure of aggregate under heating

Plate 9.4 Ejection of split aggregate material from tangential failure plane

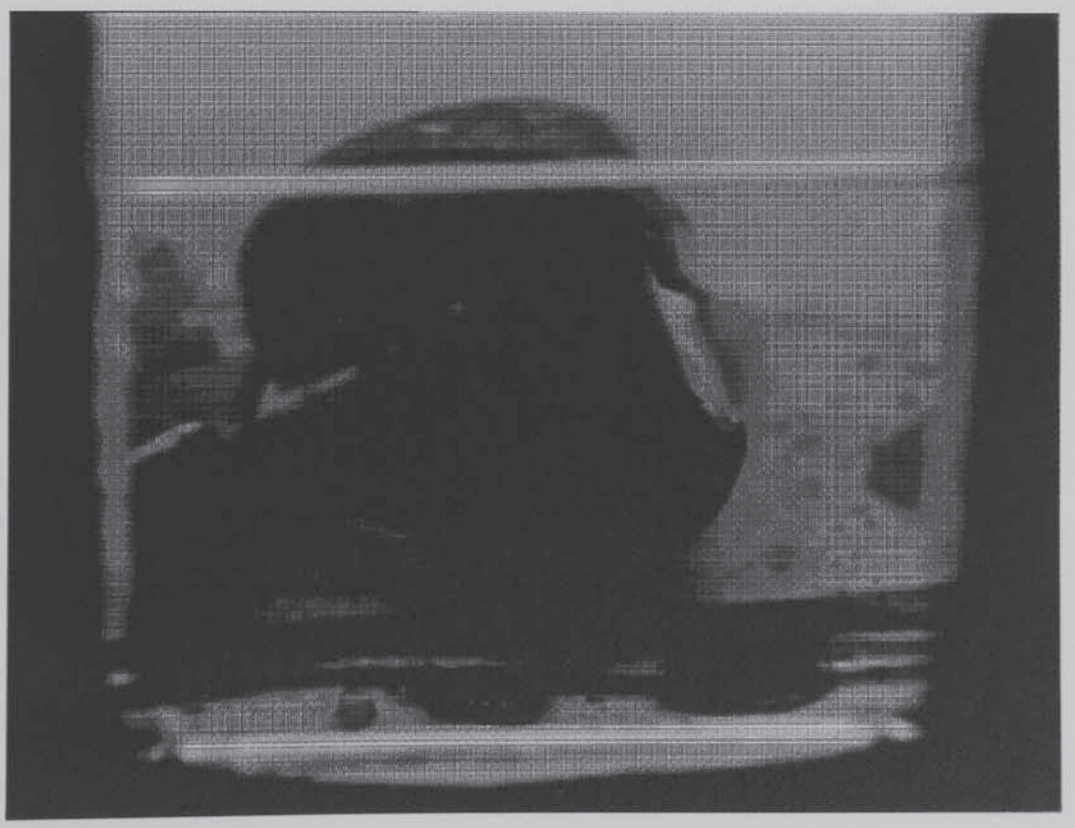

Plate 9.5 Mode of failure clearly observed as shear

9.3.2 SHEAR STRESSES IN HEATED OBJECTS

Norton (1968) used the photoelastic method to evaluate the distribution of stresses within an elastic disc, which has had its surface uniformly heated. The photoelastic method allows the resultant stresses within a plane object to be examined visually.

Norton studied a plane bakelite discs. On passing polarised light through the heated discs, the magnitude of the difference between the principal stresses was determined and, thus, so too were the principal shear stresses. Norton also studied rapidly cooled discs and found that the stresses developed were of the same magnitude but opposite sign to those developed on heating.

The stress patterns found by Norton in a disc suddenly heated to 100°C are illustrated in Figure 9.7. As predicted by Kent (1932), the shear stresses attain their maximum value at the surface and are everywhere located at 45° to the radii. Norton suggested that, as the tensile stresses have a much lower magnitude than the shear stresses, failure was due to shear alone. He substantiated this by studying the actual nature of cracking of the discs under conditions of both rapid surface heating and cooling, reproduced here in Figures 9.8 and 9.9.

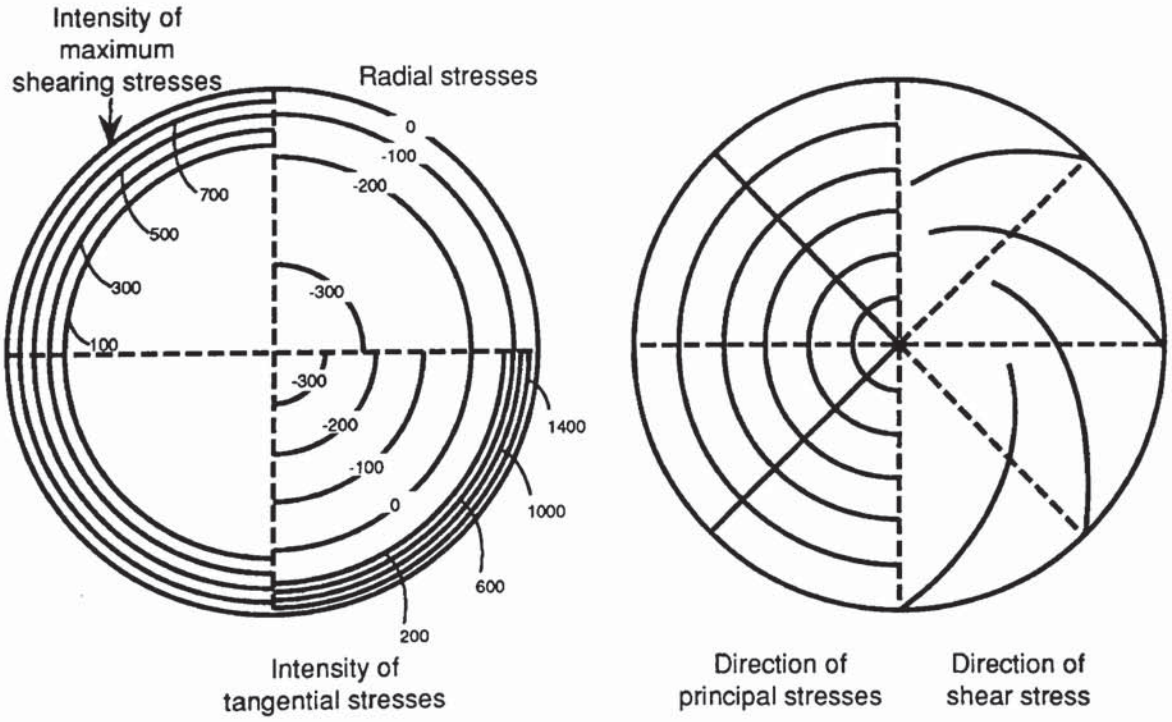

Figure 9.7 Stress patterns in heated discs (after Norton, 1968)

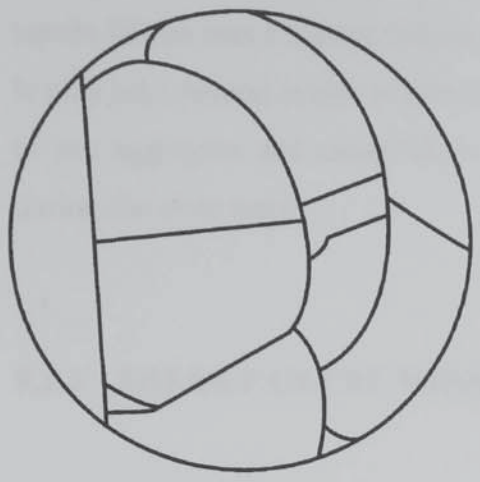

Figure 9.8.Cracking of a heated disc

Plate 9.6. Observed failure of heated aggregate

On heating, cracks were noted entering the surface at approximately 45° and as shown in Figure 9.8, tangential fracture planes were created off, having heights of approximately one quarter of the sphere's diameter. On cooling, however, Norton observed cracks entering the surface at approximately 90° as shown in Figure 9.9

Although Norton was principally concerned with the behaviour of heated discs, the crack patterns which he encountered are immediately recognisable as being similar to those observed in the aggregate heating tests. Plates 9.6 and 9.7 are directly analagous to Norton's Figures 9.8 and 9.9.

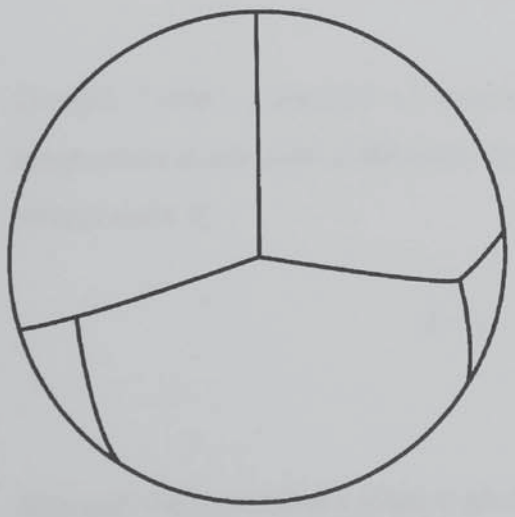

Figure 9.9. Cracking of a cooled disc

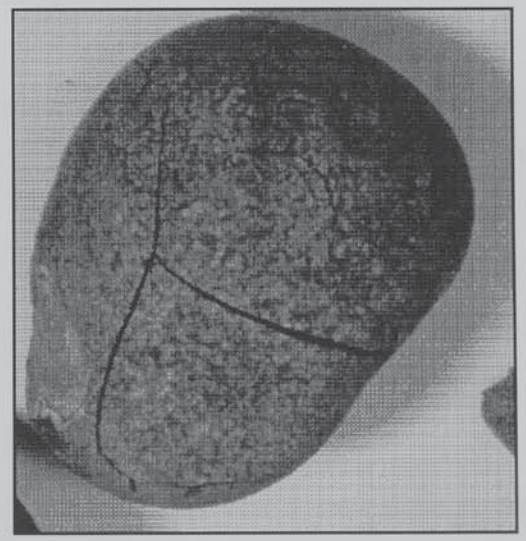

Plate 9.7 Observed failure of cooled aggregate

Furthermore, Norton suggested that failure due to shear stresses occurred suddenly, but that tensile failure was a slower failure process, with cracks growing gradually in from the surface. It may take several cycles of alternate heating and cooling before the cracks meet at the centre of the aggregate and cause failure. This corroborates the behaviour of aggregates observed during the oven tests.

9.3.3 SHEAR FAILURE MODEL OF AGGREGATE SPLITTING

9.3.3.1 Theory

Consider a spherically shaped particle of aggregate, that is heated at a uniform rate of m°C per second. The temperature within the aggregate particle itself has to satisfy the Fourier Field Equation, which may be expressed with respect to a spherical co-ordinate system as;

$$\frac{\delta^2\theta}{\delta r^2} + \frac{2}{r}\frac{\delta\theta}{\delta r} = \frac{1}{\lambda}\frac{\delta\theta}{\delta t} \qquad (9.5)$$

where;
- θ = temperature
- r = radial distance to point of interest from centre of aggregate
- t = time
- λ = thermal diffusivity of aggregate

Dougill (1965) presented an approximate solution to Equation 9.5 which described the temperature at any point a distance r from the centre of the aggregate as a function of its surface temperature θ_s;

$$\theta(r,t) = \theta_s \left(1 - \frac{R^2 - r^2}{6\lambda t}\right) \qquad (9.6)$$

Although the approximate solution given by Equation 9.6 satisfies the conditions at the interface, it does not provide the correct temperature within the aggregate at time t = 0. However, Dougill undertook a comparison with the complete solution and concluded that the approximation

described by Equation 9.6, was accurate to within 10%, for situations where $\lambda t/R^2 > 0.25$. Thus, the approximate solution becomes satisfactorily accurate after only a few minutes heating, even for aggregates which have a relatively low value of thermal diffusivity such as Lytag.

A model for the development of shear within an aggregate is proposed in Figure 9.10. It is assumed that an isothermal plane passed parallel to the heated aggregate surface and the shear strain γ due to thermal incompatability may be described at any time by;

$$\gamma = S \alpha \frac{\delta\theta}{\delta r} \tag{9.7}$$

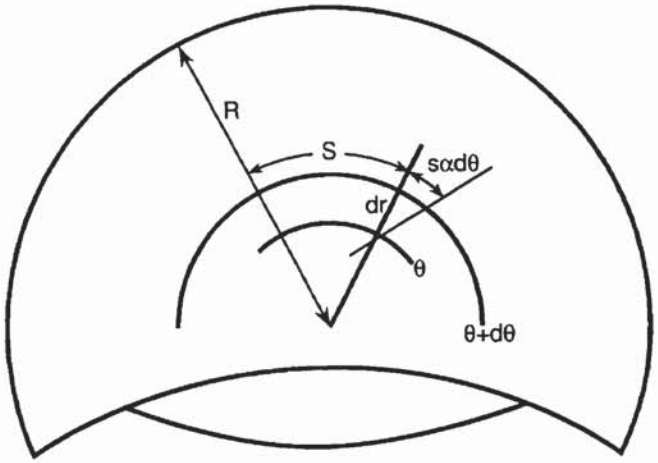

Figure 9.10 Model for shear development in a heated aggregate

Since the shear surface length S is a function of radius r and that the temperature distribution can be differentiated with respect to radius, the shear strain may be more fully described by;

$$\gamma = (2 \pi r) \alpha \left(\frac{2 \theta_s r}{6 \lambda t} \right) \tag{9.8}$$

Defining the rate of surface heating θ_s / t as m and recognising that radial distance r has a maximum value of radius R, the maximum shear strain γ_{max} developed in a heated aggregate can be described by;

$$\gamma_{max} = \frac{2 \pi}{3} \left(\frac{\alpha}{\lambda} \right) m R^2 \tag{9.9}$$

The capacity of a material to sustain shear strain is measured by its shear capacity $\gamma_{capacity}$

$$\gamma_{capacity} = \frac{2(1+\nu)}{E} F_{split} \tag{9.10}$$

A measure of the susceptibility of an aggregate to splitting is given by the ratio of the maximum thermally induced shear strain to its shears capacity, i.e. $\gamma_{max}/\gamma_{capacity}$, where;

$$\frac{\gamma_{max}}{\gamma_{capacity}} = \frac{\pi}{3(1+\nu)} \frac{\alpha E}{\lambda F_{split}} m.R^2 \tag{9.11}$$

9.3.3.2 Correlation with experimental observations

The critical rate of increase in surface temperature m_{crit} necessary to cause aggregate splitting can be obtained by rearranging Equation 9.11;

$$m_{crit} = \frac{3(1+\nu)}{\pi} \left(\frac{F_{split} \lambda}{E \alpha R^2} \right) \tag{9.12}$$

Although derived by completely independent means, Equation 9.12 contains the same parameters as those presented in Equation 9.4 for m_{fail}. The difference between both expressions lies in the Poisson's Ratio multiplier. The heating rates predicted by the different approaches are related by;

$$m_{crit} = \frac{1+\nu}{5 \pi (1-\nu)} m_{fail} \tag{9.13}$$

It was concluded in Section 9.2.4.2 that the values of m_{fail} predicted by Equation 9.4 provided a reasonable indicator of the relative performance of different aggregates but the absolute values were unrealistically high. However, application of the new aggregate splitting model gives far more reasonable estimates of the critical heating rates as detailed in Table 9.9.

On comparing these new critical heating rates to those heating rates actually observed during the oven heating tests (presented in Table 9.7), it is clear that the values predicted using Equation 9.12 are in a similar range as those encountered in the oven. Thus, the observed performance of

Gravel and Granite becomes consistent with the new failure model. However, the behaviour of Limestone and Lytag needs further explanation.

Aggregate	$\mathbf{m_{crit}}$ (°C/min)			
size (mm)	*20*	*14*	*10*	*5*
Limestone	16	33	65	258
Granite	20	42	82	326
Lytag	7	14	26	108
Greywacke	17	36	70	280
Quartzite	12	25	49	195

Table 9.9 Critical heating rates necessary to cause splitting (shear failure model)

The performance of Limestone can be explained in several ways. Most obviously the generalised material properties assumed may have been inappropriate to the Limestone aggregate actually tested. Furthermore, crushed Limestone is more angular rather than rounded and thus its mean radius is probably quite a bit shorter in practice than had been calculated based on the assumption of sphericity. As the radius exerts an inverse square influence on m_{fail}, any reduction causes a marked increase in the values predicted for m_{crit}, thus reducing the susceptibility of Limestone to splitting and allowing correlation with experimental observations.

Lytag is mechanically weak and should have been the easiest to split. Furthermore, it is a good insulator and thus could easily develop significant temperature gradients between its surface and centre. Despite its relatively low coefficient of expansion, Equation 9.4 suggests that failure stresses will be generated in Lytag by relatively low rates of heating and its observed exceptional resistance to splitting casts some doubt on the validity of Equation 9.12.

However, a closer scrutiny of the nature of the material properties of Lytag offers a possible explanation. While Lytag is a good insulator, it is also a very porous material, as suggested by its high absorption value (over 7%). Indeed, the presence of pores increases the insulating properties of Lytag. However, the presence of these pores in Lytag makes its thermal conductivity a meaningless measure of its insulating potential. Hot air can pass with relative ease through the porous surface of Lytag and by flowing through its network of internal pores can

9.4 AGGREGATE SPALLING OF CONCRETE

Section 9.3.3 has demonstrated that the thermal stability of individual aggregate particles can be predicted using a simple equation, based on the concept that splitting is a form of shear failure. Although, the ability to predict the response of individual aggregates to heating is useful, it has limited application to aggregate spalling in concrete. In the following Section, it is hoped to extend the understanding of the behaviour of individual aggregate particles that has been developed in Section 9.3.3 to encompass aggregate spalling of concrete. Initially, it is necessary to review the usefulness of techniques which previous researchers (Dougill, 1971; Wilson *et al.* 1992) have suggested for this purpose.

9.4.1 THEORIES TO EXPLAIN SPALLING OF AGGREGATES WITHIN CONCRETE

9.4.1.1 Dougill

Dougill (1971) incorporated the expressions for thermal stability (Equations 9.2 and 9.4) into his own model of aggregate spalling, which included the relevant material properties and considered a spherical particle of aggregate of radius R, Young's Modulus E_a, Poisson's Ratio ν_a, coefficient of expansion α_a, within a larger cement matrix of Young's Modulus E_c, Poisson's Ratio ν_c and coefficient of expansion α_c.

Dougill solved the equation for stress in a heated sphere, originally developed by Timoshenko (1934), subject to boundary conditions of temperature as given by Equation 9.6 and a radial displacement, u;

$$u = \alpha_c R \theta + \frac{\sigma R}{2}\left(\frac{1+\nu_c}{E_c}\right) \tag{9.14}$$

Dougill concluded that the maximum tensile stress that may be developed at the centre of a heated aggregate sphere is;

$$\sigma = \frac{2E_a\alpha_a}{1-\nu_a}\left\{\frac{R^2\ (M+5)}{30\lambda\ (M+3)}+\frac{(\alpha_c-\alpha_a)\ \theta_s}{\alpha_a\ (M+3)}\right\} \tag{9.15}$$

where;

$$M = \frac{1+\nu_a}{1-\nu_a}\left\{\frac{(1+\nu_c)\ E_a}{(1-\nu_c)\ E_c} - 1\right\} \tag{9.16}$$

He defined failure to be when this stress reached the tensile strength of the aggregate;

$$\left(\frac{M+5}{M+3}\right)\frac{m}{m_{fail}} + \frac{5.17}{(M+3)}\left(\frac{\alpha_c-\alpha_a}{\alpha_a}\right)\frac{\theta}{\theta_{fail}} = 1 \tag{9.17}$$

where; θ_{fail} = temperature of a well stirred bath of fluid, which is just sufficiently hot to cause fracture of an aggregate which is suddenly immersed in it. θ_{fail} is given by Equation 9.2

m_{fail} = heating rate required to cause fracture in a sphere of aggregate of radius R heated at a constant rate, but free of an enveloping matrix of cement. m_{fail} is given by Equation 9.4

Dougill (1965) suggested the time to splitting failure τ_{fail} for any aggregate heated at m°C per second and is given by;

$$\tau_{fail} = 0.19\left\{\frac{\frac{1}{m} - \frac{1}{m_{fail}}\left(\frac{M+5}{M+3}\right)}{\frac{\alpha_c}{\alpha_a} - 1}\right\}(M+3)\theta_{fail} \tag{9.18}$$

He simplified Equation 9.18 by setting the ratio $(M+5)/(M+3)$ to unity, based on the assumption that the parameter M, which was similar in nature to the Biot Modulus, has a value between 1 and 5. Thus he suggested a *Simplified Thermal Stress Resistance Factor* for determining the susceptibility of aggregates within concrete to splitting;

$$\left(\frac{1}{m} - \frac{1}{m_{fail}}\right)\left\{\frac{\alpha_a}{\alpha_c - \alpha_a}\left(\frac{E_a}{E_c} + 2\right)\right\}\theta_{fail} \qquad (9.19)$$

9.4.1.2 Wilson *et al.*

Wilson *et al.* (1992) presented a numerical model for spalling, which was based on the solution of Timoshenko's (1934) equation for stresses in a heated plane slab and is given below;

$$\sigma = \frac{1}{1 - \nu}\left\{-\alpha E\theta + \frac{1}{2h}\int \alpha E\theta \, dz + \frac{3z}{2h^3}\int \alpha E\theta z \, dz\right\} \qquad (9.20)$$

where;

σ	=	stress at any point z
z	=	depth below heated surface
h	=	half total slab thickness

In their model Equation 9.20 was solved using a finite difference technique and spalling was predicted when the surface stresses exceeded the material strength. Although they presented their model as a general means of predicting spalling, the high heating rates which they used resulted in spalling failure within 10 seconds at depths between 0.5 and 2 mm. Such observations are characteristic of aggregate splitting.

Wilson *et al.* reported good correlation with their own experimental results but their model seems flawed. The incredibly short time to spalling recorded in some of their experiments (as little as 0.39 seconds) raises some questions about accuracy of measurements. Furthermore, their approach to stress generation was simplistic and their material constitutive model did not include factors such as transient thermal creep, thus their model is not considered further.

9.4.2 EXPERIMENTAL INVESTIGATION OF AGGREGATE SPALLING

9.4.2.1 Background

An experimental investigation of the factors effecting the explosive spalling of concrete has been reported in Chapters 4, 5 and 6. As part of this study, a large number of concrete specimens have been exposed to heat. One of the many observations recorded was the occurrence of aggregate spalling.

The specimens examined had a range of shapes and sizes, including 300 x 300 x 50 mm slabs and 150 x 100 mm cylinders and were heated by a variety of different means including electrical radiant heating, immersion in the flame field from gas-fired burners and exposure to the BS 476:Part 20:1987 heating regime in a furnace. Regardless of the nature of the specimen and the heating arrangement, the following variables (and their effect of aggregate spalling) were examined in a consistent manner;

(i) rate of heating
(ii) water to cement ratio (w/c) of concrete
(iii) applied load
(iv) age of concrete
(v) type of aggregate

9.4.2.2 Effect of heating rate

The effect of heating rate on the occurrence of aggregate spalling in concrete is shown in Figure 9.11. It was clear that the rate of heating is important in determining the susceptibility of a particular concrete to aggregate splitting. The heating rates shown in Figure 9.11 are given in terms of a level of incident heat flux, in kW/m^2. These heat flux levels are broadly typical of those measured in real fires (Bullock, 1990, personal communication) and generate surface heating rates in concrete as detailed in Chapter 6.

The data presented in Figure 9.11 are based on the performance of a Gravel aggregate concrete

with a water/cement ratio of 0.6. The age of the concrete on testing was approximately 28 days.

Figure 9.11 suggests that heating rate effects the occurrence of aggregate spalling in a linear manner, with an increase in the rate of heating increasing the number of aggregate splits. This effect is limited, however, at both the upper and lower extremes.

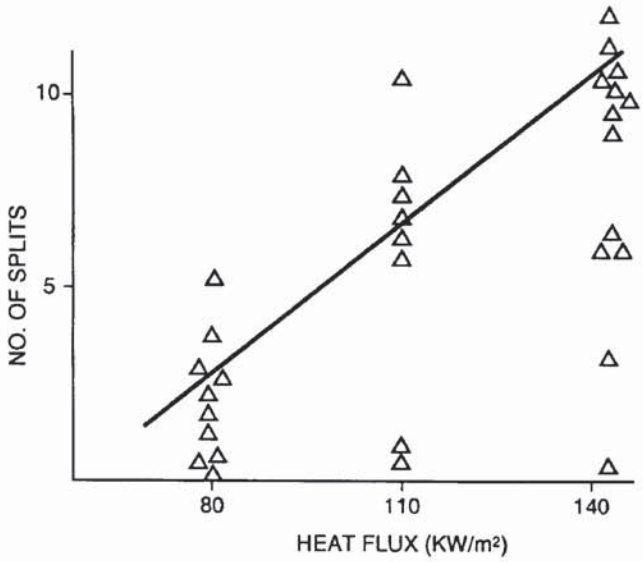

Figure 9.11 Effect of heating rate on splitting

At the lower extreme, there is clearly a threshold rate of heating, beneath which no spalling takes place. For the concrete examined, this appears to be in the order of 70 kW/m^2. At the other extreme, there is some maximum amount of spalling which can occur. This maximum is related to the size of the specimen, the grading of the aggregate within the mix and the number and size of aggregate particles at the concrete surface (surface aggregate topography).

An increased percentage of aggregate fines reduces the number of larger aggregate particles close to the surfaceand this in turn reduces the maximum amount of spalling that can occur. This effect has been confirmed by practical observations during the tests reported in Chapter 6. There is an element of probability associated with this effect, which may also be influenced by the manner in which the concrete is prepared, placed and compacted.

It was observed that concretes made with Gravel aggregates did not split when exposed to the BS.476:Part 20: 1987 standard heating regime. Some splitting of Gravel aggregate concrete did occur in the standard furnace environment, but only in those areas of the specimen that had been subjected to direct flame impingement and had suffered from particularly high local heating rates.

9.4.2.3 Effect of water/cement ratio

The effect of water/cement ratio is shown in Figure 9.12 for Gravel aggregate concrete exposed to a heating rate of 140 kW/m^2. There is no obvious relationship between the w/c ratio and the occurrence of spalling. The mixes in all cases were similar and the free water content was the only variable.

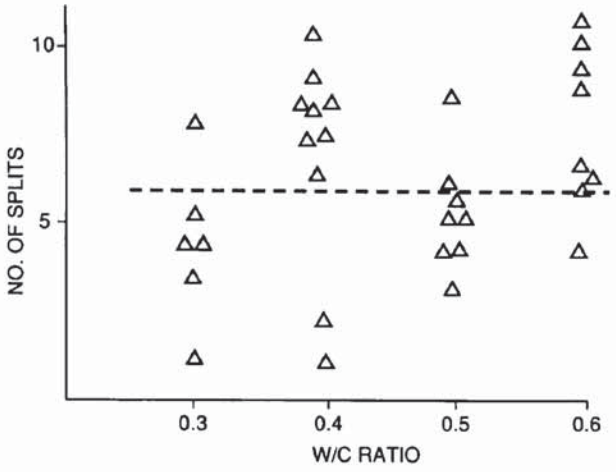

Figure 9.12. The effect of w/c ratio on splitting

It is reasonable to expect that the number of larger aggregates close to the surface would have been reasonably similar for each of the different concretes examined. It may well be that the differences observed in behaviour were associated more with the probabilistic effects of surface aggregate topography rather than any change in the w/c ratio.

9.4.2.4 Effect of applied load

The effect of applied load on the occurrence of aggregate spalling is shown in Figure 9.13. As with w/c ratio, there is no apparent relationship between the load acting on the concrete specimen and its susceptibility to aggregate spalling.

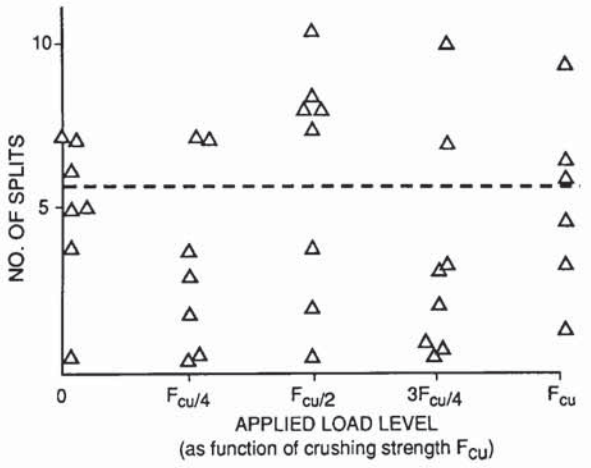

Figure 9.13. The effect of applied load on splitting

9.4.2.5 Effect of age

The susceptibility of concrete to aggregate spalling is reduced with increased age. As Figure 9.14 shows, older concretes are less susceptible to splitting than their younger equivalent. All the

concrete studied was made using Gravel aggregate and was heated by an incident flux of 140 kW/m^2. As concrete strength has been shown to be of little importance with respect to aggregate splitting (Section 9.4.2.3) the influence of age most probably is in its effect on the moisture content of the concrete.

As concrete ages, its moisture content gradually reduces from its high initial level to a steady state value. The rate of reduction depends on the nature of the concrete and the environment to which it was exposed. Figure 9.14 also shows the measured moisture content of a typical concrete specimen and its variation with time. There is a correlation between the degree of splitting and the concrete moisture content. While the susceptibility to splitting is reduced dramatically over the first 3 months after casting, it changed relatively little in the following 9 months. This correlates directly with the rate of drying of the concrete.

The importance of the free moisture content was confirmed by artificially wetting older concretes. A number of 12 month old concrete specimens were submerged in water for 7 days. In this manner their moisture contents were raised from 3 to 7.5 %. As may be seen in Figure 9.14, the soaked specimens suffered a similar degree of aggregate splitting to the younger specimens that had been tested between 1 and 3 months after casting.

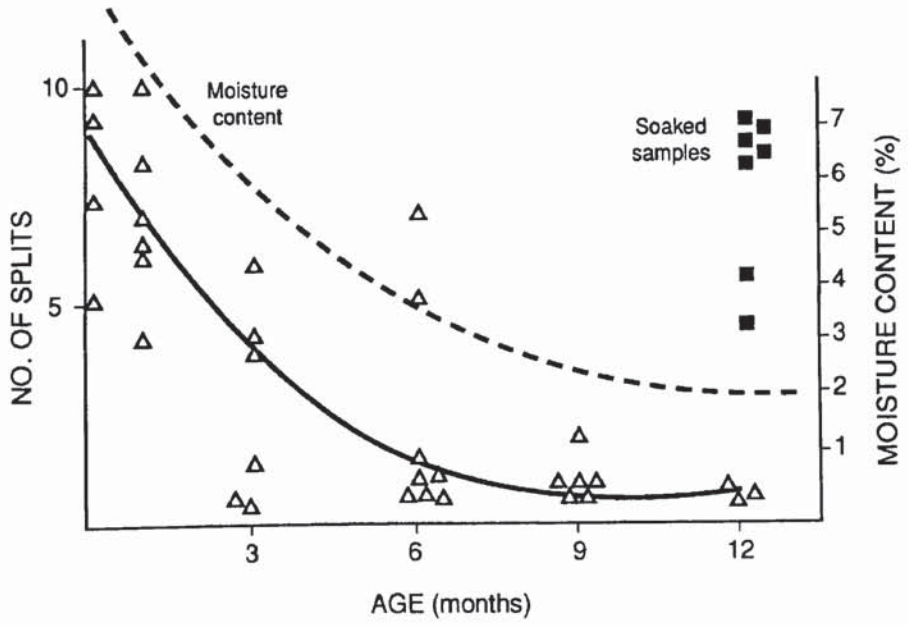

Figure 9.14. The effect of moisture on aggregate splitting

The concept of a threshold moisture content for aggregate splitting as suggested by Figure 9.14 is not new. Although, discussing spalling and not necessarily aggregate splitting, both Meyer-Ottens (1972) and Christiaanse *et al.* (1972) suggested that there is a threshold moisture content for concretes below which no spalling may occur. They both suggested a value for 4%, which is reasonably similar to the moisture content of the 3 month old concrete specimens tested in this programme.

Figure 9.14 also correlates well with American experiences of spalling, where fire resistance test procedures demand that concrete specimens not be tested until their relative humidity drops to 75% at mid-depth of the test specimen. Tests undertaken by Christiaanse *et al.* (1972) have shown that at 75% relative humidity the moisture content was approximately 3.5% in typically sized concrete fire test specimens. Figure 9.14, thus, support the perceived rarity of spalling in the U.S.A. as reported in an international survey (Malhotra, 1972).

9.4.2.6 Effect of aggregate type

Although the experimental programme concentrated on concrete made with Gravel aggregates, several other concretes were examined. Table 9.10 lists the different concrete mixes that were studied.

Concrete	Coarse	Fines	w/c ratio
I	Gravel	Gravel	0.3 - 0.6
II	Granite	Gravel	0.6
III	Lytag	Gravel	0.6
IV	Gravel	Lytag	0.6
V	Lytag	Lytag	0.6

Table 9.10 Variety of concretes examined

The concretes listed in Table 9.10 were subjected to a total heat flux of 150 kW/m^2 by positioning the specimens in front of a gas-fired radiant panel. This generated surface heating rates of 80°C per minute over the first 5 minutes. Only Concrete I suffered any splitting.

Similar concrete mixes were subjected to direct flame impingement from gas burners, which imposed surface heating rates of 100° C per minute over the first 5 minutes. Concrete mixes I, II, III and IV suffered from differing amounts of aggregate splitting as quantified in Table 9.11. Mix V did not suffer any splitting which confirmed similar observations by Austin *et al.* (1992).

Concrete	No. of splits	Ranking
I	18	5
II	4	3
III	2	2
IV	10	4
V	0	1

Table 9.11 Extent of aggregate splitting for a variety of concretes

9.4.3 DISCUSSION OF AGGREGATE SPALLING IN CONCRETE

It is clear that all concretes may suffer from aggregate spalling given suitable conditions, including sufficiently high heating rates and free moisture contents. The nature of the surrounding cement matrix is also important.

Concretes made with Lytag and Granite aggregate require particularly unfavourable conditions before they suffer from spalling. Both aggregates do split within a surrounding Gravel cement matrix, on exposure to heating rates greater than 100°C per minute. Concrete made with Lytag and Lytag fines could not be induced to spall. Austin *et al.* encountered similarly exceptional performance from an all-Lytag concrete mix, which required an imposed heating rate of 200° C per minute before suffering only slight splitting.

The experimental programme has shown that concrete made with Gravel aggregate is much more susceptible to aggregate spalling. The susceptibility to spalling reduces with increased age within the first 3 months of casting. Subsequently, its susceptibility to splitting remains reasonably constant and depends on the drying characteristics of the concrete.

For Gravel concrete, the mean number of splits observed per specimen is quite similar for a range of different applied loads and w/c ratios, as may be seen by comparing Figures 9.12 to 9.11. Aggregate spalling is independent of both these parameters.

Gravel concrete, which had been deliberately subjected to very poor compaction (almost to the degree of honey-combing) showed substantially improved resistance to aggregate splitting. A similar effect was observed when using an air-entraining agent, although only a single test was performed. Further examination of these effects is necessary.

The *Thermal Stress Resistance Factor* as defined by Dougill in Equation 9.19 requires definition of the expected heating exposure and as such is specific to particular applications. In order to illustrate the usefulness of Dougill's methodology, *Thermal Stress Resistance Factors* for a range of concrete mixes have been calculated and the results given in Table 9.12. The factors have been calculated for concrete exposed to a heating rate of 30°C per minute, which is a reasonable representation of the heating encountered in the early stages of a fire resistance test.

The thermal properties of the surrounding cement matrix were taken as follows; Poisson's Ratio $\nu_c = 0.2$; Coefficient of Expansion $\alpha_c = 12\text{x}10^{-6}/^\circ\text{C}$ and Young's Modulus $E_c = 35{,}000$ N/mm^2 . The aggregate size was 20mm. Table 9.12 also includes the ranking of observed performance of the aggregates in terms of resistance to splitting, as previously presented in Table 9.11.

Concrete Mix	**T.S.R.F. (Equation 9.19)**	**Predicted Ranking**	**Observed Ranking (Table 9.11)**
I	3.01	4	5
II	3.90	5	3
III	0.34	2	2
IV	-11.25	1	4
V	2.72	3	1

Table 9.12 Predicted behaviour of concrete mixes

Table 9.12 shows that Dougill's method does not accurately predict the behaviour of the different concrete mixes. Neither the excellent spalling resistance of the all-Lytag mix nor the high

susceptibility to spalling of the all-Gravel mix were predicted. A new approach is considered necessary, which is to be developed based upon the successful shear failure model of splitting developed for individual aggregates in Section 9.3.

9.5 NEW MODEL FOR PREDICTING AGGREGATE SPALLING IN CONCRETE

9.5.1 SHEAR FAILURE MODEL

It may be assumed that heated concrete acts as a continuum with respect to temperature as shown in Figure 9.15 allowing the temperature distribution within the aggregate to be calculated using the basic principles of heat transfer into flat plates.

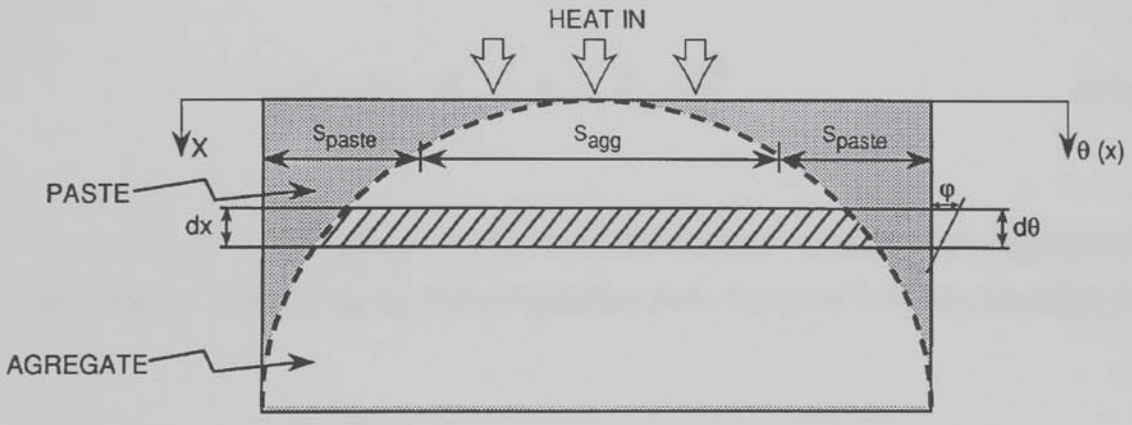

Figure 9.15 Shear development in heated concrete

The temperature at any depth x beneath the surface of a heated concrete can be described by;

$$\theta(x) = \theta_{surface} \left(1 - ERF \frac{x}{\sqrt{4\lambda t}} \right) \tag{9.21}$$

where ERF(u) is the Gaussian Error Function defined by;

$$ERF(u) = \frac{2}{\sqrt{\pi}} \int e^{-\eta^2} d\eta \tag{9.22}$$

Differentiating Equation 9.21 gives the temperature gradient;

$$\frac{d\theta}{dx} = - \frac{\theta surface}{\sqrt{\pi \tau \lambda}} e^{\frac{-x^2}{4\lambda\tau}} \tag{9.23}$$

The negative sign indicates that the temperature reduces with distance from the exposed surface. For typical aggregate sizes (i.e. less than 20mm) and diffusivities (i.e. less than 70 mm^2/min), the temperature gradient is largely governed by the surface temperature and time of exposure and can be approximated by;

$$\frac{d\theta}{dx} = - \frac{\theta_{surface}}{\sqrt{\pi \ \tau \ \lambda}} \tag{9.24}$$

Considering the situation shown in Figure 9.15, with an isothermal plane passing through both the aggregate and surrounding cement paste, the shear strain γ developed across the plane due to thermal incompatibility is given by;

$$\gamma = (\alpha_{agg} \ S_{agg} + \alpha_{paste} \ S_{paste}) \frac{d\theta}{dx} \tag{9.25}$$

where S_{agg} and S_{paste} are the lengths available for the development of shear in the aggregate and paste respectively. Substituting the thermal gradient from Equation 9.24 into Equation 9.25 gives;

$$\gamma = - \frac{\theta_{surface}}{\sqrt{\pi \ \lambda \ \tau}} (S_{agg} \ \alpha_{agg} + S_{paste} \ \alpha_{paste}) \tag{9.26}$$

The relative influence of the aggregate and the paste is a function of depth x from the heated surface. The shear lengths for depths less than R are given by;

$$S_{agg} = 2\sqrt{2 \ R \ x - x^2} \tag{9.27}$$

$$S_{paste} = n\ S_{agg}\ , \quad where \quad n = \left\{ \frac{R}{\sqrt{2\ R\ x\ \ x^2}} - 1 \right\} \tag{9.28}$$

Combining Equation 9.26 with Equations 9.27 and 9.28 the development of shear stresses across the concrete can be described by;

$$\gamma = - \frac{\theta_{surface}}{\sqrt{\pi\ \lambda\ \tau}} \left\{ S_{agg}\ (\alpha_{agg} + n\ \alpha_{paste}) \right\} \tag{9.29}$$

In order to simplify further analysis it is assumed that splitting occurs at a depth of *R/2* from the heated surface. This assumption is based on experimental observations of both this author and Dougill (1972a). Inputting $x = R/2$ into Equations 9.27 and 9.28, allows Equation 9.29 to be rewritten in more definite terms;

$$\gamma = - \frac{\theta_{surface}\ R}{\sqrt{\pi\ \lambda\ \tau}} (1.7\ \alpha_{agg} + 0.3\ \alpha_{paste}) \tag{9.30}$$

It is immediately clear that although thermal expansion of the cement paste has a role to play in the development of splitting stresses, the dominant variable is the thermal expansion of the aggregate. This confirms a previous proposal by Khoury, Sullivan and Grainger (1986), who observed that on first heating the thermal stability of the aggregate is the dominant parameter in determining material response.

The relative thermal movements of cement paste and aggregate are shown in Figure 9.16. In general, a cement paste expands up to a temperature of 100°C, after which it contracts as it loses both its free

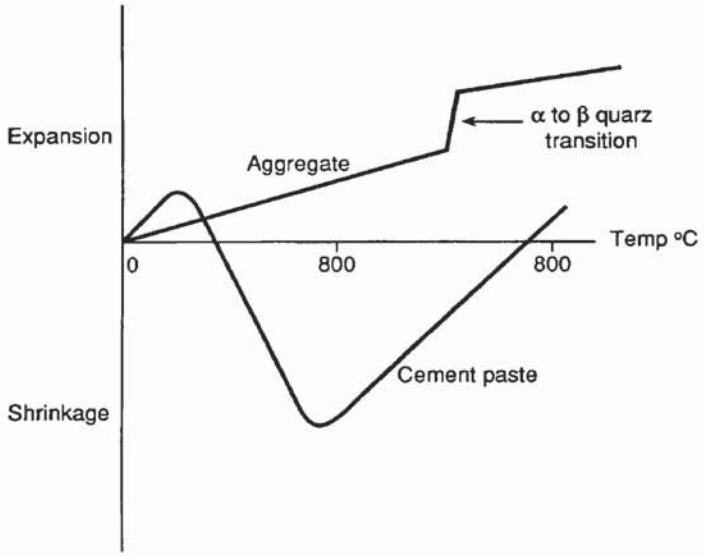

Figure 9.16 Thermal movement of aggregate and paste

water and the moisture held within its hydrated mineral constituents. Contraction of the cement paste between 100 and 400°C reduces the shear stresses acting on the aggregate resulting in an overall reduction in susceptibility to spalling. Thus, aggregate splitting is not to be expected in the range of temperatures where the cement paste is contracting. This agrees with Dougill (1972a), although he based his view on the reduction in tensile stresses within the aggregate sphere that would result from shrinkage of paste contraction.

It is difficult to assess the criterion on which to evaluate the capacity of concrete to sustain such shear strain. One possible approach is to use some basic relationships, which hold for concrete when viewed at the macro-level and to apply them at the micro-level. Adopting such an approach gives a shear capacity $\gamma_{capacity}$;

$$\gamma_{capacity} = \frac{2\ (1 + \nu)\ F_{tensile}}{E_{concrete}} \tag{9.31}$$

This relationship may be converted to a more practical format using the following simple relationships provided by Neville (1981);

$$F_{tensile} = 0.3\ (F_{cylinder})^{0.66} \tag{9.32}$$

$$F_{cylinder} = 0.8\ F_{cube} \tag{9.33}$$

$$E = 4.7\ x\ 10^3\ \sqrt{F_{cylinder}} \tag{9.34}$$

where; $F_{cylinder}$ = compressive strength of cylindrical concrete specimen (N/mm^2)
F_{cube} = compressive strength of cubic concrete specimen (N/mm^2)

Using Equations 9.32 to 9.34 the shear capacity of concrete may be expressed as;

$$\gamma_{capacity} = 4.7\ x\ 10^{-4}\ (F_{cube})^{0.16} \tag{9.35}$$

The applicability of Equation 9.35 is undoubtedly open to question. It predicts values of shear strain at failure that are much lower than those observed in tests by Neville. However, there is

no unique definition of failure for concrete and this could explain some of the difference. In addition, Equation 9.35 is based on a macro-view of concrete, whereas spalling is a local occurrence.

It is quite conceivable that a more realistic failure criterion could be derived from the stiffness and strength of the aggregate and the paste apportioned in accordance with their relative presence near the surface. However such efforts are considered unnecessary because the occurrence of spalling is influenced more by the potential development of shear strain (given in Equation 9.31) rather than the capacity of concrete to sustain it, which does not vary to the same extent.

The experimental work reported in Section 9.4.2.3 has shown this to be the case. Spalling was observed with equal frequency for concretes ranging in compressive strength from 40 to 70 N/mm^2. Thus, the very weak dependence of shear capacity on cube strength suggested by Equation 9.35 appears to accurately reflect the experimental results and is sufficiently useful for current purposes.

The propensity of any particular concrete mix to aggregate spalling may be evaluated by calculating the shear strain likely to be developed under heating (using Equation 9.30) and comparing it to the shear capacity of the concrete (as given in Equation 9.35).

9.5.2 CORRELATION WITH OBSERVED BEHAVIOUR

The shear strains developed in a range of concretes on exposure to a surface heating rate of 30°C/min over 15 minutes have been predicted using Equation 9.30. The thermal diffusivities of normal-weight and light-weight concretes have been taken as 0.8 and 0.4 mm^2/s (after Schneider, 1985). The strains predicted are shown in Table 9.13 together with the shear capacities of each concrete mix.

The Table also includes the observed ranking of the different concrete mixes, previously presented in Table 9.11. It is immediately clear from Table 9.13 that the shear failure model is superior to the previous approach suggested by Dougill (1972a), with the newly predicted ranking of all concrete mixes being accurate.

Concrete (see Table 9.9)	λ (mm^2/s)	$\alpha_{aggregate}$ ($x10^{-6}/°C.$)	α_{paste} ($x10^{-6}/°C.$)	γ $x10^{-3}$ (Equation 9.30)	Predicted Ranking	Observed Ranking
I	0.833	10.8	12.0	2.0	5	5
II	0.833	7.5	12.0	1.5	3	3
III	0.416	2.0	12.0	0.9	2	2
IV	0.833	10.8	4.0	1.8	4	4
V	0.416	2.0	4.0	0.6	1	1

Table 9.13. Ranking of thermal stability of concrete mixes using the shear failure approach

Equations 9.30 and 9.35 were also used to evaluate the influence of heating rate on the occurrence of aggregate spalling in a C40 Thames Valley Gravel concrete. The susceptibility to spalling was evaluated after 15 minutes heating. It was assumed that the concrete had a maximum aggregate size of 20mm, a thermal diffusivity of 0.8 mm^2/s and coefficients of expansion for the Gravel and the surrounding paste were $10.8x10^{-6}$ / °C and $12x10^{-6}$ /°C respectively.

The predicted behaviour compares favourably to that observed during the practical experiments reported in Section 9.4. As may be seen from the results given in Table 9.14 there was good correlation between predicted and observed behaviour.

Heating Rate (kW/m^2)	$\theta_{surface}$ (°C) as measured	γ x 10^{-4} (Equation 9.30)	$\gamma_{capacity}$ x 10^{-4} (Equation 9.35)	Predicted behaviour	Observed behaviour
80	90	4.2	8.5	no splitting	no splitting
110	240	11.1	8.5	splitting	splitting
140	350	16.2	8.5	splitting	splitting

Table 9.14. Predicted effect of heating rate on occurrence of splitting

The predicted behaviour in Table 9.14 has been calculated assuming a maximum aggregate size of 20mm. The susceptibility of concrete made with smaller aggregates to spalling can be easily derived by considering the ratio of developed to sustainable shear, giving the size of aggregate susceptible to splitting as $R \times (\gamma_{developed}/\gamma_{capacity})$. Thus, Gravel concrete heated at 110 kW/m^2 has

its aggregate in the size range 20 to 15 mm susceptible to spalling and at 140 kW/m^2 aggregate sizes 20 to 10 mm become susceptible. This approach explains why there is more spalling with high heating rates, but suggests that the actual amount is a function of the aggregate's grading.

As has been discussed in Section 9.4.2, the susceptibility of concrete to aggregate spalling is reduced with age. It has been concluded that this is due to the drying out of concrete with time, thus confirming the importance of free moisture content. In fact, the shear failure model of aggregate splitting predicts such behaviour. Mitchell (1953) provided details of the variation of the coefficient of thermal expansion of cement paste with its apparent saturation and his findings are reproduced in Figure 9.17.

These data suggest that the coefficient of thermal expansion varies from between 12 and 20 x 10^{-6}/°C with relative pore saturation. Although, the influence of the paste is secondary to that of the aggregate, such relatively large changes in its coefficient of expansion could increase the shear developed in an all-Gravel concrete, subjected to 140 kW/m^2 by about 26%, reducing the aggregate size susceptible to spalling from 10 to 8 mm.

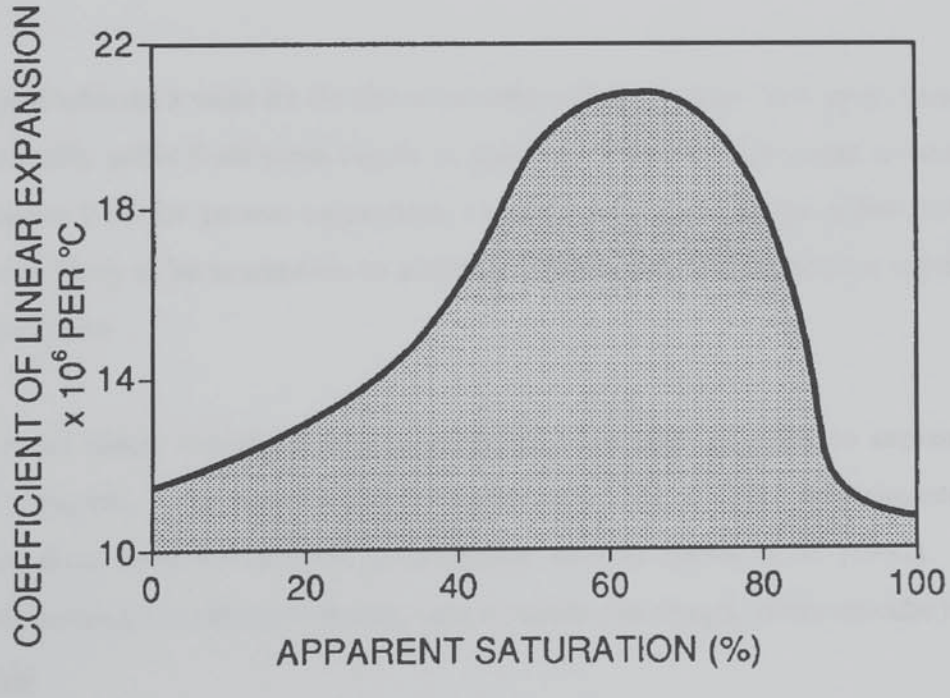

Figure 9.17 Variation of coefficient of expansion with relative pore saturation (after Mitchell, 1953)

9.6 OVERALL CONCLUSIONS REGARDING AGGREGATE SPALLING

A review has been undertaken of the various mechanisms that have been put forward by other researchers to explain aggregate spalling. An experimental programme provided evidence that these models of aggregate spalling were inaccurate. It was observed that all concrete can be susceptible to splitting under certain exposure conditions, although concretes containing certain aggregates are more susceptible than others.

A new model has been proposed to explain the splitting of individually heated aggregates. It is proposed that aggregate splitting is a form of shear failure which results from the thermal incompatability within non-uniformly heated aggregates. The model was validated against an extensive range of experimental data. Accordingly, it is proposed that the thermal stability of individual aggregates may be assessed by evaluating the parameter

$$\left(\frac{\alpha}{\lambda}\right)\left(\frac{E_{aggregate}}{F_{split}}\right) m.R^2 \qquad (9.36)$$

If an aggregate achieves a value for the above parameter that is higher than unity, then on heating it would probably suffer from some degree of splitting. Some caution needs to be exercised in using Equation 9.36 for porous aggregates, i.e. with absorption values above 3.0%, as such aggregates are likely to be susceptible to additional destructive forces from the vapourisation of contained moisture.

The basic shear failure model for aggregate splitting has been extended to explain aggregate spalling in concrete. The new model correlates well with available experimental data and observations from previous research programmes, such as Austin *et al.* (1992). The model predicts with accuracy the effects of heating rate, concrete mix design, concrete cube strength and specimen age.

The new model predicts the shear stress that can be generated in heated aggregates (using Equation 9.30) and compares it to the shear capacity of the concrete (calculated using Equation 9.35). Both Equations may be combined to give a new *Thermal Stress Resistance Factor*.

$$T.S.R.F. = \frac{\frac{\theta_{surface}\, R}{\sqrt{\pi\ \lambda\ \tau}}\ (1.7\ \alpha_{aggregate} + 0.3\ \alpha_{paste})}{4.7\ x\ 10^{-4}\ (F_{cube})} \qquad (9.37)$$

Aggregate spalling is likely to occur for concretes that have a value of the *TSRF* above unity.

Equation 9.37 has been validated against a wide range of different concrete mixes. Concretes made with Thames Valley Gravel are the most susceptible to splitting, whilst those made with Lytag aggregate are the least susceptible. Concrete made with Lytag fines are less susceptible to aggregate spalling than those made with ordinary siliceous river sand. The inherent susceptibility of concrete made with Gravel aggregate to spalling may be reduced by incorporating Lytag fines.

The most influential parameters in determining the susceptibility of concrete to spalling are the heating rate and the coefficients of thermal expansion of the coarse and fine aggregates. The moisture content of the concrete is also important, with susceptibility to spalling much reduced in concretes that have moisture contents less than 4% (by weight), which generally correlates with a specimen age of 3 months. Concrete strength and applied load does not have any effect on the occurrence of aggregate spalling.

Aggregate size is also an important parameter with concretes made using larger aggregates being more susceptible to spalling. There appears to be a threshold aggregate size, beneath which splitting is unlikely. This threshold depends on the design environment considered, but for Thames Valley Gravel generally is around 10 mm. Thus, to avoid aggregate spalling in heated concrete, the maximum size of Thames Valley Gravel used should be limited to 10 mm.

In conclusion, Equation 9.37 may be further simplified to give a simple and useful parameter for comparing the relative thermal stability of different concrete mixes;

$$\frac{R}{\sqrt{\lambda}}\ (1.7\alpha_{aggregate} + 0.3\alpha_{paste}) \qquad (9.38)$$

CHAPTER 10. CORNER SPALLING

10.1 NATURE OF CORNER SPALLING

Corner spalling involves the gradual disintegration of heated concrete and occurs at the corners or arrises of concrete members such as beams or columns. It is also referred to as corner separation or sloughing-off, because of its progressive nature. An example of corner spalling is given in Plate 10.1.

Corner spalling results from a completely different mechanism to surface and explosive spalling. Although both surface and explosive spalling may originate at the arrises of concrete members, surface and explosive spalling are differentiated from corner spalling by their violent nature.

Not only is corner spalling a more gradual and gentle failure, it also manifests itself as the removal of a small number of large pieces of concrete, whereas surface spalling removes many more smaller sized pieces of concrete. The various forms of spalling can be further differentiated by considering the time at which they occur during the standard fire resistance test (BS 476:Part 20:1987).

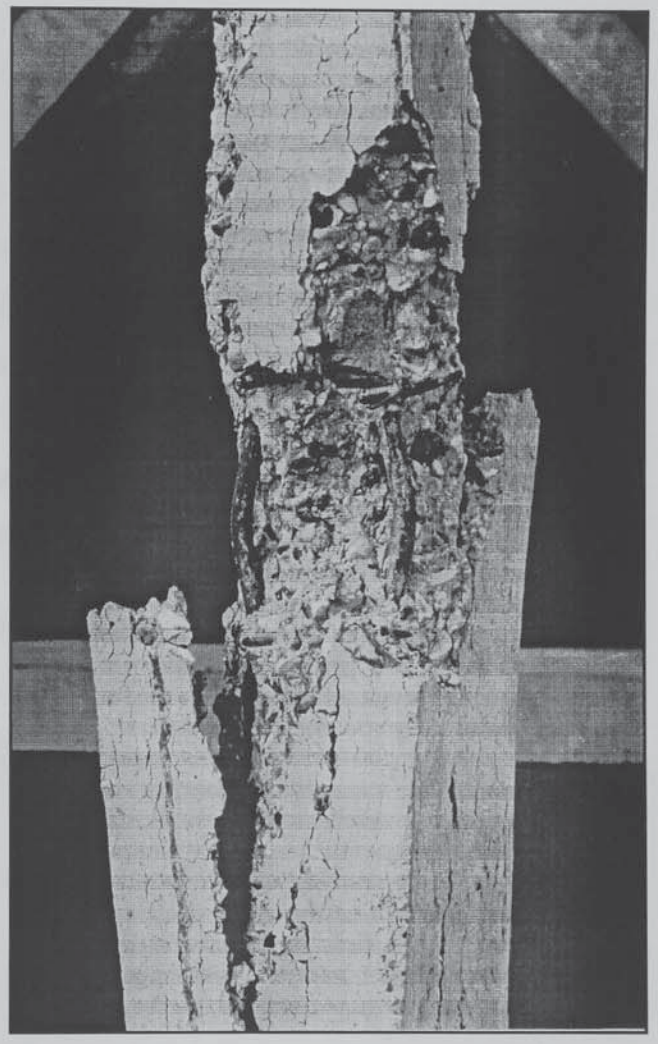

Plate 10.1 Corner spalling

It is widely agreed (Malhotra, 1984) that both surface and explosive spalling take place within the first thirty minutes of heating. Corner spalling occurs later than this and is generally considered more likely between 30 and 60 minutes. Corner spalling can have particularly serious consequences for the fire resistance of structural concrete members because the removal of large

amounts of concrete from the arrises can expose the steel reinforcement to higher temperatures thus promoting failure. Such effects are exacerbated in members subject to flexural loading.

This Chapter presents a number of possible mechanisms of corner spalling, including those discussed by Dougill (1971). The objective of this Chapter is to outline the variables that have the most effect on corner spalling, so they may be considered in subsequent discussions on suitable protection measures and design guidance on spalling in general.

10.2 MECHANISM OF CORNER SPALLING

As discussed in Chapter 3, the thermal stresses induced in a cylindrical column heated at its surface are compressive in both the tangential and longitudinal directions. However, in the radial direction the stresses are tensile and this fact may be used to explain corner spalling. By considering a prismatic column to contain a central "virtual" cylindrical rod as illustrated in Figure 10.1, it is possible to visualise how corner spalling may be a consequence of tensile stresses developed at the circumference of the virtual rod. The radial stresses σ_r developed in a solid rod heated at its circumference were calculated by Timoshenko (1934) as;

$$\sigma_r = \alpha E \left(\frac{1}{R^2}\int \theta\, r\, dr - \frac{1}{r^2}\int \theta\, r\, dr \right) \qquad (10.1)$$

where;

R = radius of rod
r = distance from centre
E = Modulus of Elasticity
θ = temperature
α = Coefficient of Expansion

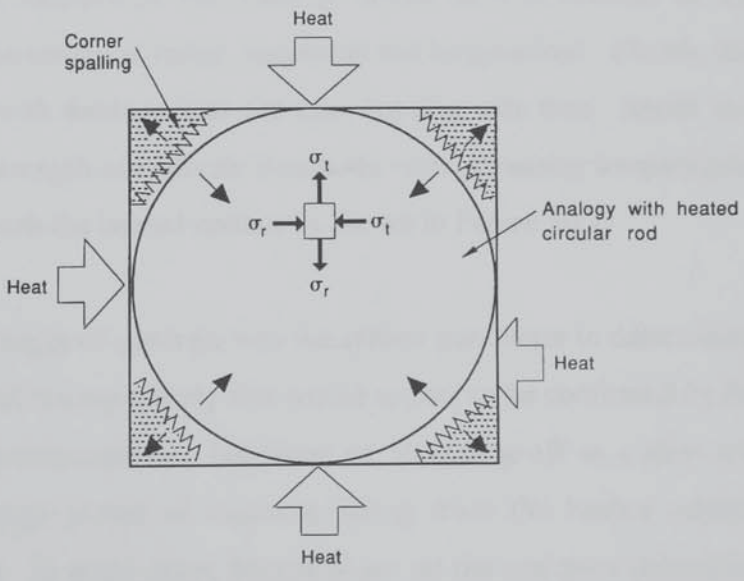

Figure 10.1 Column with virtual rod

Corner spalling is, as the name suggests, specific to the corners of square or rectangular columns and the arrises of beams. Dougill proposed the scenario shown in Figure 10.2 which gi es the distribution of temperature and radial stress in the plane that bisects a heated corner of infinite extent. The boundary conditions demand that the stresses are zero at the boundary and increase to a peak tensile alue before decreasing back to zero at large distances from the corner.

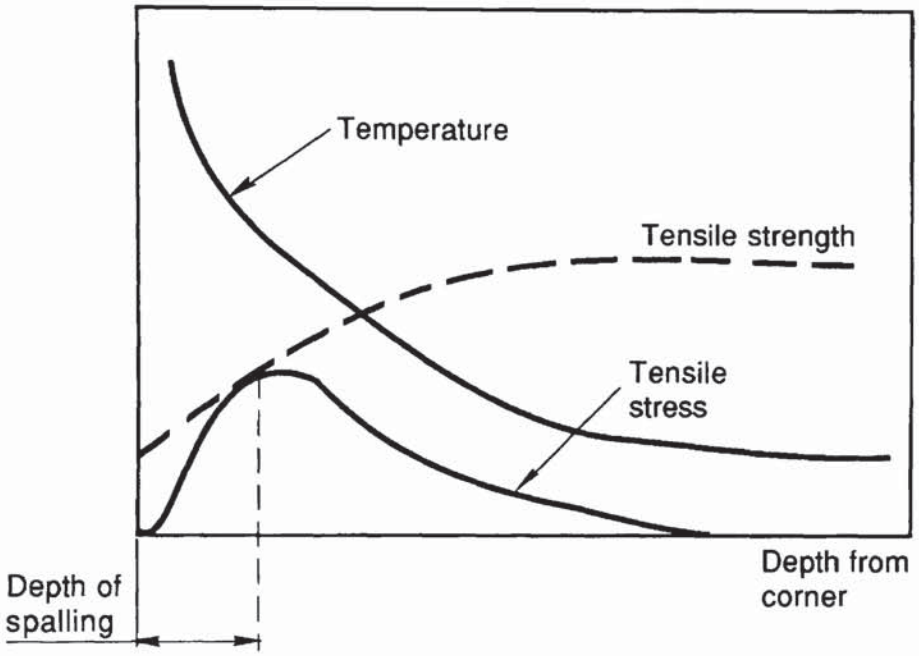

Figure 10.2 Temperature and stress de elopment at heated corner

It is difficult to ascertain the exact location of the plane of failure as it is decided by the combination of a tri-axial system of stresses, i.e. radial, tangential and longitudinal. Clearly, the combined stress state aries not only with distance from the apex but also with time. Intuiti ely, howe er, assuming that the tensile strength of concrete decreases with increasing temperature, failure will occur some distance beneath the heated surface as shown in Figure 10.2.

Dougill concluded that the tensile strength of concrete was the critical parameter in determining its susceptibility to corner spalling and retrospecti ely this would appear to be confirmed by the work of Morris (1972, personal communication). He obser ed sloughing-off as a slow and progressi e form of failure with large pieces of concrete falling from the heated corners apparently under their own self-weight. In many cases, Morris obser ed the complete debonding of a length of concrete from the corner's of columns, but the corner remained intact due to localised areas of aggregate-aggregate interlock.

Earlier work by Norton (1968), who studied the spalling of refractory bricks, confirmed the slow progressive failure with a gradual release of energy as a typical manifestation of tensile failure mode.

The importance of tensile strength may be deduced from an intuitive examination of the processes taking place in a heated column. Quite apart from the global stresses generated within the member to satisfy Equation 10.1, there are many local mechanisms for tensile failure of concrete. Bascoul *et al.* (1989) observed the microcracking of heated concrete members in directions orthogonal to the temperature gradient. Such cracks would be reduced in the immediate vicinity of the actual corner because of the reduced temperature gradient encountered and as shown in Figure 10.3 this could explain the sloughing-off of relatively large amounts of concrete.

In a heated column, the expansion of the outer layers is partially restrained by an internal cooler concrete core. Figure 10.3 shows some of the mechanisms acting at the corners of a heated column. Thus, thermal expansion imposes a thrust on the corners of the column, which are in a particularly weakened state because of their high temperatures.

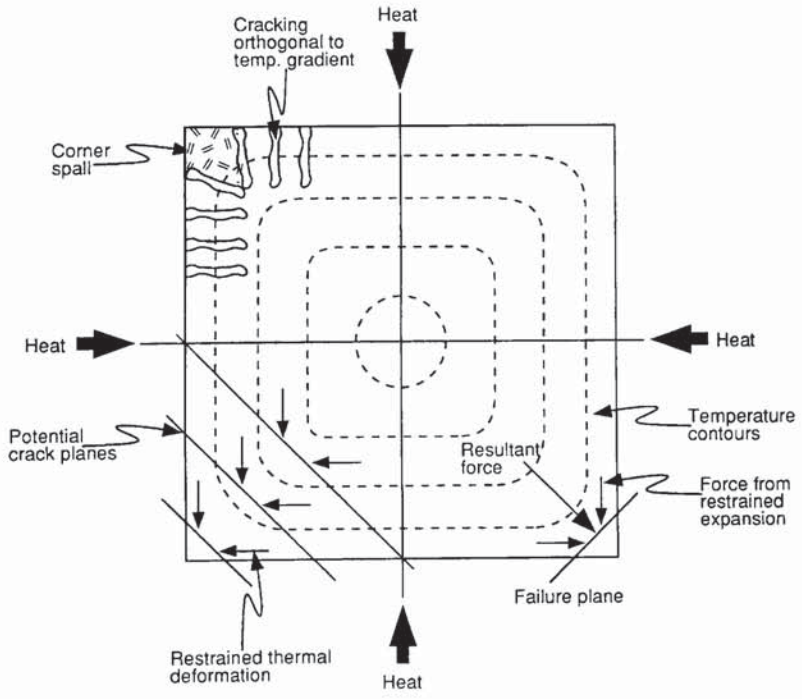

Figure 10.3 Mechanisms acting at corners of heated column

Studies of the reduction in the tensile strength of concrete at elevated temperatures provides more corroboration for the mechanism proposed for corner spalling. The work of Zoldners (1960) and Sullivan and Poucher (1971) provided some information on the effect of temperature on the flexural strength of concrete. However, Thelandersson (1971) presented information directly on the effect of temperature on the tensile strength of concrete as measured by the splitting test as given in Figure 10.4.

Figure 10.4 Reduction in tensile strength of concrete with temperature (Thelandersson, 1971)

The peak rate of loss of tensile strength with temperature shown in Figure 10.4 correlates well with the temperatures at which corner spalling has been observed in standard fire resistance tests. Morris (1972, personal communication) observed that spalling took place reasonably consistently between 30 and 60 minutes.

Figure 10.5 shows the contours of temperature that could be expected in a concrete column heated in accordance with ISO 834:1987 (after CEB, 1991). Combining information from Figures 10.4 and 10.5 shows Morris' observations on corner spalling correlate with concrete temperatures around 700° C and associated tensile strengths of roughly 20% of their ambient temperature value. There seems little doubt but that corner spalling is the result of tensile failure of concrete.

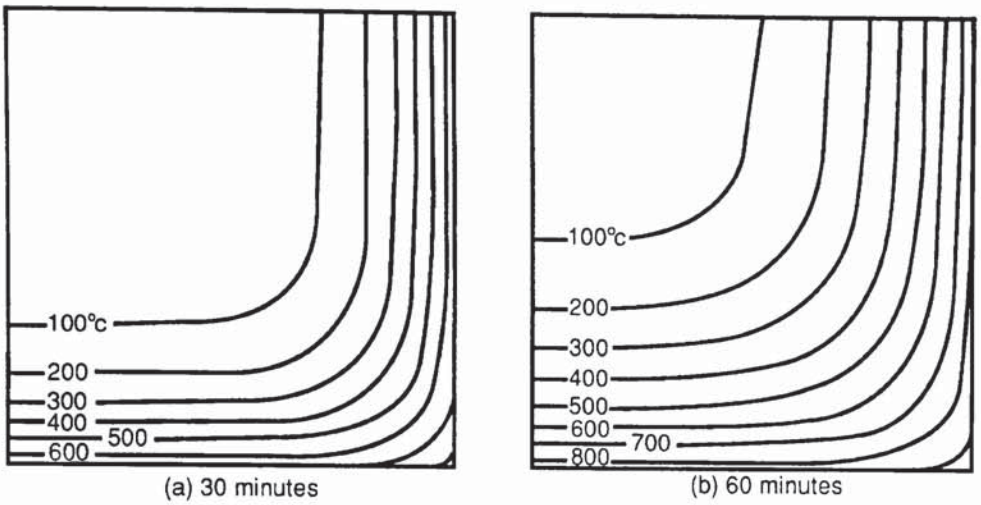

Figure 10.5 Temperature contours in concrete columns subjected to durations of heating to ISO 834:Part 1:1987 heating (after CEB, 1991)

Furthermore, Thelandersson found that the loss of tensile strength was not influenced by the rate of heating. Similarly corner spalling appears to be governed by the actual temperatures in the concrete rather than the rate of heating. This is demonstrated by the fact that slowly heated concrete, with low temperature gradients, still crumbles and sloughs-off at high temperatures.

It has been suggested by some researchers (Dougill, 1971; Sertmehemetoglu, 1977) that bursting effects due to heated reinforcement is also a contributory factor to corner spalling. This may well be the case, but Norton's (1968) observation of spalling in (unreinforced) refractory bricks and the relatively slight difference between the Coefficient of Expansion of steel and concrete would suggest that this mechanism has limited effect. Reinforcement could be influential, however, as premature fracture of the bond around the steel may provide a plane of weakness which could facilitate development of the cracks across the corner.

Malhotra (1984) observed a reduced incidence of corner spalling amongst concrete made with Lytag, crushed brick and to a lesser extent Limestone aggregates. This may be explained by their reduced coefficients of expansion, which would tend to minimise the global stresses generated by temperature gradients across the heated section. Furthermore, the reduced conductivity of concretes made with these aggregates keeps temperatures lower and delays strength loss. In fact, Zoldners (1960) observed a reduced rate of tensile strength loss amongst concretes made with lightweight aggregate. A similar reduced strength loss could be expected for crushed or angular aggregates because of improved aggregate to paste bond and aggregate interlock.

10.3 DISCUSSION OF CORNER SPALLING

Corner spalling is generally considered to be an inevitable consequence of exposing concrete to prolonged durations of heating. It is the natural manifestation of tensile strength loss at high temperatures and the complete degradation of bond between the aggregate and the cement matrix.

Measures to alleviate the consequences of corner spalling have concentrated on protection rather than prevention. Malhotra (1972) suggested that provision of supplementary reinforcing mesh within the depth of the concrete cover effectively reduces the amount of concrete that may be lost on spalling due to the physical retention of the weakened concrete by the steel mesh.

The provision of a supplementary reinforcement mesh was recommended by the Institution of Structural Engineers and the Concrete Society (1978) for concrete with cover depths greater than 40 mm. However, such reinforcement mesh may be difficult to place on site and can cause problems at connections. Furthermore, cover requirements for durability may conflict with the need to place the mesh within 20 mm of the concrete face. Supplementary reinforcement does not represent an ideal solution to the problem.

The mechanism of corner spalling proposed earlier in this Chapter would suggest that there are two possible approaches to its prevention. In the first instance the concrete could be designed so as to have a minimal coefficient of thermal expansion. This could be achieved by using particular aggregates and would have the effect of reducing the global tensile stresses predicted by Equation 10.1. The outcome of such an approach would most likely be the increase in the concrete temperatures necessary for spalling or in effect an increase in fire resistance. However, local destructive mechanisms such as loss of aggregate bond would still be possible and the absence of sloughing-off could not be guaranteed. The guidance given in Chapter 9 regarding the assessment of the thermal stability of aggregates is also appropriate for corner splitting.

A second and more desirable approach to prevention of corner spalling would be to increase the tensile strength of the concrete. In theory, this could be achieved by using a higher grade of concrete but in practice the gain in tensile strength is minimal and as outlined in Chapter 7 other problems may occur with regards to explosive spalling.

Alternative means of achieving higher tensile strengths for concrete through mix design could be investigated. One might consider intuitively that a reduction in the aggregate to cement ratio would improve the tensile strength, although a cursory examination by Thelandersson (1971) showed that the benefits were limited. The angularity, surface texture and grading of the component aggregates are also factors which could effect the elevated temperature tensile strength of concretes. Some research into mix design and tensile strength of concrete could prove fruitful in enhancing the fire resistance of columns.

Artificial means of increasing the tensile strength of the concrete such as implantation of steel or glass fibres could be considered. Low melting temperature polypropylene fibres such as those examined in Chapter 7 for the treatment of explosive spalling would not be suitable, as high temperature tensile strength is required. Although, steel or glass fibres represent a reasonable preventative measure, they could be difficult to mix evenly on-site. However, once placing and compacting issues were resolved, they might be an option for ready-mixed concrete. In a similar manner, factory conditions may make fibres a suitable form of protection for the arrises of precast concrete beams, particularly if they could be placed locally to the arrises.

10.4 CONCLUSIONS

Corner spalling is the natural degradation of concrete due to loss of tensile strength at high temperatures. It may be alleviated by using concrete with a low coefficient of thermal expansion or a low value of thermal conductivity. Corner spalling can be prevented by using concretes which can maintain a reasonable tensile strength at high temperatures. Concrete made with lightweight aggregate satisfies all the above criteria and accordingly is reasonably resistant to corner spalling. Further research is necessary to ascertain whether other concretes can have their resistance to corner spalling improved by increasing their tensile strength through mix design or by artificial means such as addition of fibres.

CHAPTER 11 CONCLUSIONS

Spalling at elevated temperatures can significantly reduce the fire resistance of concrete constructions and consequently the factors that influence the occurrence of spalling are of interest for structural fire safety design.

The unexpected damage caused to a concrete construction by spalling can render fire safety design calculations inaccurate and lead to significantly reduced levels of safety for concrete structures in the event of fire. The inability to predict the occurrence of spalling has been a limiting factor in the development of robust models of the response of concrete structures to fire.

This Thesis has suggested that spalling can be categorised as;

(i) Surface spalling
(ii) Explosive spalling
(iii) Aggregate spalling
(iv) Corner spalling

Each category of spalling has its own causative factors which have been identified. It has been shown that many of these factors exert opposing influences on the different types of spalling, thereby explaining much of the confusion that has existed regarding spalling.

11.1 SURFACE SPALLING

Surface spalling is the result of pore pressures beneath the heated concrete surface exceeding the material's strength. Thus, the factors which increase the susceptibility of a concrete to surface spalling are those which tend to increase the magnitude of the pore pressures which can be developed on heating. Such factors include increased rate of heating, increased pore saturation and reduced permeability. The resistance of concrete to surface spalling is largely a function of its tensile strength.

Many of the factors that affect surface spalling tend to vary locally at a concrete's surface due to variables such as degree of compaction and size and position of aggregates. Therefore, the actual locations at which surface spalling may occur are subject to an element of randomness. However, an empirical failure envelope has been produced (Figure 8.5) to allow the susceptibility of a concrete to surface spalling to be evaluated from a knowledge of the concrete's tensile strength and the pore pressures likely to be developed.

11.2 EXPLOSIVE SPALLING

The factors that influence the explosive spalling of concrete were the subject of an extensive experimental investigation. After examining the response of a number of different concretes to a range of simultaneous heating and loading environments, it was concluded that explosive spalling may result from either of two distinct mechanisms.

11.2.1 PORE PRESSURE INDUCED EXPLOSIVE SPALLING

The development of pore pressures within a heated concrete can result in explosive spalling. The main factors which influence pore pressure development have been identified as concrete permeability, porosity, pore saturation and rate of heating. The material resistance of a concrete to pore pressure induced explosions has been modelled empirically and a correlation established with tensile strength.

The pore pressures developed in heated concretes generally tend to be quite small in magnitude and thus can be easily counteracted by low levels of applied load. Hence, pore pressure induced explosive spalling occurs more frequently in unloaded or lightly loaded concrete members. Explosive spalling was observed more frequently in concretes with lower water/cement ratios, because of their reduced permeability. Small specimens were also more susceptible to spalling because of the relatively high rate at which they can be heated.

11.2.2 THERMAL STRESS INDUCED EXPLOSIVE SPALLING

Explosive spalling may also result from the development of excessive thermally induced stresses within a heated concrete member. The combination of imposed load stresses with those induced by heating can cause violent destructive failure when they exceed the concrete's strength. Experimental evidence has shown that the concretes subjected to lower levels of net effective stress, i.e. the sum of the load and thermally induced stresses less the pore pressure, are not as susceptible to explosive spalling. Similarly, concretes having higher levels of compressive strength do not spall as easily.

However, such concretes tend to be less permeable and therefore more susceptible to pore pressure induced spalling. A balance exists between the load levels needed to resist pore pressure induced spalling and those that can result in stress induced spalling. This balance depends on the likely magnitude of the pore pressures, the degree of thermal expansion expected and the compressive strength of the concrete.

The influence that many parameters exert on the occurrence of spalling may have opposing effects on the different mechanisms of explosive spalling. Therefore, it has been proposed that there is no single set of conditions that define when spalling will occur. Instead, the range of mechanisms that can result in spalling have been identified allowing the relative influence of any single parameter to be assessed within the total context of the concrete's likely behaviour.

This Thesis presents methodologies for assessing the susceptibility of any particular concrete to explosive spalling from either pore pressures or thermal stresses. These methodologies could be incorporated into existing behavioural models, allowing explosive spalling to be considered within the predicted response of a concrete to fire. However, the experimental programme reported in this Thesis has clearly demonstrated the importance of probability associated with explosive spalling. This suggests that development of more definitive models of explosive spalling than those proposed here, could be very difficult. Despite these problems, there is much scope for further work.

11.3 AGGREGATE SPALLING

This Thesis proposes that aggregate spalling is a form of shear failure which results from the thermal incompatibility within non-uniformly heated aggregates. A model for splitting of individual aggregate particles has been developed and validated against an extensive range of experimental data. This basic model of aggregate behaviour was developed to consider the spalling of concrete and a simple and useful parameter defined for comparing the relative thermal stability of different concrete mixes.

The most influential parameters in determining the susceptibility of concrete to aggregate spalling are the heating rate and the coefficients of thermal expansion of the coarse and fine aggregates. Moisture content of the concrete is also important, with susceptibility to spalling much reduced in concretes that have moisture contents less than 4% (by weight), which generally correlates with a specimen age of 3 months. Concrete strength and applied load does not have any effect on the occurrence of aggregate spalling.

Aggregate size is also an important parameter with concretes made using larger aggregates being more susceptible to spalling. A threshold aggregate size was observed, beneath which aggregate spalling was less likely. This threshold depends on the design environment considered, but for Thames Valley Gravel generally is around 10 mm. Thus, to avoid aggregate spalling in heated concrete, the maximum size of Thames Valley Gravel used should be limited to 10 mm.

11.4 CORNER SPALLING

Corner spalling is generally considered to be an inevitable consequence of exposing concrete to prolonged durations of heating. It is the natural manifestation of tensile strength loss at high temperatures and the complete degradation of bond between the aggregate and the cement matrix.

Measures to alleviate the consequences of corner spalling have concentrated on protection rather than prevention, e.g. provision of supplementary reinforcing mesh. The mechanisms of corner spalling proposed in this Thesis suggest that there are two possible approaches to its prevention. In the first instance the concrete could be designed so as to have a minimal coefficient of thermal

expansion, e.g. by using particular aggregates. A second and more desirable approach to prevention of corner spalling would be to use concretes which can maintain a reasonable tensile strength at high temperatures, e.g. concrete made with lightweight aggregate. Further research is necessary to ascertain whether other concretes can have their resistance to corner spalling improved by increasing their tensile strength through mix design or by artificial means such as addition of fibres.

11.5 FURTHER WORK

This Thesis has highlighted the need for further work in many areas. The factors which affect the development of pore pressures in heated concrete specimens are critical in determining its susceptibility to both surface and explosive spalling. However, the actual measurement of these pore pressures in non-sealed concrete specimens has proven very difficult. Closer attention to the design of suitable instrumentation could eliminate the need for indirect measurements of pore pressures and could provide valuable data to correlate pressure models.

Pore pressures are greatly influenced by concrete permeability. The manner in which the permeability of concrete changes at elevated temperatures needs further practical investigation. The influence of load, tensile strength, aggregate type, and effects such as creep need to be examined in the context of pore pressure generation.

This Thesis has highlighted the increased susceptibility of high strength concrete to explosive spalling. Preventive measures such as addition of air-entraining agent or polypropylene fibres have appeared promising, but their usefulness requires further examination. The application of these measures to the prevention of corner spalling could also be studied.

The existence of two different modes of explosive spalling needs to be established further, by undertaking a similar programme of simultaneous heating and loading of concrete specimens, but under lower levels of load. The importance of specimen size also requires further examination, particularly in the context of more severe heating regimes.

REFERENCES

Abrams, M.S. (1971) Compressive strength of concrete at temperatures to 1600F.Special Report SP 25, American Concrete Institute, Detroit, United States, pp 33-59.

Ahmed, G.N. and Huang, C.L. (1990) Modelling of concrete slabs under fire. *Chemical Engineer Communication,* **91**, 241-253 .

Akhtaruzzaman, A.A. (1973) The effect of transient and steady state temperatures on concrete. PhD Thesis, Imperial College, London.

Akhtarruzaman, A.A. and Sullivan, P.J. (1970) *Explosive spalling of concrete exposed to high temperature*. Concrete Structures and Technology Research Report, Imperial College, London.

Anderberg, Y. (1976) *Fire exposed hyperstatic concrete structures - An experimental and theoretical study*. Bulletin 55. Division of Structural Mechanics and Concrete Construction, Lund Institute of Technology, Sweden.

Anderberg, Y. and Thelandersson, S. (1976) *Stress and deformation characteristics of concrete at high temperatures - Experimental investigation and material behaviour model*. Bulletin 54. Division of Structural Mechanics and Concrete Construction, Lund Institute of Technology, Sweden.

Ashton, L.A.and Bate, S.C. (1960) The fire resistance of prestressed concrete beams. *Proceedings of the Institution of Civil Engineers*, **9**, 15-38.

Ashton, L.A.and Davey, N.(1953), Investigations of building fires - Part 5. *National Building Studies Research Paper 12*, HMSO, London.

Austin, S., Robins, P. and Richards, M. (1992) Jetblast temperature resistant concrete for harrier aircraft pavements. *The Structural Engineer*,**70(23/24)**, 427-432.

Bascoul, A.,Ollivier, J. and Poushanchi, M. (1989) Stable microcracking of concrete subjected

to tensile strain gradient. *Cement and Concrete Research,* **19(1)**, 81-88.

Bažant, Z. and Thonguthai, W. (1978) Pore pressure and drying of concrete at high temperatures. *Proceedings of the American Society of Civil Engineers (Journal of Engineering Mechanics Division)*, **104 EM5**, 1059-1079.

Bažant,Z. and Thonguthai, W.(1979) Pore pressure in heated concrete walls - theoretical prediction. *Magazine of Concrete Research,* **31(107)**, 67-75.

Bažant, Z. and Raftshol, W. (1982) Effect of cracking in drying and shrinkage specimens. *Cement and Concrete Research,* **12**, 209-226.

Bolton, A. (1994) Island strife. *New Civil Engineer*, 6th October, 14-21.

Bottke H. (1931) Behaviour of reinforced concrete structures in fire. *Beton und Eisen*,**30**, Germany.

Bremer, F. (1967) Multi-layer (Double-wall) prestressed concrete pressure vessel. *Nuclear Engineering and Design*, **5**, 183-190.

BS 476:Part 1:1953 Fire tests on building materials and structures. British Standards Institution, London.

BS 476:Part 8:1972 Test methods and criteria for the fire resistance of elements of building construction. British Standards Institution, London.

BS 476:Part 20:1987 Fire tests on building materials and structures. British Standards Institution, London.

BS 812:Part 2:1975 Methods for sampling and testing of mineral aggregates, sands and filters - physical properties. British Standards Institution, London.

BS 1881:Part 114:1983 Methods for determination of density of hardened concrete. British

Standards Institution, London.

BS 1881:Part 116:1983 Methods for determination of compressive strength of concrete cubes. British Standards Institution, London.

BS 1881:Part 117:1983 Methods for determination of tensile splitting strength. British Standards Institution, London.

BS 1881:Part 122:1983 Methods for determination of water absorption. British Standards Institution, London.

BS 5950:Part 1:1985 Structural use of steelwork in building. British Standards Institution, London.

BS 6319:Part 7:1985 Testing of resin and polymer/cement compositions for use in construction - Method of measurement of tensile strength. British Standards Institution, London.

Building Research Establishment (1988) *Design of normal concrete mixes.* Building Research Establishment report 106, Department of Environment, HMSO, London.

Carrasquillo, R. and Slate, F. (1983) Microcracking and definition of failure of high- and normal-strength concretes. *Cement, Concrete and Aggregate*, **5(1)**, 54-61.

Chapman, D.A. and England, G.L. (1976) Effect of moisture migration on shrinkage, pore pressure and other concrete properties. *Transactions, Fourth International Conference on Structural Mechanics in Reactor Technology*. San Francisco.

Christiaanse, A., Langhorst, A. and Gerriste, A. (1972) *Discussion of fire resistance of lightweight concrete and spalling*. Dutch Society of Engineers (STUVO), Report 12, Holland.

Collins, R.J. (1989) *Porous aggregates in concrete - sandstones from NW England.* BRE Information Paper IP 16/89, Building Research Establishment, Watford.

Comité Euro-International du Béton (CEB) (1991) *Fire Design of Concrete Structures in*

accordance with CEB/FIP Model Code 90. Bulletin d'Information No.208, CEB, Switzerland.

Connolly, R.J and Kirby, J.A. (1993) Theoretical background to a computer program to predict the thermal response of materials to fire. BRE Note N 102/93, Building Research Establishment, Watford.

Connolly, R.J., Kirby, J.A. and Barnes N. (1994) A parametric study of the influence of boundary conditions in using THELMA. BRE Note 149/94, Building Research Establishment, Watford.

Copier, W.J. (1979) *Spalling of normalweight and lightweight concrete on exposure to fire*. Report **24(2)**, Heron, Holland.

Cruz,C.R. and Gillen, M. (1990) Thermal expansion of Portland cement paste, mortar and concrete at high temperatures, *Fire and Materials*, **4(2)**, 1-5.

Davey, N. and Ashton, L.A. (1953) *Investigation of building fires - Part V Fire tests on structural elements*. National Building Studies Research Paper No.12, Department of Scientific and Industrial Research, HMSO, London.

Dayan, A. and Gluekler, E. (1982) Heat and mass transfer within an intensely heated concrete slab. *International Journal of Heat and Mass Transfer*, 25(10), 1461-1467.

Deidrichs, U., Jumpannen, U.M., Morita, T., Nause, P. and Schneider, U. (1994) Concerning spalling behaviour of high-strength concrete columns (personal communication)

Dougill, J.W. (1965) Some effects of thermal volume changes on the properties and behaviour of concrete. *Proceedings, International Conference on the Structure of Concrete*, 1-15.

Dougill, J.W. (1971) The effect of high temperature on concrete with reference to thermal spalling. PhD Thesis, Imperial College, London.

Dougill, J.W. (1972a) Modes of failure of concrete panels exposed to high temperatures, *Magazine of Concrete Research*, **24(79)**, 71-76.

Dougill, J.W. (1972b) *A note on the mechanics of spalling in concrete*. Appendix to Fire Research Memorandum No.70, Joint Fire Research Organisation, Borehamwood.

Ehm, H. (1966) Contribution to calculation of fire loaded beam type reinforced concrete elements. PhD Thesis, Technical University of Braunschweig, Germany.

Endell, R. (1929) Tests on the length and structure changes of concrete aggregates and cement mortars at temperatures up to 1200°C. In *Deutscher Ausschuß für Stahlbeton*, **60**, W.Ernst and Son, Berlin.

England, G. (1971) Migration of moisture and pore pressures in heated concrete. *Proceedings of First International Conference on Structural Mechanics in Reactor Technology*, **3 (H)**,Berlin, 22-26.

England, G., Greathead, R. and Khan, S. (1991) Influence of high temperature on water content, permeability and pore pressures in concrete. *Transactions of Structural Mechanics in Reactor Technology*, **H(02/1)**, Japan, 31-36.

ENV 1992-1-2:1994 Code of practice for the design of concrete structures - Fire design. Comité Européen de Normalisation available through British Standards Institution, London.

Gary, M. (1916) *Fire tests on reinforced concrete buildings* (in German) Verlag Wilhelm Ernst und Sohn, Heft 11, Germany.

Goto,S. and Roy, D. (1981) Effect of w/c ratio and curing temperature on the permeability of hardened cement paste. *Cemente and Concrete Research*, **11**, 575-579.

Grunberg, G.(1925) *Physik*, **35**, p548, Germany.

Gustaferro, A.H.and Carlson, C.C. (1962) Interpretation of the results of fire tests on pretsressed concrete building components. *Journal Prestressed Concrete Institute*, **7(5)**, Chicago,14-22.

Hanneman, M.and Thomas, H. (1959) Resistance of reinforced concrete elements and floors in

fires, In *Deutscher Ausschuß für Stahlbeton*, **132**, W.Ernst and Son, Berlin.

Harada, K. and Terai, T. (1991) Heat and mass transfer in an intensely heated mortar wall. *Proceedings of 3rd International Symposium on Fire Safety Science*, Edinburgh, 781-790.

Harmathy, T.Z. (1966) Experimental study on moisture and fire endurance. *Fire Technology*, **2(1)**, 52-59.

Harmathy, T.Z. (1967) Moisture sorption of building materials, Technical Paper 242, National Research Council of Canada, Ottawa.

Harmathy, T.Z. (1969a) *Simultaneous moisture and heat transport in porous systems with particular reference to drying*. Research Paper No. 407, National Research Council of Canada, Ottawa.

Harmathy, T.Z. (1969b) Moisture and heat transport with particular reference to concrete. Paper to *49th Annual Meeting of Committee on Performance of Concrete - Physical Aspects*, Canada.

Hassenjager, (1935) The behaviour of concrete and reinforced concrete in fire and the design of expansion joints in reinforced concrete construction. PhD Thesis, Technical University of Braunschweig, Germany.

Herbst, H.J. and Schneider, U. (1990) Moisture distribution measurements for describing transport processes in heated concrete. In *Proceedings of Second Workshop on Mechanical Behaviour of Concrete under Extreme Thermal and Hygral Conditions*, 7-21.

Hertz, K. (1984) Heat induced explosion of dense concretes. Report No.166, Institute of Building Design Technology, University of Denmark.

Hertz, K.D. (1992) Danish investigation of silica fume concretes at elevated temperatures. *American Concrete Institute Materials Journal*, July/August, 345-347.

Heuze, F.E. (1983) High Temperature Mechanical, Physical and Thermal Properties of Granitic

Rocks - A Review', *International Journal of Rock Mechanics*, **20(1)**, 3-10.

Hognestad, E., Hanson, N. and Mc Henry, D. (1955) concrete stress distribution in ultimate strength design. *Journal of American Concrete Institution*, **52**, 455-479.

Huang, C., Stang, H. and Best, C. (1979) Heat and moisture transfer in concrete slabs. *International Journal of Heat and Mass Transfer*, 22 (2), 257-266.

Hughes, D.C. (1985) Pore structure and permeability of hardened cement paste. *Magazine of Concrete Research*, **37(133)**, 227-233.

Institution of Structural Engineers and Concrete Society (1978) *Design and detailing of concrete structures for fire resistance*, Interim Guidance by a Joint Committee of the Institution of Structural Engineers and The Concrete Society, Institution of Structural Engineers, London.

ISO 834: Part 1:1987 Elements of building construction - General requirements for fire resistance testing, British Standards Institution, London.

Joint Committee on the Fire Grading of Buildings (1946) *General Principles and Structural Precautions*. Post-War Building Studies No.20, HMSO, London.

Jumpannen, U-M. (1989) Effect of strength on fire behaviour of concrete, *Nordic Concrete Research*, Publication No. 8.

Kalos, G.M. (1973) *Influence of the carbonisation of the concrete on the explosive spalling under fire conditions*. Report 673, Techical Chamber of Greece, Greece.

Kawagoe, K. (1958) Fire test on prestressed concrete slab. In *Proceedings of Symposium on Prestressed Concrete and Composite Beams*, Braunschweig, Germany.

Kent, C.H.(1932) Thermal stresses in spheres and cylinders produced by temperatures varying with time. *Transactions of American Society of Mechanical Engineers*, **54(18)**, 185.

Kordina, K., Ehm, C. and Schneider, U. (1984) Effects of biaxial loading on the high temperature behaviour of concrete. *Proceedings of First International Symposium on Fire Safety Science*, 281-290.

Kupfer, H., Hilsdorf, H. and Rusch, H. (1969) Behaviour of concrete under biaxial stress. *Journal of American Concrete Institute*, **8**, 656-666.

Khan, A. (1990) Pore pressure and moisture migration in concrete at high and non-uniform temperatures. PhD Thesis. University of London.

Khoury, G.A., Grainger, B. and Sullivan, P.J. (1985) Strain of concrete during first heating to 600°C under load. *Magazine of Concrete Research*, **37 (133)**, 195-215.

Lawson, R.M. (1985) *Fire resistance of ribbed concrete floors*. Report No.107, Construction Industry Research Information Association, London.

Lewis, W.K. (1921) *Industrial Engineering and Chemistry*, **13**, 427.

Lie, T.T. (1984) A procedure to calculate fire resistance of structural members. *Fire Technology*, **14(1)**, 28 - 85.

Malhotra, H.L. (1956) The effect of temperature on the compressive strength of concrete. *Magazine of Concrete Research*, **8(23)**, 84-90.

Malhotra, H.L. (1969) *Fire Resistance of structural concrete beams*. Fire Research Note No.741, Joint Fire Research Organisation, Borehamwood.

Malhotra, H.L. (1970) *Effect of age on the fire resistance of reinforced concrete columns*. Fire Research Memorandum Note No.1, Joint Fire Research Organisation, Borehamwood..

Malhotra, H.L. (1971) Concrete beams and fire. *Concrete*, **12(2)**, 63-65.

Malhotra, H.L.(1972) *Survey on spalling - Results of a questionnaire*. Fire Research Memorandum 70, Joint Fire Research Organisation, Borehamwood.

Malhotra, H.L. (1984) *Spalling of concrete in fires*. Technical Note 118, Construction Industry Research and Information Association, London.

Manson, S.S. (1952) Behaviour of materials under conditions of thermal stress. *Proceedings of Heat Transfer Symposium,* University of Michigan, United States, 9-75.

Marshall, A.L.(1972) The thermal properties of concrete. *Building Science*, **7**, 167-174.

Mc Cready, D.W., Mc Cabe, H.J. and Marshall, W.R. (1940) *Journal Transactions of American Institute of Civil Engineers*, **136**, 183

Meyer-Ottens, C. (1972) The question of spalling of concrete stuctural elements of standard concrete under fire loading. PhD Thesis, Technical University of Braunschweig, Germany.

Meyer-Ottens, C. (1977) Spalling of normal concrete elements under fire stress - causes and preventive measures (in German). BRE Translation No.2058, Building Research Establishment, Watford.

Mitchell, L.J. (1953) Thermal expansion tests on aggregates, neat cement pastes and concretes. *Proceedings of American Society of Testing and Materials*, **53**, 963.

Mustapha K. (1994) Modelling the effects of spalling on the failure modes of concrete columns in fire, PhD Thesis, University of Aston in Birmingham.

Nekrasov, K.D., Zhukov, V.V. and Shevchenko, V.I. (1967) Investigation of the heating of large blocks of refractory concrete from one side. *Refractories* (Translated from Ogneupony), **6**, 21-22, New York.

Neville, A.M.(1981) *Properties of concrete*. 3rd Edition, Pitman International, London.

Nisugi, N., Kono, T. and Sugawara, M. (1959) Fire Resistance of prestressed concrete beam. *Journal of Japanese Society of Civil Engineers,* **44 (9)**, 16-20.

Norton, F.H.(1968) *Refractories*, 4th Edition, Mc Graw-Hill, New York.

Orchard, D.F.(1976) *Concrete Technology Volume 3 - Properties and Testing of Aggregate.* 3rd Edition, Applied Science Publishers, London.

Piasta, J. (1984) Heat deformations of cement paste phases and microstructure of cement paste. *Matérieux et Constructions*, **17(102)**,415-420.

Purkiss, J.A. (1995) *Fire safety engineering design of structures*. Technical Communications (Publishing)Ltd. and Butterworth-Heinemann, London.

Rickenstorf, G. (1970) Spalling of temperature loaded plain, reinforced and prestressed concrete building elements. *Proceedings of the Sixth Congress of the Fédération Internationale de la Précontrainte (F.I.P.)*, Prague, 56-65.

Robinson G.S. (1967) Behaviour of concrete in bi-axial compression. *Proceedings of American Society of Civil Engineers*, United States, 71-85.

Rogers, G.F. and Mayhew, Y.R. (1991) *Thermodynamic and transport properties of fluids.* Fourth Edition, Basil Blackwell Ltd., Oxford.

Saito, H. (1965) *Explosive spalling of prestressed concrete in fire*. Occasional Report No.22, Building Research Institute, Japan.

Sanjayanan, G. and Stocks, L. (1993) Spalling of high strength silica fume concrete in fire. *American Concrete Institute Materials Journal*, March/April, 170-173.

Sarvaranta, L., Elomaa, M. and Järvelä, E. (1993) A study of spalling behaviour of pan fibre-reinforced concrete of thermal analysis. *Fire and Materials,* **17**, 225-230.

Schneider, U. (1973) Zur kinetik festigkeitsmindernder reaktionen in normalbetonen bei hohen temperaturen. Disseratation, Technical University of Braunschweig, Germany.

Schneider, U. (1977) Strength and temperature deformation of concrete under steady and non-steady temperature influence. *Die Bautechnik*, **4**, 123-132.

Schneider, U. (1985), *Properties of materials at high temperatures - concrete*, International Union of Testing and Research laboratories for Materials and Structures (RILEM), Kassel University Press, Germany

Schneider, U., Herbst, H-J. and Diederichs, U. (1985) Permeability and porosity at elevated temperature, *Proceedings of 8th International Conference on Structural Mechanics in Reactor Technology*.

Schneider, U. (1986) Modelling of concrete behaviour at high temperatures. In *Design of structures against fire* (ed. Anchor, R.D, Malhotra, H.L. and Purkiss, J.A.), Elsevier Applied Science Publishers, London, pp 53 - 69.

Sertmehemetoglu, Y. (1977) On the mechanism of spalling of concrete under fire conditions. PhD Thesis, Kings College, London.

Shirley S.T., Burg, R.G. and Fiorato, A.E. (1987) *Fire endurance of high strength concrete slabs*. Research Paper 871210, Construction Technology Laboratories Inc., Illinois, United States.

Shorter, G.W.and Harmathy, T.Z. (1965) Moisture Clog Spalling. In *Proceedings of Institution of Civil Engineers*, **20**, 75-90.

Skinner, B.T.(1966) Thermal expansion (Section 6) - Handbook of physical constants. *Geologocal Society of America Memoir*, **97**, pp 75-95.

Sullivan, P.J.E. and Poucher, M.P. (1971) The influence of temperature on the physical properties of concrete and mortar in the range 20°C to 400°C. In Proceedings of *Symposium on Effects of Temperature on Concrete*, SP-25, American Concrete Institute, Detroit, 103-135.

Thelandersson, S. (1971) *Effect of high temperatures on tensile strength of concrete*. Report by Division of Structural Mechanics and Concrete Technology, Lund Institute of Technology, Sweden.

Thelanderson, S.(1974) *Mechanical behaviour of heated concrete under torsional loading at transient high temperature conditions*. Bulletin No. 46, Lund Institute of Technology, Sweden.

Thomas, F.G.and Webster C.T. (1953) *Investigations on building fires - Part 6*. National Building Studies Research Paper 18, HMSO, London.

Timoshenko, S.(1934) *Theory of Elasticity*. Engineering Societies Monograph, Mc Graw-Hill, London.

Venecanio, D. (1990) Thermal imcompatibility of concrete components and thermal properties of carbonate rocks. *American Concrete Institute Materials Journal*, Nov/Dec, 602-607.

Weigler, H. and Fischer, R. (1968) Beton bei temperaturen von 100°C bis 750°C. *Beton*, **2**, 1-8.

Woodside, W. and Kuzmak, J. (1958) Effect of temperature distribution on the moisture flow in porous media. *Transactions of American Geophysical Union*, **39(4)**, 670-680.

Wilson, R., Taylor, G., Platten, A. and Fletcher, A. (1992) Mathematical modelling of thermal stresses resulting from transient heat transfer in concrete at high temperatures. In *Proceedings of International Conference on Materials and Design against Fire*, Institution of Mechanical Engineers, London, 33-37.

Winslow, D.N. and Diamond, S. (1970) A Mercury Intrusion Porosimetry study of evolution of porosity in Portland Cement. *Journal of Materials*, **5(3)**, 564-585.

Wu, G.Y.,(1986) Heat Resistant Concrete Pavements. *Military Engineer*, **8(509)** , 487-489.

Zhukov, V.V. (1975) *Explosive failure of concrete during a fire* (in Russian). Translation No.DT 2124, Joint Fire Research Organisation, Borehamwood.

Zhukov, V.V. (1994) *Forecast of a brittle failure of concrete by fire*. Scientific Research Institute for concrete and reinforced concrete, Moscow.

Zoldners, N.G. (1960) Effect of high temperature on concrete incorporating different aggregates. *Proceedings of American Society for Testing and Materials*, **60**, 1087-1108.

APPENDIX DESIGN OF TEST RIG TO BS 5950:Part 1:1985

A.1 OBJECTIVE

To design a test rig that will allow delivery of 70 N/mm^2 uniform compressive stress to a cylindrical concrete specimen (150 mm diameter, 100 mm deep). A schematic of the loading frame is shown in Figure A.1.

A.2 ANALYSIS OF LOADS ACTING

A.2.1 Calculation of Design Moments and Forces

The load is applied over each quadrant of the cylindrical concrete specimen.

Surface Area (A) = 100 (118 - 8) = 1.1 x 10^4 mm^2

Design stress (σ) = 70 N/mm^2

Required loading force (F) = $\sigma . A$ = 7.7 x 10^5 N

Design load on steel beam = 800 kN

Design Bending Moment (M) = 160 kNm at mid-span

Design Shear Force (V) = 400 kN at mid-span

A.2.1.2 Choice of Steel Section Size

Universal Beam Section : 305 x 127 x 48 UB (Grade 50)

A.3 CHECK CAPACITY OF BEAM TO BS 5950:Part 1:1985

BS 5950 Reference

Section Definition

Table 6 $P_y = 355 \text{ N/mm}^2$

$$\epsilon = 0.88 \ , \ \frac{b}{T} = 4.5 \ , \ \frac{d}{t} = 29.7$$

$$\text{as } \frac{b}{T} < 9.5\,\epsilon \text{ and } \frac{d}{t} < 39\epsilon$$

$\therefore$ Section is Compact

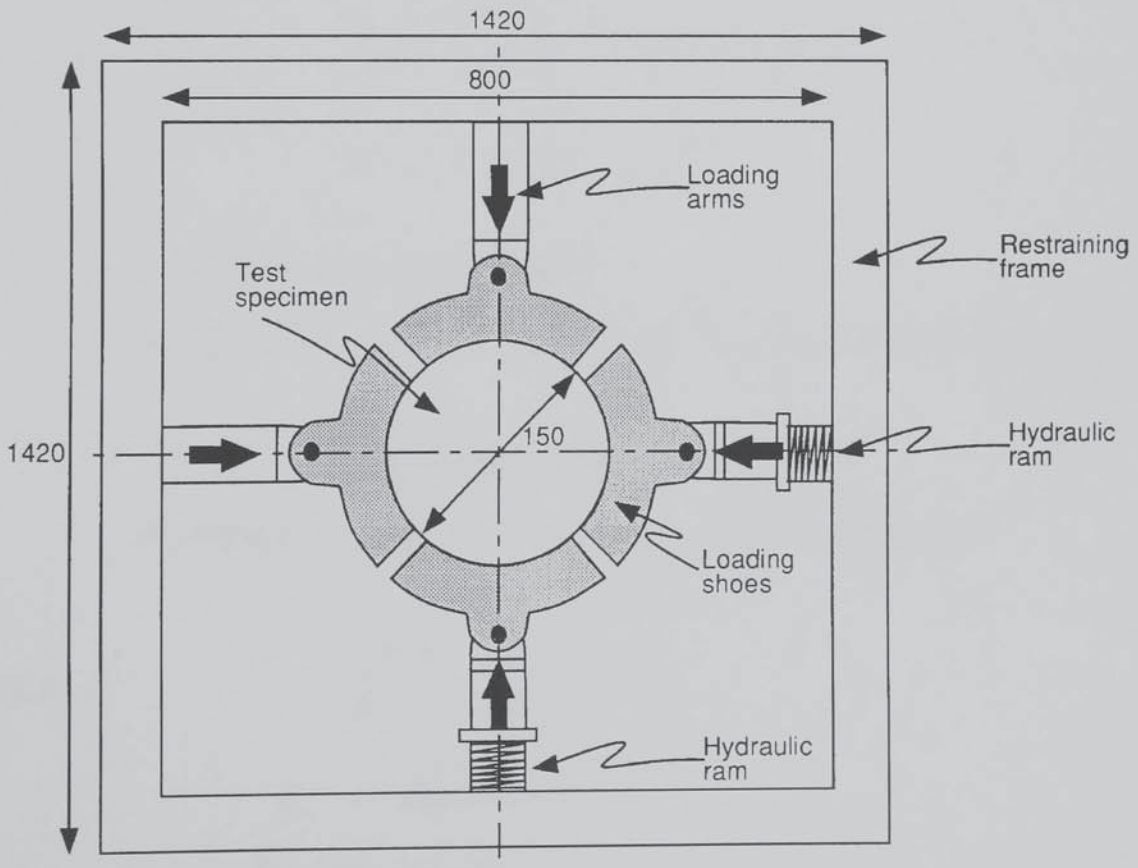

Figure A.1 Schematic of Loading Frame

BS 5950 Ref.

Moment/Shear Capacity

Cl.*4.2.3* Shear capacity (P_v) = $0.6\ P_y\ A_v$

P_y = 355 N/mm^2

A_v = shear area = t . D = 2762 mm^2

$\therefore$ Pv = 588 kN

Cl.4.2.6 0.6 Pv = 353 kN

This is less than the design shear force (v) of 400 kN, so design must consider moment with co-acting shear.

Cl.4.2.6 $M_c = P_y (S - S_v \rho_1) \leq 1.2\ P_y . Z$

$$\rho_1 = \frac{2.5\ F_v}{P_v} - 1.5 = 0.2$$

$$S_v = \frac{t\ D^2}{6} = 142.5 \times 10^3 \text{ mm}^3$$

$$S = 706 \times 10^3 \text{ mm}^3$$

$\therefore$ Moment capacity (M_c) = 240 kNm

As this is greater than the Design Moment (M_{des}), section size is adequate.

Axial Load Capacity

Applied axial load (F) = 400 kN using the simplified approach.

Cl.4.8.2
$$\frac{F}{A_e\ P_y} + \frac{M_x}{M_{cx}} \leq 1$$

A_e = effective area = 60.8 cm^2

F = 400 kN

M_x = applied moment = 160 kNm

BS 5950 Ref.

M_{cx} = moment capacity = 240 kNm

$$\frac{400 \times 10^3}{60.8 \times 10^2 \times 355 \times 10^3} + \frac{160}{240} = 0.85 \leq 1$$

$\therefore$ Section is acceptable

Cl.4.5.2

Bearing Check

Cl.4.5.2.1

$P_w = (b_1 + n_1)\, t\, p_c$

Cl.4.5.1.3

b_1 = stiff bearing length = T = 2 . t

= 14 + 2 (8.9)

n_1 = 155.2

t = web thickness = 8.9 mm

p_c = compressive strength

Cl.4.5.2.1

$$\lambda = 2.5 \frac{d}{t} = 2.5 \frac{(262.5)}{8.9}$$

= 74.3

Table 27(c)

p_c = 205 N/mm^2

P_w = (150 + 310) x 8.9 x 205 x 10^{-3}

= 840 kN > 800 kN

$\therefore$ No stiffners necessary.

Check on Central Deflection

$$\delta = \frac{W1^3}{48E1} = \frac{800 \times 10^3 \times (800)^3}{48\,(205 \times 10^3)\, 9500 \times 10^4}$$

δ = 0.4 mm This is acceptable

A.4 CHECK ON WELD CONNECTING BEAMS

BS 5950 Ref.
Cl.6.6.5 Use 6 mm surround fillet weld (E51)

$$\rho_w = 255 \text{ N/mm}^2$$

Weld length = (200 x 2) + (12.5 x 2) = 810 mm

Weld capacity = $255 \times 10^{-3} \times 6 \times 810$ = 1239 kN

This is greater than reaction force of 400 kN, so welds are adequate.

A.5 DESIGN OF LOADING PLATES

For bending about the X-X axis, assume design is controlled by stiffness requirements. The trial design is shown in Figure A.2.

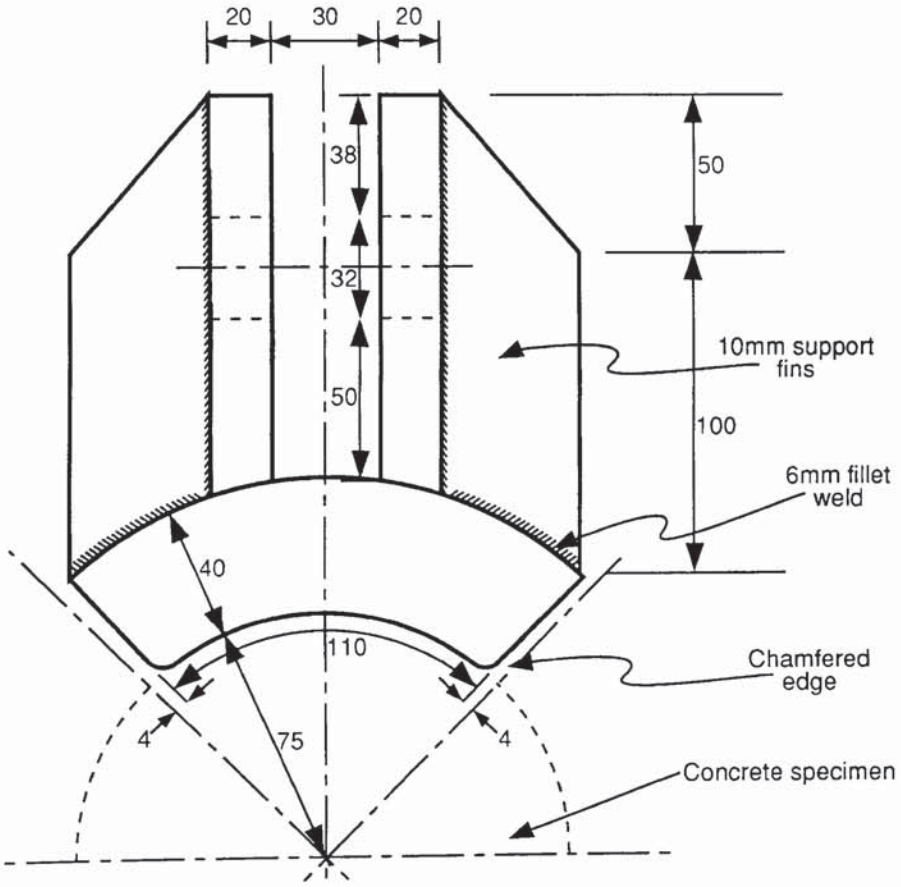

Figure A.2 Loading arm

$$\bar{y} = \frac{(40 \times 110 \times 20) + (100 \times 20 \times 90) \times 2}{(40 \times 110) + (100 \times 20 \times 2)}$$

$$\bar{y} = 53.3 \text{ mm}$$

$$I_{NA} = \frac{110 \times 40^3}{12} + 100 \times 40 \times 33.3^2$$

$$+ 2 \times \frac{20 \times 100^3}{12} + 2\ (20 \times 100 \times 36.7^2) = 1{,}419 \text{ cm}^4$$

$$E_s = 205 \text{ kN/mm}^2$$

$$\therefore \quad E_s I_s = 2909 \times 10^6 \text{ N mm}^2$$

$$E_c = 5.5 \sqrt{F_{cu}} = 5.5 \sqrt{40} = 35 \text{ kN/mm}^2$$

$$I_c = \frac{\pi d_c^4}{64}, \text{ where } d_c = \text{specimen diameter} = 150 \text{ mm}$$

$$= 2458 \text{ cm}^4$$

$$E_c I_c = 745.5 \times 10^6 \text{ N mm}^2$$

$$\therefore \quad \frac{E_s I_s}{E_c I_c} = 3.9$$

(This stiffness ratio is acceptable)

A.6 DESIGN OF CONNECTION TO SPREADER PLATE

Specify connections made of 30 mm Grade 8.8 bolts

P_s = 421 kN (double shear)

F_v = $400 < 421$ ∴ acceptable

Min. Edge Distance = 1.25 . d = 38 mm

ρ_{bs} = D . T . ρ_{bs} = $30 \times 40 \times 970 \times 10^{-3}$ = 1,164 kN

Designed connection are OK for bearing